Biological studies on different cellular responses to bioactive compounds of natural and synthetic origin

By

Sanjima Pal

[LIFE07201004004]

National Institute of Science Education and Research Bhubaneshwar

A thesis submitted to the

Board of Studies in Life Sciences

In partial fulfillment of requirements

For the Degree of

DOCTOR OF PHILOSOPHY
of
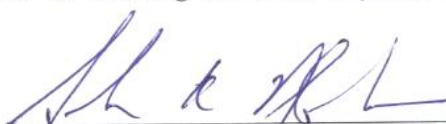# HOMI BHABHA NATIONAL INSTITUTE

August, 2016

Homi Bhabha National Institute

Recommendations of the Viva Voce Committee

As members of the Viva Voce Committee, we certify that we have read the dissertation prepared by **SANJIMA PAL [HBNI Roll No. LIFE07201004004]** entitled, **"Biological studies on different cellular responses to bioactive compounds of natural and synthetic origin"** and recommend that it may be accepted as fulfilling the thesis requirement for the award of Degree of Doctor of Philosophy.

Chairman - < Prof. SURESH K. ABRAHAM >   **Date: 17-08-2016**

Guide / Convener – Dr. V BADIREENATH KONKIMALLA   **Date: 17-08-2016**

External Examiner – Prof. SURESH K. ABRAHAM   **Date: 17-08-2016**

Member 1– Dr. ASIMA BHATTACHARYYA   **Date: 17-08-2016**

Member 2- Dr. HARAPRIYA MOHAPATRA   **Date: 17-08-2016**

Final approval and acceptance of this thesis is contingent upon the candidate's submission of the final copies of the thesis to HBNI.

I/We hereby certify that I/we have read this thesis prepared under my/our direction and recommend that it may be accepted as fulfilling the thesis requirement.

Date: 17-08-2016

Place: Bhubaneswar

Guide: Dr. V Badireenath Konkimalla

STATEMENT BY AUTHOR

This dissertation has been submitted in partial fulfillment of requirements for an advanced degree at Homi Bhabha National Institute (HBNI) and is deposited in the Library to be made available to borrowers under rules of the HBNI.

Brief quotations from this dissertation are allowable without special permission, provided that accurate acknowledgement of source is made. Requests for permission for extended quotation from or reproduction of this manuscript in whole or in part may be granted by the Competent Authority of HBNI when in his or her judgment the proposed use of the material is in the interests of scholarship. In all other instances, however, permission must be obtained from the author.

Sanjima Pal

DECLARATION

I, hereby declare that the investigation presented in the thesis has been carried out by me. The work

is original and has not been submitted earlier as a whole or in part for a degree / diploma at this or

any other Institution / University.

Sanjima Pal

Bhubaneswar

Date:

List of Publications from the Thesis

Journals

1. Induction of autophagic cell death in apoptosis-resistant pancreatic cancer cells using benzo[α]phenoxazines derivatives, 10-methyl-benzo[α]phenoxazine-5-one and benzo[α]phenoxazine-5-one. **Sanjima Pal**, Sunita Salunke-Gawali and V. Badireenath Konkimalla. **2016**; 16 (doi: 10.2174/1871520616666160624091519) (**Accepted**)

2. Sulforaphane regulates phenotypic and functional switching of both induced and spontaneously differentiating human monocytes. **Sanjima Pal**, V. Badireenath Konkimalla. International Immunopharmacology, **2016**; *35*, 85-98. (doi: 10.1016/j.intimp.2016.03.008)

   Data on sulforaphane treatment mediated suppression of autoreactive, inflammatory M1 macrophages. **Sanjima Pal, V. Badireenath Konkimalla. Data in Brief, **2016;** *7,* 1560–1564. (doi:10.1016/j.dib.2016.03.105)

3. Hormetic potential of Sulforaphane (SFN) in switching cells' fate towards survival or death. **Sanjima Pal,** V. Badireenath Konkimalla. Mini Reviews in Medicinal Chemistry, **2015**; *16.* (doi: 10.2174/1389557516666151120115027)

4. Targeting a chemorefractory COLO205 (BRAF-V600E) cell line using substituted benzo[a]phenoxazines† **Sanjima Pal,** V. Badireenath Konkimalla, Laxmi Kathwate, Soniya S. Rao, Shridhar P. Gejji, Vedavati G. Puranik, Thomas Weyhermüller and Sunita Salunke-Gawali. RSC Advances, **2015**, *5*, 82549. (doi:10.1039/c5ra14949e)

In Communications

1. Sulforaphane targets endogenous FasL to attenuate collagen mediated inflammatory responses in THP1 derived macrophages.

Conferences and Workshops

1. Attended a workshop on "Scientific communication" conducted by Welcome trust-DBT Alliance, April, 2014

2. Presented a poster entitled, "Regulation of Toll like Receptor 4 in B16 tumor bearing B6 mice: An implication in tumor induced immune regulation" **Sanjima Pal**, Pratheek BM, Sujay Singh, Prasanta Maiti and Subhasis Chattopadhyay; InCoFIBS-**2010** at National Institute Technology, Rourkela, Odisha.

Others (Published)

1. Reaction between lawsone and aminophenol derivatives: Synthesis, characterization, molecular structures and antiproliferative activity; Laxmi Kathawate, Pranya V Joshi, Tapan Kumar Dash, **Sanjima Pal**, Milind Nikalje, Thomas Weyhermüller, Vedavati G Puranik, V Badireenath Konkimalla, Sunita Salunke-Gawali. Journal of Molecular Structure, **2014**, *1075*, 397-405.

2. Separation and isolation of tautomers of 2-hydroxy-4-naphthoquinone-1-oxime derivatives by liquid chromatography: Antiproliferative activity and DFT studies; Yogesh Shinde, Stephen Sproules, Laxmi Kathawate, **Sanjima Pal**, V Badireenath Konkimalla, Sunita Salunke-Gawali. J. Chem. Sci., **2014**, *126*, 213-225.

3. Molecular structures and antiproliferative activity of side-chain saturated and homologated analogs of 2-chloro-3-(<i>n</i>-alkylamino)-1,4-napthoquinone; **Sanjima Pal**, Mahesh Jadhav, Thomas Weyhermüller, Yogesh Patil, M Nethaji, Umesh Kasabe, Laxmi Kathawate, V Badireenath Konkimalla, Sunita Salunke-Gawali. Journal of Molecular Structure, **2013**, *1049*, 355-361.

Sanjima Pal

DEDICATIONS

To my family

ACKNOWLEDGEMENTS

I feel immensely honored to get this opportunity to convey my deepest sense of gratitude to everyone who has guided and supported me during my PhD work.

This PhD work would have not been possible without the help and support of many people. Firstly, I express my gratitude to my Guide, Dr. V Badireenath Konkimalla for introducing me to the fields of chemical biology of medicinal agents and granting me complete freedom to explore my potential and help me out in all types of circumstances. I appreciate all his contributions of time, ideas, and funding to make my Ph.D. experience productive.

I am thankful to Prof. V. Chandrasekhar, (Director, NISER) and Prof. T. K. Chandrashekar (Ex-Director, NISER) for providing me an opportunity to work in this premiere institute.

I would like to thank my Doctoral Committee Members; Prof. Jgneshwar Dandapat (Dept. of Biotehnology, Utkal University, Bhubaneswar Dr.Harapriya Mahapatra (Dean, NISER), and Dr.Asima Bhattacharyya (NISER) for their expert comments, critical analysis of my data and helpful suggestions towards the progress of my work.

Dr. Sunita Salunke-Gawali (Dept. of Chemistry, Savitribai Phule Pune University, Pune) and her lab members have contributed immensely to my Ph.D work. The group has synthesized and provided all the derivatives of benzo [α] phenoxazines for the biological studies reported in this dissertation. I appreciated their collaboration and the impressive skills of developing novel molecules with possible bioactivities.

I am indebted to NISER, DAE for awarding me a Junior and Senior Research Fellowships from 2010-2015. I am also equally grateful to Innovative Young Biotechnology Award scheme grant (Ref. No. BT/05/IYBA/2011), Department of Biotechnology for being an integral part of financial support to this Ph.D works. I would like to convey my special thanks to blood bank and Super Religare Laboratories Ltd (SRL) at Kalinga Hospital Limited, Bhubaneswar for providing their facilities.

It was a great pleasure getting a lab member like, Tapan Kumar Dash who always supported and helped me in innumerable ways without complaining.

I would like to acknowledge Dr. Subhasis Chattopadhyay, NISER who taught me immunology as well as various techniques (cell culture, flow cytometry) at some points during my tenure as a Ph.D. student. I would also extend my special thanks to all the faculties, scientific officers, scientific and technical staff members of School of Biological Sciences, and members of

NISER administration, accounts, library, stores and purchase; all of whom always have provided adequate support to complete my Ph.D work.

It was nice to have batch mates like Pratibha Verma, Sushri Priyadarshini, Lopamudra Das, Usha Pallavi Kar, Ashutosh Kumar Jha, and Santosh Kumar Singh who have always made the days in NISER very lively and pleasant. I am especially grateful to Uday Singh, Santosh Kumar for all the help, supports and also making the lab atmosphere lively and cheerful. I will also cherish my stay during my PhD spent with my wonderful roommate Renuka Pradhan and my ever supportive juniors, Vikram Singh Meena, Ankit Tiwari and Mitali Mishra. Guys, without your moral support and encouragement this journey would have not been possible. I am also blessed with a large friend circle outside NISER. I would like to thank all of them for all their moral support and encouragement throughout this journey. Some of them deserved to be mentioned here are Indrani Das, Anirban Baral, Milan Banik, Sharmistha Dam were the one who had actually motivated me for pursuing PhD and were a constant source of encouragement. I also thank all others not mentioned here and who have been equally helpful towards me in various ways.

I am also thankful to my parents, my siblings (brother and sister) and brother in law for being on my intensive support system at all times. It was only your loves, blessings and beliefs in me that made me through the entire voyage and have made this day possible. Lastly, my love will always be for a little angel, my nephew '**Ryan**' who brought only good lucks for me from the day he has arrived in the world.

Sanjima Pal

CONTENTS

SYNOPSIS

Homi Bhabha National Institute

Ph. D. PROGRAMME

1. **Name of the Student:** SANJIMA PAL

2. **Name of the Constituent Institution:** National Institute of Science Education and Research (NISER)

3. **Enrolment No. :** LIFE07201004004

4. **Title of the Thesis:** Biological studies on different cellular responses to bioactive compounds of natural and synthetic origin

5. **Board of Studies:** Life Sciences

1.   Introduction

A chemical entity can be defined as a bioactive substance if it causes any reactions or triggers any response or displays either any beneficial or toxic effects on the living tissues. Plants are one of the richest hubs of bioactive chemical diversity. However, chemical synthesis methods have employed as alternative means to develop new sets of bioactive scaffold structures or modify existing phytochemicals. Collectively, all experimental data unleashed thousands of bioactive compounds of natural and synthetic origins, exhibiting from non-cytotoxic to cytoprotective to cytotoxic activities against various diseases e.g. cancers, infectious and autoimmune diseases (AD). Despite of the studies and progress in biomedical research, about 13% of all annual deaths have been registered due to cancer [1] and 1% of the worldwide population (more than 75% are women) are suffering from any autoimmune inflammatory arthritis e.g. rheumatoid arthritis (RA) or osteoarthritis (OA) [2]. The increasing global burden of diseases, treatment mediated side-effects or cell types associated intrinsic chemo-resistance let researchers to continue thrive for discovering or developing new therapeutic agents from any sources possible and exploring their therapeutic efficacy.

2.   Scope and Organization of the Present Thesis

According to current status about 49% of drugs available are either natural products or their synthetic derivatives [1]. Moreover, cell based studies defining the bioactivities of few interesting synthetic chemicals families which may be considered as anti-cancer chemotherapeutic agents in future. This thesis work mainly focused on understanding the bioactivities or cellular responses (either immune-modulatory anti-autoimmune or anti-cancer) to

    I.   Plant **derived sulforaphane (SFN)**

    II.   Synthetic fluorescent **benzo[α]phenoxazines (BPZ)**

using different *in vitro* experimental models and approaches.

3. **Non cytotoxic immune-modulatory and specificity studies of bioactive isothiocyanate, Sulforaphane (SFN) using *in vitro* monocyte/macrophage model for autoimmunity**

3.1. Introduction

Cruciferous plant-derived isothiocyanates (ITCs), SFN [(R)-1-isothiocyanato-4-(methylsulfinyl)-butane] has already established as promising multi-targeting, anti-proliferative, anti-metastatic, anti-angiogenic, anti-inflammatory, anti-cancer chemopreventive agent [3]. Hormetic SFN can promote both cell survival and cytotoxic within a spectrum of *in vitro* applied concentrations [4]. In a recent review, we mapped and proposed a network of multi-targeting, intra-cellular concentration and time dependent hormetic signaling events by SFN [5]. But studies emphasizing SFN (at *in vitro* non cytotoxic immune modulatory concentration) mediated shifting of monocytes (Mn) differentiation into specific (phenotypes and functions) macrophage (MΦ) population are unavailable.

Polarization and plasticity are the hallmarks of development and activation of the Mn/MΦ system. M1-MΦs initiate pro-inflammatory responses and mount T_H1 responses whereas M2-MΦs develop immune-suppression through activating T_H2 type response [6]. Unidirectional M1 polarization (increase in ratio of M1 cells to M2 cells) is one of the major determining events for the development and persistence of inflammation during autoimmunity e.g. arthritis [7]. M1-MΦs are the active participants in magnifying the inflammatory responses against body's own tissues or proteins (e.g. against extracellular matrix protein collagens in arthritis) during any chronic inflammatory arthritis such as RA and OA. Published reports also revealed these aggressive, pro-inflammatory M1-MΦs and degraded/soluble form of collagens as active biomarkers for RA condition [8. 9]. On contrary, the presence or longer survivability and activity of immune-suppressive M2-MΦs is preferred in such conditions.

During synovial inflammation, effector cells are often characterized by a unique resistance to Fas-related apoptosis and intracellular control or distribution of both Fas and FasL proteins affect

death of auto-reactive T cells and agonistic therapeutic interventions have been found beneficial for arthritis [10]. *In vitro* studies also unleashed, the presence of soluble collagens in culture media is capable of generating auto-reactive, apoptosis resistant (Fas mediated signal) but collagen restricted T cells [8]. However, reports are unavailable whether the soluble collagens and SFN can regulate Fas/FasL system within Mn/MΦ cells *in vitro*.

In last decade, immune suppressive SFN has used as an alternative therapeutic measure for treating inflammatory arthritis. Experimental evidences suggested the cytotoxic effects of SFN either on auto-reactive tissue fibroblasts or T_H1 cells [11, 12]. However, reports regarding the effects of SFN on another major contributor of RA/OA pathogenesis, auto-reactive M1-MΦs are unavailable. Therapeutic interventions upon polarization of Mn differentiation to M2 or switching plasticity of M1-MΦs (converting them into M2) have recognized as beneficial approaches in various animal and human disease models. If at non cytotoxic concentration, phytochemical SFN holds characteristics to polarize Mn differentiation into immune suppressive M2 type and concomitantly converts existing M1 cells into M2 type, it may be proposed as a Mn/MΦ mediated therapeutic intervention in chronic inflammatory autoimmune conditions e.g. arthritis.

3.2. Aims and objectives

(a) Establishment of an *in vitro* collagen-induced inflammatory, autoimmune condition with human monocytic cell line, THP1 and human peripheral blood derived monocytes.

(b) Evaluation of the roles of immune-regulatory candidate-SFN in generating anti-autoimmune responses *in vitro*.

(c) *In vitro* evaluation of differential regulation on endogenous Fas/FasL proteins within developed autoimmune model (soluble collagen induced) and SFN treated THP1 cells (differentiating Mn or differentiated MΦs).

3.3. Materials and methods

Human monocytic cell line THP1 is an excellent model to study Mn to MΦ differentiation and polarization using conventional inducers [13]. For this study, THP1 cells were differentiated using

20ng/ml phorbol 12-myristate 13-acetate (PMA). To establish positive controls, following 6 h of PMA treatment (complete adhesion) differentiating Mns were polarized toward classical M1 type with LPS (100 ng/ml) and IFN-γ (20 ng/ml) together and alternative M2 type using IL-4 (20 ng/ml) and IL-13 (20 ng/ml) together. To evaluate Mn differentiation polarizing roles of soluble collagens [soluble human collagens (I-IV): 1 µg/ml and soluble chicken collagen-II: 20 µg/ml] and 10 µM SFN were introduced separately or together in culture media (after 6 h of PMA addition). Differentiating Mns were collected after 24 h and phenotypes and functional characterization were performed using microscopy, flow cytometry, sandwich ELISA and western blotting. Each working concentration (no adverse effect on cell survival) was determined by XTT cell survival assay [14].

For switch/plasticity experiments, PMA differentiated THP1 derived MΦs have been used and soluble collagens or SFN alone or together were added after Mn adhesion (6 h after PMA addition) and kept for another 48 h. Soluble collagen /SFN pretreated MΦs were washed with PBS and incubated for another 24 h with fresh culture media along with/without SFN. MΦ specific functional and phenotypic characteristics were assessed using sandwich XTT assay, sandwich ELISA, flow cytometry, western blotting.

3.4. Results and Discussion

a) These present findings demonstrated the ability of soluble collagens of various origins (human and chicken) or types (I-IV of human) in developing pro-inflammatory, autoimmune conditions *in vitro.* This *in vitro* model may be useful to unleash the cellular mechanisms responsible for the development and persistence of chronic inflammatory conditions in ADs e.g, RA and OA.

b) Our findings suggest, both SFN and soluble collagens can polarize *in vitro* THP1-Mn differentiation. As observed in conventional M1 polarizing differentiating THP1-Mns (LPS+IFNγ induced) production or expression of several pro-inflammatory biomarkers (IL12p70, surface CD14, CD197 and endogenous COX-2, iNOS) were upregulated in soluble collagens treated cells. Downregulation in several anti-inflammatory biomarkers e.g. IL10 and surface CD36, CD206 were also observed in these auto-reactive cells. While non-cytotoxic,

SFN treated differentiating Mns resembled to M2 polarizing Mns and also showed to inhibit *in vitro* soluble collagens mediated M1 polarization.

c) Non cytotoxic (here 10μM), anti-inflammatory SFN involves MAPKs, especially MEK1/2 and JNK1/2 while polarizing THP1-Mn to M2 cells.

d) Current dissertation also suggest, SFN regulates the plasticity of already differentiated auto-reactive (here soluble collagen induced) M1-MΦs and coverts them into M2 cells.

e) Indicating a possible similarity with any auto-reactive immune cells i.e. existence of altered Fas/FasL mediated apoptosis, endogenous FasL maturation (absence of 26 kDa product) process was observed to be inhibited in soluble collagen (non-apoptotic) induced auto-reactive M1 polarizing Mns. While SFN promoted FasL maturation during and after THP1 differentiation to M1 cells, dampening the *in vitro* autoimmune condition.
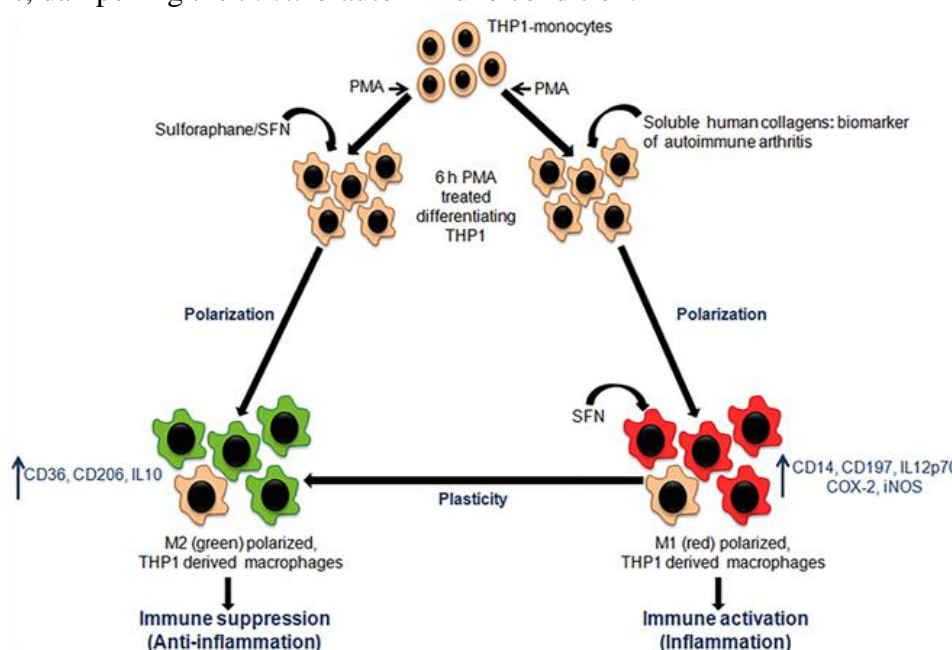
Figure 1: *In vitro* SFN mediated regulation in Mn/MΦ model for arthritis

3.6. Conclusions

SFN switches THP1 derived Mns differentiation (PMA induced) towards M2-MΦs depending on MEK1/2 and JNK1/2 (members of MAPK pathways) activity. These SFN polarized M2 type Mns/MΦs are capable of suppressing *in vitro* soluble collagens induced pro-inflammatory autoimmune responses by shifting M1-MΦ plasticity towards M2 types and induced endogenous FasL maturation in M1-MΦs.

4. Screening for bioactivities and mechanistic characterization of novel, synthetic benzo[α]phenoxazines (BPZ) in different *in vitro* experimental models

4.1. Introduction

Unavailability of any reliable plant sources (no reports available in literature), intrinsically fluorescent BPZs were synthesized using chemical synthesis methods. These ligands [e.g., Nile red (9-diethylamino-5H-benzo[α]phenoxazine-5-one)] have been in use in wide ranges of biological applications for at least last few decades. This class of compounds is one of the most popular redox-sensitive (real-time probe to detect intracellular changes in pH) florescent dyes and often used to stain intra-cellular lipid droplets or proteins in SDS-PAGE or organelle organization [15]. Several BPZs have also been reported as antitumor, antibiotic and antiprotozoal activities [16-18].

Despite of these published reports (endogenous targets and biological applications) on BPZs, studies regarding cell based incorporation, cytotoxicity and possibility to be specific anti-cancer pro-drugs/drugs are limited. However, no evidences are available regarding the induction of non-apoptotic cell death pathways by BPZs in any cancer models.

4.3. Aims and objectives

a) Determination of anti-proliferative effect and cellular internalization of chemically synthesized BPZs.

b) Evaluation of differential cellular responses (apoptosis and autophagy) to synthetic BPZs.

4.4. Materials and methods

20mM concentration stock of three newly synthesized BPZs, **1B** (**10-chloro-benzo[α]phenoxazine-5-one**), **2B** (**10-methyl-benzo[α]phenoxazine-5-one**) and **3B** (**benzo[α]phenoxazine-5-one**) were prepared in dimethyl sulfoxide (DMSO) and kept at -20 °C.
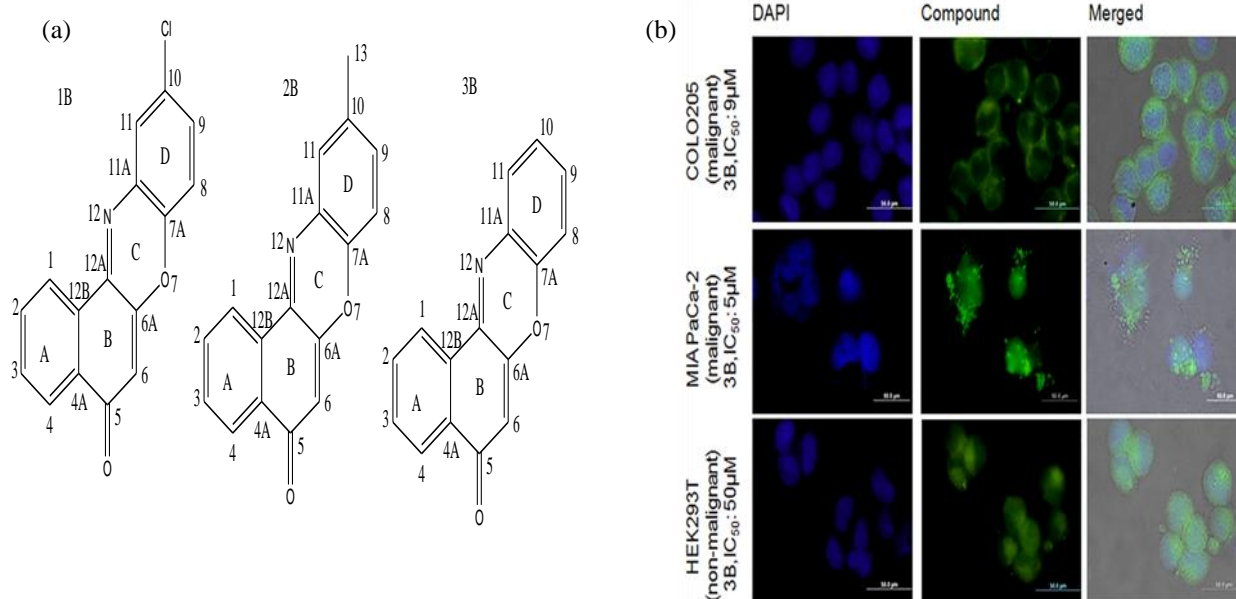
Figure 2: (a) Molecular structure of 1B, 2B and 3B; (b) Cellular internalization of fluorescent BPZ (3B)

Human colon cancer cell line, COLO205 (BRAF-V600E) was maintained in RPMI and pancreatic cancer cell line, MIAPaCa-2 (p53-R248W, KRAS-G12D, mutated DPC4 /SMAD family member 4 and CDKN2A / p16 / p16INK4a) and a non malignant human embryonic kidney cell line, HEK293T (possesses SV40 virus large T antigen mediated inactivated wild type /wt p53, KRAS, BRAF) were maintained in DMEM growth media respectively containing 10% heat-inactivated FBS (5% FBS during experiments) and 1% pen-strep at 37°C in 5% CO_2. XTT assay, colonogenic assay, flow cytometry and fluorescent microscopy based compound internalization/accumulation studies, annexin-V/ 7-AAD assay, DNA fragmentation assay and western blots (for the biomarkers of apoptosis and autophagy) were performed to assess the malignant cells specific bioactivity of the tested BPZs.

4.5. Results and discussion

1. Current experimental findings suggest, tested intrinsically fluorescent BPZ derivatives are membrane permeable. Both **2B** (IC_{50}: 13μM in COLO205 and 20μM in MIA PaCa-2) and **3B** (IC_{50}: 9μM in COLO205 and 5μM in MIA PaCa-2) are biologically active in malignant cells and significant anti-proliferative, anti-colonogenic and cell cycle blocking agents.

2. Current studies also featured the anti-cancer specificity of **2B** and **3B** as they remained significantly ineffective in non-malignant cells (HEK293T) even after treating with very high (non permissible) concentration (50μM).

3. Despite of accumulating into both malignant and non-malignant cells, **1B** showed insignificant anti-proliferative activity within *in vitro* permissible limit.

4. Current studies also demonstrated, both **2B** and **3B** induced apoptosis only in chemorefractory COLO205 cells and cytotoxic autophagy in chemorefractory, apoptotic resistant MIA PaCa-2 cells.
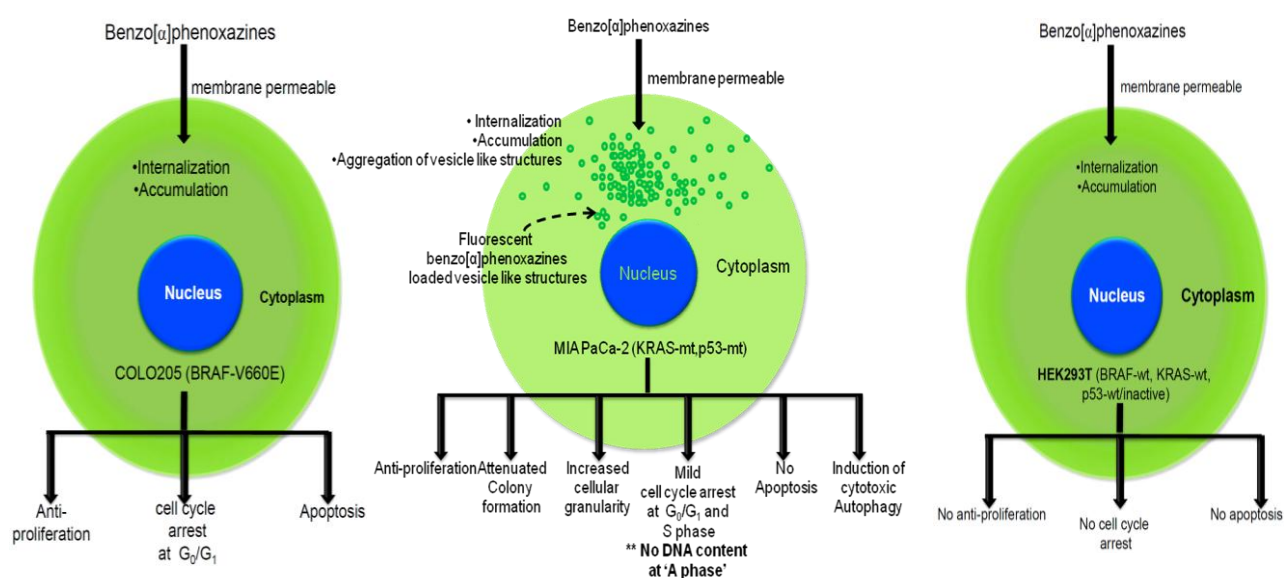
Figure 3: Schemes summarizing the results reported for BPZ induced bioactivities

4.6. Conclusions

Synthetic **2B** and **3B** (order of efficacy **3B >2B >>1B**) are highly specific (only active in malignant cells) pro-apoptotic and pro-death autophagy inducing agents for malignant cells. However, insignificant cytotoxicity yet capacity to internalize into any cell type indicated an alternative usage of **1B** as non- cytotoxic fluorescent dye. Moreover, all of these three ligands may also be used as basic scaffold structures in developing new sets of anti-cancer agents.

5.   Bibliography

[1]   Mangal, M.; Sagar, P.; Singh, H.; Raghava, G.P.; Agarwal, S.M. NPACT: Naturally Occurring Plant-based Anti-cancer Compound-Activity-Target database. *Nucleic Acids Res,* **2013**, *41* (Database issue), D1124-1129.

[2]   Gibofsky, A. Overview of epidemiology, pathophysiology, and diagnosis of rheumatoid arthritis. *Am J Manag Care,* **2012**, *18* (13 Suppl), S295-302.

[3]   Amjad, A.I.; Parikh, R.A.; Appleman, L.J.; Hahm, E.R.; Singh, K.; Singh, S.V. Broccoli-Derived Sulforaphane and Chemoprevention of Prostate Cancer: From Bench to Bedside. *Curr Pharmacol Rep,* **2015**, *1* (6), 382-390.

[4]   Bao, Y.; Wang, W.; Zhou, Z.; Sun, C. Benefits and risks of the hormetic effects of dietary isothiocyanates on cancer prevention. *PLoS One,* **2014**, *9* (12), e114764.

[5]   Pal, S.; Konkimalla, V.B. Hormetic potential of Sulforaphane (SFN) in switching cells' fate towards survival or death. *Mini Rev Med Chem,* **2015**.

[6]   Mills, C.D.; Kincaid, K.; Alt, J.M.; Heilman, M.J.; Hill, A.M. M-1/M-2 macrophages and the Th1/Th2 paradigm. *J Immunol,* **2000**, *164* (12), 6166-6173.

[7]   Li, J.; Hsu, H.C.; Mountz, J.D. The Dynamic Duo-Inflammatory M1 macrophages and Th17 cells in Rheumatic Diseases. *J Orthop Rheumatol,* **2013**, *1* (1), 4.

[8]   Lin, Y.P.; Su, C.C.; Huang, J.Y.; Lin, H.C.; Cheng, Y.J.; Liu, M.F.*, et al.* Aberrant integrin activation induces p38 MAPK phosphorylation resulting in suppressed Fas-mediated apoptosis in T cells: implications for rheumatoid arthritis. *Mol Immunol,* **2009**, *46* (16), 3328-3335.

[9]   Haringman, J.J.; Gerlag, D.M.; Zwinderman, A.H.; Smeets, T.J.; Kraan, M.C.; Baeten, D.*, et al.* Synovial tissue macrophages: a sensitive biomarker for response to treatment in patients with rheumatoid arthritis. *Ann Rheum Dis,* **2005**, *64* (6), 834-838.

[10]   Peng, S.L. Fas (CD95)-related apoptosis and rheumatoid arthritis. *Rheumatology (Oxford),* **2006**, *45* (1), 26-30.

[11] Choi, Y.J.; Lee, W.S.; Lee, E.G.; Sung, M.S.; Yoo, W.H. Sulforaphane inhibits IL-1beta-induced proliferation of rheumatoid arthritis synovial fibroblasts and the production of MMPs, COX-2, and PGE2. *Inflammation,* **2014**, *37* (5), 1496-1503.

[12] Kong, J.S.; Yoo, S.A.; Kim, H.S.; Kim, H.A.; Yea, K.; Ryu, S.H*., et al.* Inhibition of synovial hyperplasia, rheumatoid T cell activation, and experimental arthritis in mice by sulforaphane, a naturally occurring isothiocyanate. *Arthritis Rheum,* **2010**, *62* (1), 159-170.

[13] Auwerx, J. The human leukemia cell line, THP-1: a multifacetted model for the study of monocyte-macrophage differentiation. *Experientia,* **1991**, *47* (1), 22-31.

[14] Kathawate, L.; Joshi, P.V.; Dash, T.K.; Pal, S.; Nikalje, M.; Weyhermüller, T*., et al.* Reaction between lawsone and aminophenol derivatives: Synthesis, characterization, molecular structures and antiproliferative activity. *Journal of Molecular Structure,* **2014**, *1075* (0), 397-405.

[15] Alba, F.J.; Bartolome, S.; Bermudez, A.; Daban, J.R. Fluorescent Labeling of Proteins and Its Application to SDS-PAGE and Western Blotting. *Methods Mol Biol,* **2015**, *1314*, 41-50.

[16] Chadar Dattatray; Rao S. Soniya; Khan Ayesha; Gejji P. Shridhar; Kiesar, B.S.; Thomas, W*., et al.* Benzo[a]phenoxazines and benzo[a]phenothiazine from vitamin K3: synthesis, molecular structures, DFT studies and cytotoxic activity. *RSC Advances,* **2015**, *5*, 57917–57929.

[17] Motohashi, N. [Interaction between 9-substituted benzo[alpha]phenoxazine derivatives and DNA and relationships to their antibacterial activities]. *Yakugaku Zasshi,* **1982**, *102* (7), 646-650.

[18] Wesolowska, O.; Molnar, J.; Westman, G.; Samuelsson, K.; Kawase, M.; Ocsovszki, I*., et al.* Benzo[a]phenoxazines: a new group of potent P-glycoprotein inhibitors. *In Vivo,* **2006**, *20*(1), 109-113.

LIST OF ABBREVIATIONS

µ	Micro
µl	Microlitre
µM	Micromolar
7-AAD	7-aminoactinomycin D
APC	Allophycocyanin
ARE	Antioxidant response element
ATCC	American Type Culture Collection
Atg	Autophagy-related gene
BITC	Benzyl isothiocyanate
B-ME	β-Mercaptoethanol
BPZ	Benzo [α] phenoxazine
BSA	Bovine serum albumin
Coll/s	Collagen/s
Conc.	Concentration
COX-2	Cyclooxygenase-2
CYP 450	Cytochrome P-450
DAPI	4',6-diamidino-2-phenylindole
DMEM	Dulbecco's Modified Eagle's medium
DMSO	Dimethyl sulphoxide
DNA	Deoxyribonucleic acid
DTT	Dithiothreitol
ECL	Enhanced chemiluminescence
EDTA	Ethylenediaminetetraacetic acid
ELISA	Enzyme-linked immunosorbent assay
Em	Emission
ER	Endoplasmic reticulum
ERK	Extracellular-signal-regulated protein kinase
EtBr	Ethidium bromide
Ex	Excitation
FACS	Fluorescence-activated cell sorting
FBS	Foetal bovine serum
FITC	Fluorescein isothiocyanate
GST	Glutathione S-transferase
h	Hour
HDAC	Histone deacetylase
HRP	Horseradish peroxidase
Hsp	Heat-shock protein
IC$_{50}$	Inhibitory concentration $_{50}$
ILs	Interleukins
iNOS	Inducible nitric oxide synthase
IR	Infra red
ITC/s	Isothiocyanate/s

IκB	Inhibitor of NF-κB
JNK 1/2	Jenus kinase 1/2
KCl	Potassium chloride
Keap-1	Kelch-like ECH-associated protein 1
L	Litre
LC3	Microtubule-associated protein 1 light chain 3
LPS	Lipopolysaccharide
Macrophage/s	MΦ/s
Malignant	M
MAPK	Mitogen activated protein kinase
MFI	Mean fluorescence intensity
min	Minutes
ml	Millilitre
mM	Millimolar
mmol	Millimoles
Monocyte/s	Mn/s
MRP	Multidrug resistance proteins
MS	Mass spectrometry
Mutant	mt
NaCl	Sodium chloride
NaN$_3$	Sodium azide
NCCS	National Centre for Cell Sciences
NF-κB	Nuclear factor-kappa B
NO	Nitric oxide
Non-malignant	NM
Not determined	ND
Nrf-2	Nuclear factor erythroid-derived 2-like 2
Nrf2	NF-E2-related factor-2
O.D	Optical density/Absorbance
OA	Osteoarthritis
p38	p38 protein kinase
PAGE	Polyacrylamide gel electrophoresis
PBS	Phosphate buffered saline
PE	Phycoerythrin
PEITC	Phenethyl isothiocyanate
Pen-Strep	Penicillin-streptomycin
PFA	Paraformaldehyde
PGE-2	Prostaglandin E-2
PI	Propidium iodide
PI3K	Phosphatidylinositol 3-kinase
PMA	Phorbol 12-myristate 13-Acetate
PMS	N-methyl dibenzopyrazine methylsulfate
PVDF	Polyvinylidene difluoride membrane
RA	Rheumatoid arthritis

RIPA buffer	Radio immuno precipitation assay buffer
RPMI 1640	Rosewell Park Memorial Institute medium
RT	Room Temperature
SDS	Sodium dodecyl sulfate
Sec	Seconds
SFN	Sulforaphane
TAE	Tris-acetate-EDTA
TBS	Tris buffer saline
TBST	Tris buffer saline-Tween 20
TLRs	Toll-like receptors
Wavelength	wl
WB	Western blotting
Wild type	wt
XTT	2,3-bis-(2-methoxy-4-nitro-5-sulfophenyl)-2H-tetrazolium-5-carboxanilide)

LIST of TABLES

LIST of FIGURES

differentiation of human monocytes

CHAPTER-1

Introduction and Review of Literature

1. BIOACTIVE AGENTS

A compound is considered bioactive or 'biologically active' when it attributes any direct effect (positive or negative) in one or more component(s) of living organisms, tissues or cells. They can be found in plant or animal or produced synthetically. Depending on the substance, organisms/cell (cancerous or healthy) types, concentrations used, the dose, bioavailability and exposure time, bioactive agents display both cytotoxic as well as non-cytotoxic effects. Biologically active substances always remained a centre of attraction to research community. Knowledge of the biophysical, chemical properties as well cellular responses exerted by a bioactive agent has contributed immensely in understanding and determining the specific usages for human benefits [1].
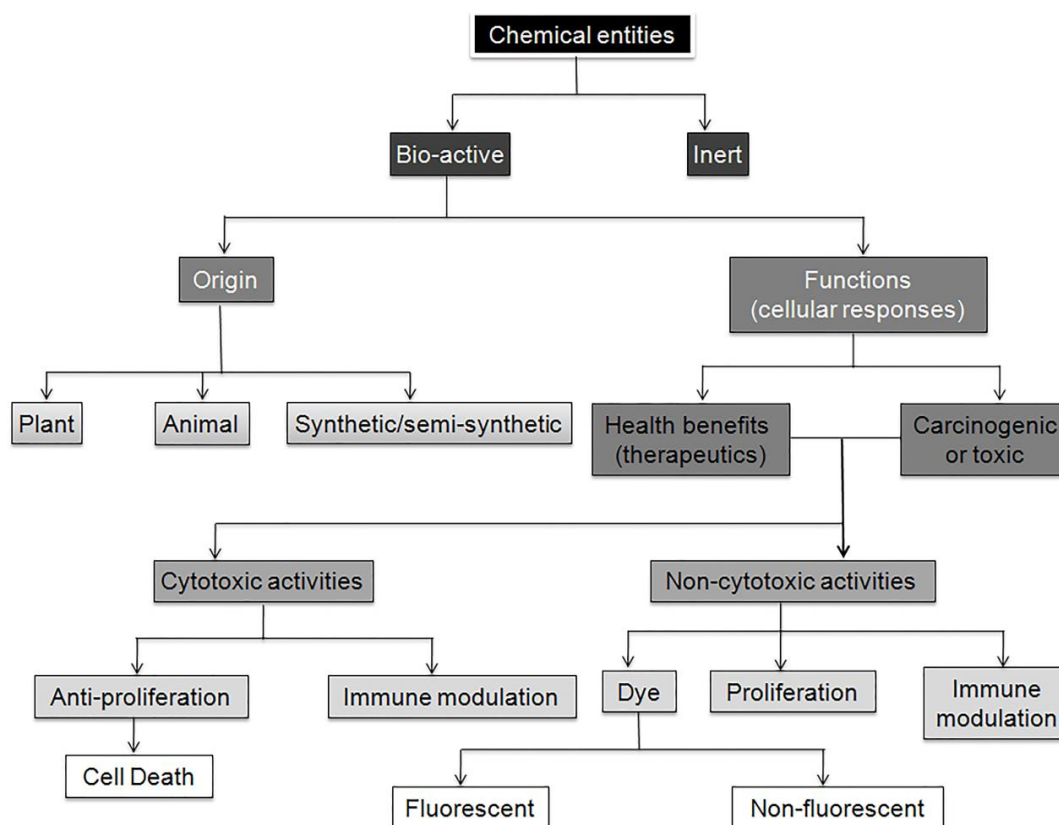
Fig.1.1. Multiple variables or parameters to explore the functions of a bioactive agent

1.1. Phytochemicals

Plants are a major hub of biologically active compounds that elicit diverse pharmacological or toxicological effects [2]. These plant derived bioactive ligands are named *phytochemicals* and majority of them are secondary metabolites. Herbal agents easily conglomerate with other entities,

Review of literature

adapt well with surroundings, followed by change intracellular environments and eventually get metabolized. Throughout history, natural products have played a dominant role in the treatment of human ailments.

Within animal body these agents commence several alterations in bio-molecular activities before getting excreted through urine. As per the current status, major lead scaffold structures of about 49% of available drugs (especially) were found in plants [3]. These plant derived secondary metabolites have been of great interest for medical practitioners and researchers from time immemorial. These structurally unique phytochemicals function by novel mechanisms of action and isolation from the natural sources have led to their discovery. On the other hand, several bioactive compounds are consumed by the body in the form of diet either to maintain the homeostasis or as a preventive measure.

Successful isolation and characterization of active ingredients and understanding their mechanistic roles have invoked researchers world-wide to investigate such naturally occurring bioactive compounds. Researchers have been greatly successful in isolating the active ingredient and exploring their mechanism of action at a molecular level. Still majority of these bioactive compounds suffer major biochemical and pharmacokinetic (absorptivity, short half-life and hydrophobicity) limitations in clinical setting as in the case of curcumin and theaflavin.

Despite of these setbacks, researchers have been quite successful in exploring new bioactive compounds from cocktail of chemicals present in plants and evaluating their biological properties of existing potential phytochemicals in disease perspectives.

So far thousands of chemopreventive bioactive phytochemicals have been documented. Among those agents, the following are the most effective in reducing the proliferative activity of cancer cell; tea polyphenol epigallocatechin-3-gallate (EGCG), curcumin, resveratrol, lycopene, pomegranate extracts, luteolin, genistein, piperin, β-carotene and sulforaphane (SFN) [4]. Not only cancer chemoprevention, application of phychemicals had been proven to be effective against microbial, viral and protozoal infections e.g. artemisinin [5].

1.2. Chemically synthesized bioactive chemicals

Synthetic compounds gained popularity as an alternative source of medicine for past few decades. Researchers apply chemical synthesis methods for the betterment of shortcomings found in bioactivity (modification of novel scaffold structures found in plant sources, increment in half life and tissue absorption) or scaling up the availability of many phytochemicals (industrial benefits) and also development of new sets of bioactive scaffold structures which are not available naturally. Though few of them have appeared to be as good as natural bioactive ligands, yet manifestation of adverse effects, cost of synthesis sometimes reverted back the scientific community towards discovery and utilization of phytochemicals.

Despite of these, chemical synthesis remains unchallenged alternative when bioactive lead scaffold structures are not available from any plant or animal sources or any structural modifications required for improving the activity of the bioactive phytochemicals.

1.1.1. Sulforaphane (SFN)

Isothiocyanate or ITC (–N=C=S) is a bioactive sulfur containing electrophile [6-8]. ITCs can be produced by plants after enzymatic conversion of metabolites called glucosinolates e.g. allyl isothiocyanate or can have synthetic/semi synthetic origins e.g. phenyl isothiocyanate. Among all available natural or synthetic ITCs, allyl isothiocyanate (AITC), phenethyl isothiocyanate (PEITC) and sulforamate or (±)-4-methylsulfinyl-1-(S-methyldithiocarbamyl)-butane has been particularly shown to exert similar anticancer properties against a broad range of cancers. Apart from biological applications, ITCs also have almost unchallenged applications in amino acid sequencing by the Edman degradation.

Cruciferous vegetables such as broccoli and cabbages are the natural sources of ITCs [9, 10]. These plants are considered as the natural cocktail of various membrane-permeable, chemopreventive, cytoprotective, anticancer organo-sulfur ITCs e.g. sulforaphane/ SFN/(R)-1-isothiocyanato-4-(methylsulfinyl)-butane, glucosinolates (GS), S-methyl cysteine sulfoxide,

vitamins (E,C,K) and minerals (zinc, selenium and iron) of which a particular ITC, SFN has acquired most attention as a potential drug candidate [8]. SFN has also been reported as hormetic agent [11, 12].
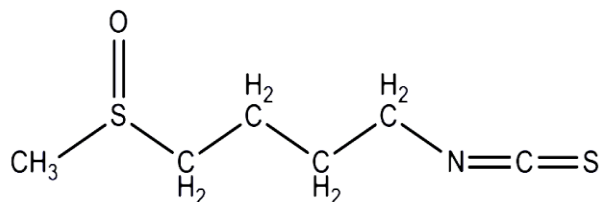
Fig.1.2. Molecular structure of SFN. The N=C=S moiety is reported to be important for its bioactivity.

SFN attracted much attention due to its profound growth inhibitory pro-apoptotic activity. The the induction of apoptosis observed as a primary effect following SFN and other ITCs treatment is attributed mainly to the -N=C=S moiety commonly present in these family of compounds. Activities of SFN and its analogues differ depending on the oxidation state of sulphur and number of methylene groups: CH_3-SO_m-$(CH2)_n$-NCS, (m=0, 1 or 2 and n=3, 4 or 5).

It can exist in both R and S isoforms where, R-SFN is the naturally occurring and better bioactive one [13]. Talay *et al*. also designed and synthesized about thirty-five bi-functional ITCs as structural analogues of SFN capable of inducing both Phase-I and II enzyme systems that are metabolically much more stable than natural SFN itself [14]. Kim *et al.* showed that the SFN analogues with oxidized sulfurs e.g. alyssin, erysolin and alyssin sulfone are much potent inducer of ROS and subsequent apoptosis than its non-oxidized sulfur containing analogues (erucin and berteroin) [15].

SFN or its sulphide or sulphone analogues also elevate both quinone reductase and GST activities in cancer model cell lines and other mouse tissues (liver, glandular stomach, fore-stomach, lung and proximal small intestine) [16]. In a recent review, Dinkova-Kostova *et al.* also discussed the studies conducted for human safety, metabolism, and efficacy of glucosinolates and isothiocyanates. They also provided a list with available information about protection of central nervous system and carcinogenesis by PITC and SFN in various rodent models [17].

Review of literature

1.1.1.1. Origin, isolation and metabolism

In 1992, Talalay *et al.* from Johns Hopkins University was the first group to isolate this dietary component from SAGA broccoli (*Brassica oleracea italica*) [8]. Cruciferous vegetables rich in myrosinases (β-thioglucosidase family, EC 3.2.3.147) are involved in the biosynthesis of SFN from glucosinolate (GS) [18]. Myrosinases catalyze degradation of β-thioglucoside bond of GS molecules resulting in the formation of glucose, sulphate and a diverse group of aglycones as by-products those further undergo non-enzymatic intra-molecular rearrangements (Lossen rearrangement) and eventually form multiple bioactive ITCs or nitriles [17]. Upon consumption, the gastrointestinal tract rich in microflora take up the responsibility of converting GS to SFN, preserving the nutritive value of these cooked crucifers [19]. Conaway *et al.* observed that the bioavailability of ITCs from fresh broccoli is approximately three times greater than that of cooked/steamed brocoli possessing inactivated myrosinase [20]. The overall process of SFN synthesis from GS inside plants, followed by their entry inside cells after exposure, subsequent metabolism, degradation and excretion through urine has been vividly discussed by Wu *et al.* in 2009 [21].

The rate of ITC uptake and intracellular accumulation depends upon temperature, pH, Fe^{2+} content, molecular structure and intracellular glutathione (GSH) concentration [22]. Following cellular uptake, SFN reacts rapidly with free GSH to form covalent adducts elliciting inhibitory effect depending on its thiol-modifying activity [7, 23-26]. SFN has extremely high affinity towards some thiol-containing cysteines and ε-amino-containing lysines leading to the formation of thiocarbamates and thiourea, respectively. It mainly targets only those cysteine residues that have functional implication in respective protein activity or highly conserved in vertebrates [27]. SFN and its analogs (chemically synthesized/modified) have very high passive cellular diffusion rate and can rapidly reach an intracellular concentration 100-200 fold within 0.5-3 h of exposure [28, 29].
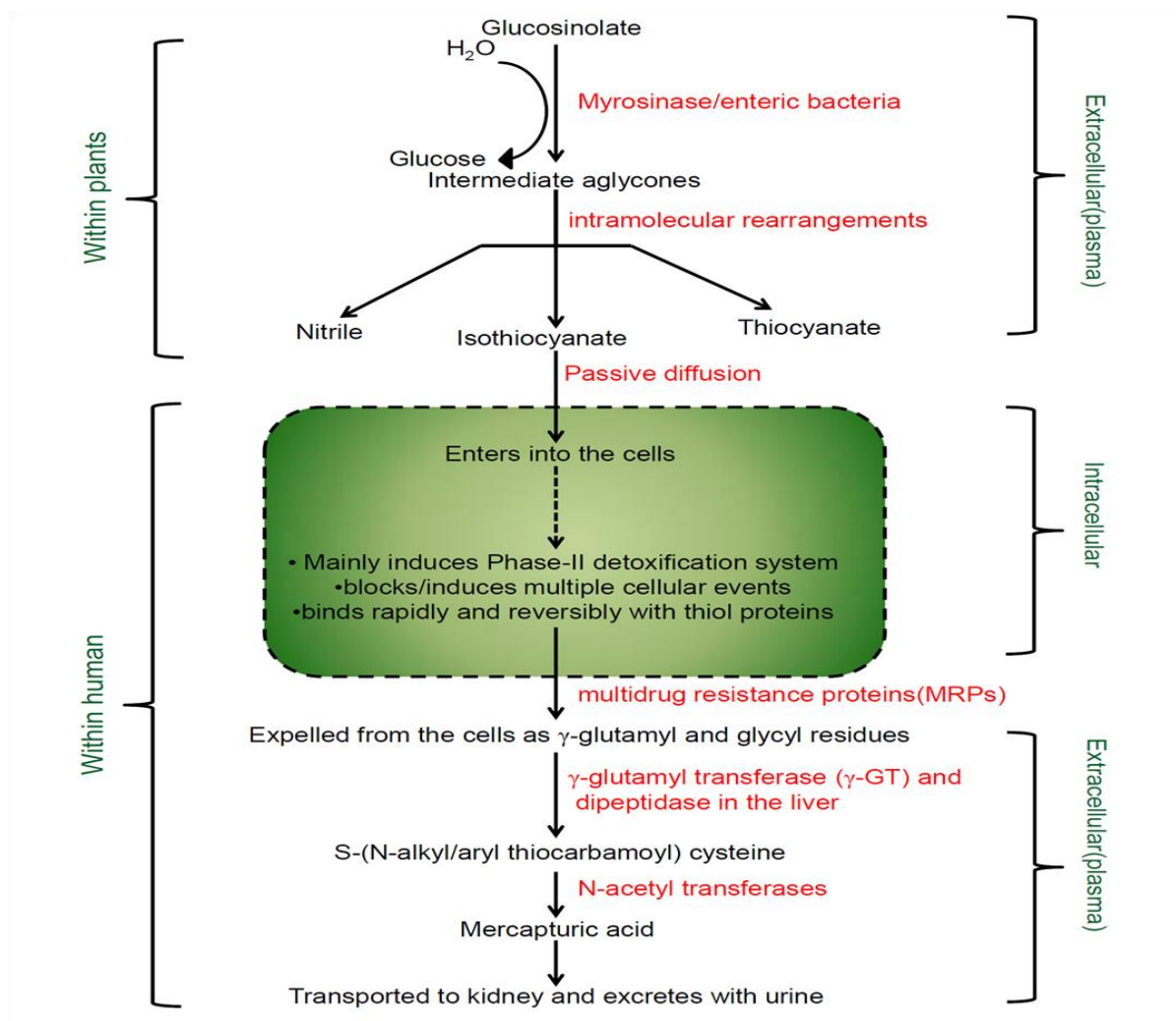
Fig. 1.3. A brief schematic diagram illustrating the various transformations undertaken by GS (precursor of SFN) from its biosynthesis in the plant system to metabolism and formation of by-products in the human system

1.1.1.2. Molecular targets for diverse bioactivities of SFN

SFN has almost two decades of rigorous research history exploring its potential as a anticancer drug candidate. Owing to dampen the patho-physiological conditions, SFN and other bioactive ITCs serve multi-faceted roles and target a vast array of bio-molecules involved in various cellular processes. **Fig.1.4** illustrates a few bio-molecular targets and associated cellular pathways that are both positively as well as negatively regulated by SFN. As such, SFN directly or indirectly interacts with a large number of molecules involved in a variety of cellular events and can regulate them at various levels (RNA/Protein) [12]. Several techniques e.g. affinity chromatography, radio-labelling, microarray, mass spectroscopy and 2D gel electrophoresis, site directed mutagenesis,

mass spectrometry, functional or conformational inhibition of selected proteins have been used so far to identify the cellular protein targets of SFN [27, 30-32]. This way, identifying interacting partners of SFN promises a great potential in targeted drug discovery, at both design and screening level.

From published reports, it is demonstrated that the prime mechanism by which SFN protects cells is through a molecular master redox switch, Nrf-2. Upon activation, Nrf-2 promotes transcriptional induction of ARE regulated genes involved in Phase-I and II detoxification system [33]. Therefore, targeting Nrf-2 is one of the major mechanisms by which compounds from ITC family exert protection against electrophiles and oxidants. Cellular level of Nrf-2, is tightly maintained by active Cullin3 (Cul3)/Kelch-like ECH-associated protein 1 (Keap1)-dependent polyubiquitination system and that SFN interacted with atleast four cysteine residues including Cys^{151} present in Keap1 protein forming thionoacyl adducts with protein thiols. Only in the absence or presence of low concentrations (1%) of fetal bovine serum, SFN aggravated the phagocytic activity in RAW264.7 cells and this aggravation occurs in an Nrf-2-independent manner as observed in peritoneal macrophages of nrf-$2^{-/-}$ mice.

SFN efficiently stimulated iron efflux through ferroportin-1 (the sole iron exporter in mammals) in bone marrow-derived and peritoneal primary macrophages and a murine macrophage cell line, J774.1 [34]. In this process, it followed both Nrf-2-dependent and independent mechanism and affected the level of hepcidin mRNA. SFN can also control cellular damages mediated by several oxidative stressors such as menadione, *tert*-butyl hydroperoxide, 4-hydroxynonenal and peroxynitrite in human adult retinal pigment epithelial cells (ARPE-19), human HaCaT keratinocytes and L1210 murine leukemia cells *via* activating Nrf-2 pathway. SFN also prevented loss of the biomarkers of epithelial-mesenchymal (EMT) transition, E-cadherin and overexpression of α-smooth muscle actin, by inducing Nrf-2 in tissue fibrosis model, rat tubular epithelial NRK-52E cells. It blocks metastasis by inhibiting the expression of EMT associated proteins such as β-

catenin, vimentin, twist1 and ZEB1 thereby concomitantly inducing apoptosis by inhibiting Bcl2, XIAP and phosphorylation of FKHR.

SFN can scavenge free radicals directly or indirectly through the transcription factor, Nrf-2 and exerts neuroprotection both at *in vitro* and *in vivo* conditions. In a study it protected ROS (reactive oxygen species) exposed or hemin or glucose deprived hippocampal neurons from death. In SFN pre treated cultured cortical astrocytes, the levels of a marker of DNA/RNA oxidation, 8-hydroxy-2-deoxyguanosine was reduced (determined by immunostaining) and cells become resistant to death following ischemia or reperfusion. To date there are sufficient reports associated SFN-mediated Nrf-2 activation with alteration of neuron-glia interactions that ultimately resulted in neuroprotection [35]. In patient-derived hONS cells, a model system for Parkinson's disease (PD), L-SFN enables to restore metabolic deficits *via* Nrf-2 pathway after activating its function and expression both at transcriptomic and protein level [36].

It also induces expression of genes encoding members of the cytosolic class α, μ, π and θ GST and certain microsomal transferases (MGST2 and MGST3) and regulates pregnane-X receptor, peroxisome proliferator-activated receptor-γ (PPARγ) and CAATT/enhancer binding protein β (C/EBPβ) [37]. It has been reported that higher dietary intake of glucoraphanin as well as SFN is associated with reduction in the flux of homocysteine *via* the trans-sulfuration pathway resulting in the lowered expression of enzymes of GSH biosynthesis. This particular ability of SFN eventually establishes the intestinal barrier against oxidative stress.

SFN inhibits expression of β-catenin, sterol regulatory element-binding protein (SREBP) -1, -2 and fatty acid synthase, p66(shc), tautomerase activity of macrophage migration inhibitory factor (MIF) [38-40]. From chromatin immunoprecipitation (ChIP) and electrophoretic mobility shift assay (EMSA) is has been shown that SFN can also inhibit TNF-α-induced endothelial lipase expression by inactivating of NFκB. SFN upregulates Hsp27 mediated proteasomal activity (especially rapid removal of misfolded and oxidized proteins) to prevent complications associated with age-related diseases [41]. Following the similar degradation (proteasome-mediated) pathway SFN suppresses

polycomb group of proteins (e.g., Bmi-1, Ezh2) and histones after methylation and ubiquitination [42]. SFN also induces generation of a novel gasotransmitter, H_2S to regulate cell growth and other associated functions [43]. In addition, elicited inactivation of HIF1α has been found in SFN pre-treated cells and turn them sensitive towards TRAIL (TNF-related apoptosis-inducing ligand)-induced apoptosis at hypoxic conditions [44]. Altogether these results suggest potential applications of this phytochemical in prevention of cancer, autoimmune diseases, transplantation surgeries and other genetically-defined pathologies.

Using mass spectroscopy technique, interaction of SFN with more than 30 proteins and covalent modification of Cys303 and Cys[347] in both α- and β- tubulins is reported [31]. Though, SFN has neither any significant affinity to DNA or RNA nor causes any significant cleavage in DNA strands, above mentioned covalent binding potential is an early sequence of events for its pro-apoptotic activity. SFN can also suppress tissue specific function of 6-phosphofructo-2-kinase/fructose-2,6-biphosphatase4 (PFKFB4) by inhibiting the expression and function of its modulator, HIF-1α. From a recent study, SFN involvement in transcriptomic and proteomic regulation of few members of aldo-keto reductase family such as AKRB10, AKR1C1, AKR1C2, AKR1C3, NQO1 and ALDH3A1 is reported.

CDC2 kinase, Rb (retinoblastoma tumour suppressor) protein are the key tagerts in SFN-mediated cell cycle arrest [45]. Reports also suggest that SFN treatment mediates dose- and time-dependent induction of pro-apoptotic proteins e.g., Bax and Bak and simultaneously causes a conformational change, followed by mitochondrial translocation of Bax [46]. Various apoptotic markers e.g. cytosolic release of cytochrome-c and Smac/DIABLO, activation of caspase-9 and caspase-3, induction of Apaf-1 have been observed following SFN treatment.

It is well-known that SFN impairs redox-sensitive DNA binding of proteins e.g. NFκB-DNA binding. With the aid of redox regulators, thioredoxin (Trx) it specifically targets and blocks NFκB binding at DNA without affecting IκB degradation [47]. It also elicits cardioprotection indirectly through targeting several biomolecules involved in anti-oxidative events.

In vitro, SFN and its metabolites SFN-N-acetylcysteine and SFN-cysteine trigger competitive inhibition of HDAC activity, reduce both global and local histone acetylation status, followed by inducing epigenetic modification in human colon cancer [48], prostate cancer [49] and breast cancer model [50]. In a nutshell, SFN can directly regulate gene promoter activity through down-regulating histone deacetylase activity and alters gene promoter methylation in indirect ways e.g. by modulating non-coding micro-RNAs [51].

Still it is required to analyse the SFN regulated signalling pathways which leads to tissue protective immune-modulation and extremely important to screen out some key molecules directing the cytoprotective versus cytotoxic activity of SFN. However, its immune-modulatory target molecules and roles in autoimmunity are less understood. Therefore, in this thesis, investigations have been performed to explore the immune-chemical biology of the action of the SFN.
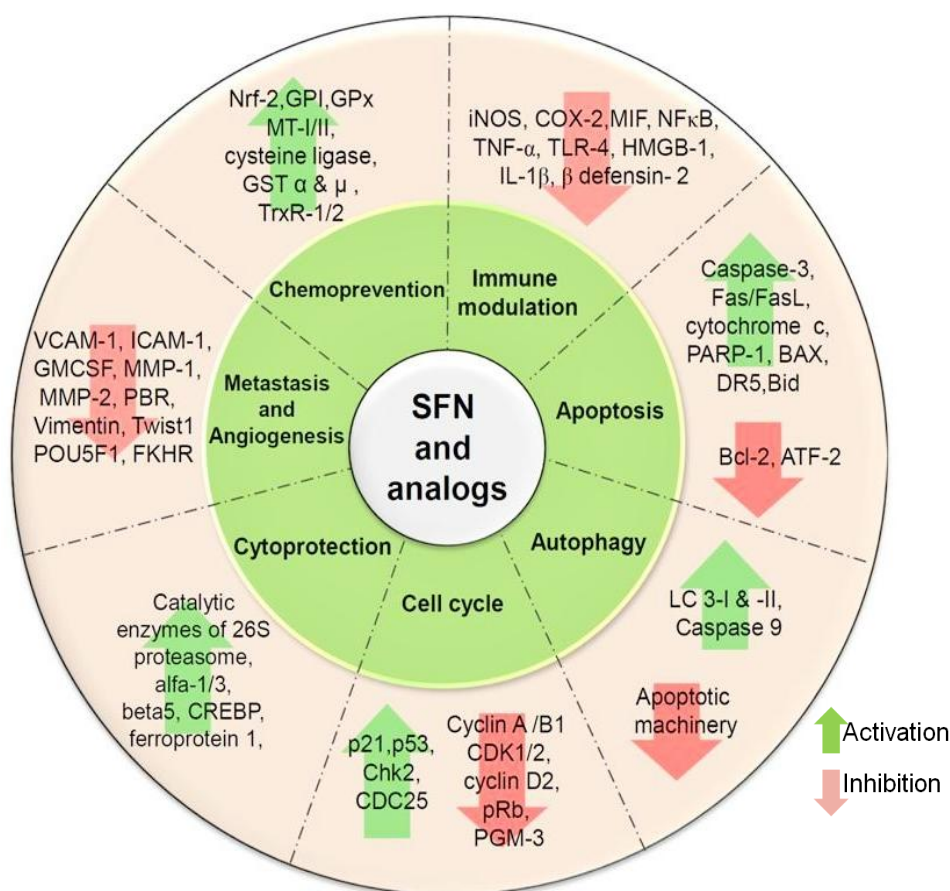
Fig.1.4. SFN & its analogs directly or indirectly targets multiple macromolecules associated with major intracellular pathways

1.1.1.3. *Notable biological properties of SFN*

Despite being a small chemical entity, SFN is extremely bioactive and alone capable of functioning as a potential modulator of various cellular and physiological pathways of cell survival, proliferation, invasion, angiogenesis metastasis, cell death and ageing either by directly binding with the protein or indirectly inducing/suppressing their activities or gene expressions. For last two decades research was directed towards rationally translating this magic molecule from bench to bedside by conducting clinical trials under different disease conditions besides patenting them for exploring other activities. Several clinical trials are being conducted with this multi-targeting molecule (either alone or in combination) either in healthy individuals or for possible therapy against various disease conditions such as prostate cancer, breast cancer, melanoma, autism, cardiovascular diseases, etc. Such data show the level of progress and the importance gained by this small molecule. Most of the trials have been reached upto phase II stage without any observed adverse effects. Tomczyk *et al.* also proposed that individuals' genetic makeup is one of the crucial factors in determining the bioavailability, tissue distribution as well as anti-proliferative chemopreventive efficacy of SFN and other ITCs [52]. In different experimental disease models or directly in patients, it suppressed the incidence and progression of several malignant tumors of different tissue origin (colon, pancreas, breast, prostate, kidney, overy, lung and gastric) along with detoxification pathway [53]. Apart from anti-tumor effects, SFN exhibits profound anti-inflammatory and anti-microbial activity [54]. Below sub-toxic concentration *in vitro*, SFN promotes cell survival [53, 55, 56]. Upon initial increment in exposure time and concentration, it mildly arrests cell cycle progression at various phases while at higher concentration triggers cell death by every possible ways especially through apoptosis. Following **Table-1.1.** has summarized the ongoing clinical trails that are conducted using SFN to develop better therapeutics.

	Title of the trial	Diseases	Phase	I.D no.	Descriptions
1	SFN in Treating Patients With Recurrent Prostate Cancer	Adenocarcinoma of the Prostate; Recurrent Prostate Cancer	II	NCT01228084	Measuring anti-tumor activity of SFN through determining the proportion of patients who has showed 50% decline in prostate specific antigen [PSA] levels within 20 weeks after treatment.
2	Broccoli Sprout Extracts Trial	COPD	II	NCT01335971	Investigating the role of SFN to increase Nrf2 activity and downstream antioxidant expression in alveolar macrophages, bronchial epithelial cells, PBMCs, expired breath condensate (EBC), nasal epithelial cells of COPD patients.
3	SFN-rich Broccoli Sprout Extract for Autism	Autism	II	NCT01474993	Measuring efficacy and cytotoxicity of orally administered SFN rich brocoli sprouts as well as its effect on social responsiveness (primary outcome) and other behavioral symptoms of autistic males
4	Chemoprevention of prostate Cancer, HDAC Inhibition and DNA Methylation	Prostate cancer	II	NCT01265953	Investigating the mechanisms by which SFN prevents the development of human colorectal and prostate cancer cells via altering HDAC activity.
5	Study to Evaluate the Effect of SFN in Broccoli Sprout Extract on Breast Tissue	Breast cancer	II	NCT00982319	Assessing the toxicity of SFN rich brocoli sprouts on breast tissue and its effect on the expression of some key molecules associated with breast cancer progression.
6	Pilot Study Evaluating SFN in Atypical Nevi-Precursor Lesions	Atypical Nevi; Melanoma	0	NCT01568996	Evaluating the role of SFN to prevent melanoma progression by altering some key events involved.Also study the expression of STAT3 molecule pattern in nevi,a primary lesion which ultimately develop into melanoma.
7	Effects of SFN on Normal Prostate Tissue	Prostate cancer	I/II	NCT00946309	To study and comapare the growth inhibitory effect of SFN on prostate cancer cells as well as normal prostate tissue.
8	Effect of SFN in Broccoli Sprouts on Nrf2 Activation	Cystic Fibrosis	-	NCT01315665	To study the effect of SFN, isolated from macerated broccoli sprouts on healthy as well as cystic fibrosis volunteer via inducing Nrf2 mediated antioxidant pathway.
9	Topical Application of SFN-containing Broccoli Sprout Extracts on Radiation Dermatitis	Breast Cancer; Dermatitis	II	NCT00894712	Evaluate the preventive effect of SFN on dermatitis associated with external-beam Radiation Therapy for Breast Cancer
10	Cross-Over Broccoli Sprouts Trial	Healthy	I	NCT01008826	Modulation of preventive biomarkers expression associated with the exposure of the air-borne pollutant phenanthrene and also the level of metabolites formed due to exposure of hepatocarcinogen aflatoxin B1.
11	Effect of Broccoli Sprout on Blood Levels of SFN to Reduce Responsiveness of Immune System	Healthy	-	NCT01357070	Evaluate the anti-inflammatory effect of SFN on white blood cells undergoing inflammatory stress also its protective effect on artherosclerosis by dampening the activation of leukocytes.
12	Effects of SFN on Immune Response to Live Attenuated Influenza Virus in Smokers and Nonsmokers	Healthy	-	NCT01269723	Studying the ability of SFN to modulate inflammed innate immunity in response to live attenuated Influenza Virus infection in Smokers and Nonsmokers

Review of literature

13	Broccoli Sprout Intervention in Qidong, P.R. China	Environmental Carcinogenesis	II	NCT01437501	pharmacodynamic evaluation of the effect of SFN/glucoraphanin rich juices in Qidong, P.R. China population by measuring the of urinary levels of variousair-borne toxins those are known to be high in this population.
14	Effects of 2 Different Broccoli Sprout Containing Supplements on Nasal Cells in Healthy Volunteers	Healthy	-	NCT01129466	To study and compare the alteration of nasal cell HO-1 expression induced by SFN (SFN)-containing nutritional supplements.
15	Broccoli Sprout Extract in Treating Women Who Have Had a Mammogram and Breast Biopsy	Breast Cancer; Precancerous Condition	II	NCT00843167	Evalute the role of SFN rich broccoli sprout extract to prevent the growth of tumor cells or any abnormal cells, ductal carcinoma in situ and/or atypical ductal hyperplasia formed due to breast cancer progression.
16	Dietary Interventions in Asthma Treatment: Sprouts Study	Asthma; Allergy	I/II	NCT01183923	Modulation of preventive biomarkers expression associated with the exposure of the air-borne pollutant phenanthrene and also the level of metabolites formed due to exposure of hepatocarcinogen aflatoxin B1.
17	Diet and Vascular Health Study	Cardiovascular disease	-	NCT01114399	To study the role of SFN in cadiovascular disorders by measuring various biomarkers e.g. blood lipid profiles(cholesterol); Pulse wave velocity (PWV), Augmentation index (AIx) and Ambulatory Blood Pressure Measurements (ABPM).
18	SFN as an Antagonist to Human PXR-mediated Drug-drug Interactions	Healthy	I	NCT00621309	Examining the role of SFN in preventing various adverse drug-drug interaction through modulation of cytochrome P450 3A4 (CYP3A4) expression and activity

Table-1.1. A brief summary of information available from clinical trials database (http://clinicaltrials.gov) until 2014.

1.1.1.3.1. *Hormetic action of SFN*

The concept of 'hormesis' (to excite) is an age old phenomenon first described by Schultz (1888) and coined by Southam and Ehrlich later in 1943 [57]. Hormesis phenomenon is characterized by a biphasic dose response curve where an agent is capable of eliciting low dose stimulation and a high dose inhibition [58-60]. Below a certain threshold (intracellular concentration or time of exposure), hormetic agents induce pro-survival signals and on contrary, above the threshold activate pro-death signals. But at this particular borderline (area differ depending on the type of hormetic agent), both the signaling events occur in a mutually exclusive manner balancing the effects exerted by each other.
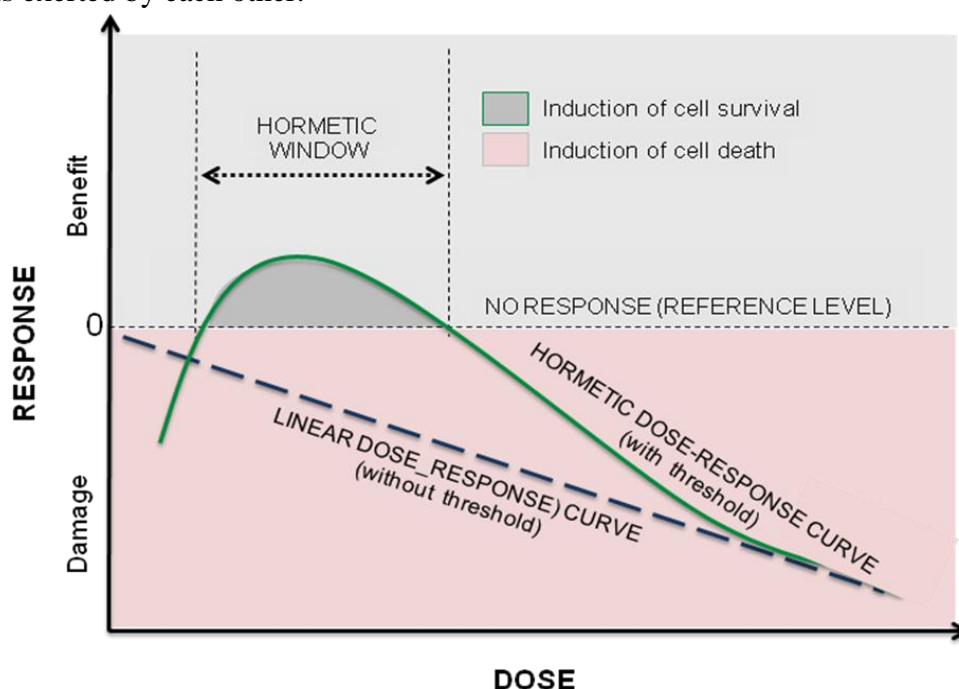
Fig. 1.5. The hormetic dose-response and linear no-threshold relationship curves. Above bioactive compound specific hormetic window toxic or other harmful effects have been observed while an apparent improvement is observed within hormetic window.

SFN also demonstrates biphasic dose responses following entering into cells [61]. Upon entering into the cells, at first it alkylates and depletes cellular thiols, damages the mitochondria and elevates ROS levels leading to mild cellular stress [62-65]. Altogether these activities provide an adaptive condition for the cells to battle against future chronic oxidative stress. At this stage, SFN acts as a pro-survival agent and either directly or indirectly alters the endogenous signaling molecules associated with survival autophagy induction or apoptosis inhibition.

Review of literature

However, with longer incubation or higher accumulation, SFN turns deleterious for exposed cells. Therefore, it uninhibitedly targets pro-apoptotic biomolecules and causes cellular demise *via* apoptosis. In a recent review, we enlighten the hormetic potential of SFN in switching cellular fate, survive or demise [12]. Based on the published results and possible interacting partners, a network of SFN induced hormetic signaling events along with a list of bio-molecular partners has been deduced in this review.

Being a hormetic agent SFN has the potential to regulate or determine cellular fate from survival to death or *vice versa*. SFN's role in promoting cell death as well as survival signals is well established. However, there is a lack in understanding its effects in altering cellular phenotypes and functions without inducing cell death. Although published results indicated such possibilities, a thorough attention and evaluation needs to establish such cell fate changing potential of SFN.
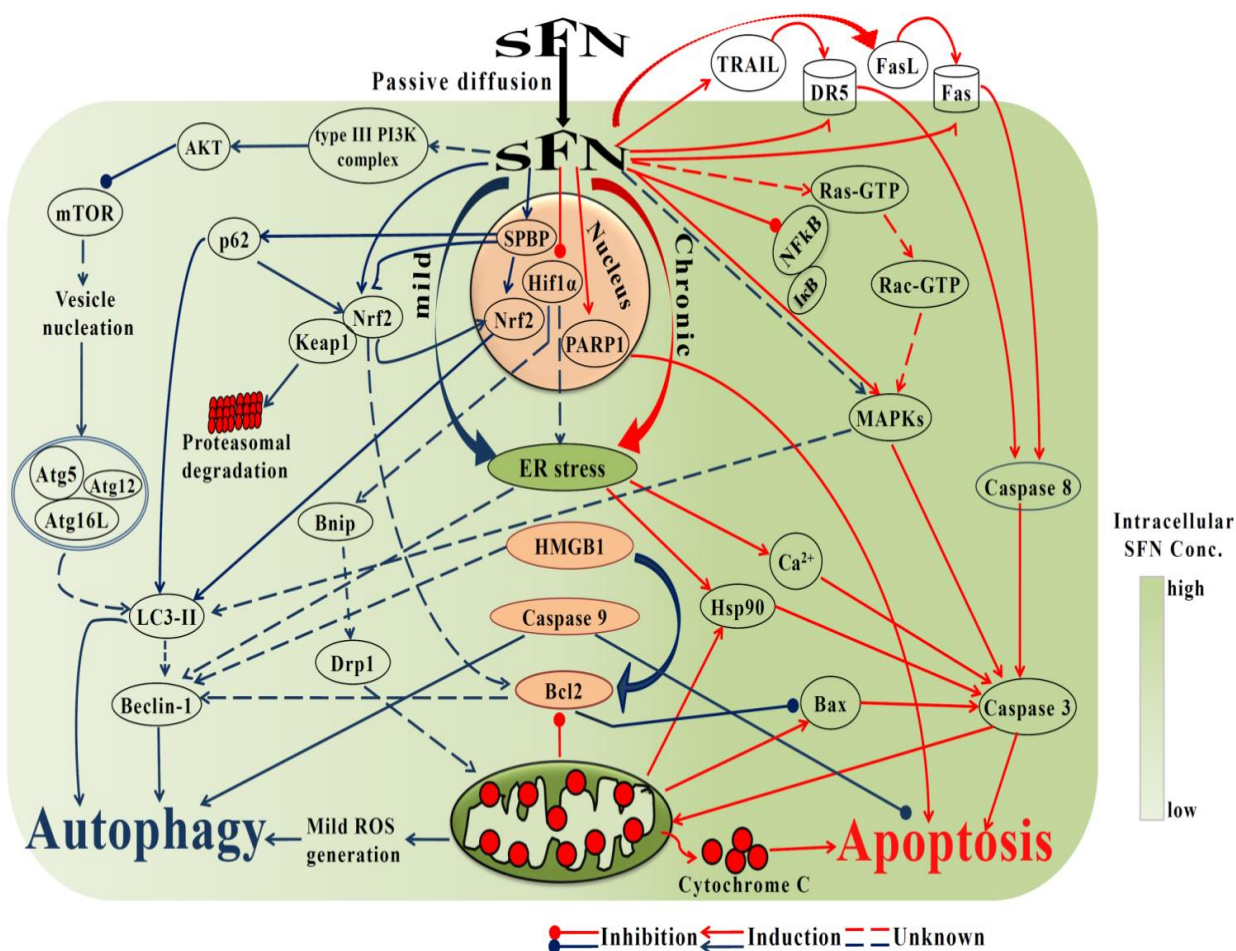
Fig.1.6. Signaling events maintaining 'hormesis' in SFN exposed cells

1.1.1.3.2.   *Non-cytotoxic chemo-preventive activity of SFN*

SFN has been studied extensively for its anticancer efficacy and the underlying mechanisms using cell culture and preclinical models. Simultaneously, SFN and its analogs have also been implicated to have a chemopreventive role for multiple diseases [66, 67]. Enhanced emphasis on its different arrays of chemo-preventive activities will help us to better understand the clinical utility of this nutraceutical [68].

To establish a chemopreventive agent, an extensive preclinical mechanistic evaluation with a focus on defining biomarkers of activity is required [69]. For SFN mediated chemoprevention, it has been observed that Nrf-2 serves as such pivotal nodal points [68, 70]. It regulates the activation and phosphorylation status of Nrf-2 proteins by modulating the activity of many intracellular kinases, which bring forward the nucleo-cytoplasmic trafficking of Nrf-2 or alter the Nrf-2 protein stability. After entering into a cell, immediately SFN draws the activation of intracellular phase-II chemopreventive systems through Nrf-2/Keap-1.

However, now it is clear that there are multiple cellular signaling events activated in response to SFN other than Nrf-2/Keap1 pathway, including suppression of cytochrome P450 enzymes, induction of apoptotic pathways, cell cycle arrest and inhibition of angiogenesis and progression of anti-inflammatory activity [71-77]. Altogether, these SFN induced cellular events exert synergistic effect to cancer cell demise and exert proper chemoprevention.

1.1.1.3.3.   *Cytotoxic anticancer activity of SFN*

Certainly, SFN is one of the most explored ITCs and drug candidates for cancer treatment [78-87]. Beyond a concentration threshold SFN noncompetitively exerts pro-death activities. However, below that threshold (specifically within a micro-environment dependent concentration window) it promotes pro-survival autophagy and far below that window remains latent [61]. The mechanisms it mainly attributes in killing tumor or other altered conditions (infections, autoimmunity) especially cellular demise are cell cycle arrest, epigenetic modifications, eventually and apoptosis. Apart from

this, SFN is capable of inhibiting cancer cell migration and invasion by suppressing epithelial-mesenchymal transition (EMT) process and expression of α-Sma, Slug, Twist, MMP-2, MMP-9 and phosphorylation of Akt Ser473), p-S6, and MAPKs (p38, ERK, JNK1/2) [74, 88-90]. Such mechanisms are the undoubtedly the most elaborately studied anticancer bioactivities of SFN. Interestingly, it differentially protects normal and healthy cells from cytotoxicity by inducing cell death pathways only in altered or cancerous cells. Therefore, SFN can recognize altered microenvironments in or around tumor cells and selectively kill them [80, 91]. Though published reports suggested several, only four major targets (pathways) are discussed below.

1.1.1.3.3.1. Cell cycle arrest

Arresting the cell cycle progression is one of the major mechanisms by which SFN exerts anti-cancer activity [92]. Researchers have rigorously studied to identify the key target molecules (e.g.p53, Cyclin D1, p21,p27, phosphorylation of CDK1 and CDC25B at inhibitory sites) of SFN that might be involved in cell cycle arrest depending on the cellular status or extracellular environment [90, 92]. SFN have been shown to block G2/M phase arrest in tumor cells [92, 93]. However, many published reports also suggest prominent discrepancy in cell cycle phases arrested by SFN [94-99]. However, limited studies have been performed to identify the exact switching force (at protein or genetic level) of SFN mediated differential cell cycle arrest. SFN role in augmenting the cell cycle arrest above hormetic window have been discussed in the recent review [12].

1.1.1.3.3.2. Epigenetic modifications

Epigenetic modification is critically involved in embryonic development and other ageing processes and any kind of alteration in the epigenetic level causes any age-related diseases like cancer, cardio-vascular and neurodegenerative disorders. Epigenetic mechanisms in cancer cells comprise (i) post-translation deacetylation and methylation of histone protein (ii) DNA global hypomethylation; (iii) hypermethylation at the promoter sites of tumour suppressor or cell cycle, cell differentiation and apoptosis regulatory; and (iv) post-transcriptional regulation of gene

expression by noncoding microRNAs. These epigenetic aberrations can be readily inhibited by both synthetic agents and natural components of diet. According to the published reports, SFN is a standout inhibitor of HDAC activity in cancer cells [100] and also causes effective up-regulation of transcriptional activity of certain genes involved in epigenetic modification and also in restoration of active chromatin structure [51]. SFN potentially alters the epigenetic patterns by modulating the levels of S-adenosylmethionine and S-adenosyl-homocysteine or activity of enzymes that catalyses DNA methylation and histone modifications by histone deacetylase [51, 101-104].Thus SFN mediated therapeutic interventions seems to be a potentially effective epigenetic modification causing cancer preventive strategy.

1.1.1.3.3.3. Apoptosis induction

Although sporadically *necrosis* has been reported [92] to be induced by SFN but promotion of apoptosis mediated cell death in different arrays of cancers e.g prostate cancer, osteosarcoma, leukemia, lung cancer, glioblastoma, breast cancer, hepatocellular carcinoma, colon cancer, melanoma cancer [92-95, 105-112] had been reported to be predominant. SFN targets both intrinsic (mitochondria mediated) and extrinsic (Fas/FasL) pathways in cancer cells to induce apoptosis [95]. Increased ROS, Ca^{2+} production, caspase-3, -8, and -9 activation, induction of mitochondrial dysfunction (decreased the levels of $\Delta\Psi m$),ER stress and inhibition of aldehyde dehydrogenase 1 (ALDH1) activity, increased annexin V-binding capacity, Bad, Bax, Bid, cytochrome C expression, Fas, Fas-L, caspase-8, Endo G, AIF, decreased Notch-1, c-Rel, Bcl-2, Bcl-XL, XIAP and survivin expressions are the major outcomes of SFN mediated pro-apoptotic effects [95, 106, 110, 113]. Published report also suggested the pro-apoptotic efficiency of SFN in the malignant cells with impaired apoptotic machinery [114]. All these findings simultaneously indicated that SFN is a promising and safe strategy for treating tumor development, promotion and pathogenesis.

However, in non-malignant cells SFN selectively inhibits apoptosis and promotes cell survival. In a recent report, SFN prevented cardiomyocytes from hypoxia/reoxygenation injury *in vitro via*

activating SIRT1 pathway and subsequently inhibiting the ER stress-dependent apoptosis by inhibiting associated pro-apoptotic molecules (GRP78, CHOP and caspase-12) [106].

Hormetic, SFN treatment associated apoptosis induction mechanisms, molecular targets had been vividly discussed in a recent review [12] under the section entitled *"SFN Mediates Selective Induction of Growth Arrest and Apoptosis above the Hormetic Threshold"*.

1.1.1.3.3.4. Synergistic anti-cancer activity of SFN

From investigations so far it has been observed that SFN has pronounced tissue type independent synergistic effects on cellular demise when combined with other conventional drugs e.g. cisplatin,curcumin, bortezomib, dibenzoylmethane, doxorubicin, selenium, indole-3-carbinol (I3C), 3,3'-diindolylmethane (DIM), arsenic trioxide (ATO), tamoxifen, ibuprofen, TRAIL, gemcitabine, azathioprine, eugenol nobiletin [106, 113-128]. The major advantages of these combinatorial therapeutic protocols were to lower the dose to be administered and simultaneously downregulate the associated toxicity.

In the recent review [12] under the section entitled, *"Application of Cytotoxic or Protective Role of SFN in Developing Combinatorial Therapeutic Approaches"* several published reports have been cited to establish its synergistic role in combinatorial anticancer therapy.

Although several studies, clinical trials (**Table.1.1**) are being organized with ITCs but to establish them (especially SFN) as potential standout chemotherapeutic agents there are multiple anticancer mechanisms, targets that need to be addressed.

1.1.1.3.4. Promotion of cell survival autophagy by SFN

Autophagy is an evolutionarily conserved process that mediates transportation of misfolded, exhausted, aggregated proteins or damaged organelles to lysosomes for degradation [129]. Activation of autophagic pathway in tumor cells may promote prolonged survival after sacrificing some of the neighbours cells (tumor/healthy). However, published reports also suggested that both gain and loss of autophagy might be involved in tumor progression [130]. Induction of autophagy

represents one of the defense mechanisms against anti-cancer drug-induced apoptosis in various types of cancer cells. Few reports also suggested that inhibition of autophagy is not exclusive to apoptosis induction as other types of cell deaths are likely to be happened [131]. But only a few reports are available in the context of above mentioned cellular response by SFN.

Due to its hormetic characteristics, SFN is efficient in promoting both apoptosis and survival autophagy and can switch the signals in either direction following any permissible alteration in the micro-environment by external stimuli [12]. Herman *et al.* first reported SFN as a ROS dependent inducer of cell survival autophagy (formation of acidic vesicular organelles and active form of LC3-II A, increased expression of SPBP, Nrf-2 p62/SQSTM1, formation of aggresome-like structure/ALS, covalent modification of cytoplasmic α- and β-tubulin without affecting proteasome activity) in chemo-resistant prostate cancer cells [132, 133]. SFN induced autophagy preferably depends upon activity of mitochondrial respiratory chain enzymes. Naumann *et al.* also showed how intracellular ROS conc. determines and co-induces of autophagy and apoptosis in a mutually exclusive fashion in pancreatic cancer cells [134]. SFN activates ubiquitin-proteasome system (UPS) in β-cells to ameliorate ER stress along with upregulation of Bcl-2 proteins and protects them FFA-induced cell death [135].

SFN has been shown to alleviate caspase-9 dependent as well as p53-independent autophagy in multiple p53 mutant pancreatic carcinoma cells (AsPc-1, MIAPaCa-2, Panc-1, Capan) and a wide range of phenotypically different breast cancer cell lines [136]. Utilization of synthetic inhibitors or specific siRNA against caspase-9 had shown to exert negative effect on SFN induced cytoprotective autophagic flux and concomitantly enhanced apoptosis. Meanwhile reports suggest, treatment of SFN in combination with autophagy inhibitors e.g, 3-methyladenine (3-MA), could enhance significantly apoptosis in human colon cancer cell lines [137, 138]. These studies clearly confirmed the existence of hormetic window and also demonstrated that treatment with relatively high concentrations of SFN for longer period has better pro-apoptotic effects while treatment with lower concentrations for shorter period exhibit cytoprotective effect by inducing cell survival autophagy

After critically analyzing all the above mentioned scenarios, in our recent review we proposed the concentration and time dependent selectivity (malignant vs. non-malignant) of SFN's bioactivities [12]. How it only promotes autophagy mediated survival rather inducing cell death at low concentration and helps the exposed cells to be adapted for future stress. However, altered status of intracellular, molecular machinery (within malignant cells) renders SFN to accumulate beyond a cell and cancer type specific sub-toxic limits, lead it to cause apoptosis mediated cell death. For better comprehension, current scenario of *in vitro* SFN mediated induction of both cell survival autophagy and apoptosis has been illustrated in a schematic diagram and published in a review [12].
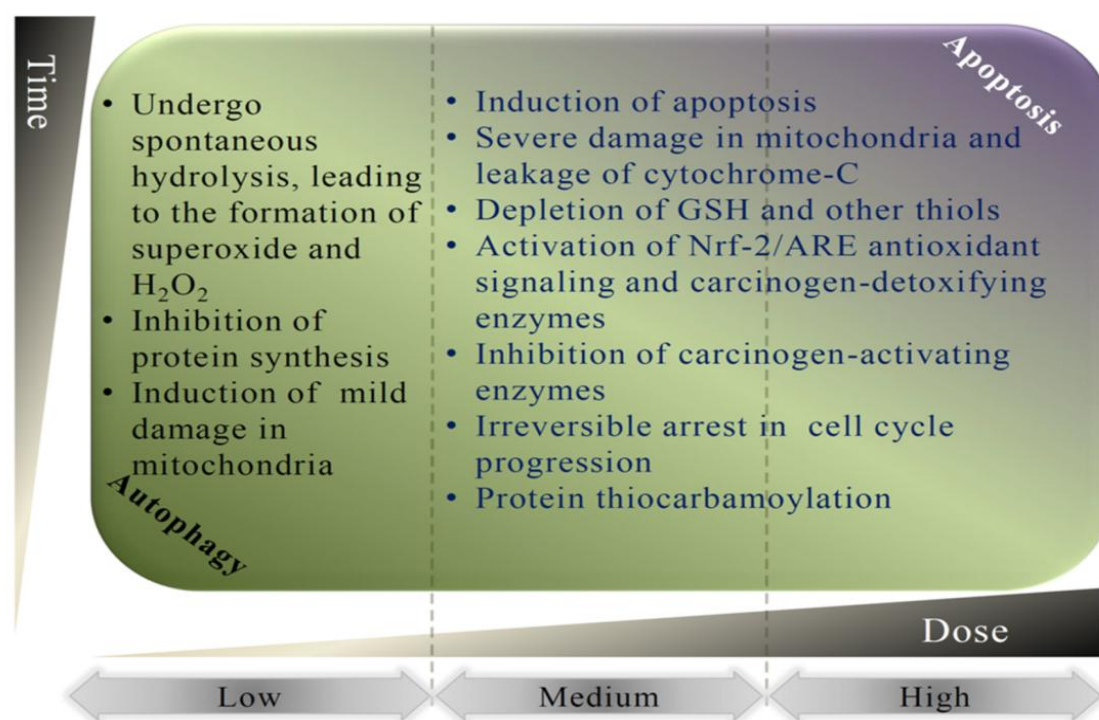
Fig.1.7. Intracellular concentration and exposure time dependent paradoxical effects by hormetic SFN (**adapted from Mini Rev Med Chem. 2015, 16**)

1.1.1.3.5.   Anti-inflammatory and immune-modulatory activity of SFN

Existing evidences suggest that SFN acts as an anti-inflammatory antioxidant and often play an effective role in various infectious disease conditions or inflammation associated immune related disorders [139]. Upon realization of its hormetic potential (no cell killing and promotion of cell survival at low conc.), SFN has attracted several researchers to develop various anti-inflammatory,

cell survival promoting therapeutic approaches. Here, a few publications had cited to demonstrate it immune suppressive potential, especially at any chronic inflammatory condition.

In a study it was demonstrated that SFN suppressed chronic obstructive pulmonary disease (COPD) by blocking *de novo* synthesis of IL-8 and MCP-1 and promoting Nrf-2 nuclear translocation expression of NADPH quinone oxidoreductase-1, HO-1 and glutamate cysteine ligase [140-142]. However, SFN triggered phagocytic ability of non-typeable *Haemophilus influenza* and *Pseudomonas aeruginosa* infected alveolar macrophages in COPD [140]. SFN treatment had been shown to be effective in both experimental inflammatory bowel disease *in vivo* [143], epidermolysis bullosa simplex [144].

SFN had been shown to suppress respiratory syncytial virus replication mediated bronchopulmonary inflammation [145], epithelial injury, mucus cell metaplasia, influenza-A virus replication or its entry [146] and indirectly musculoaponeurotic fibrosarcoma viral infection [147]. Simultaneously, SFN is capable of promoting expression of various antiviral mediators e.g. RIG-I, IFN-β and MxA without any infection. Apart from these anti-viral activities, SFN can exert antibacterial activities, especially inhibits *Helicobactor pylori* infection. [148-156].

SFN has been reported to suppress various chronic inflammations by targeting TLR4 signalling events [25, 157]. Reports also indicated, sub-cytotoxic SFN can downregulate multiple inflammatory responses (increased NO, PGE-2, TNFα production, iNOS and COX-2, IL-1 expression) in LPS stimulated RAW264.7 cells, peritoneal macrophages and lung epithelial cells [158-165]. Oral administration of SFN also inhibited premature death caused by LP-BM5 retrovirus infection with concomitant restoration of T-cell and B-cell mitogenesis (partially), Th1/Th2 balance, hepatic vitamin-E level, reduction of hepatic peroxidation level and excessive free radical generation [166]. However, sub lethal dose of SFN retarded the T cell activation and expansion mediated by combination of anti-CD3 and anti-CD28 antibody with concomitant decrease in IL-2 production [167, 168]. Therefore, a significant inhibition of pro-inflammatory activated T cell

proliferation and associated IL-2 production upon SFN treatment may be employed as a cost effective dietary therapeutic agent during autoimmune or transplantation conditions

Such immunosuppressive activities of SFN has also been reported to prevent or control various autoimmune diseases [169], however, this area of research is still in its stage of infancy. Th1 and Th2 balance is one of the major determining factors for autoimmune disease associated pathogenesis. In general SFN negatively modulates the secretion of many pro-inflammatory cytokines IL-1β, IL-6, TNF-α, IFN-γ and also immunosuppressive cytokine IL-4 and growth factors like PDGF and VEGF, key players in multiple disease pathogenesis [164, 168, 170, 171]. Recently, it has been shown that in the atopic dermatitis (a chronic pruritic inflammatory skin disease) SFN triggers Th2 chemokines production, HO-1 expression, impairs NFκB expression [172]. SFN administration also resulted in reduction of type-1 diabetes associated pathogenesis [173, 174]. Recently, few studies also reported SFN mediated suppression of collagen type-II (CII) induced rheumatoid arthritis in mice model, hyperplasia, CII specific T cell, fibroblasts proliferation and downregulated production of associated IL-17, TNFα, IL-6 and IFN-γ from spleen and lymph node cells [159, 161, 170, 175].

Therefore, it is interesting and need of the hour to carry out various experimental approaches establishing SFN as an anti-inflammatory, anti-autoimmune agent.

1.1.1.4. *Undefined bioactivities of SFN*

With most features of an ideal therapeutic molecule such as easy availability, high bio-absorptivity, low cost purification with good yield and therapeutic efficiency, SFN stand out as attractive molecule to serve as potential lead compounds in various pathological conditions, more prominently in cancers. Despite of handful of reports available on SFN treatment mediated regulation of biological processes in favor of anti-inflammatory responses, few interesting aspects of SFN activities in the context of autoimmune diseases is still obscure.

Monocytes/macrophages polarization and plasticity plays important disease pathogenesis promoting and maintaining roles in inflammatory autoimmune diseases e.g. chronic inflammatory arthritis. SFN have been observed to induce cell death in autoreactive T cells and Fibroblasts. But no reports have been published so far suggesting monocyte differentiation and macrophage plasticity targeting beneficial role of SFN in autoimmunity. **Fig. 1.7** displays currently known and unknown but possible anti-autoimmune-modilatory activities of SFN.
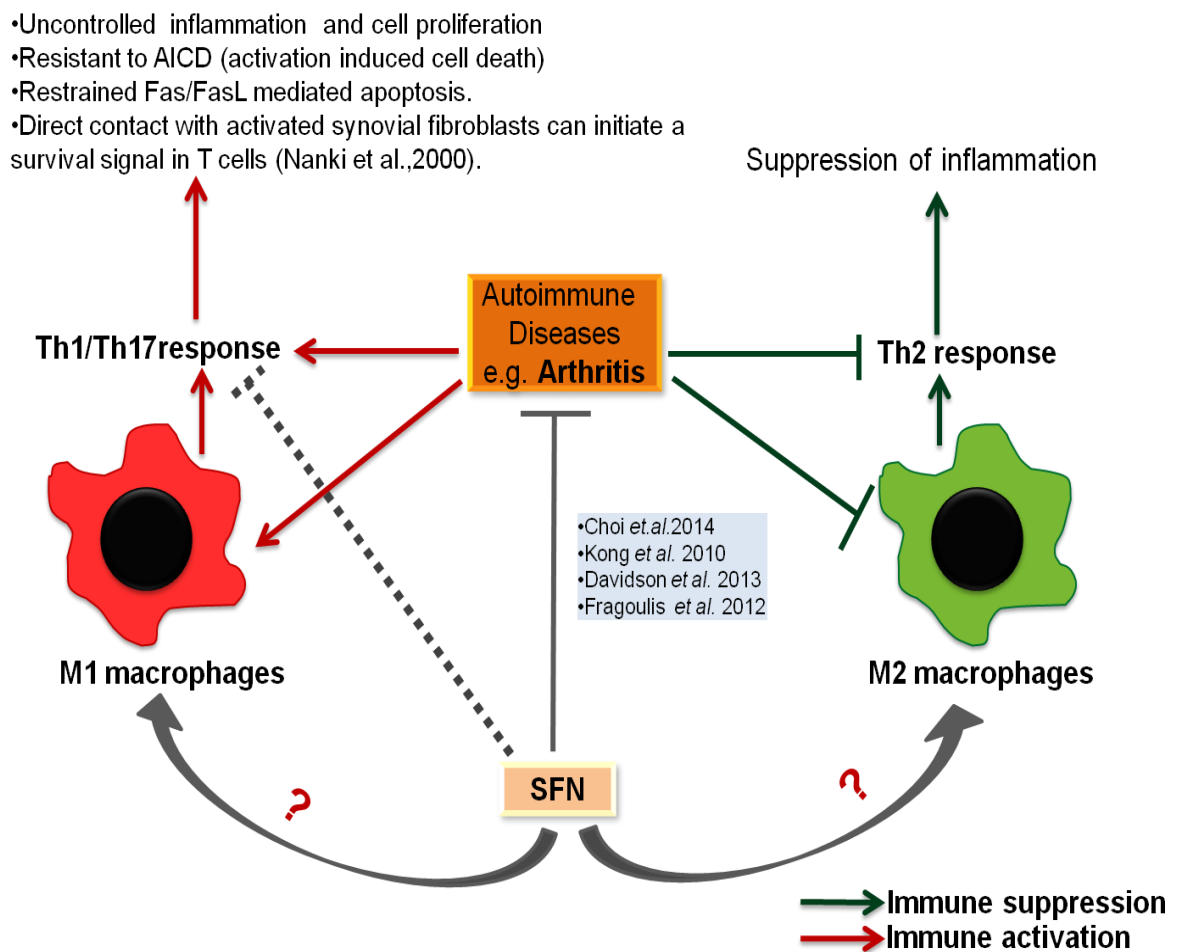
Fig 1.8. Schematic diagram illustrating undefined roles of SFN in autoimmune disease (e.g. arthritis) pathogenesis

1.2.1. *Benzo[α]phenoxazine (BPZ)*

Epidemiological studies provide evidences that chemically synthesized or modified semi-synthetic compounds are equally capable of killing cancerous or microbes infected cells. However, when a bioactive chemical entity appears to be intrinsically fluorescent and selective chemo-toxic towards altered self or infected cells, it attributes added advantages.

BPZs are similar intrinsically fluorescent compounds with varying degrees of bioactivities. They have generally been employed as fluorescent dye or probe when found almost non cytotoxic to the cells and used as anticancer agents when found to be selectively cytotoxic to tumor cells at physiologically attributable low concentrations.

1.2.1.1. *Molecular structures of BPZs*

Benzophenoxazines molecules formation took place when phenoxazine skeleton have been extended by adding fused benzene rings to the a–c or h–j faces. These molecules appeared as 'angular' or 'linear' depending on the orientation of the ring fusion [176].

BPZs are the benzophenoxazines in which a benzene ring have been fused at [a] or [α] faces. These molecules show out-of-plane vibrational deformations by infra red spectroscopy which is characteristic for the condensed benzene nucleus localized in the position [α] at the phenoxazone skeleton [177]. Substituents that freely donate and/or accept electron density on benzophenoxazine cores can, in some orientations, impart the intrinsic fluorescence. The first synthesized, notably fluorescent BPZ was Meldola's Blue, but Nile Red (9-diethyl amino-5-H benzo[α] phenoxazine-5-one) and Nile Blue are frequently used in contemporary science [178, 179].

These compounds showcase some desirable attributes as fluorescent probes and dyes e.g. reasonably high fluorescence quantum yields in apolar solvents and fluoresce at reasonably long wavelengths [176, 180, 181].

However, their structural integrity have made them almost insoluble in aqueous media where their quantum yields get dramatically reduced and caused a major road block in their usages

especially a drug candidates. **Fig.1.8** displays the general molecular structures of phenoxazines, BPZs and a most famous BPZ derivative, Nile red.
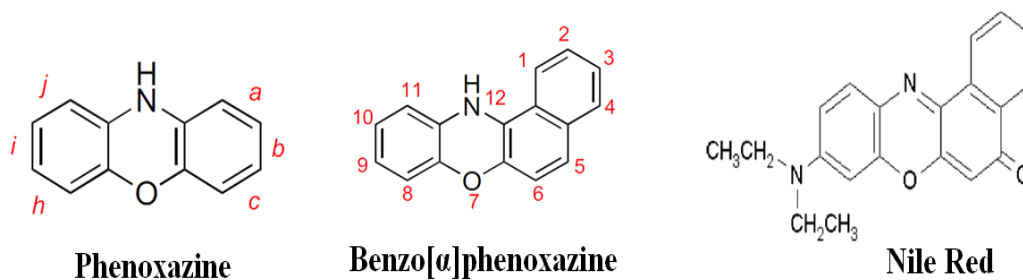
Fig.1.9. Molecular structures of BPZs e.g. Nile red

1.2.1.2. *Source and synthesis*
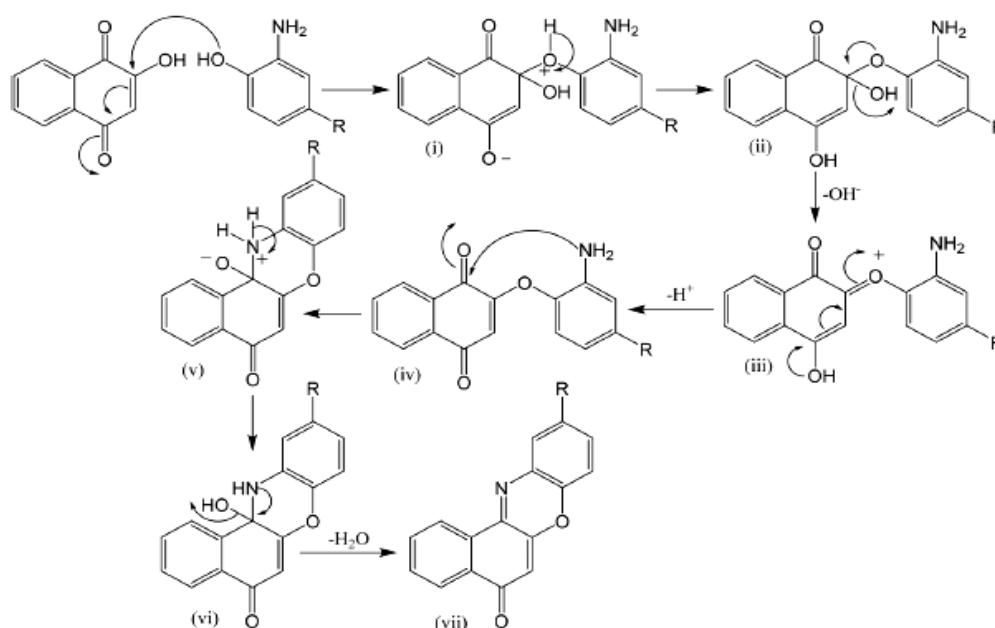
Fig.1.10. Reaction mechanism involved in the chemical synthesis of BPZ derivatives (**adapted from RSC Adv., 2015, 5, 57917**)

So far, no reports have been published suggesting any reliable natural sources of BPZs. Therefore, BPZ derivatives have always been synthesized using various chemical synthesis methods. In this dissertation, three derivatives of **benzo[α]phenoxazine-5-one (R=Cl, CH₃, H)** have been chosen to study their anticancer effects. These derivatives of our interest have been synthesized by Michael addition of the phenolic hydroxyl groups of 4R-2-aminophenol **(R = Cl; 1B, CH₃; 2B and H; 3B)** to 2-hydroxy-1,4-naphthoquinone [182]. **1B, 2B** and **3B** are the minor products of the reaction between 2-hydroxy-1,4-naphthoquinone and aminophenol derivatives. The overall reaction mechanism has presented in **Fig.1.9**.

The 1,4-Michael addition–elimination of the hydroxyl group of the aminophenol to the C(2) carbon of 2-hydroxy-1,4- naphthoquinone results in species (iv), and further 1,2-addition of the amino group of aminophenol to the carbonyl carbon C(1) generates an aminol as unstable intermediate (vi). Further dehydration of (vi) results in the different derivatives, **1B** to **3B**.

1.2.1.3. *Notable biological properties of BPZs*

BPZs have extensively been characterized as inert to bioactive intrinsically fluorescent chemical entities. Bioactive BPZs have shown arrays of biological activities those have been discussed in following sections.

1.2.1.3.1. BPZs as fluorescent dyes or probes

Compounds belong to this class are the extremely efficient oxidation reduction indicators and acid-base indicators for aqueous and anhydrous media. Their ability of changing their redox status depending on the intracellular pH have led them to become *in vitro* real-time probes for detecting minute changes in intracellular pH [183, 184]. Such polarity sensitivity feature had also been utilized to improve biocompatibility of nano-pores and drew a potential impact in nano-medicine [185].

These types of compounds have also widely used as dyes for labelling different biomolecules (e.g. intracellular lipid droplets, proteins) and staining and quantifying proteins in SDS-poly acryl amide gels and lipids in thin layer chromatograms [178, 186-192]. Strong binding affinity of them allowed the rapid monitoring of the total protein patterns of SDS gel and western blotting [191, 193]. Hydrophobicity of protein-SDS complexes or mutant *vs* wild type proteins can also be determined by the BPZs [194]. Studies have been done with nile red to monitor the production of primary and secondary metabolites by living organisms in suspension culture [195]. Nile red had also reported as a fluorescent core shell nanoparticle chemosensor for detecting Cu^{2+} in aqueous solution or lipid (negatively charged) cation (Ca^{2+} or $Cu^{+2/3}$) interaction in different types of mixtures [196-198]. Published reports also suggested that BPZs can be used to determine the polarity

of cellular lipids (e.g. polar membrane lipid; phospholipids *vs* neutral lipid, esterified cholesterol and triglycerides) [186, 189].

A wide range of endogenous targets, pharmacological studies and applications are reported for BPZ derivatives, but, only limited numbers are thoroughly explored for anticancer activity in this class.
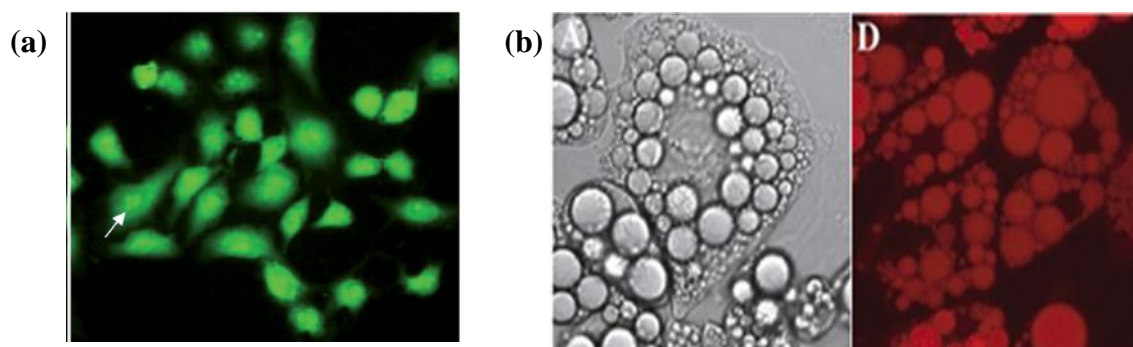
Fig.1.11. Examples of cellular internalization or intracellular macromolecule binding role of BPZ derivatives. **(a)** Fluorescence microscopy image of HeLa cells following intracellular accumulation of a derivative of BPZ (**adapted from RSC Adv, 2015, 5, 57917–57929**). (b) Application of Nile red as intracellular lipid binding fluorescent dye (**adapted from Mol. Ther, 2004, 9, 209–21**).

1.2.1.3.2. Biomacromolecular targets of BPZs

BPZ possess strong affinity towards all possible biomolecules present inside a cell, e.g DNA, lipids and protein. Recently a group has showed that BPZ can act as topoisomerase II inhibitor by direct binding [199].

BPZs are structurally similar to DNA intercalating groups phenothiazines and phenoxazines. Therefore, BPZs can directly intercalate to the DNA and inhibit DNA-dependent RNA polymerase [200]. A few novel BPZs were also reported to bind directly to G-quadruplex (G rich protein sequence at the promoter of various genes) [201].

1.2.1.3.3. Anticancer, Anti-inflammatory and immune modulatory activity of BPZs

Above mentioned properties together may attribute to alterations in the intracellular metabolisms; microenvironments arose by the acquisition of one or more than one mutations during cancer development and progression or microbial/protozoan infection.

Streptomyces antibioticus produced natural antibiotic, Actinomycin D (Dactinomycin) is a phenoxazine derivative and one of the most well-known chemotherapeutic anti neoplastic drugs. The molecule has been characterized by phenoxazine ring bound to two cyclic pentapeptides and this particular molecular makeup potentiated their intercalation through DNA, thereby inhibiting DNA-dependent RNA polymerase. The presence of the phenoxazine moiety in the structure of any chemical entity hints that other phenoxazine derivatives could also possess antitumour activity. The early studies, however, did not reveal many promising drug candidates among the phenoxazines, presumably because of their poor water solubility. Studies also revealed a few soluble moieties, e.g. 2-amino-4,4•-dihydro-4•,7-dimethyl-3H-phenoxazine-3-one with promising anti-proliferative, immunosupressive, antibacterial and antiviral activities [202]. Published reports also demonstrated a cancer chemopreventive and effective multidrug resistance (MDR) inhibitory role of phenoxazine and phenothiazines group of molecules in different carcinogenesis models [200].

BPZs are structurally similar to phenothiazines and phenoxazines and also have been observed to possess some structural features important for their MDR reversal activity. A few experimental evidences also suggested that the BPZs are better MDR modulators than simple phenoxazine scaffold and capable of inhibiting P-gp significantly [200].

BPZs have also reported to induce cell survival inhibitory effects in human gastric carcinoma by downregulating endogenous c-KIT expression [201]. Some BPZ derives have also been reported to be pro-apoptotic to tumor cells [199].

Apart from these, recent studies have also documented their profound anti-bactericidal [203, 204], anti-inflammatory [205] and anti-protozoal [206] activities.

1.2.1.4. *Undefined bioactivities of BPZs*

BPZs are intrinsically fluorescent molecules and a potential family to be established as anticancer agents. The present chapter under **section 1.2** had already provided an overview on the present state of knowledge on the impact of BPZ on biomolecules and indicated their potential applications to prevent various disease pathogenesis.
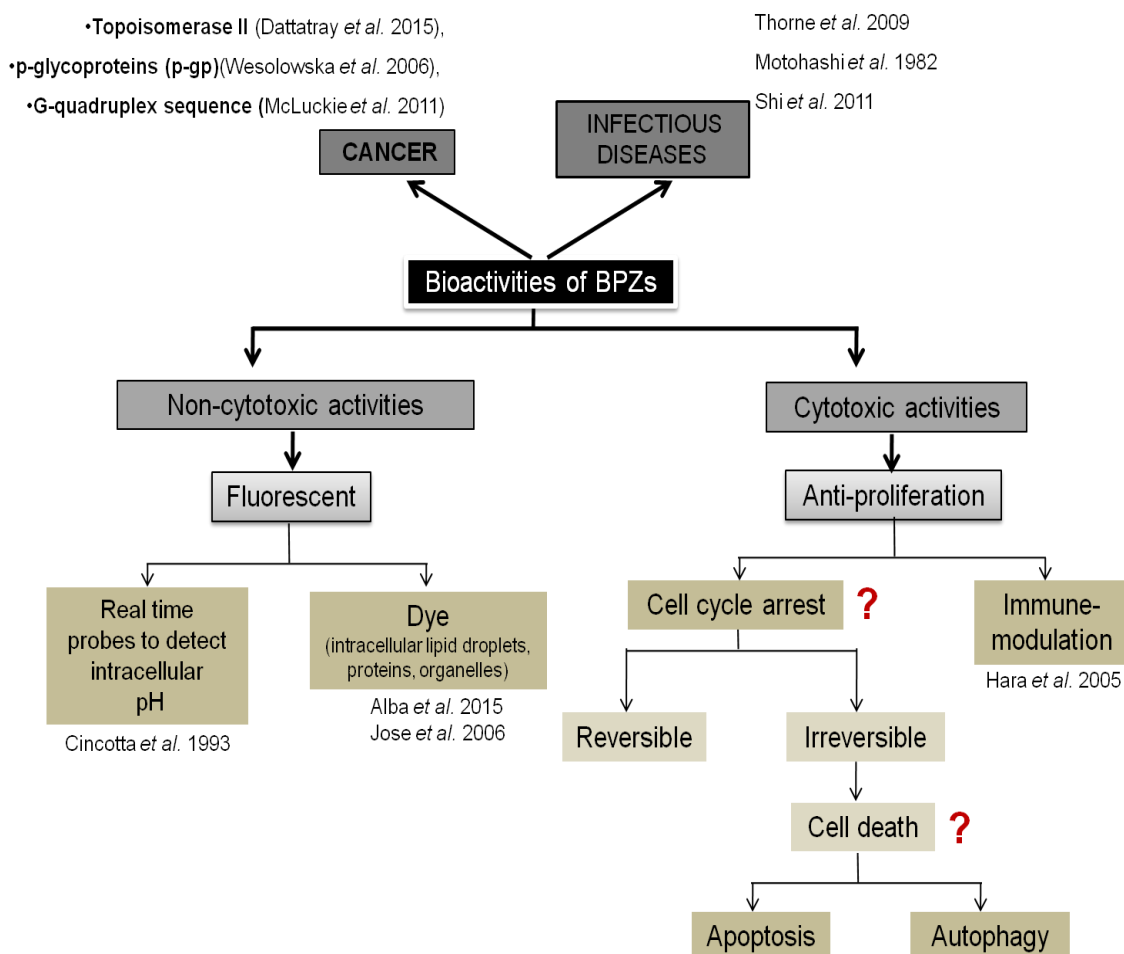
Fig.1.12. Bioactivities of BPZs: implications in human benefits. Question marks defining the undefined bioactivities of BPZs

A wide range of endogenous targets, applications are reported for BPZ derivatives, but, only limited numbers are thoroughly explored for cellular model based selective pharmacological roles especially anticancer activities. Only a few published reports suggested that BPZ derivatives can reduce chemically induced tumor formation.

To date, there is no cell based or animal studies available suggesting a potential ability of BPZ derivatives to induce any non-apoptotic cell death pathways (e.g senescence, autophagy) at any malignant conditions. Moreover, no studies have been done so far indicating BPZ class of molecules might have great implications for the treatment in those types of cancer cells those are also intrinsically resistant to apoptosis-mediated cell death. **Fig.1.11** displays few possible but unknown bio-activities (indicated with question marks) of BPZs.

Review of literature

Therefore, extensive studies on BPZ class of molecules may have great implications in those cancer treatments in which cells are intrinsically resistant to apoptosis-mediated cell death as well as chemorefractory.

These representative ligands belong to BPZ family are newly synthesized and their potential bioactivities are unknown. Therefore, in this dissertation, investigations had been commenced to explore the chemical biology of the action of the three newly synthesized BPZs.

CHAPTER-2

Aims and Objectives

The principle **aim** of this thesis work was to understand and report the chemical biology of actions in terms of either immune-modulatory anti-autoimmune or anti-cancer bioactivities of

I.   Plant **derived sulforaphane (SFN)**

II.   Synthetic fluorescent **benzo[α]phenoxazines (BPZ)**

using different *in vitro* experimental disease models and approaches.
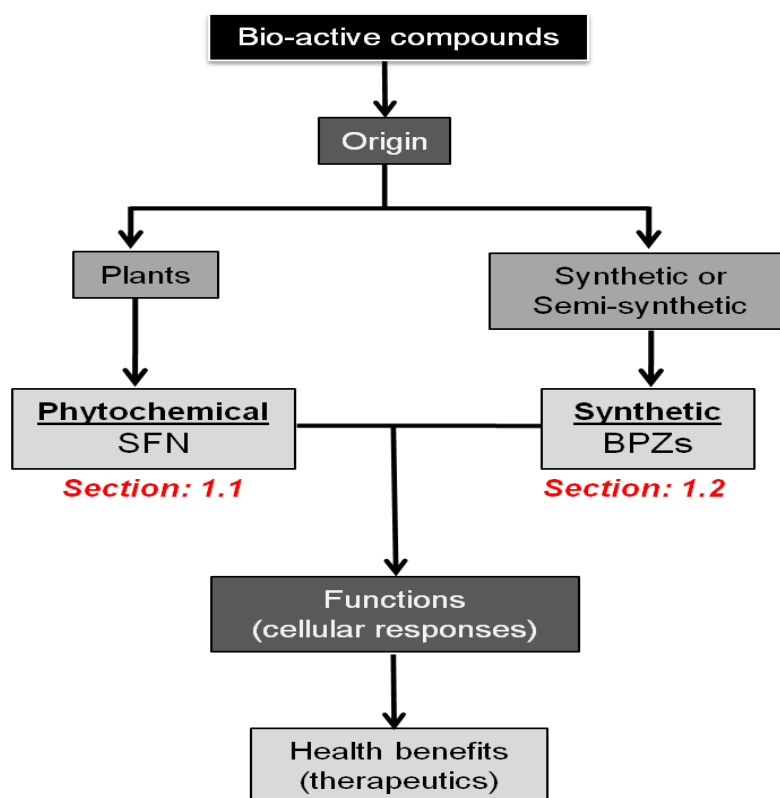
Fig.2.1. Bioactive compounds of different origins evaluated for the therapeutic interventions

Chapter-4, -5 and **-6** demonstrate the experiments and results to describe a specific chemical biology of the action of a bioactive phytochemical, SFN whose anti-autoimmune-modulatory role is less understood. The specific objectives for this study are as follows:

- Non cytotoxic immune-modulatory and specificity studies of bioactive ITC, SFN using *in vitro* monocyte/macrophage (Mn/MΦ) model mimicking autoimmune conditions

- SFN regulates phenotypic and functional switching of spontaneously differentiating human peripheral blood derived monocytes (Mns).

- *In vitro*, SFN and soluble collagens mediated regulation of endogenous FasL proteins in an monocyte/macrophage (Mn/MΦ) model: implications

Chapter-7, describes the attempts made to explore few selective undetermined cellular responses to three synthesized fluorescent derivatives of BPZs and their therapeutic implications in various cancers perspectives e.g. colon and pancreatic cancer respectively. The specific objective for this work is given as follows:

- Screening for bioactivity and characterizing the mode of cell death for few novel, synthetic benzo[α]phenoxazines (BPZs) in different cancer cell line models
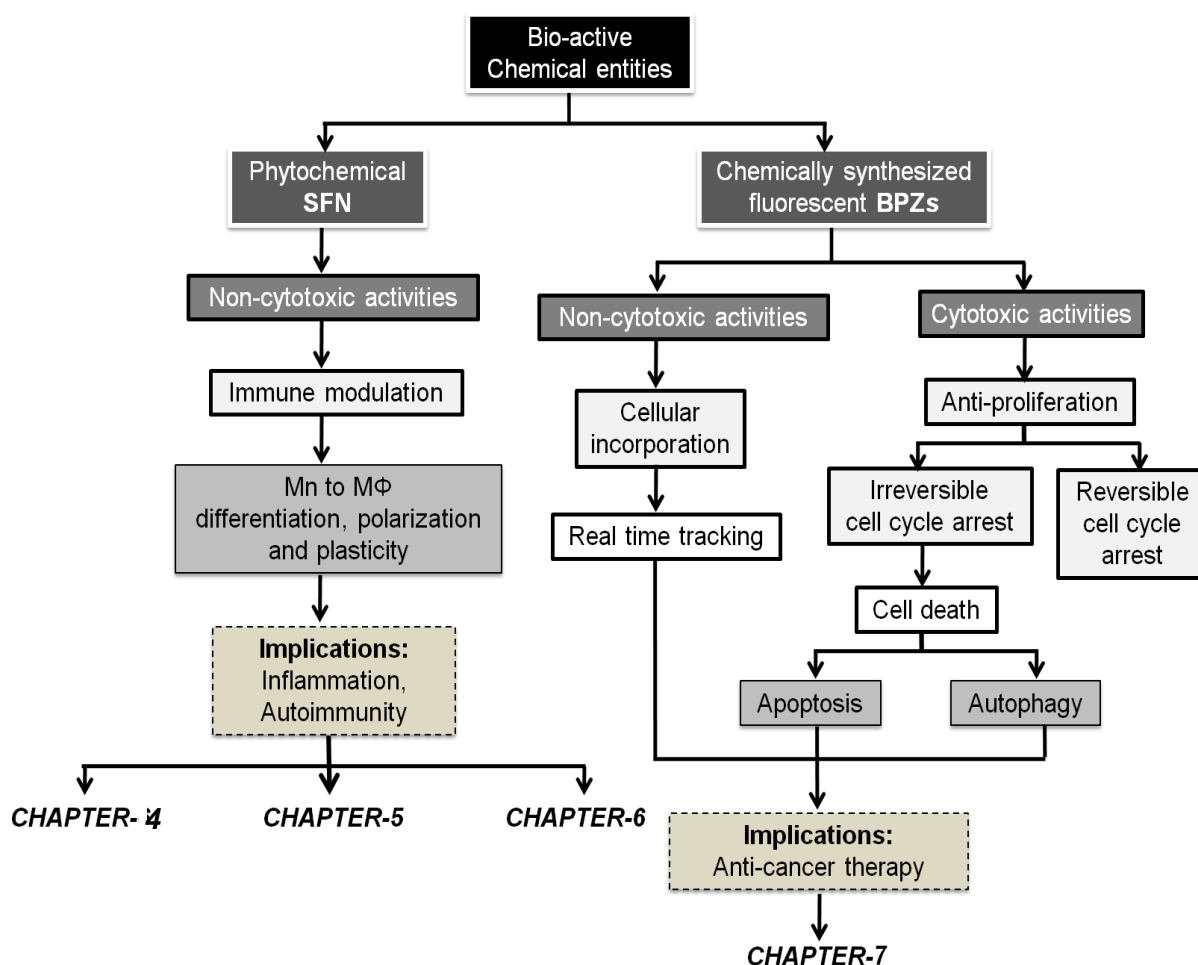
Fig.2.2. Schematic illustrations of aims and objectives of the current study

CHAPTER-3

Materials and Methods

3.1. PROPAGATION OF MAMMALIAN (HUMAN) CELL LINES

3.1.1. THP1 cell line

Human monocytic leukemic cell line THP1 was procured from ATCC, USA (Cat No. TIB-202). This cell line was selected for this study because it has no prominent chromosomal aberration and an established monocytes/macrophages model in which PMA enable to induce differentiation and differentiated cells remained responsive to any external immune-modulators [207-212].

Cells were maintained in culture media RPMI 1640 supplemented with 10% FBS and 1% Pen-Strep at 37 °C in 5% CO_2 in air. Cells were passaged before they reached maximum concentration to prevent unwanted differentiation or death in either 75 cm^2 or 25 cm^2 tissue culture flasks (T75/T25) (Corning, USA).

To set up an experiment or to give a passage, at first spent media containing cells were centrifuged at 950 rpm for 5mins. Cell pellets were dissolved into fresh media and counted (**see section 3.1.5**). Numbers of cells were seeded as per the requirement of each experiment. THP1 monocytes never maintained beyond 40 passages (counted from the first time it was received).

3.1.1.1. *Differentiation of THP-1*

1×10^4 or 0.5×10^6 THP1 cells (monocytes) in suspension were used to differentiate into matured monocytes/macrophages (adherent cells) in 96 well plates and 6 well plates/35mm dishes respectively. Cells were incubated with 20 ng/ml of differentiating agent, phorbol 12-myristate 13-acetate (PMA) for specified time points (24 h-48 h) at 37 °C in 5% CO_2.

Table.3.1. Chemicals used to regulate THP1 cell line differentiation

Sr. No.	Materials	Company	Cat.No.
1	RPMI 1640	HIMEDIA	AL162S
2	FBS [US origin]		RM9970
3	Pen-strep		A001
4	Trypsin-EDTA		TCL007
5	PBS		ML023
6	PMA	Sigma	P8139-1MG
7	Collagen		**C9301,** Chicken sternal cartilage, type-II
			C5483, Human, type-I
8	LPS from *E.coli* 0127:B8		L3129
9	Recombinant Human IL-4		I4269
10	Human IL-13 variant		SRP3076
11	Human IFNγ		SRP3058
12	Collagen	Millipore	**CC052,** Human, type II.
			CC054, Human, type III
			CC076, Human, type IV
13	Acetic acid[HPLC grade]	Rankem	A0042
14	L-SULFORAPHANE	MP Biomedicals	0219378210
15	Trypan Blue (0.4%)		1691049
16	SP6000125	Calbiochem	420119
17	PD 98059		513000
18	SB 203580		559389

3.1.2. COLO205 cell line

BRAF(V600E) harbouring human malignant colon cancer cell line COLO-205 [213, 214] (procured from NCCS, Pune, India) was maintained in complete growth media constituted with RPMI 1640 medium, 10% FBS and 1% Pen-Strep at 37°C with 5% atmospheric CO_2. Cells were

Material and Methods

grown in 75 cm2/25 cm2 tissue culture flasks (T75/T25) (Corning, USA) and passaged before they reached maximum concentration to prevent crowding induced cell death. Spent media containing cells were centrifuged at 950 rpm for 5mins. Supernatants were discarded and cell pellets were dissolved into fresh media, followed by cell numbers were counted in hemocytometer (**see section 3.1.5**). To set up experiments, cells were then distributed into either 24 well/6 well/96 well plates at required numbers.

3.1.3. MiaPaCa-2 cell line

Human malignant pancreatic cancer cell line MIA PaCa-2 possesses mutations both in several gatekeeper genes (e.g, p53-R248W, DPC4 /SMAD family member 4 and CDKN2A / p16 / p16INK4a) as well as oncogene (e.g, KRAS-G12D) [215, 216]. This adherent malignant cell line was also procured from NCCS, Pune, India and grew at 37 °C with 5% atmospheric CO_2, in complete growth media constituted with DMEM (HIMEDIA-AL007A) medium 10% FBS and 1% Pen-Strep. Cells were grown in 75 cm^2/25 cm^2 tissue culture flasks (T75/T25) (Corning, USA) and passaged before they reached maximum concentration to prevent differentiation or death. Spent media containing cells were centrifuged at 950 rpm for 5 mins. Cell pellets were dissolved into fresh media and counted (**see section 3.1.5**). To set up experiments, cells were then distributed into either 6 well/96 well plates at required numbers.

3.1.4. HEK293T cell line

Human non-malignant human embryonic kidney cell line, HEK293T possesses both wild type KRAS-wt and BRAF-wt but harbours simian virus 40 [SV40] large T antigens which inactivate p53-wt and imparts the immortality [217]. Similar protocol (**see section 3.1.3**) was followed to maintain, count, and use HEK293T cells for experiments.

3.1.5. Cell counting

Cell counts were performed using 0.4% trypan blue reagent. A 10 µl medium-suspended cell was mixed with 90 µl trypan blue solution. This mixture incubated 30 sec-1 min to give the dye a chance

to penetrate into the non-viable cells; leaving the viable cells unstained. Then 10 µl sample of this trypan blue-stained cell mixture was transferred to the edge of a cover-slip coated hemocytometer and immediately placed under the microscope (at 10X) for cell counting.

3.1.6. Cryopreservation and defrosting

Cells having low passage numbers were cryo-preserved into liquid nitrogen for long-term storage. Either suspension or freshly suspended adherent cells were centrifuged at 950 rpm for 5 minutes at room temperature. Supernatant was discarded**.** Approximately $1x10^6$ cells were resuspended in 1 ml freezing media (5% DMSO in FBS). Cell suspensions were then stored in 1.5 ml cryo vials (Tarsons) and kept aseptically in -20 °C Freezing Container, (Tarsons) for approximately 12 h. Then vials were transferred to a -80 °C freezer overnight and followed by to liquid nitrogen for long-term storage.

To defrost, the vials were taken out of the liquid nitrogen tank, thawed at 37 ºC water bath. Then those defrosted cells were directly added to 5 ml pre-warmed media in T25 culture flasks. Flasks were incubated for 3-4 hours before the medium was refreshed.

3.2. CELL LYSATE PREPARATION

Whole cell lysates were prepared to perform immune-blotting (conducted to identify various endogenous proteins and β-actin as loading control). To prepare the lysates from different experimental set ups; cells were collected with ice cold phosphate buffered saline (PBS) and centrifuged. As per the requirements, the supernatants were discarded immediately; followed by pellets were resuspended into a cocktail of 1X protease inhibitors (#158837, MP Biomedicals) and lysis buffer **(see section 3.2.1** and **3.2.2**). Following complete lysis of the cells, protein quantification was performed with the lysates (**see section 3.3**). Later, 1X sample reducing loading buffer (see section 3.4) was added into the lysates, denatured for 5 minutes at 100°C and stored at -20°C.

3.2.1. Laemmli lysis methods

Post treatment cells (COLO205, HEK293T) were harvested with ice cold PBS and centrifuged. Supernatant was discarded and 1X cocktail of protease inhibitor was added into each sample to dissolve the pellet. Followed by cells were lysed with Laemmli lysis buffer and total protein concentration was measured. Each sample was stored at -80 °C freezer for western blotting. Before immunoblotting 1X Laemmli loading buffer was mixed with each cell lysate.

Table.3.2. Laemmli lysis buffer composition

Concentration	Reagents
50mM	Tris buffer pH-8,
150mM	NaCl
1%	Triton X-100

3.2.2. RIPA lysis methods

At first cells (THP1, MiaPaCa-2, and HEK293T) were harvested with ice cold PBS in 1.5ml eppendorf tubes and later drained using centrifuge. Ice cold RIPA lysis buffer along with 1X protease inhibitor cocktail (1:1) were added into each cell pellet (500 µl per $5x10^6$ cells/ml). Cell lysates were maintained in constant agitation (1000 rpm) for next 30 min at 4 °C. Followed by those lysates were centrifuged at 12000 rpm at 4 °C for 20 min. Supernatants were collected in fresh tubes and kept at -80°C freezer for western blotting.

Table.3.3. RIPA lysis buffer composition

Concentration	Reagents	Cat. No.	Company
150 mM	NaCl	S3014	Sigma
1.0%	Triton X-100	194854	MP Biomedicals
0.5%	sodium deoxycholate	210290680	MP Biomedicals
0.1%	SDS	210291880	MP Biomedicals
50 mM	Tris, pH 8.0		

3.3. WHOLE CELL PROTEIN QUANTIFICATION

To ensure equal loading in each well of the gels used for western blot, the amount of protein in cell lysates was quantified using either Bradford protein Assay (Bio-Rad Laboratories, USA) or nanodrop-2000 (Thermo scientific, USA) at 280 nm. BSA (Sigma) (concentrations range 0-1000 µg/ml) had been used for standard curve preparation for Bradford assays. The standard samples

Material and Methods

were prepared as described in **Table.3.4.** Then 250 µl of 1x dye reagent was mixed (using multi channel pipette) with 5 µl of each standard solution or diluted (1:10) experimental samples (prepared in deionised water) in 96 well plates. Those solution mixes were incubated at room temperature for at least 5min. Absorbance of each well was taken at 595 nm using micro plate reader (Bio-Rad, USA). Averages of the blank values were subtracted from the average of each standard or sample value. Standard curve was plotted using 595 values (Y axis) of each standard dilution *vs* their concentration (X axis). Later Unknown sample concentrations were determined using formula obtained from the standard curve.

Table.3.4. Plan for BSA standard dilutions

Sr. No.	Concentration (mg/ml)	Volume from 2mg/ml BSA stock (µl)	De-ionized water (µl)	Total Volume (µl)
1	Blank	0	30	30
2	0.0625	0.9375	29.0625	30
3	0.125	1.875	28.125	30
4	0.25	3.75	26.25	30
5	0.5	7.5	22.5	30
6	1	15	15	30

3.4. PROTEIN SAMPLE PREPARATION FOR PROTEIN ELECTROPHORESIS

Before performing immunoblotting, each sample was taken out from the freezer and melted at 4 °C. Samples were boiled at 100 °C for 8 mins with equal amount of sample loading buffer.

Table.3.5. Protein loading buffer composition

Concentration	Reagents	Cat. No.	Company
4%	SDS		
10%	β-ME	M6250	sigma
20%	glycerol	219399690	
0.004%	bromo-phenol blue	215250605	MP Biomedicals
0.125M	Tris-Cl pH-6.8		

3.5. WESTERN BLOT TECHNIQUE

3.5.1. Buffers and reagents

Table.3.6. Resolving Gels composition (5ml)

Components	8% (ml)	10% (ml)	12% (ml)
H_2O	2.3	1.9	1.7
30% Acrylamide-bis acrylamide mix	1.3	1.7	2
1.5M Tris-Cl pH-8.8	1.3	1.3	1.3

10% SDS	0.05	0.05	0.05
10% APS	0.05	0.05	0.05
TEMED	0.003	0.003	0.003

Table.3.7. Stacking Gels composition (3ml)

Components	5% (ml)	Cat. No.	Company
H_2O	2.1		
30% Acrylamide-bis acrylamide mix	0.5	1610156	Bio-rad
1M Tris-Cl pH-6.8	0.380	T5941	Sigma
10% SDS	0.03	210291880	MP Biomedicals
10% APS	0.03	219055680	
TEMED	0.003	219401925	

Table.3.8. 10X Migration/ running buffer composition

Components	Amount
Tris-base	30 gm
Glycine	144 gm
SDS	10 gm
H_2O	1000ml
pH - 8.3	

Table.3.9. 10X TBS buffer composition

Components	Amount
Tris-base	24.23 gm
NaCl	80.06 gm
H_2O	1000ml
pH - 7.6	

Table.3.10. 1X TBST buffer composition

Components	Amount	Cat. No.	Company
10X TBS	100ml		
Tween-20	1ml	210316880	MP Biomedicals
H_2O	900ml		

Table.3.11. 1X Transfer buffer composition

Components	Amount	Cat. No.	Company
Glycine	14.4 gm	219482590	MP Biomedicals
Tris-base	3.02 gm	T1503	Sigma
Methanol	100ml	154903	
H_2O	900ml		
To transfer large proteins (>100 KDa), 0.1% SDS was added to 1X transfer buffer			

3.5.2. Western blot analysis

Along with pre-stained protein loading marker (#SM0671, Fermentas), equal amount of

each protein sample was separated electrophoretically in 8-12% (depending on the primary protein

of interest, mentioned in table) SDS-PAGE. Upon proper separation of bands (decided from the appearance of prestained marker), the resolved proteins were electro-blotted (15-17 v for 1 h) from the gel to methanol pre-activated PVDF membrane using semidry transfer system.

- ***Transfer of proteins to PVDF membrane:*** Depending on the molecular weight of the protein in interest, equal amount protein from each cell lysate was transferred onto two types of PVDF membranes (IPVH15150, 0.44μm, Millipore, USA) or (#162-0177, 0.22 μm, Bio-rad, USA) by semi-dry electro-blotting (Bio-rad, USA). When protein of interest was low molecular weight (< 40 KDa), 0.22 μm PVDF membranes have been used.

Upon completion of transfer, membranes were incubated with blocking buffer; (5% skimmed milk in TBST, #180020, MP Biomedicals) for 1hr at room temperature on a rocker. The membranes were then incubated overnight (approx 12 h at 4-8 °C in moist chamber) with different primary antibodies (dilutions were prepared as per manufacturer's instruction). Following incubation, primary antibody coated membranes were washed twice with TBST and once with TBS respectively.Membranes were incubated with secondary anti-rabbit HRP conjugated IgG (goat) for next 1h at room temperature. After incubation, once again membranes were washed twice with TBST and once with TBS respectively.

Chemiluminescence was detected under Gel Doc-XRS (Biorad) upon addition of enhanced chemiluminescence ECL kit following manufacturer's instructions.

Table.3.12. List of antibodies and chemi-luminescence reagents used in immune-blotting

Sr. No.	Antibody	Mol. Wt. (KDa)	Type	Cat No.	Dilution	% of SDS-PAGE	Company
1	Rabbit anti human Caspase3	17, 19, 35	Primary	#9665	1:1000	10%	
2	Rabbit anti human LC3A/B-I/II	14, 16	Primary	#4108	1:1000	12%	
3	Rabbit anti human Atg-7	78	Primary	#8558	1:1000	8%	
4	Rabbit anti human β-actin	45	Primary	#4970	1:1000	Depending on the protein of interest	Cell Signalling

5	Rabbit anti human iNOS	130	Primary	#2977	1:1000	8%	
6	Rabbit anti human Cox-2	74	Primary	#4842	1:1000	8%-10%	
7	Rabbit anti human Fas	40	Primary	#4233	1:1000	8%	
8	Rabbit anti human FasL	26, 40	Primary	#4273	1:1000	10%	
9	Rabbit anti human beclin-1	60	Primary	#3495	1:1000	8%	
10	Goat anti rabbit HRP tagged IgG	-	Secondary	#7074	1:3000	-	
11	20X LumiGLO® Reagent and 20X Peroxide	-	ECL (enhanced chemiluminicence) kit	#7003S	As per manufacturer's instruction	-	

Table.3.13. 1X Reprobing buffer composition

Components	Amount
Tris-Cl	3.78 gm
SDS	10 gm
H_2O	500ml
pH should be 6.7	

3.6. FLOW CYTOMETRY

3.6.1. Determination of cell phenotype:

Cells from each experimental set ups were harvested with ice cold PBS after specified time points. Then samples were centrifuged (5000 rpm for 5min at 4°C) and pellets were dissolved with 50 μL FACS buffer containing 1X PBS, 0.1% BSA (Sigma, A7906), 0.01% NaN_3(Sigma, S2002).

Table.3.14. 1X PBS composition, pH-7

Components	Amount	Cat. No.	Company
NaCl	8.0 gm		
Na_2HPO_4	1.16 gm	194739	MP biomedicals
KH_2PO_4	0.2 gm	194727	
KCl	0.2 gm	60128	Sigma
H_2O	1 L		

Flow cytometric measurements were performed using a four colour FACS-Calibur (Becton Dickinson). FSC (Forward scatter determines size) and SSC (side scatter determines cellular granularity) was used to identify healthy live cell populations. Auto-fluorescence was recorded by

analysing unstained cells in the all four Laser channels. For detecting the expression of cell surface markers, monoclonal mouse anti-human antibodies are added into each experimental set up and incubated for 30 min at 4˚C at the dark condition. Following incubation samples were washed and resuspended in 400µl FACS buffer and approx 10,000 events was recorded for each sample within a constant window.All data was analysed using Cell Quest Pro software.

Table.3.15. Fluorophore tagged antibodies for flow cytometry

Material	Company	Cat.No.
PE Mouse Anti human CD14	BD biosciences	555398
APC Mouse Anti-Human CD36		550956
FITC- Anti-Human CD206		551135
FITC-Anti-Human CD197[CCR7]		560548

3.6.2. Uptake and retention studies

About $1x10^6$ cells were incubated with fluorescent compounds (here BPZs) separately in growth media at 37°C. Cells were harvested at indicated time points, 15 min, 2 h and 24 h. Followed by cells were washed with ice cold PBS. Finally, single cell suspensions were prepared in 500 µL of PBS. The mean fluorescence intensity (MFI) was determined at a compensated FL1 voltage (selected based on excitation/emission wavelength of compounds of interest) using a FACS-Calibur flow cytometer (BD Biosciences). 5000 gated live events were taken from the forward vs. side scattering plots to analyse the extent of the compound uptake into the cells after each indicated time point. Histograms were obtained by comparing the mean fluorescence intensity of the test samples with that of the DMSO treated control samples.

3.6.3. Annexin-V/7AAD assay

Alteration in membrane asymmetry is one of the early hallmarks of apoptosis induction. A calcium-dependent phospholipid-binding protein, Annexins V have high affinity towards phosphatidylserine (PS). Fluorophore tagged Annexin-V is a flow cytometry probe that easily detect early apoptotic cells. 7-amino-actinomycin (7-AAD) is a standard plasma membrane impermeable

flow cytometric viability probe that distinguishes viable from nonviable cells. Annexin-V/7AAD assay is a quantitative method to determine the percentage of cells within a population that are actively undergoing apoptosis and are at the early stage (still alive). In healthy cells, PS remains at the cytosolic side of the plasma membrane whereas during early stage of apoptosis, PS translocates to the extracellular membrane and concomitantly gets accessible to any fluorescently labeled Annexin V. At the advent of apoptosis, cells remain alive and easily expel 7-AAD. Though 7-AAD failed to evade into viable cells with intact membranes but it easily enters into the dead and damaged cells. Therefore, cells displaying only Annexin V staining but 7-AAD negative are at the early stages of apoptosis. During late-stage apoptosis, cell membranes completely lose its integrity, there turned positive for both Annexin V and 7-AAD staining [218]. Cells those appeared positive for both PE Annexin V and 7-AAD were considered either in the end stage of apoptosis, are undergoing necrosis, or are already dead. Cells that stain negative for both PE Annexin V and 7-AAD are alive and not undergoing measurable apoptosis. Here staining was performed as per the protocol mentioned in the user's guide of the detection kit (BD biosciences #559763).

1×10^6 live cells were seeded into 24-well plates containing complete growth medium (5% FBS and 1% pen-strep) in the absence or presence of the test compounds and incubated at 37 °C under 5% CO2. After 2 h and 24 h of treatment, the cells were collected and washed twice with ice cold PBS.

Followed by single cell suspensions were prepared using 1X binding buffer (BD biosciences) supplied with the kit. Independently 100 µl of each experimental single cell suspension containing 1×10^5 cells were transferred to 5 ml tubes. 5 µl of PE Annexin V (supplied with the kit) and 5 µl 7-AAD (supplied with the kit) were added together into these solutions.Reaction mixtures (cells in staining solutions) were vortexed gently and incubate for 15 min at RT (25 °C) in the dark.400 µl of 1X binding buffer was added to each tube. Samples were acquired by flow cytometry within 1 hr from the time of staining.

The gated population (5000 cells/gate) obtained from the scatter plots and the cells undergoing apoptosis upon compound/ DMSO (solvent control) treatment were determined and represented in terms of percentage.

3.7. DNA FRAGMENTATION ASSAY

Degradation of nuclear DNA into nucleosomal units is a hallmark of apoptotic cell death. Following induction of apoptosis, activated executioner enzyme caspase 3, cleaves Inhibitor of Caspase activated DNase (ICAD) and releases it binding partner, Caspase-activated DNase (CAD). Upon release, CAD gets activated, concomitantly cleaves exposed and accessible DNAs (tightly wrapped around histones, core protein of nucleosomes) at inter nucleosomal linker sites, at approximately 200-bp intervals. Therefore, DNAs isolated from apoptotic cells appeared as ladder (around 200-bp or multiple of it) in highly concentrated agarose gels [219].

1×10^{6} cells per ml were cultured into 65 mm dishes containing complete growth medium (5% FBS and 1% pen-strep) and incubated with the test compounds for 48 h at 37 °C under 5% CO2. Buffer containing 10 mM Tris–HCl (pH 8), 150 mM NaCl, 5 mM EDTA and 0.5% Triton X-100 was used to rupture the cell membrane. 1 mg/ml RNaseA (MP Biomedicals, #0107680) were added into the lysates, vortexed and incubated for 1 h at 37°C.Followed by 0.1 mg/ml proteinase-K (MP Biomedicals, #9398125) was added into the same lysates for another 2 h under the same conditions. Chromosomal DNA was extracted from the lysates using a 25:24:1 phenol: chloroform: isoamyl alcohol mixture (MP Biomedicals, #154903),) after vortexing for 20 sce. Lysate/ phenol/chloroform/ isoamyl alcohol mixtures were centrifuged at 10000g for 5 min to separate aqueous phase and organic phase. Aqueous phase was removed carefully and kept at separate tubes. DNA was left to precipitate overnight at -20°C by adding equal volume of isopropyl alcohol. DNA-isopropyl alcohol solutions were centrifuged at 12000 g for 15 min at 4°C. Supernatants were discarded and pellets were air dried, resuspended into 20μl Tris-acetate EDTA buffer. The quality (260/280 absorbance ratio should be ≥1.8–2.0) of extracted DNA was assessed using NanoDrop

UV/Vis spectrophotometer (Thermo scientific). 2 µl of sample loading buffer (0.25% bromophenol blue, 30% glycerol in water) was added with required amount of each DNA samples. To observe any fragmented chromosomal DNA. Equal amounts (in terms of DNA content) of the individual samples were loaded and electrophoresed on 1.8% agarose gel (Conda, #8012) containing 0.1 mg/ml ETBr (MP Biomedicals, #802511).

Table.3.16. 50X TAE buffer composition

Components	Amount	Cat. No.	Company
Tris-base	121 gm		
Acetic acid	28.6 ml		
0.5 M EDTA pH-8.0	50 ml	194822	MP Biomedicals
H_2O	500ml		

3.8. ENZYME-LINKED IMMUNOSORBENT ASSAY (ELISA)

Sandwich ELISA was performed to detect and quantitate the concentration of soluble cytokines (soluble proteins in cell culture medium) in each experimental sample using capture and detection antibodies. Sandwich ELISA generally measures the amount of antigens (for this study, cytokines) between two layers of either monoclonal or polyclonal antibodies (capture and detection antibodies which specific for two different antigenic sites of same cytokine). The advantage of sandwich ELISA is that the sample does not have to be purified before analysis, and the assay can be very sensitive (up to 2 to 5 times more sensitive than direct or indirect).

Supernatants were collected after 24 & 72 hrs from stimulated/treated and resting THP1 and stored at -80 ˚C until analysis. IL-10, IL-12p70 levels were measured by ELISA (BD biosciences) according to manufacturer's instructions. Each kit comprised of two monoclonal antibodies (capture and detection) which recognize a single epitope in respective cytokines and allows fine detection and quantification of small differences at any experimental conditions.

Table.3.17. ELISA kit used for detecting secreted cytokines

Material	Company	Cat. No.
HU IL-10 OPTEIA SET	BD biosciences	555157
HU IL-12p70 OPTEIA SET		555183

Table.3.18. Coating Buffer composition

Components	Amount	Cat. No.	Company
NaHCO$_3$	7.13 gm	300185	MP Biomedicals
Na$_2$CO3	1.59 gm	191437	
H$_2$O	1.0 L		
Maintain pH to 9.5 with 10 N NaOH. Freshly prepare or use within 7 days of preparation, stored at 2-8°C.			

Table.3.19. Assay diluent composition

Components	Amount
PBS	1 L
FBS	10%
pH -7, Freshly prepared , stored at 2-8°C storage.	

Table.3.20. Wash buffer composition

Components	Amount
PBS	1 L
Tween-20	0.05%
Freshly prepared, stored at 2-8°C storage.	

Capture antibody was diluted in coating buffer and 100 μl per well of diluted mixture was added into 96 well plate. Each plate was sealed with parafilm and incubated overnight at 4 °C. After incubation, solution (capture antibody in coating buffer) was discarded and each well was washed 3 times with wash buffer (≥ 300 μl/well). After last wash, plate was inverted on an absorbent paper to remove any residual buffer. Plates were blocked with assay diluent (≥ 200 μl/well) and again incubated at RT for 1 h. Washing step was repeated following proper incubation. Meanwhile standards were prepared in assay diluents (as instructed by manufacturer). Samples dilutions were also taken out from -80 °C freezer and kept at ice. 100 μl of each standard, sample, and control were pipetted into appropriate wells, followed by sealing with parafilm and incubation for 2 h at RT. 5 times aspirate/wash each well as mentioned in washing step. 100 μl of working detector (Detection Antibody + SAv-HRP reagent) mixture was added to each well, followed by sealing with parafilm and incubation for 2 h at RT. Wells were washed 7times following washing step, but were soaked in wash buffer for 30 sec for each wash. Next, 100 μl of 1X substrate solution

(Tetramethylbenzidine/TMB and hydrogen Peroxide (H_2O_2) mix (Bangalore GeNei^{TM} #106035) was added to each well. Without plate sealer plates were incubated for 30 min at RT in the dark. At last 50 μl of stop solution (2 N H_2SO_4) were added to each well and absorbance was acquired at 450 nm within 30 min of stopping reaction.

3.9. MICROSCOPY

3.9.1. Inverted phase contrast microscopy

To determine the different stages of the monocytes to macrophages differentiation, or morphological changes of the cells following a treatment cells were observed by phase contrast microscopy (Zeiss) at indicated time points from the addition of any bioactive agents especially external immunomodulatory stimuli (solvents or SFN or soluble collagens) and cytotoxic agents in the culture media respectively.

3.9.2. Fluorescence microscopy

About 1×10^4 cells were grown on UV sterilized cover slips (12 mm) placed in each well of a 24-well plate (BD bioaciences) containing complete growth medium. The cells in each well were then treated with the fluorescent compounds and incubated for up to 24 h at 37 °C under a continuous flow of 5% CO_2. Post incubation, the cells were washed twice with PBS before fixing with 2% PFA (Himedia, GRM3660). The cells were kept in the fixing solution for 5 mins. Followed by the washed again with PBS and nuclei were counterstained with DAPI (MP Biomedicals, #15757405). After 5 min cover slips containing cells were washed twice with PBS and transferred inversely into mounting media (MP Biomedicals). Images were captured at both at 20 X and 40 X magnifications using a fluorescence microscope (Olympus) under appropriate wavelength filters.

3.10. CYTOTOXICITY ASSAY (XTT ASSAY)

The second generation tetrazolium dye, 2,3-bis-(2-methoxy-4-nitro-5-sulfophenyl)-2H-tetrazolium-5-carboxanilide) (XTT), can be effectively used to measure cell growth and drug

sensitivity in tumor cell lines [220]. Upon reduction (breakage of positively-charged quaternary tetrazole ring) this colorless or slightly yellow compound XTT form soluble formazan product and turned brightly orange. Therefore, real-time assays can be done using this dye. Due to net negative charge, XTT gets easily excluded from entering live cells. But considerable evidence suggests that the dye reduction occurs at the cell surface facilitated by trans-plasma membrane electron transport mediated by reductants of mitochondrial oxidoreductases. However, the sensitivity of an XTT assay is greatly improved by the usage of an intermediate electron carrier, PMS (N-methyl dibenzopyrazine methyl sulfate) which drives faster reduction of XTT and the formation of its formazan derivative. Altogether, PMS performed as the activation reagent in the XTT Cell Proliferation Assay. Published reports suggest, PMS mediates XTT reduction by picking up electrons at the readily accessible site in the plasma membrane and forms a reactive intermediate that eventually reduces XTT to its highly pigmented formazan product. Dead cells lose activity of its mitochondrial oxidoreductases, failed to conduct above mentioned reaction for the formation of bright orange fromazan dye.

100 µl of media containing $1x10^4$ cells was placed into each well of a 96-well plates (BD biosciences) and incubated for a minimum of 8 h for cell adherence (adhered cells) or used immediately (only for suspension cells). Later, the cells were incubated independently with either increasing concentrations (10^{-8} to 10^{-4} M) or respective working concentrations of tested compounds at 37 °C in a 5% CO2 incubator for either 72 h or indicated time points respectively. Each experimental 96-well plate had cells treated with DMSO (0.1% to 0.5%) or acetic acid (0.01%) as the solvent control.

Duplicate wells were used for each treatment. Post incubation, 50 µl of an assay mix consisting of 49 µL XTT (MP Biomedicals, #158788), and 1 µL PMS (MP Biomedicals, #194595) was added to each well. After about 6-8 h incubation, the enzymatic activity of the mitochondrial dehydrogenase (releases an orange coloured formazan dye after cleaving the XTT) present in

Material and Methods

metabolically active cells (live) was measured. The intensity of this coloured product denotes the number of live/ active cells present.

A micro-plate reader (iMark, Biorad) was used to measure the intensity of the absorbance from the coloured product formed by setting the wavelength at 490 nm with a reference wavelength of 655 nm.

The percentage cell viability was calculated using the following equation,

Cell viability (%) = (O.D $_{sample}$ /O.D $_{solvent\ treated\ control}$) x 100

O.D$_{sample}$: Intensity obtained from the cells incubated with the compounds at various conc.

O.D$_{solvent\ treated\ control}$: Intensity of the cells incubated with solvents alone.

Cell survival curves were prepared using MS-Excel software. Sigmoid curves were plotted using Origin Pro software and the IC$_{50}$ concentrations of the test compounds were determined from the same.

3.11. COLONY FORMATION ASSAY

The significant decrease in the number of viable cells detected by XTT may be attributed either to decreased cell proliferation or increased cell death or both. To determine occurrence of any of such phenomenon as probable anti-cancer mechanism of a cytotoxic compound, *in vitro* colony formation assay was performed using only adherent cell lines. *In vitro* assessments of altered colony formation ability by anticancer agents treated tumor cells often display significant correlation with *in vivo* growth delays and cell cycle changes [221-223].

Cells were plated in 35 mm (BD biosciences) dishes at 2500 cells per dish and incubated until they adhered properly. Later adhered cells were exposed to bioactive compounds for 24 h in 5% FBS containing complete growth media. After that indicated time period spent media were replaced with fresh one (without the compounds) after a through wash with PBS. Cells were incubated for next 15 days, while fresh media have been added after every two days. Cells were again washed with PBS after discarding the spent media. Washed cells were incubated with fixing

solution (ice-cold 100% methanol) for 10 min. Followed by distinct colonies were visualized after staining the fixed cells with 1% (w/v) crystal violet (sigma) in 35% methanol. For better clarity cells were washed with deionised water thoroughly. Images of inverted plates along with colonies were taken by ChemiDoc-XR system, Bio-Rad under trans-illumination. Images were processed using Quantity One software, Bio-Rad.

3.12. CELL CYCLE ANALYSIS

Selective anti-cancer activity of a bioactive agent is often determined by its ability to halt cell cycle progression of malignant cells leaving non-malignant cells unaffected. Similarly, here the effects of bioactive compounds on cell cycle progression were studied using flow cytometry (BD Biosciences).

1×10^6 cells/ml was seeded at 24 well plates with 5% FBS containing complete growth media. Following their proper adhesion to the bottoms of the wells, cells were exposed to the test compounds with the indicated concentrations for 24 h. At the end of the incubation, the spent media were discarded after centrifuging at 3000 rpm for 5 min. Cells pellets were dissolved with ice cold PBS and repeat the previous step. After discarding the PBS, cells were fixed using 3% paraformaldehyde for 5 mins. Once again cell pellets were obtained after centrifuging at 1500 rpm for 5min. Cell pellets were dissolved and DNA content of these fixed cells was stained with 500 μl PI (MP Biomedicals #19545810) solution (50 μg/ml PI, 0.5 mg/ml RNaseA and 0.1% Triton X-100). Incubate for 40min at 37 °C. Cells were washed with PBS, followed by centrifuged (as 1500 rpm for 5 min) and resuspended into 500 μl PBS. 5000 live gated events were acquired using a flow cytometer. Cell Quest Pro software was used to generate histograms based on the DNA content in each phase of the cell cycle.

3.13. STATISTICAL ANALYSIS

All analysis was performed using Microsoft Excel, Origin-Pro8 and. Statistical analyses were done using respective softwares (e.g: ***Cell-Quest Pro*** software for flow cytometry) used for

each techniques. All data were normalized to respective control values for each assay and presented as means ± SD or means ± SE (e.g. bar graphs).

The results displayed in **chapters 4-7** were expressed as either mean ± SD or mean ± SEM. Data were compared by unpaired student's t-test (using GraphPad software) between SFN treated sets with conventional M1 cells or soluble collagen treated set. Differences were considered statistically significant only when obtained p-values found to be less than or equal to 0.05.

CHAPTER-4

Non Cytotoxic Immune-Modulatory and Specificity Studies of Bioactive Isothiocyanate, Sulforaphane (SFN) Using *In Vitro* Monocyte/Macrophage Model for Autoimmunity

Results: Cellular responses to phytochemical, SFN

4.1.   BRIEF BACKGROUND INFORMATION

Functional phenotypic plasticity is one of the important characteristic features of the cells belonging to monocyte/macrophage (Mn/MΦ) lineage [224, 225]. Presence of more pro-inflammatory Th1-cytokines than Th2 cytokines in surroundings drives monocytes differentiation/activation towards classical M1 type. These cells are characterized as highly aggressive, inflammatory and inducers of various autoimmune diseases. While an increment in amount of Th2 cytokines alternatively shifts their activation towards anti-inflammatory M2 type (initiate Th2 humoral responses, allergic responses and wound healing mechanisms following any inflammatory assault) [226-229]. Cumulatively, M1 to M2 ratio is contemplated as an integral factor in maintaining physiological homeostasis and any uncontrolled drift towards either form always results in disease manifestation and pathogenesis. A therapeutic intervention that capable of balancing macrophage plasticity under any external or internal influence is considered as one of the most powerful means to suppress cartilage or bone erosion and subsequent development of inflammation (observed in chronic arthritis, tissue injury, fibrosis and so on) [230-232].

The peripheral monocytes are already programmed to sense and then migrate to the inflamed tissues. In patients with inflammatory diseases, such peripheral monocytes efficiently identify and automatically extravasate (movement through tissues) to the place of inflammation, e.g. synovial joints in RA. Upon arrival at the inflamed point, monocytes immediately get influenced by the micro-environmental cues and subsequently differentiate into pro-inflammatory M1 macrophages, activating various collagenases in tandem [233-238]. These proteases accelerate the degradation of articular cartilage or bone collagens (degradation and enzymatic modification of collagens) deteriorating the condition further. In RA and OA conditions, soluble degraded forms of collagens are detected both in the serum and synovial fluids and mount inflammatory responses at a higher magnitude [233, 239-241].

Results: Cellular responses to phytochemical, SFN
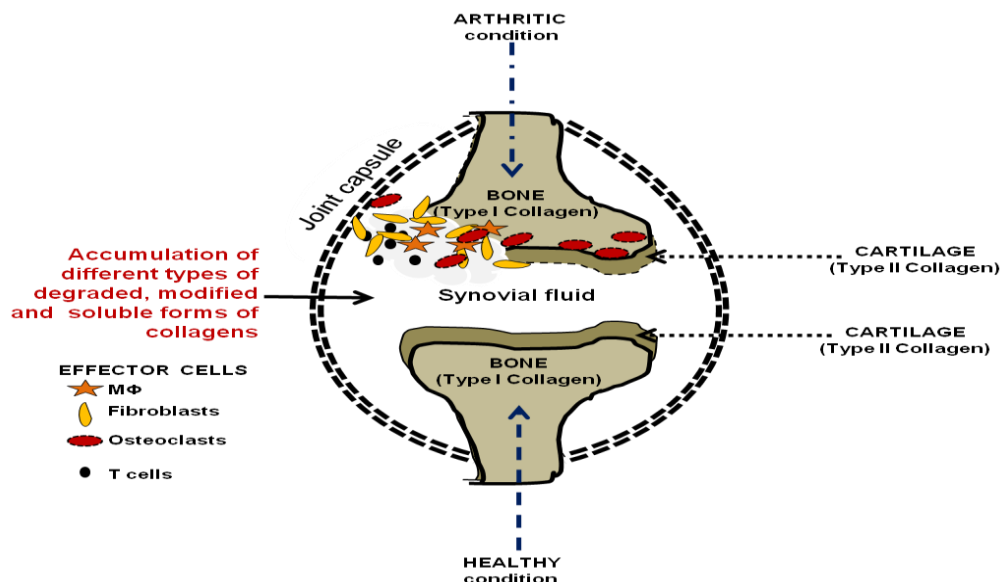
Fig. 4.1. Accumulation of soluble collagens at synovial fluids of arthritic (e.g. RA) joints. (***Adapted from Schurigt et al. 2013, Chapter 13; ISBN 978-953-51-0916-7***) MΦ/s = macrophage/s, Mn/s = maoncyte/s

According to published reports, both M1 macrophages and soluble forms of collagens in synovial fluids are sensitive biomarkers for any inflammatory, chronic arthritis e.g. RA [233, 236]. Later, Meng FW *et al*. demonstrated that the soluble forms of collagens derived from inflamed tissue extra cellular matrices (ECM, hubs of collagens) are also capable of influencing macrophage function and phenotype [242]. Altogether all these events lead to persistence of the diseases and monocytes/macrophages mediated inflammatory damages in autoimmunity represents a promising target for the treatment.
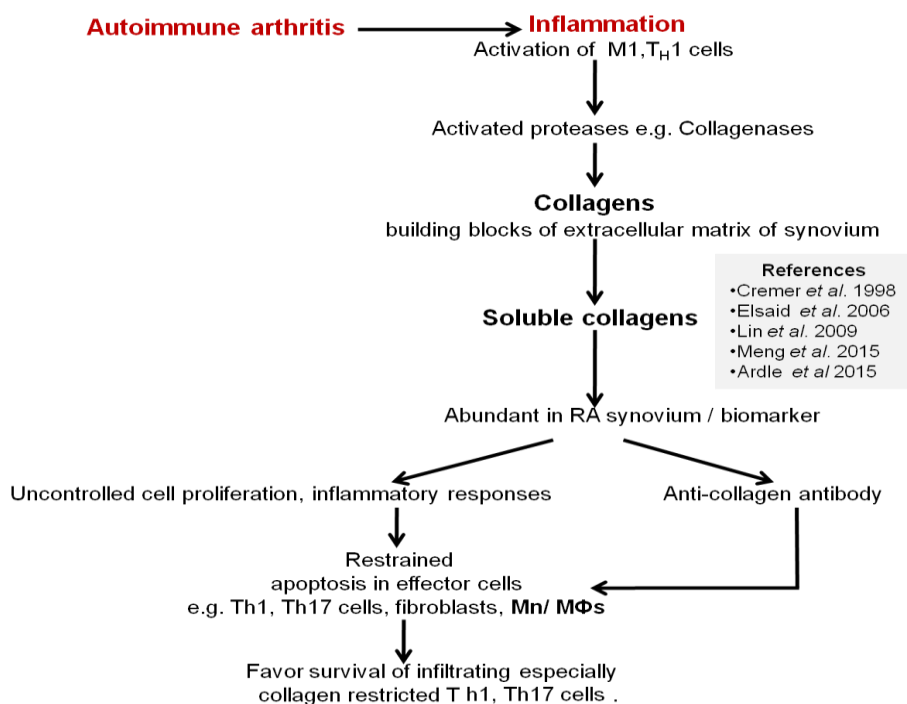
Fig. 4.2. Schematic diagram showcasing the role of soluble collagen in arthritis associated autoimmunity MΦ/s = macrophage/s, Mn/s = maoncyte/s

Results: Cellular responses to phytochemical, SFN

Over the years, several mice/rats models e.g. collagen-induced rheumatoid arthritis (CIRA) have been developed to study the diseases associated pathogenesis and underpinning cellular mechanisms [243-245]. However, using such models at a prescreening stage (especially to study activities of a specific immune cell population) to identify anti-autoimmune (e.g. anti-arthritic) agents is rather expensive and not feasible at times. Heterogeneity of body's immune system (consists of different cell population) also make it difficult to study cellular changes and underpinning mechanisms in a whole model animal. Moreover recent reports state that owing to multiple reasons, studies from such animal models may not be directly extrapolated to human conditions [243, 246-248]. Therefore, for initial screening, an *in vitro* cell type specific model would be more reliable and cost effective to study the mechanism of macrophage plasticity and behavior.

Without any external influence by disease specific inducers (self antigens or antibodies etc.), i*n vitro* generation of conventional M1 or M2 cells using Th1 and Th2 cytokines are one of the most well studied areas of macrophage biology. Classical M1 cells generation and activation has been observed when differentiating Mns were exposed to standard doses of interferon-γ (IFNγ) and LPS. Alternative activation (M2 type) takes place upon co-treatment of differentiating Mns with interleukins IL-4 and IL-13 [249-251]. In last five years, few sporadic reports had been published on ability of trace amount of soluble collagens (in culture media) to develop collagen specific autoimmune pro-inflammatory Th1 cells that *in vitro* mimic and perpetuate collagen induced pathogenesis during bone erosion or disease progression [252-254]. According to the immunological phenomenon, Th1 cells have capacity to promote M1 activation [255]. Thus, in principle soluble collagen can be used as inducer of autoimmune inflammation *in vitro* in a monocytes/macrophage (Mn/MΦ) model that can be used to pre-clinically screen new compounds with desired immune-modulatory role. For this purpose, an *in vitro* inflammatory Mn/MΦ based autoimmune conditions was established using THP1 monocytes and acid soluble collagen.

Lowering the M1 to M2 ratio for regaining a homeostatic state is a need of hour in combating multiple inflammatory disease pathogenesis. Application of an anti-inflammatory agent

Results: Cellular responses to phytochemical, SFN

that is not only capable of suppressing the consequence (inflammation) but also capable of altering the cause (macrophage phenotype) of the pathogenesis by favoring the downregulation of inflammation may have great implication as therapeutic strategy.

Upon SFN treatment, induction of an array of both anti-inflammatory and apoptosis signals within SFN treated autoimmune responsive, collagen restricted T cells and fibroblasts had already been reported [159, 170, 256]. Despite of clear indications from the published results, only a few studies had demonstrated beneficial effects of broccoli sprout derived or pure sulforaphane (SFN) in other experimental models for inflammatory as well as autoimmune diseases; mainly involving self restricted, immunogenic Th17 cells [169, 257]. However, the concept of anti-inflammatory SFN facilitating alteration in monocytes polarization, macrophage phenotypes (surface markers), plasticity (phenotype shifting without induction of cell death) and function (cytokine production) at autoimmune condition is still obscure.

In this chapter, an *in vitro* soluble collagen induced, an *in vitro* Mn/MΦ specific inflammatory model was developed and simultaneously non-cytotoxic yet anti-inflammatory effect of hormetic phytochemical, SFN was studied using this model system. To identify and validate soluble collagen induced functional M1 macrophage generation and their functional and phenotypic modification (immune suppressive M2 macrophage generation) upon SFN treatment, appropriate established biomarkers for M1 and M2 were used. Simultaneously, involvements of some other key immune regulators (such as MAPKs, p38/ ERK/ JNK) during the hypothesized M1/M2 switching were also investigated.

4.2. METHODS

4.2.1. *In vitro* THP1 cell culture and treatment

THP1 cells were maintained and differentiated following the protocol mentioned at **section 3.1.1** and **3.1.2.**

4.2.1.1. Polarization of THP1 differentiation

PMA-treated THP1macrophages can be used as a macrophage polarizing model to estimate the immune-modulatory or polarizing/switching ability of any compounds [207, 208]. It has unique characteristics as a model to be transformed or polarized into different types of macrophages. According to the recent reports PMA differentiated THP1 derived macrophages display slightly M2 functional profiles but depending on the micro-environments (presence of inflammatory or anti-inflammatory inducers) THP1 derived macrophages can acquire respective M1 or M2 profiles [250].

Shifting/polarizing THP1 differentiation is a topic of interest for few decades and the protocol is quite established [250]. In our study we slightly modified the established protocol depending on the requirement of the experiments. 20 ng/ml PMA was added in the culture media for 6 h and then cells were exposed to a combination of PMA with Th1 cytokines, LPS (100 ng/ml) and IFNγ (20 ng/ml) to polarize them into functional M1 macrophages. Similarly, when combination of PMA and Th2 cytokines (20 ng/ml IL-4 and 20 ng/ ml IL-13) were added after 6 h of PMA treatment, cells turned into M2 polarized macrophages and portray a M2 profile. Such *in vitro* M1/M2-polarized THP1 macrophages were generated and employed into several experiments to serve the purpose of positive control for the study of SFN induced THP1 polarization.

4.2.1.2. Generation of autoimmune responsive differentiating/polarized THP1

To generate autoimmune responsive M1-polarized THP1 derived macrophages, THP1cells were treated with PMA for 30 h - 54 h and polarizing them with soluble human or chicken collagens (chicken collagen type II/ human collagen type I/II/III/IV) for 24 h - 48 h (added 6 h after PMA**).** After 48h from the addition of PMA adhered differentiated THP1 macrophages were washed with PBS and PMA fresh media were added into them. In an experimental set soluble collagen was added together with SFN and in another setup 48 h old soluble collagens (I-IV) pre-exposed cells were treated with SFN containing PMA free media.

4.2.1.3. *To study the effect of SFN on THP1 differentiation and polarization*

To examine the role of SFN during THP1monocytes/ macrophages differentiation/ polarization, 6 h PMA treated differentiating THP1 cells were exposed to non cytotoxic dose (10 µM) of SFN and incubated for next 24 h- 48 h. To study the ability of SFN to polarise monocytes/ macrophages differentiation, cells were collected after 30h from the initial PMA treatment. Whereas to demonstrate its role in macrophage plasticity, SFN were added into 54 h old differentiated polarized macrophages following the wash with PBS and exposed cells were incubated for another 72 h.

For switch/plasticity experiment, already polarized, differentiated and auto-reactive (1 µg/ml soluble collagens treated) M1 type macrophages (6 h + 48 h) have been washed with PBS followed by incubating with fresh complete media containing non-cytotoxic but immune suppressive concentration of SFN (10 µM) and used for flow cytometry and western blotting.
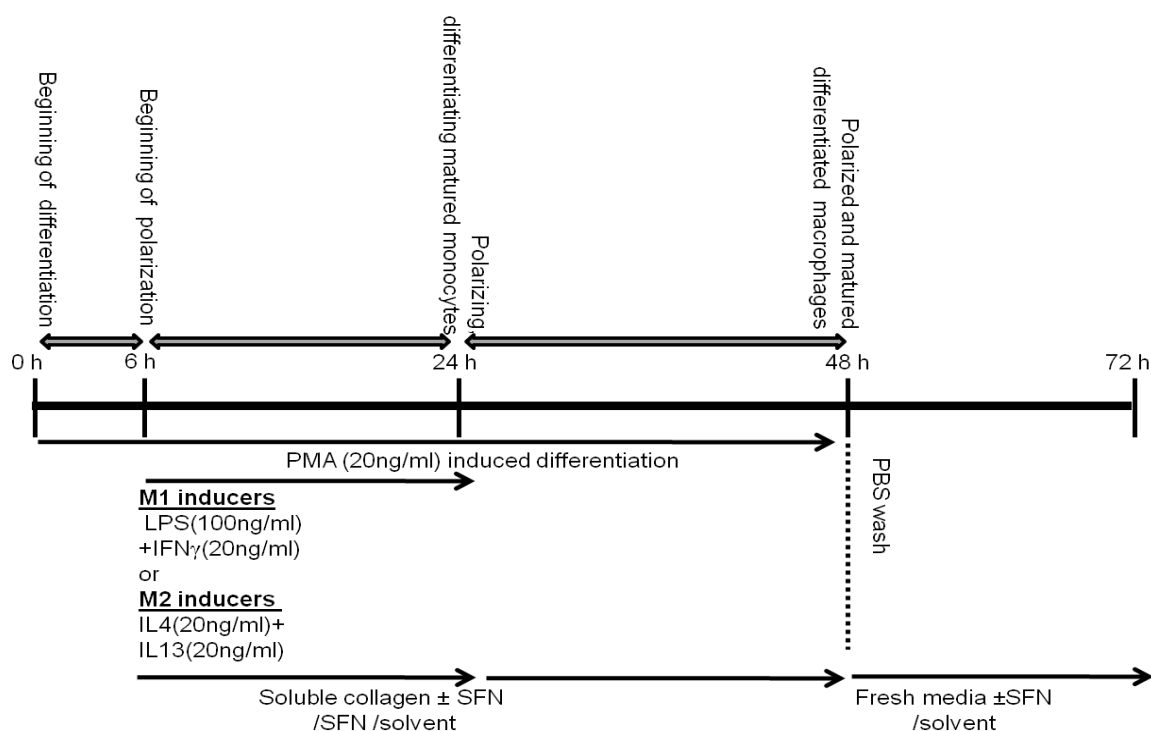
Fig. 4.3. Schematic illustration of experimental plans using human monocytic cell line, THP1

Not only cell survival, effect of SFN in monocytes/macrophages differentiation in the presence/absence of 20ng/ml PMA was also evaluated. Protocol was slightly modified and a separate study was performed using XTT cell survival assay. At first cells were treated with/without

Results: Cellular responses to phytochemical, SFN

SFN and incubated for 24 h at 37 ℃ with 5% CO_2 (Well A). Following the 24 h incubation cell supernatants were taken out and added in separate wells (**well B**) and equal amount of fresh media were added into the previous wells (**well A**). If cells are differentiated (macrophages stage) in presence of SFN (without PMA), then live cells would have adhered and found in the 'well A' whereas live floating cells (monocytic stage) will be found in 'well B'. If SFN is incapable of inducing differentiation signals like PMA (here 20 ng/ml), then all live cells would be found in 'well B'. Overall experimental plan has been described in **Fig.4.3.**

4.2.2. Phase contrast microscopy

To determine the morphological changes with monocytes differentiation/maturation to macrophages, combination of PMA with either SFN or soluble collagens alone or together exposed THP1 cells were observed under phase-contrast microscopes. Following 24 h and 72 h (**see section 4.2.1**) of incubation (after 6 h from the initial PMA treatment) under 5% CO_2 at 37°C, images were taken using Olympus camera. Image processing has been done using Image-J 1.4 software.

4.2.3. Cell viability assay

Cell proliferation assay was performed to evaluate the effect of either SFN or conventional M1 or M2 inducers or soluble collagens on differentiating THP1-monocytes survival and proliferation. Cell viability at the different the stages of monocytes to macrophages maturation (**see section 4.2.1**) was measured using XTT assay as described in **section 3.10.** Triplicate wells were used for each treatment for which the standard deviation was determined.

4.2.4. Cell differentiation assay

To examine whether SFN can acts as a differentiating agent like PMA, another XTT based assay was performed (**see section 4.2.1.3**). At first THP1-Mn cells seeded at 96 well plates ('**well A**') and cells were treated with solvent control or 10 µM SFN in the presence/absence of 20ng/ml PMA (final volume in each well, 100 µl). Following the 24 h incubation, 100 µl supernatants (containing floating, un-differentiated cells) were collected from wells (**well A**) and added in corresponding

Results: Cellular responses to phytochemical, SFN

separate wells (**well B**). Equal amounts (100 µl) of fresh media were also added into empty wells (**well A**). 50 µl solution containing XTT and PMS (50:1) was added in each well at indicated time point and percentage of live cells (either at floating undifferentiated or adhered, differentiated state) was determined as described previously.

4.2.5. Western blotting and analysis

Differentially treated both differentiating/ already differentiated THP1 cells (initial seeding was 0.5×10^6 cells/ml) were harvested with ice cold PBS after indicated time points (**see Fig. 4.3** and **section 4.2.1**). Protocols discussed in **section 3.2** to **3.5** had been used to perform western blotting using the whole cell lysates obtained from above mentioned harvested samples.

Normalized density of each observed protein band on the membranes was determined after subtracted from the background density using Quantity-one Basic software (Biorad) and comparative bar-graphs were prepared using Microsoft-Excel. Experiments were performed with biological triplicates for each treatment for which the standard deviation was determined.

4.2.6. Flow cytometry and analysis

To optimize the working concentration for PMA, about 0.5×10^6 THP1 monocytes have been seeded along with or without varying concentration of PMA (20 ng/ml, 50 ng/ml and 100 ng/ml) and incubated for 48 h at 37 °C in 5% CO_2. Cells were harvested with cold PBS and immediately stained with anti-CD36-APC (differentiation as well as M2 Marker) to estimate the level of THP1 differentiation and basal level M2 polarization (mimic natural differentiation) upon PMA treatment using FACS calibur.

To determine the conventional M1 or M2 polarization along with SFN or soluble collagens induced polarization (after 6 h+ 24 h from PMA treatment) or SFN induced switching of macrophage plasticity (after 6 h+ 48 h+ 24 h from PMA treatment) four M1/M2 specific surface markers were examined. Four fluorophore tagged flow cytometry specific monoclonal antibodies have been used CD36, CD206-FITC (M2 Marker), CD14-PE (M1 Marker) and CD197-FITC (M1

Results: Cellular responses to phytochemical, SFN

Marker) [256, 258-262] (**see section 3.6.1**). Following each indicated time points cells were harvested with cold PBS and immediately stained with antibodies to estimate the level of M1/M2 polarization or switching of plasticity using FACS calibur.

Comparative bar-graphs were prepared using Microsoft-Excel. Experiments were performed with biological triplicates for each treatment for which the standard error was determined.

4.2.7. Cytokine measurement

After indicated time points (**see section 3.8**), cell supernatants were collected and preserved at -80 °C freezer. Cytokine productions associated with M1/M2 polarization eg. IL10 (M2 Marker) and IL12p70 (M1 Marker) [263] were determined as per the manufacturer instructions using these cell supernatants.

Comparative bar-graphs were prepared using Microsoft-Excel. Experiments were performed with biological triplicates for each treatment for which the standard deviation was determined.

4.3. RESULTS

4.3.1. Development of *in vitro* monocyte/macrophage (Mn/MΦ) based (THP1 derived) experimental autoimmune model

4.3.1.1. *Assessment of PMA dose dependent differentiation of THP1 monocytes*

Body's default monocytes differentiation is partially M2 type and *in vitro* PMA has been shown to perfectly mimic the natural signal by drifting monocyte differentiation towards partially M2 type. Considering CD36 as one among such markers for THP1 monocytes to macrophage differentiation, current study was performed to feature the level of default differentiation (increase in CD36+ cells) in THP1 monocytes treated with various concentrations (20 ng/ml, 50 ng/ml and 100 ng/ml; selected based on published reports) of PMA for 48 h. A comparative flow cytometry based study revealed, almost similar amount of CD36 protein expression and percentages of CD36+ cells when THP1-Mns were treated from either 20ng/ml (lowest concentration) PMA or 100ng/ml

Results: Cellular responses to phytochemical, SFN

(highest concentration) independently (**Fig 4.4**). Microscopic images at **Fig.4.5** displayed that 20ng/ml PMA alone does not exert any adverse effect on THP1 proliferation. Therefore, for further studies 20ng/ml PMA was used as optimal concentration for the induction of differentiation in THP1.
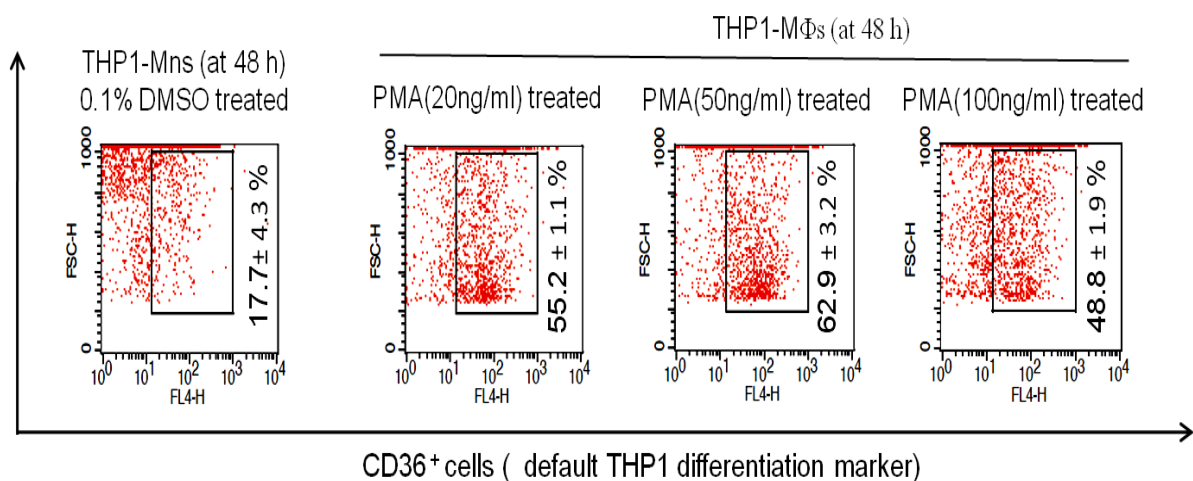
Fig. 4.4. Estimation of basal level of PMA dose dependent THP1 differentiation. Data shows PMA concentration dependent significant promotion of differentiation in THP1 (increase in default differentiated CD36$^+$ cells) after 48 h. For further studies, 20ng/ml PMA was used. Mns = monocytes; MΦs = macrophages

4.3.1.2. PMA induced differentiation is associated with time dependent morphological changes

A matured macrophage is morphologically distinct entity from its progenitor Mn. In presence of 20ng/ml PMA, post 48 h it was observed that the floating and round shaped THP1 monocytes adhered to the surface of tissue culture plates and following adhesion, differentiated morphologically distinct macrophages (adhered and elongated) (**Fig.4.5.i-iii**). At 24 h after PMA treatment, cells acquired a specific morphology that is partially similar to macrophages but completely adhered to the plates, indicating they are undergoing differentiating (**Fig.4.5.ii**). Post 48 h, removal of both PMA and other components from the culture media did not cause any change in the morphology of macrophages like cells (**Fig.4.5.iii**). In our study, PMA (20 ng/ml) treated THP1 not only acquired desired macrophages like morphological changes with times but also there is also a significant increase in differentiation marker (surface CD36) expression after 48 h (**Fig.4.4**).

i) Undifferentiated THP1-Mns (without PMA)

ii) Differentiating THP1-Mns (at 24 h, with 20ng/ml PMA)

iii)Differentiated (PMA free fresh media after 48 h), completely differentiated THP1-MΦs (at 72 h)

Determined time points to get Mn/MΦs at different stages during differentiation

0 h: begining of differentiation
6 h: begining of polarization
24 h: ongoing differentiation and polarization
48 h: completion of differentiation and polarization

Fig. 4.5. Differential morphological features of THP1 derived monocytes, differentiating monocytes and matured macrophages. Based on the differential morphological features, time points to acquire monocytes/ macrophages at the different stages of their PMA induced differentiation process were determined. Mns = monocytes; MΦs = macrophages

4.3.1.3. *Autoimmune inflammatory responses by soluble collagens from self (human) and non-self (chicken) origins*

Soluble forms of collagens of self (human type-I, 1μg/ml) and non-self (chicken sternum, type-II, 20μg/ml) origins were used to determine and subsequently develop an *in vitro* model to study the cellular mechanisms in auto-immune inflammatory arthritis conditions. Differentiating THP1-Mns (20ng/ml PMA treated for 6 h) were exposed to both types of soluble collagens separately for next 24 h. Cells were harvested and western blotting was performed with the whole cell lysates of each experimental samples determining the accumulation of two pro-inflammatory proteins, COX-2 and iNOS. Representative results (**Fig.4.6**) suggest, each type of soluble collagen can induce COX-2 and iNOS at protein level while undergoing differentiation and *in vitro* mimic the inflammatory autoimmune symptoms registered in arthritis progression.

Results: Cellular responses to phytochemical, SFN
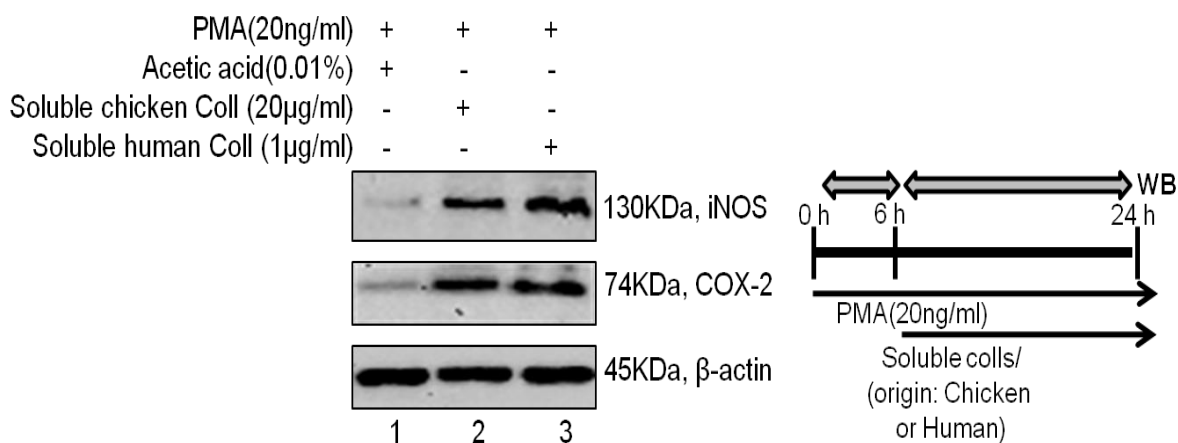
Fig. 4.6. *In vitro***, soluble collagens (Chicken and human) mount autoimmunity associated inflammatory responses.** At indicated doses soluble forms of collagens of self and non self origins induced pro-inflammatory proteins, COX-2 and iNOS in 20 ng/ml PMA induced differentiating THP1 monocytes (at 24 h). Coll/s = collagen/s

4.3.1.4. In vitro pro-inflammatory concentrations of soluble collagens exert no adverse effect on differentiating THP-1 proliferation

In the current experiment, differentiating THP1-Mns (20ng/ml PMA treated for 6 h) were exposed to both types of soluble collagens separately for next 24 h. At this time point, cell viability was measured by the XTT assay (**Fig.4.7.i**) as described in **section 3.10** and morphological changes have been observed under microscope (**Fig.4.7. ii**). It has been observed, both types of collagens (human type-I, 1µg/ml and chicken sternum, type-II, 20µg/ml) exerted no adverse effect in cellular proliferation as well as morphology as compared to solvent control treated cells (**Fig.4.7 and Fig.4.5**). Altogether representative results (**Fig.4.7**) suggested the efficiency of these soluble collagens as non-cytotoxic, in *vitro* non-cytotoxic inflammatory autoimmune response inducers.
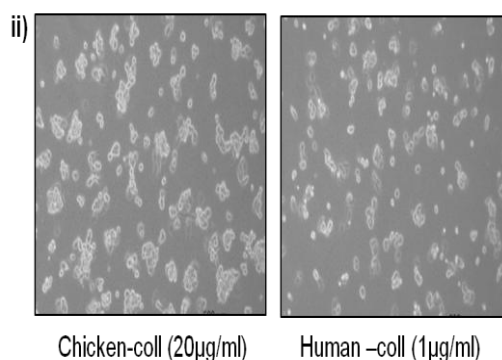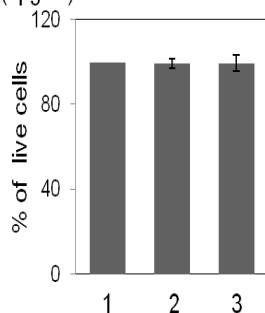
Fig. 4.7. Working concentrations of soluble forms of collagens (Chicken and human) are non cytotoxic to differentiating THP1 monocytes. Coll/s = collagen/s

4.3.1.5. *In vitro, pro-inflammatory concentrations of soluble collagens are non-apoptotic to differentiating THP-1*

As development of apoptosis resistance is associated with the arthritis associated pathogenesis, current experiment was performed to determine the autoimmune responsive, inflammatory self or non self originated soluble collagens are pro-apoptotic or not. Once again, differentiating THP1 monocytes (20 ng/ml PMA treated for 6 h) were exposed to both types of soluble collagens separately for next 24 h. Cells were harvested and western blotting was performed with the whole cell lysates of each experimental samples to determine the accumulation of established apoptosis marker, cleaved form of caspase-3 (17-19 KDa band) (**see section 3.5**). Representative result (**Fig.4.8**) suggested, each type of soluble collagens (human and chicken) failed to induce caspase-3 activation. Therefore, at the working concentrations, they remained inefficient enough to induce apoptotic signals in differentiating THP1 monocytes (at 24 h).
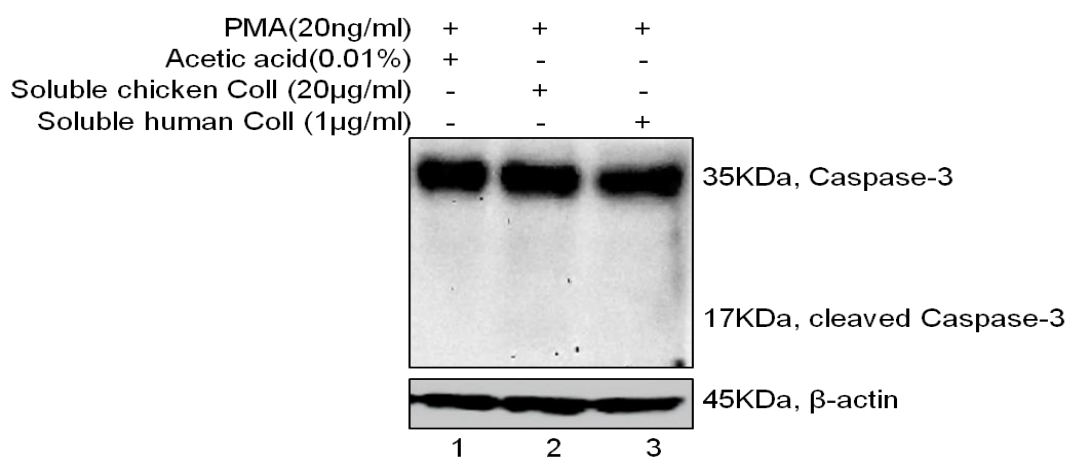
Fig. 4.8. *In vitro,* **soluble collagens are inflammatory but non-apoptotic.** At indicated inflammatory concentrations, both soluble forms of collagens of different orinns failed to induce apoptosis in differentiating THP1 monocytes (at 24 h). Coll/s = Collagen/s

4.3.1.6. *Collagen type dependent (human, type I-IV) differential auto-immune type inflammatory responses*

Soluble forms of both type I and II collagens are the two established biomarkers for bone and cartilage degradation in arthritis respectively. Here, soluble forms of four types of collagens of self origin (human type-I, II, III, IV, 1 µg/ml) were used to determine a valid cellular inflammatory

Results: Cellular responses to phytochemical, SFN

response (COX-2 induction) associated with auto-immune arthritis progression. For the current experiment, differentiating THP1 monocytes (20 ng/ml PMA treated for 6 h) were exposed to each soluble collagen for next 48 h at 37 °C, 5% CO_2. Followed by cell were washed with PBS and incubated for another 24 h with PMA as well as soluble collagen free media at same conditions. To determine the accumulation of a pro-inflammatory and arthritis associated protein, COX-2 in whole cell lysates, these collagen pre treated cells were harvested at indicated time point (72 h post collagens exposure) and western blotting was performed. Representative result (**Fig.4.9**) suggests each type of soluble collagen has shown efficacy in inducing cellular inflammatory symptoms of arthritis (induction of COX-2). However, *in vitro* both human soluble collagen type-I (1µg/ml) and type-II (1µg/ml) were observed to induce comparatively higher amount of COX-2 than collagen type-III (1µg/ml) and type-IV (1µg/ml).
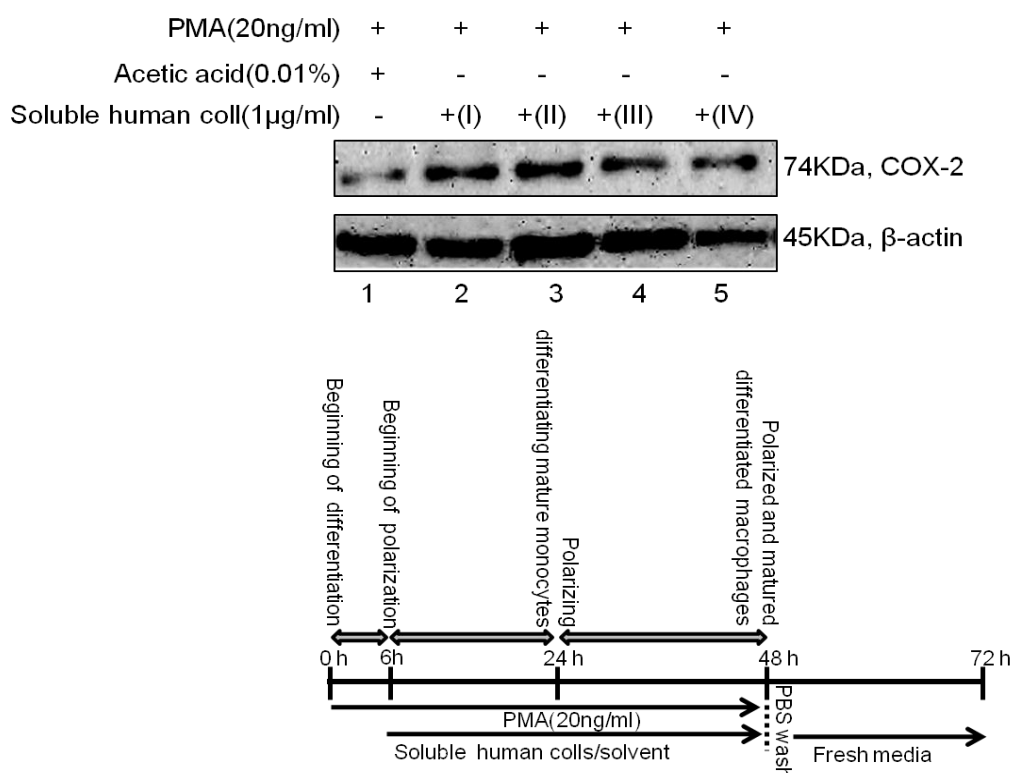
Fig. 4.9. Soluble form of human collagens (I-IV) mount inflammatory response *in vitro*. Western blot analysis was perfomed to delineate how during PMA mediated differentiation, presence of trace amount of soluble form of human collagens (1 µg/ml) in culture media developed pro-inflammatory, autoimmune responsive matured macrophages (induced COX-2 expression at 72 h old cells, both PMA and collagens (I-IV) have been washed out after 48 h). Coll/s = Collagen/s

Results: Cellular responses to phytochemical, SFN

4.3.2. Dose and time dependent effects of SFN on PMA induced, differentiating THP1-monocytes

4.3.2.1. SFN differentially affects survival of THP1 derived monocytes and PMA induced differentiating monocytes

PMA (20ng/ml) induced differentiation in THP1 monocytes. Within 48 h from the initial PMA treatment, THP1 cells completely differentiated into macrophages **(see section 4.2.1).** Comparative studies on concentration dependent cytotoxic effect of SFN on survival of PMA treated (differenting/differentiated) and untreated (undifferentiated) THP1 cells were performed and survival curves were also constituted. **Fig.4.10.i.** displays that PMA differentiated THP1 cells (48 h old matured macrophages) are more resistant to SFN induced cytotoxicity (at any concentration) than THP1 monocytes (undifferentiated). Treatment with 10 µM of SFN brought about a significant difference in number of viable cells (expressed in percentages) in PMA treated or untreated THP1 cells. It was a primary indication that 10 µM of SFN can be used as non-cytotoxic working concentration to study the functional effect of SFN specifically on differentiating monocytes or completely differentiated macrophages. This data also indicated the probable resistance of partially M2 type (default) macrophages against SFN mediated cytotoxicity (at 10 µM or higher dose) as compared to inactivated monocytes.

Results: Cellular responses to phytochemical, SFN
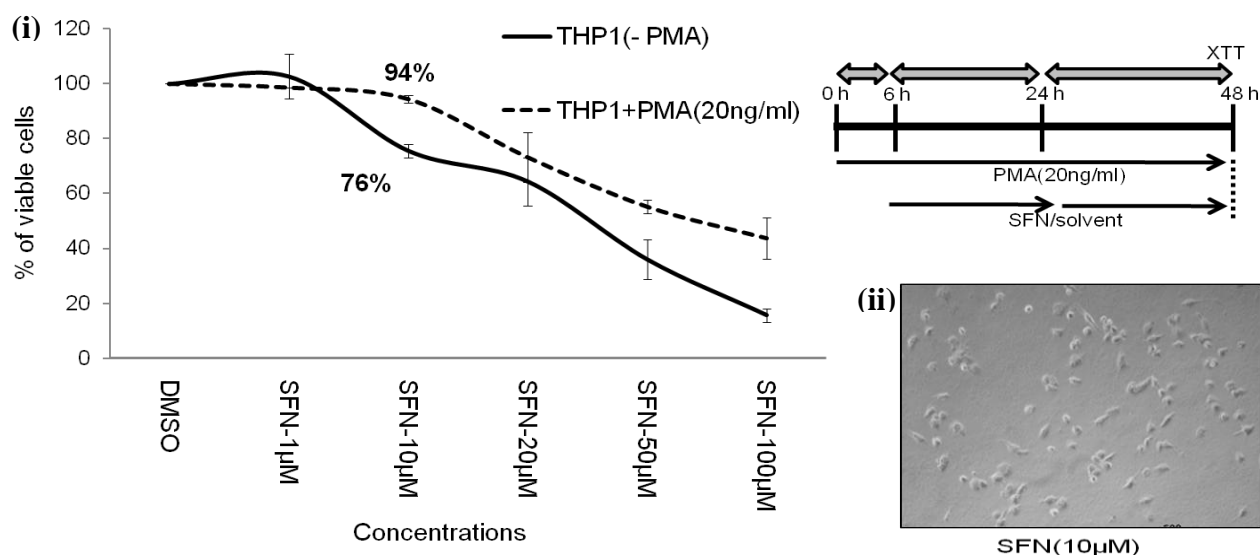
Fig. 4.10. **Determination of differential (monocytes *vs* macrophages) cellular response (cytotoxicity) to SFN**. **(i)** Cell survival curves showing SFN induced dose dependent differential antiproliferation of THP1 derived monocytes and macrophages. **(ii)** Microscopic image of 10 µM SFN treated THP1 deived macrophages (at 48 h).

4.3.2.2. *SFN does not exert or inhibit differentiation signals to THP1 monocytes*

This experiment (**see section 4.2.5**) was performed to evaluate whether at non cytotoxic (10 µM) conc. SFN is capable to acting as a differentiation inducer like PMA. It was observed that SFN is incapable of exerting any differentiation signal to the THP1 (no increase in the adherent cell numbers at respective **'well A'** as compare to DMSO treated monocytes) and most of the live cells were found in supernatant or at floating state (like THP1 monocytes) (**Fig. 4.11.a**).

As following 24 h of combined treatment of PMA(20 ng/ml) and SFN(10 µM) to THP1, almost 95% cells were found in adherent, differentiated condition and only a mild amount of live cells (approximately 9%) were found at floating state (**well B**).

Microscopic images showcased at **Fig.4.11.b.** also suggest, below subtoxic dose (at 10 µM), SFN neither induce differentiation (cells remained at the monocytic stage) nor promote any adverse effect (no cell death/cytotoxicity).

Results: Cellular responses to phytochemical, SFN

(b)

DMSO (0.1%)   10 µM SFN   100 µM SFN
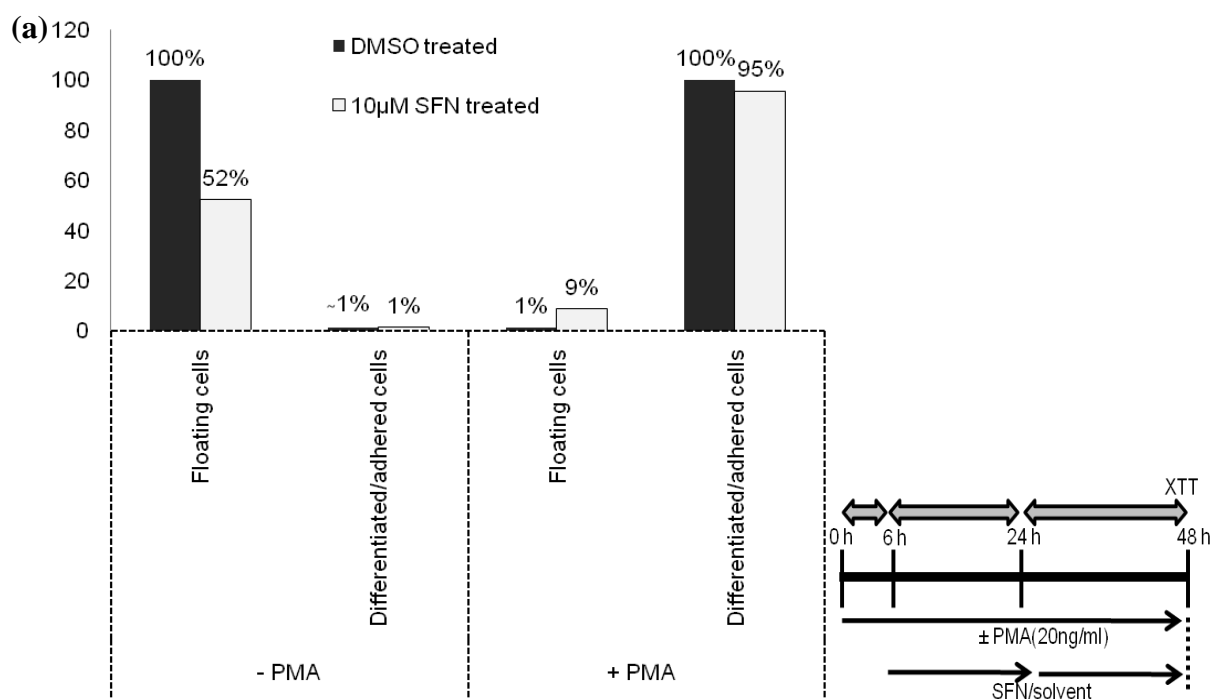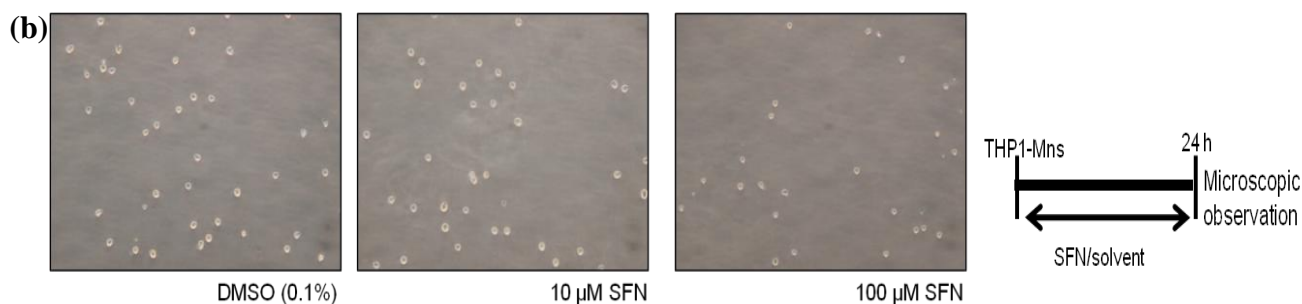
Fig. 4.11. Influence of SFN exposure on THP1 differentiation. (a) Level of cellular adherence following 48 h of 10 µM SFN treatment (with/without 20 ng/ml PMA) was studied by XTT assay. (b) In the absence of PMA, THP1 monocytes (5 X10^4 cells/well) was treated with either 0.1% DMSO or different concentrations of SFN (10 µM and 100 µM) for 24 h and cellular (THP1-monocytes) morphology was observed under inverted microscope at 10X magnification.

4.3.2.3. SFN induces concentration dependent apoptosis in PMA differentiating THP1

Differentiating (6 h from the 20 ng/ml PMA exposure) THP1 monocytes were treated with varying concentrations (1 µM, 10 µM, 50 µM) of SFN and incubated for another 24 h. Following incubation, western blot was performed with the whole cell protein lysates (RIPA lysates to determine accumulation of apoptosis marker, caspase-3). We observed that both at 1 µM and 10 µM concentration, SFN did not induce any apoptosis signal (absence of cleaved or active form of caspase-3) in differentiating monocytes. At higher concentration (here 50 µM) SFN turns pro-apoptotic for this *in vitro* model by activating caspase-3 (formation of cleaved caspase-3, 17KDa band). This result (**Fig. 4.12**) was an indication that 10 µM conc. can be a used to evaluate non-apoptotic role of SFN in this *in vitro* model for monocytes/ macrophages.
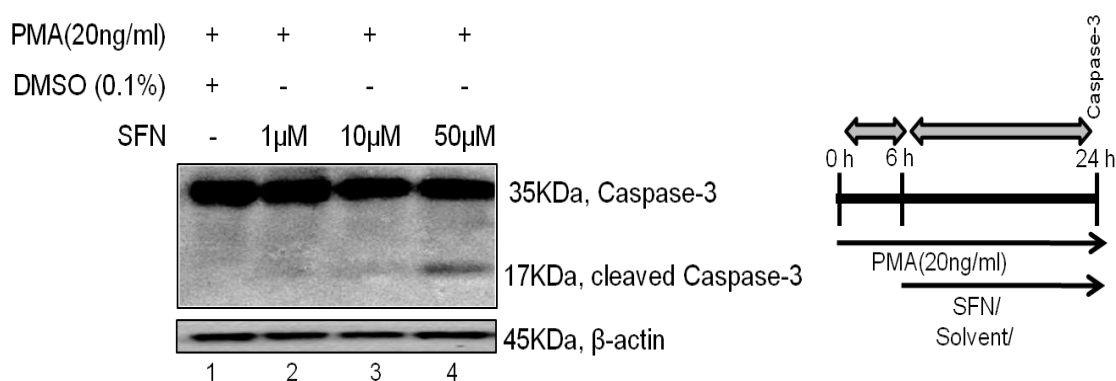
Fig. 4.12. Dose dependent caspase-3 activation by SFN. *In vitro,* below or at 10µM SFN also failed to induce apoptosis biomarker, caspase-3 activation in differentiating monocytes.

Results: Cellular responses to phytochemical, SFN

4.3.2.4. *SFN suppresses accumulation of inflammatory marker, COX-2 at a non-cytotoxic/non-apoptotic concentration*

Not only dose dependent cytotoxicity, current study was also performed to demonstrate whether within 24 h of treatment at determined non-cytotoxic, non-apoptotic concentration (1 µM and 10 µM) SFN is capable of suppressing inflammatory inducer (here COX-2) in differentiating THP1 monocytes. As SFN was dissolved into DMSO, 0.1% solvent treated cells have been used as control for this study. Western blot analysis has demonstrated 10 µM SFN suppressed the intracellular accumulation of inflammatory marker, COX-2 within differentiating monocytes. Though 1µM SFN was non-cytotoxic yet it failed to suppress COX-2 accumulation. At determined cytotoxic concentrations of SFN, 20 µM and 50 µM, COX-2 protein expression was inhibited at equal measures in treated differentiating cells. This observed absence of COX-2 protein may be possible due to death of SFN treated THP1 cells at these cytotoxic concentrations.

Compiling all these above mentioned results, a potential immune suppressive yet non cytotoxic concentration of SFN (10 µM for PMA exposed THP1) was determined. New experiments which may explain the probable roles of SFN on monocytes to macrophages differentiation, polarization and plasticity as well as implication for the treatment of autoimmune (soluble collagen mediated) inflammatory conditions were carry out.
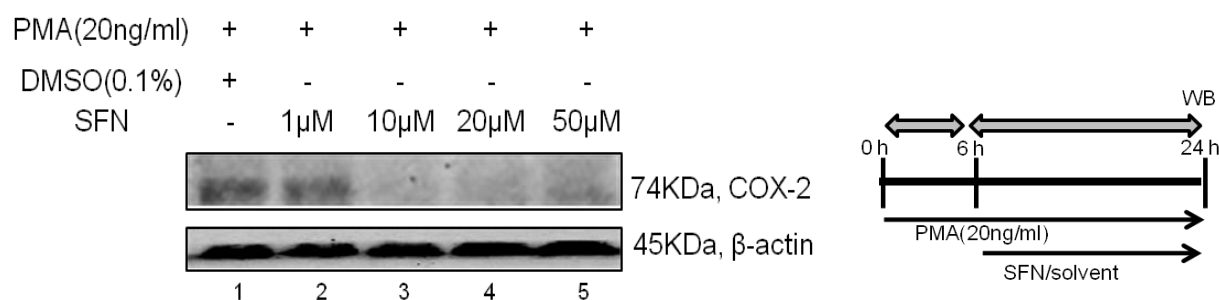
Fig. 4.13. Western blot analysis to determine anti-inflammatory response by SFN. Current experiment confirmed that without inducing significant cell death, minimum 10µM SFN is required to establish significant immune-suppression by PMA induced differentiating Mns. 10µM dose SFN enable to reduce the level of a pro-inflammatory M1 marker, COX2 protein in SFN exposed monocytes.

4.3.3. Regulation of SFN mediated immune-suppression by MAPK inhibitors

Here, we examined whether pre-inhibition of MAPKs (p38, MEK1/2, JNK1/2; potential regulators of innate immunity [264]) during differentiation (1 h before SFN treatment) can alter SFN mediated suppression of COX-2 in differentiating (20 ng/ml PMA treated for 6 h +24 h) THP1 monocytes. Before treating differentiating monocytes with 10 μM SFN for 24 h, we exposed the cells to 10 μM concentration of each MAPK inhibitors (**Table.4.1.**) for 1 h (after 5 h from initial PMA treatment and washed them with PBS. Considering COX-2 as one of the authentic targets of SFN mediated immune suppression, only MEK1/2 and JNK1/2 individual and dual inhibitions were able to reverse the SFN mediated suppression of COX-2 moderately. We also observed that p38 inhibition (when both MEK1/2 and JNK1/2 were uninhibited) could not resume COX-2 accumulation**.** Interestingly, overall COX-2 accumulation in MAPKs pre-inhibited, differentiating THP1-Mns was lower than only 0.1% DMSO exposed cells.

Table.4.1. List of MAPK inhibitors used

Inhibitor	Target MAPKs	Working conc.
PD98059	MEK1/2	10 μM
SB203580	P38	10 μM
SP600125	JNK1/2	10 μM

Results: Cellular responses to phytochemical, SFN

(a) PMA(20 ng/ml), DMSO (0.1%), Soluble human collagen (1 µg/ml), SFN (10 µM), PD98059 (10 µM), SB203580 (10 µM), SP600125 (10 µM)

74 KDa, COX-2
45 KDa, β-actin

(b)
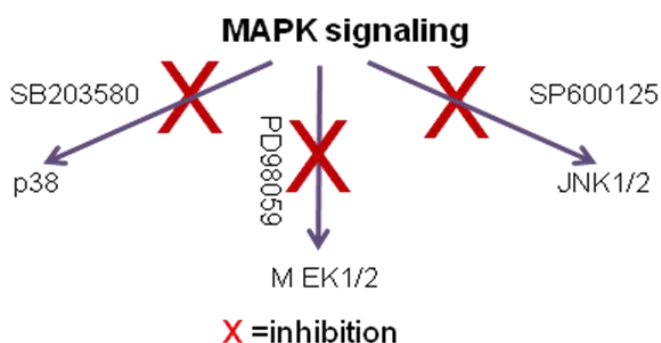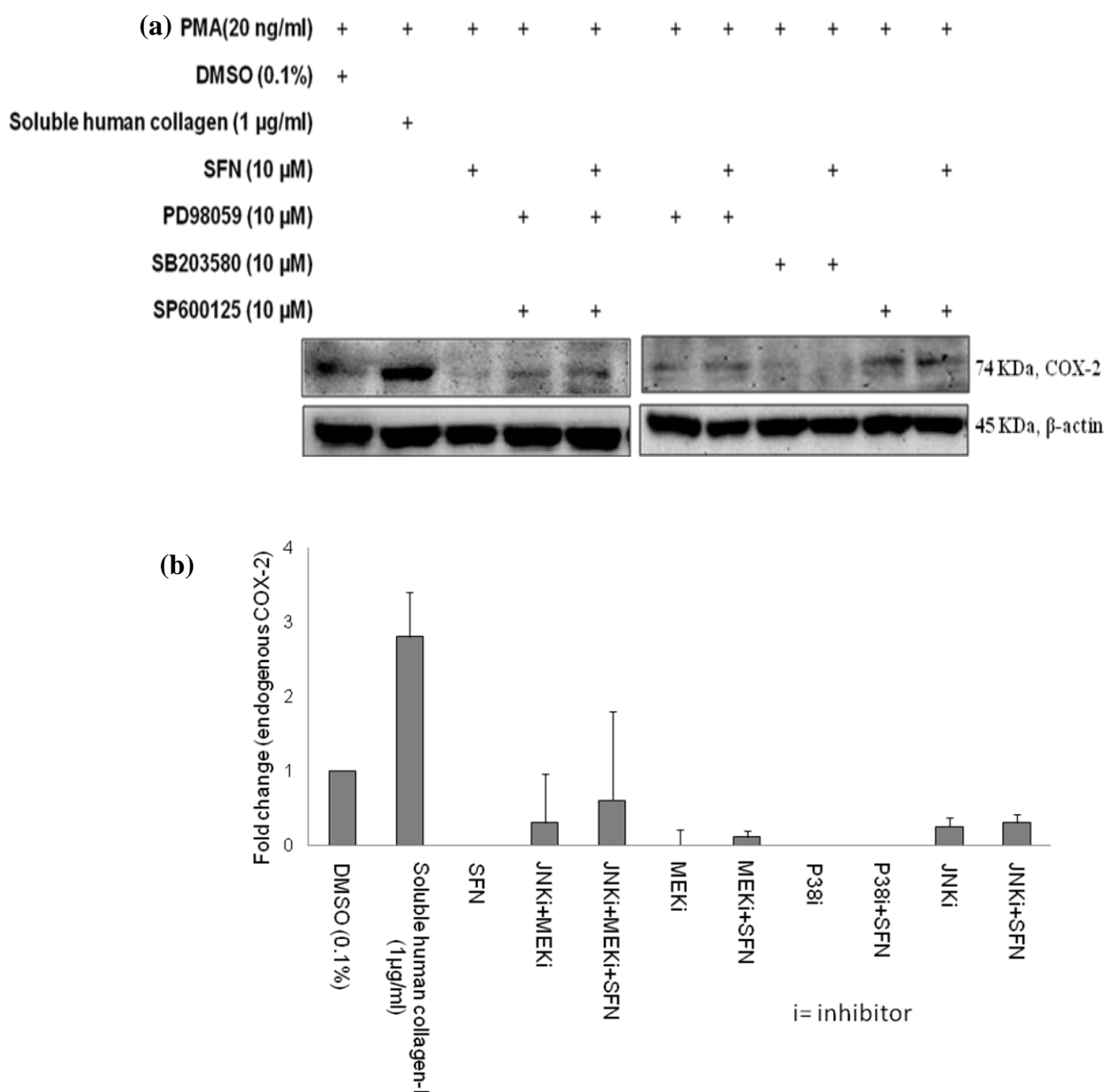
Fig.4.14. Involvement of MAPKs in SFN mediated anti-inflammatory response during THP1 monocytes polarization. (a) Western blot pictures are displaying COX-2 accumulation in 24 h SFN treated/untreated but MAPK pre-inhibited (for 1 h before SFN exposure) differentiating THP1 monocytes. **(b)** Representative bar graphs obtained by densitometric analysis using Quantity-one. Working concentration and specification of each inhibitor has been described in **Table.4.1**.

4.3.4.   SFN induces M2 polarization in differentiating THP1 monocytes

4.3.4.1. Below sub-toxic concentration, SFN represses accumulation of endogenous biomarker

for M1 polarization

According to our earlier study it has been observed, 10µM (non cytotoxic) SFN reduced COX-2 enzyme accumulation during THP1 derived monocytes to macrophage differentiation. In this current experiment we compared this COX-2 suppressing activity of SFN (completely shut down) with the conventional M1 (100ng/ml LPS and 20ng/ml IFNγ driven) and M2 (20ng/ml IL4 and 20ng/ml IL13 driven) polarizing THP1-Mns. The endogenous marker profile of SFN treated cells (**Fig.4.15. Fig.4.15. lane-4**) matched with that of the conventional M2 inducers (IL4+IL13) treated cells (**lane-3**) whereas M1 inducers (LPS+IFNγ) treated cells (**Fig.4.15. lane-2**) showed elevated level of COX-2 accumulation defining their inflammatory characteristics. However, at non cytotoxic concentration (10 µM) SFN demonstrated potential immune-suppressive effect by downregulating the COX-2 protein level (**Fig.4.15. lane-5**) in the conventional M1 polarizing cells.

Results: Cellular responses to phytochemical, SFN
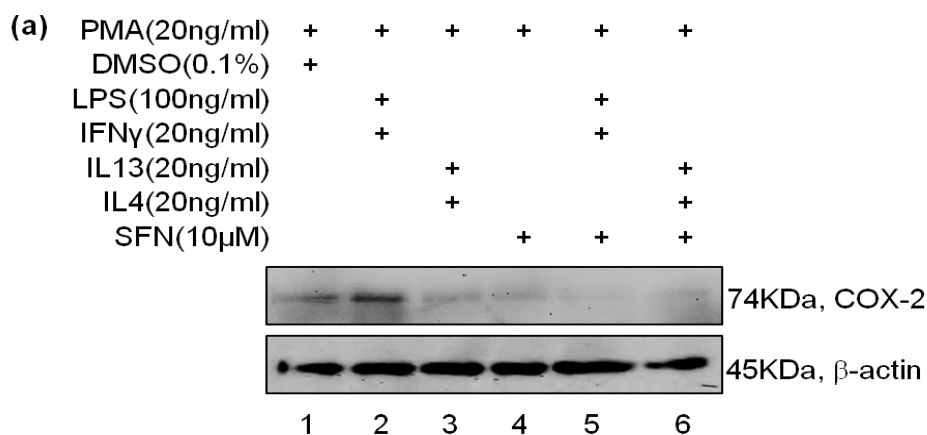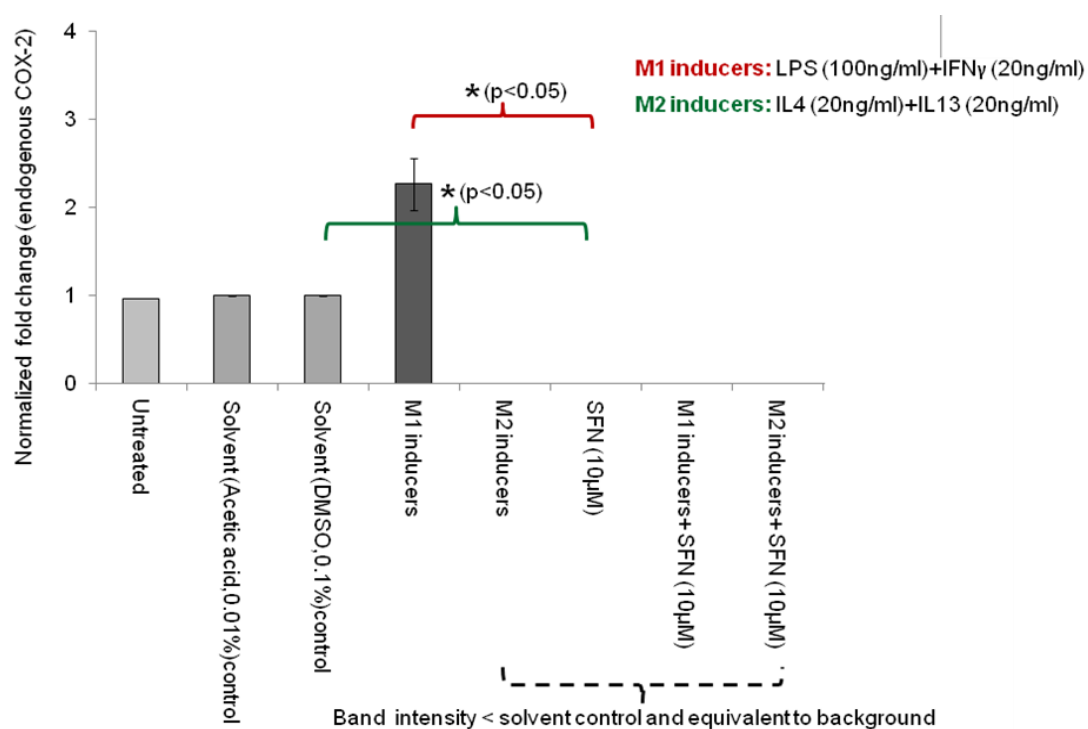
Fig. 4.15. SFN polarizes THP1-monocytes differentiation towards M2 type (a) The status of endogenous M1 biomarkers (COX-2) during PMA induced THP1 differentiations (after 24 h) were detected by western blotting. A bar graph (b) was obtained from representative blot by using Quantity-one-densitometric analysis. Error bars represent mean ± SEM (standard error of means). 'p value' obtained using unpaired-student's t-test.

4.3.4.2. SFN treated differentiating THP1 monocytes display M2 polarization specific phenotypes

Expression of surface CD14 (M1 marker) and surface CD36 (M2 marker) upon 24 h treatment with 10µM SFN or optimal concentrations of IFNγ/LPS (M1 inducers) or IL-4/IL-13 (M2 inducers) in PMA-differentiating THP1 cells were analyzed and compared. From the results, conventional M2 polarizing cells showed significantly higher surface expression of surface CD36 (MFI: 95.4 ± 0.4) in comparison to the IFNγ/LPS treated cells (MFI: 60.5 ± 6.4). When the impact of non-cytotoxic but anti-inflammatory (10 µM) SFN treatment on these differentiating Mns was determined and a significant ($p<0.05$) increase in the expression of surface CD36 (MFI: 85.1 ± 5.9) was observed (**Fig.4.16.a**). Surprisingly, a significant but contrasting pattern was observed when expression of surface CD14 (MFI for SFN or IFNγ/LPS treated cells are 5.1±0.4 and 12.6 ± 1.3 respectively) on

Results: Cellular responses to phytochemical, SFN

treated differentiating THP1-Mns were examined (**Fig.4.16.b**). These results clearly indicated that SFN directs THP1-Mn differentiation towards alternative activation (M2 type) mode.

As no cytotoxicity was observed by XTT assay at the concentrations employed for either M1 or M2 polarizers or SFN (10 µM), the observed effects only conveyed the immune suppressive, M2 polarizing effects of SFN during Mn differentiation **Fig.4.16.a.**

Results: Cellular responses to phytochemical, SFN
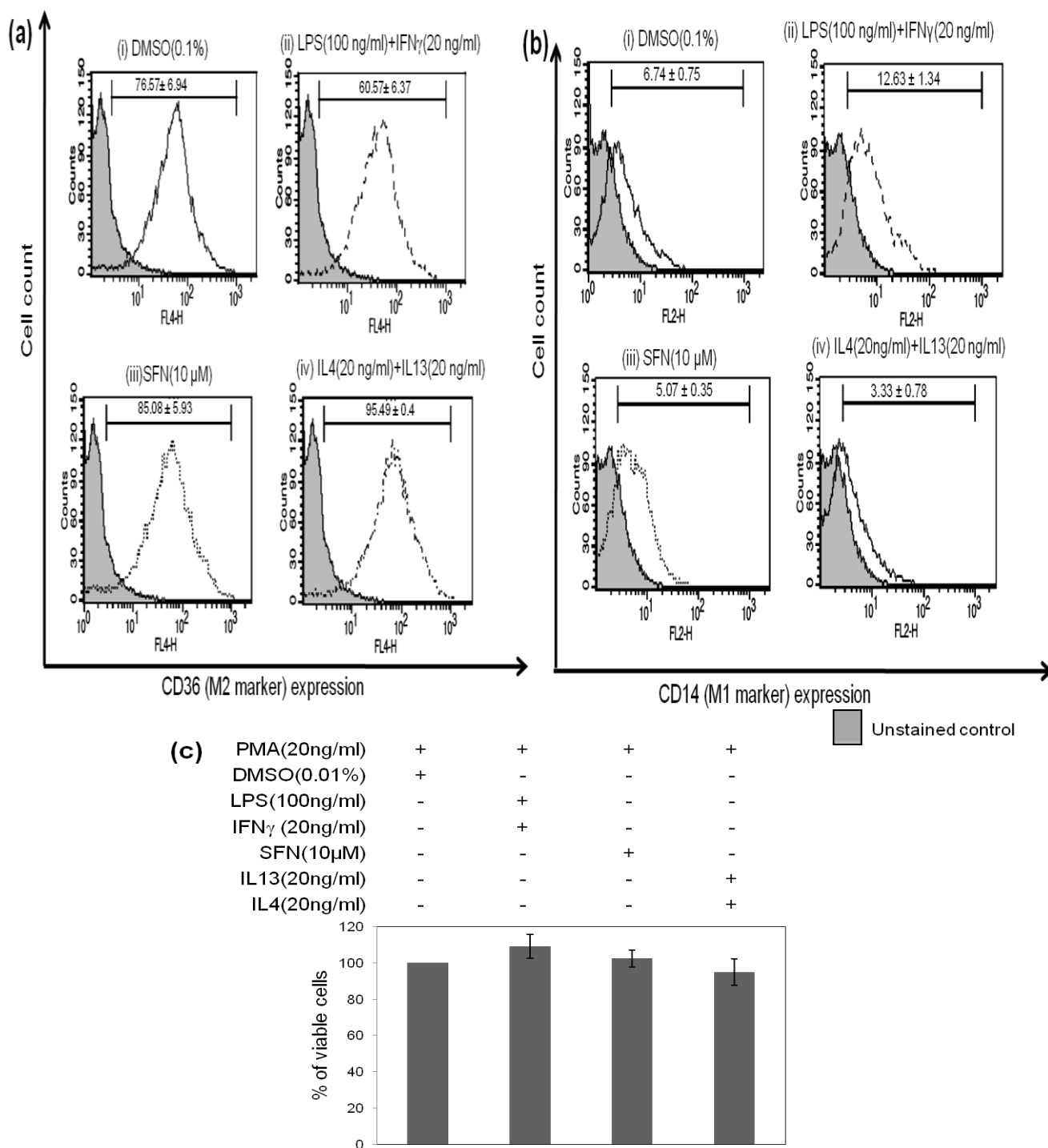
Fig. 4.16. Effect of SFN treatment on M1 and M2 specific cellular surface markers. Cells (differentiating THP1monocytes) were harvested after 24 h treatment and stained with fluorescently labeled monoclonal antibodies specific for CD14 (early pro-inflammatory early M1 marker), CD36 (anti-inflammatory M2 marker) and were analyzed by flow cytometry. Following treatment with (i) DMSO (solvent control) (ii) LPS/IFNγ (iii) SFN and (iv) IL-4/IL-13 at indicated concentrations for 24 h, histograms showing surface expression of **(a)** CD36 and **(b)** CD14 proteins were obtained. **(c)** No cell deaths were observed in all indicated treatment conditions. Error bars represent mean ± SD Data are representative of triplicate experiments.

4.3.4.3. SFN alters microenvironments in favor of M2 polarization

SFN has been shown to regulate the production of both pro and anti-inflammatory cytokines both *in vivo* and *in vitro*. Microenvironments of M1 (LPS and IFNγ) and M2 (IL13 and IL4) inducers treated THP1 derived differentiating Mns (at 24 h from the treatment) were studied after collecting the corresponding supernatants at the indicated time points and results were compared with that of the 10 µM SFN treated cells. Here we determined the production of both pro-inflammatory M1 polarizing cytokine, IL-12p70 (active form of IL12) and anti-inflammatory M2 polarizing cytokine, IL-10 by 10 µM SFN or M1/M2 inducers (alone or together with SFN) exposed differentiating Mns (protocol at **section 4.2.7**).

Studies using sandwich-ELISA demonstrated (**Fig.4.17**) that M1 polarization influencing cytokine, IL12p70 level was abrogated in the presence of either SFN (28.1 ± 2.1 pg/ml) or M2 inducer cytokines, IL-4/IL-13 (29.9 ± 15.03 pg/ml) as compared to the 0.1% DMSO (36.4 ± 4.4 pg/ml) treated or M1 inducers, IFNγ/LPS treated (87.7 ± 1.5 pg/ml) cells. Additionally, upregulation of a M2 polarization influencing cytokine IL10 was observed in those cells (**Fig.4.17**) However, microenvironment of M1 inducers treated cells were found to accumulate significantly higher amount of IL12p70 (p<0.0001) and lower amount of IL10 (105.4 ± 5.7 pg/ml, p <0.001) than that of the SFN treated cells (IL10: 181.5 ± 3.2 pg/ml) (**Fig.4.17**). When the differentiating Mns (6 h PMA treated) were treated together with M1 inducers and SFN (10 µM), a contrasting pattern was observed and indicated the development of M2 polarizing microenvironment in presence SFN.

Results: Cellular responses to phytochemical, SFN

PMA(20ng/ml)	+	+	+	+	+	+
DMSO(0.1%)	+	-	-	-	-	-
LPS(100ng/ml)	-	+	-	-	+	-
IFNγ(20ng/ml)	-	+	-	-	+	-
IL13(20ng/ml)	-	-	+	-	-	+
IL4(20ng/ml)	-	-	+	-	-	+
SFN(10µM)	-	-	-	+	+	+
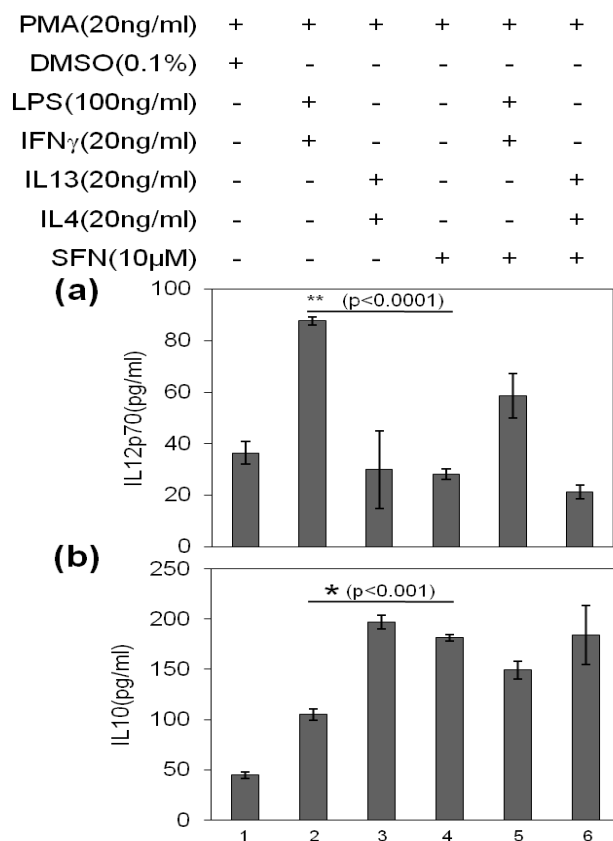
Fig. 4.17. SFN induces M2 polarization specific cytokine production. To quantify the level of **(a)** M1 polarization favoring cytokine, IL12p70 and **(b)** M2 polarization favoring cytokine, IL10 in the microenvironment of 24 h treated (M1/M2 inducers or SFN) /untreated differentiating (PMA induced) THP1 monocytes, sandwich ELISA were performed. Error bars represent mean ± SEM (standard error of means). p-values obtained using unpaired-student's t-test in Graph pad.

4.3.5. Soluble human collagen induces M1 polarization in differentiating THP1 monocytes

4.3.5.1. *Soluble human collagen elevates endogenous pro-inflammatory biomarker to direct monocytes polarization towards M1 type*

6 h PMA induced, differentiating THP1-Mns was treated with bone erosion biomarker, soluble human collagen-I, M1 inducers, SFN and solvent controls (acetic acid and DMSO) independently for 24 h and intracellular accumulation of endogenous inflammatory biomarker, COX-2 protein was determined by western blotting.

As compared to solvent or SFN treated cells, pro-inflammatory M1 marker, COX-2 protein expression was up regulated in both M1 inducers and soluble human coll-I treated cells (**Fig.4.18**). Results suggested an *in vitro* pro-inflammatory M1 inducing effect of soluble human collagen-I in differentiating THP1 monocytes.

Results: Cellular responses to phytochemical, SFN

PMA(20 ng/ml)	+	+	+	+	+
Acetic acid 0.01%)	+	-	-	-	-
DMSO (0.01%)	-	+	-	-	-
LPS(100 ng/ml)	-	-	-	-	+
IFNγ (20 ng/ml)	-	-	-	-	+
Soluble human coll-I(1 µg/ml)	-	-	-	+	-
SFN(10 µM)	-	-	+	-	-

74KDa, COX-2

45KDa, β-actin

    1   2   3   4   5
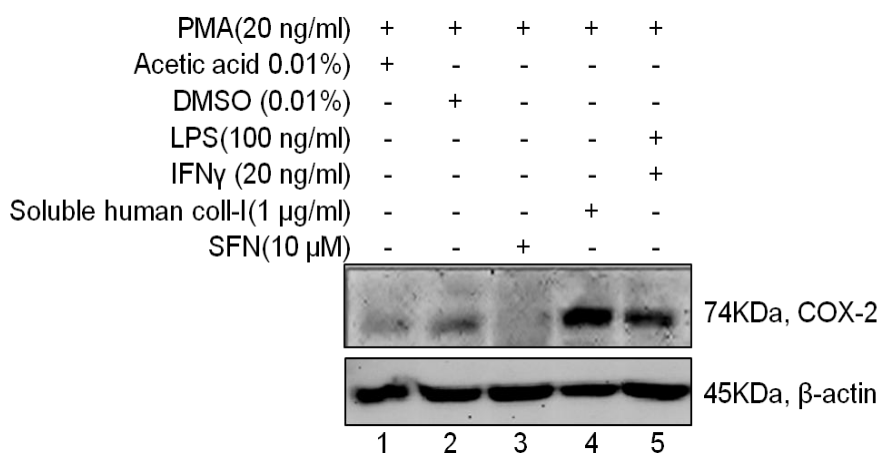
Fig. 4.18. Soluble coll acts as M1 polarizer during THP1 differentiation. Like M1 inducers (IFNγ + LPS; **lane-5**), soluble human collagen-I also polarized 20 ng/ ml PMA mediated THP1 monocytes differentiation towards M1 type (up regulates endogenous marker, COX-2, lane-4). This effect is completely opposite to effect shown by M2 polarizer, SFN **(lane-3).** Coll = Collagen

4.3.5.2. *Soluble human collagen treated differentiating THP1 monocytes display M1 phenotype*

6 h PMA induced, differentiating THP1 monocytes was treated with bone erosion biomarker, soluble human collagen-I, M1 inducers, SFN and solvent control (acetic acid) independently for 24 h and phenotypes of treated cells were determined using flow cytometry. Soluble collagen-I (1µg/ml) induced expression of M1 polarization marker, surface CD14 (MFI: 10.7±2.2, **Fig.4.19.b.ii**) but significantly ($p<0.05$) reduced expression of a M2 polarization marker, surface CD36 surface (MFI: 59.2±1.4, **Fig.4.19.a.ii**) as compared to respective 0.01% acetic acid treated differentiating THP1 monocytes (solvent control, MFI for CD36: 65.3±1.3 and MFI for CD14: 4.2±1.4) (**Fig.4.19.a.i and b.i** respectively). However, insignificant differences had been observed when phenotypes (surface CD14 and CD36 expression) of collagen-I exposed cells were compared with conventional M1 inducers treated differentiating cells (**Fig.4.19.c**). Interestingly, surface CD36 expression was found to be elevated and CD14 was reduced when differentiating cells were exposed to both soluble human collagen-I and SFN together at the time of beginning of polarization. (**Fig.4.19.a.iii and b.iii** respectively)

Data are represented as histograms (**Fig.4.19.**) formats and respective comparative analysis obtained after analyzing all the data shown in have been displayed as bar graphs (**Fig.4.19.c**).

—

Therefore, further experiments were carried out with soluble collagen induced M1-macrophages and

SFN induced M2-macrophages.

Results: Cellular responses to phytochemical, SFN

(c)								
PMA(20ng/ml)	+	+	+	+	+	+	+
DMSO(0.01%)	+	-	-	-	-	-	-
Acetic acid(0.01%	-	+	-	-	-	-	-
LPS(100ng/ml)	-	-	+	-	-	-	-
IFNγ (20ng/ml)	-	-	+	-	-	-	-
Soluble human coll-I(1µg/ml)	-	-	-	+	-	+	-
SFN(10µM)	-	-	-	-	+	+	-
IL13(20ng/ml)	-	-	-	-	-	-	+
IL4(20ng/ml)	-	-	-	-	-	-	+
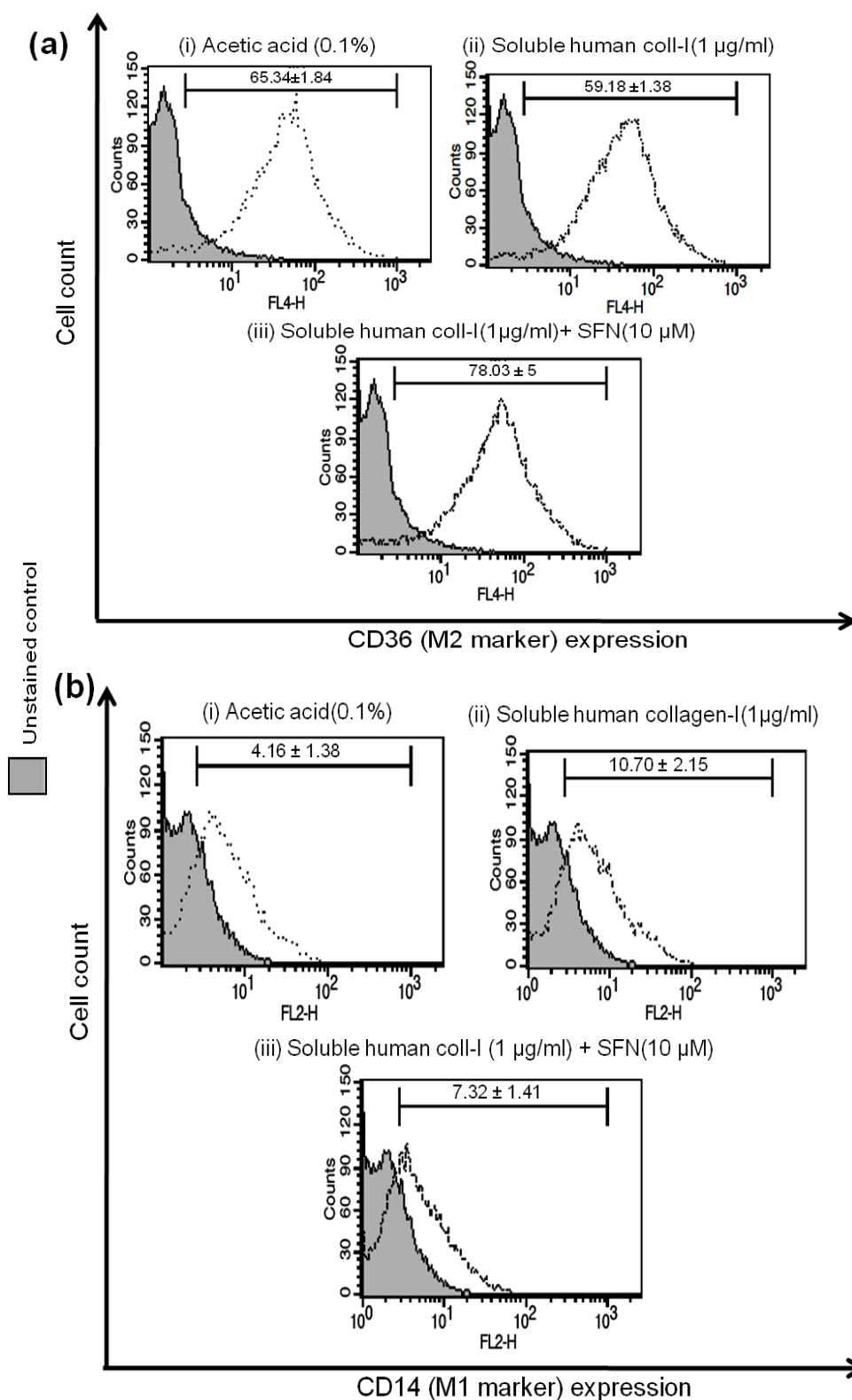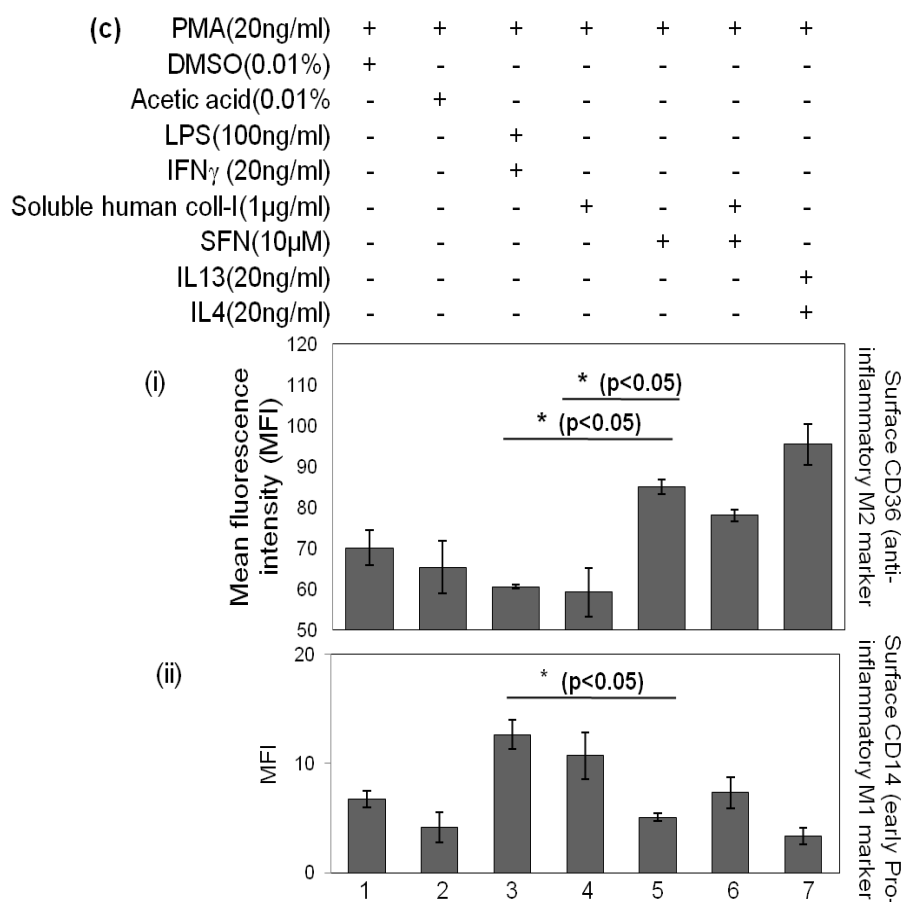
Fig. 4.19. Soluble collagen-I treated differentiating cells showcase M1 polarizing phenotypes. Cells were harvested and stained with fluorescently labeled monoclonal antibodies specific for CD14 (early pro-inflammatory M1 polarization marker), CD36 (anti-inflammatory M2 polarization marker) and analyzed by flow cytometry. Following treatment with (i) acetic acid (solvent control) (ii) Soluble human coll-I (iii) Soluble human collagen-I and SFN together at indicated concentrations for 24 h, histograms showing surface expression of **(a)** CD36 and **(b)** CD14 proteins were obtained. **(c)** Bar graphs are displaying the surface expression of M1/M2 biomarkers at indicated dose and conditions (after analyzing data displayed at both at **Fig. 4.16**. and **4.17**). Asterisk denotes P values compared with SFN treated cells using unpaired-student's t-test. Data are representative of three replicate experiments. Coll = collagen

4.3.5.3.   *Soluble human collagen alters microenvironments in favor of M1 polarization*

Like M1 inducers (**Fig.4.20. lane-5**), soluble human collagen-I also polarized PMA mediated THP1 differentiation towards functional M1 type (up regulates production of active form of pro-inflammatory cytokine IL12p70 (**Fig. 4.20. lane-4**). Interestingly presence of SFN and soluble collagen-I together during PMA induced differentiation (from 6 h of PMA treatment) significantly reduced pro-inflammatory cytokine, IL12p70 production **(Fig. 4.20 lane no. 2 and 4)**.

PMA(20 ng/ml)	+	+	+	+
Acetic acid 0.01%)	+	-	-	-
Soluble human coll-I(1µg/ml)	-	+	-	-
Soluble human coll-I (1µg/ml)+SFN(10 µM)	-	-	-	+
SFN(10 µM)	-	-	+	-
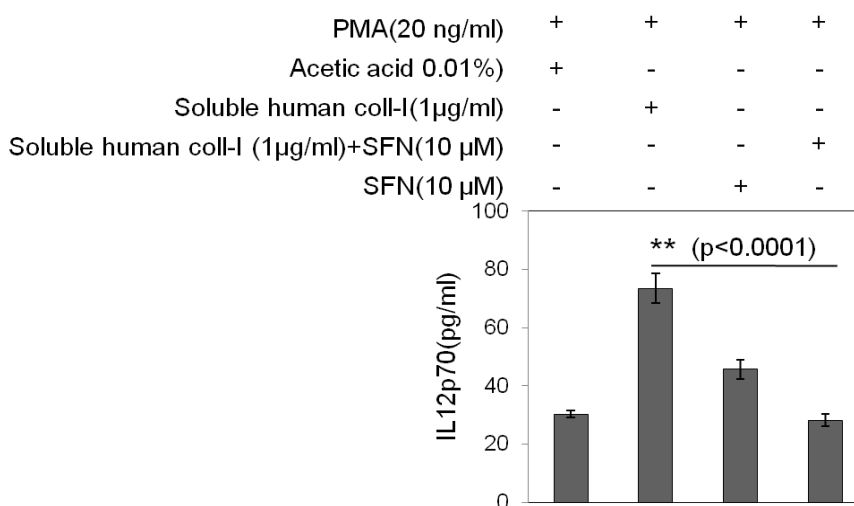
Fig. 4.20. Soluble human collagen-I draws functional differentiation of THP1 monocytes. Like M1 inducers (IFNɣ+LPS) soluble human collagen-I induced functional polarization of M1 type cells (up regulated production of active form of pro-inflammatory cytokine IL12p70). This effect got reversed in presence of SFN together with soluble human coll-I. Asterisk denotes p values compared with SFN treated cells using unpaired-student's t-test. Data are representative of three replicate experiments. coll= collagen.

4.3.6. SFN regulates phenotypes and functional plasticity of *in vitro* polarized, autoreactive M1 macrophages

4.3.6.1. SFN suppresses pro-inflammatory, endogenous COX-2 in autoreactive M1 macrophages

As described in the **Fig.4.1,** soluble colls (human I-IV or chicken-II) or SFN exposed PMA treated completely differentiated THP1macrophage (after 6 h+72 h from initial PMA treatment) were used to evaluate the effects of SFN on already polarized macrophages plasticity. Western blot analysis with whole cell (differentiated, matured macrophages) protein lysates revealed that observed SFN induced suppression of COX-2 was independent of PMA treatment (washed out after 48 h from SFN treatment) (**Fig.4.21).** Two potential pro-inflammatory biomarkers, iNOS and COX-2 were observed to be elevated in either soluble human coll-I induced or chicken collagen-II induced M1 like cells (**Fig.4.21.a** and **c** respectively)**.** However, in completely M1 polarized macrophages downregulation of iNOS and COX-2 protein expression had been observed only in presence of SFN (**Fig**.**4.21.a, c)** No cells death observed in these already polarized, differentiated,

Results: Cellular responses to phytochemical, SFN

and matured macrophages **(Fig.4.21.b)**. Further experiments also revealed that SFN can switch any

type of autoreactive M1 cells (soluble collagen II-IV induced) into M2 cells **(Fig.4.21.c)**.

PMA (20 ng/ml)	+	+	+	+	+
Acetic acid (0.01%)	+	-	-	-	-
Soluble human coll-I (1 µg/ml)	-	+	-	+	+
SFN(10 µM)	-	-	+	-	+
10 µM SFN (post PBS wash)	-	-	-	+	-

(a)

130KDa, iNOS (M1 marker)

74KDa, COX-2 (M1 marker)

45KDa, β-actin

(b)

(C) Post PBS wash

PMA(20ng/ml)	-	-	-	-	-	-
Acetic acid(0.01%)	+	-	-	-	-	-
Chicken collagen (20µg/ml)	-	+	+	+	-	-
SFN (10µM)	-	-	-	-	-	+
Chicken collagen (20µg/ml)+SFN(10µM)				-	+	-
Post PBS wash	-	-	++	+-	-	-

130KDa, iNOS

74KDa, COX-2

***Post PBS wash**
Addition of chicken collagen (20µg/ml): ++
Addition of SFN (10µM): +-

45KDa, β-actin

Results: Cellular responses to phytochemical, SFN

(d) Soluble human coll(1µg/ml)   -   +(II)   +(II)   +(III)   +(IV)

SFN(10 µM)   +   -   -   -   -

SFN (post PBS wash)   -   -   +   +   +

74KDa, COX-2

45KDa, β-actin

1   2   3   4   5

Fig.4.21. SFN regulates already polarized macrophage plasticity at endogenous level. (a) Western blots demonstrates the status of COX-2 and iNOS proteins in already differentiated (after 72 h) and polarized (SFN/ soluble coll-I induced) MΦs. **(b)** Data obtained from XTT assay demonstrates no cell deaths in all indicated treatment conditions. Error bars represent mean ± SD **(c)** *In vitro* SFN switches soluble chicken collagen-II induced M1 cells. **(d)** Not only soluble human collagen-I, SFN is efficient enough to suppress inflammatory response (COX-2 protein induction) developed by soluble human collagens (II-IV) induced autoreactive M1 macrophages. Coll = collagen

4.3.6.2. SFN increases M2 phenotypic markers in soluble collagens induced M1 population

Similarly surface CD36 (M2), CD197 (M1) and CD206 (M2; mannose receptor) expression on the alreadyM1/M2 polarized but completely differentiated macrophages were determined using flowcytometry. In this study, soluble collagen I-IV exposed M1 macrophages cells were defined as CD197$^+$CD206$^-$ cells whereas SFN exposed M2-macrophages were defined as CD197$^-$CD206$^+$ cells (displayed as dot plots and bar diagrams). With the absolute numbers of macrophages belong to various populations (M1 *vs* M2) were determined**.** Surface expression of the individual receptors were also evaluated and expressed as histograms.

Surface expression of CD197 (M1 marker) was abrogated in SFN induced M2 cells but there was mild induction in the surface expression of CD206 (M2 marker) in those cells (**Fig.4.22.a**). Therefore, the CD197$^+$CD206$^-$ population was found to be extremely less in number in SFN induced M2 macrophages (**Fig.4.22.a**). However, combined treatment with soluble human collagen-I and SFN during polarization also led to generate lesser number of CD197$^+$CD206$^-$ cells as compared to that found in only soluble human coll-I pre-treated macrophage population (**Fig.4.22.a**).

As expected, in soluble collagen I-V induced completely differentiated, matured M1 macrophages, surface expression of CD197 was significantly high but surface expression of CD206 was low. Proportion of M1 (CD197$^+$CD206$^-$) cells was higher than M2 (CD197$^-$CD206$^+$) cells when cells were pretreated with only soluble collagens exposed matured macrophages and SFN exposure to these polarized cells for last 24 h significantly lowered the number of M1 cells. Interestingly, CD36$^+$ cells were found to be significantly higher in numbers in all experimental set ups where the polarized matured macrophages (soluble collagen I-IV pre exposed M1 cells) were exposed to SFN for last 24 h (**Fig.4.22**).

We observed that the number of autoimmune responsive macrophages (CD197^{high} CD36$^{extremely\ low}$ CD206^{none}) are significantly higher only in soluble collagens pre-exposed THP1 derived macrophages than only SFN exposed M2 macrophages (CD197$^{extremely\ low}$ CD36^{high} CD206^{high}) or soluble collagen and SFN co-treated 72 h old completely differentiated macrophages. Further XTT assay had demonstrated that at any experimental condition (SFN treatment together with soluble human colls or alone), matured M1/M2 macrophages remained unharmed (**Fig.4.22**)

Results: Cellular responses to phytochemical, SFN

(a)

CD206 : M2 marker

CD197 : M1 marker

Acetic acid (0.01%)

Solvent control — CD206: 1.03 ± 0.15 — CD197: 2.6 ±1.18

Soluble human coll-I induced M1 cells

M1>M2 — CD206: 0.92 ± 0.15 — CD197: 9.35 ±1.36

SFN induced M2 cells)

M2>M1 — CD206: 4.14 ± 0.44 — CD197: 2.29 ± 0.4

Soluble human coll-I + SFN treated M2 polarized cells + SFN(24h)

M2>M1 — CD206: 1.2 ± 0.66 — CD197: 3.35 ± 1.01

Soluble human coll-I induced M1 cells + SFN(24h)

M2>M1: Plasticity — CD206: 2.16 ± 0.66 — CD197: 4.08 ± 1.5

Results: Cellular responses to phytochemical, SFN

(b)

Acetic acid (0.01%)

SFN (10 µM) induced M2 cells

Soluble coll-I (1 µg/ml) induced M1 cells

Soluble coll-I(1 µg/ml) induced M1 cells + 10 µM SFN(24 h)

Soluble coll-I (1µg/ml) + 10 µM SFN pretreated MΦs

CD36 (M2 marker) expression

(c)

	1	2	3	4	5	6	7	8	9	10
Acetic acid	+	–	–	–	–	–	–	–	–	–
SFN	–	+	–	–	–	–	–	–	–	–
Soluble human coll-I(1µg/ml)	–	–	+	+	–	–	–	–	–	–
Soluble human coll-II(1µg/ml)	–	–	–	–	+	+	–	–	–	–
Soluble human coll-III(1µg/ml)	–	–	–	–	–	–	+	+	–	–
Soluble human coll-IV(1µg/ml)	–	–	–	–	–	–	–	–	+	+
SFN (Post PBS wash)	–	–	–	+	–	+	–	+	–	+

Results: Cellular responses to phytochemical, SFN

(d)

	Control (0.01% acetic acid)	SFN induced M2 cells	Coll-I induced M1 cells	Coll-I induced M1 cells+ SFN(24h)	Coll-II induced M1 cells	Coll-II induced M1 cells+ SFN(24h)	Coll-III induced M1 cells	Coll-III induced M1 cells+ SFN(24h)	Coll-IV induced M1 cells	Coll-IV induced M1 cells+ SFN(24h)
▫% of CD197	6.2	5.1	21.0	8.9	12.3	2.7	7.8	3.1	6.4	3.1
▪% of CD206	3.1	11.6	1.7	6.0	2.5	4.1	1.9	4.3	1.0	5.4

✶✶ M2>M1: indication of effect of SFN on macrophage plasticity
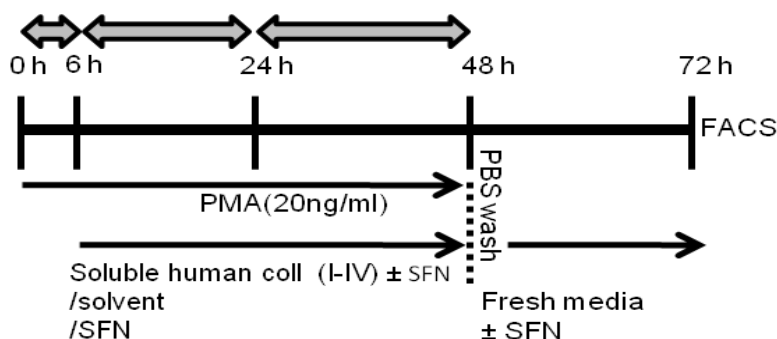
Fig.4.22. SFN regulates phenotypic plasticity of soluble collagen I-IV induced M1 macrophages. (a) Histograms and dot plots are showing the level of surface CD197 (M1 marker) and CD206 (M2 marker) expression on macrophages derived after treating THP1-Mns with indicated doses and combinations of PMA, coll-I and SFN. **(b) Activation of M2 marker, CD36 expression and (c) induction of CD36+ cells number upon SFN treatment:** Matured and polarized macrophages (soluble collagens induced M1 type) were harvested after 72 h from initial polarization and surface CD36 expression (in terms of MFI) and absolute number of CD36$^+$ cells at each experimental condition were determined by flow cytometry. **(d) SFN regulates the number of CD197+ cells (M1 type) and CD206+ cells (M2 type):** Percentages of CD197$^+$ cells (M1 type) and CD206$^+$ cells were determined in the harvested, polarized and completely differentiated macrophages at 72 h. A comparative bar graph is displaying CD197$^+$ and CD206$^+$ cells at each experimental condition (described schematically). Error bars represent mean ± SEM.

Results: Cellular responses to phytochemical, SFN

4.3.6.3. SFN alters cytokine milieu to suppress functionally active auto-reactive M1 macrophages

Not only phenotypes SFN also altered the extra cellular micro-environments of already polarized macrophage populations by regulating the ratio of pro-inflammatory to anti-inflammatory cytokines. **Fig.4.23.** displays the ratio of IL12p70 (pro-inflammatory M1 cytokine) to IL10 (anti-inflammatory M2 cytokine) in all experimental conditions. Amount of IL12p70 was higher in the supernatants obtained from soluble collagen-I and II induced M1 polarized macrophage cultures than that of SFN induced M2 cells [**Fig.4.23.a**]. SFN not only reduced the IL12p70 amount in the supernatants of M1 polarized macrophages but also increased the production of IL10 by those cells [**Fig.4.23.b**]. Altogether, IL12p70 to IL10 ratio was lower in SFN exposed macrophages, at any experimental conditions (**Fig.4.23.c**).
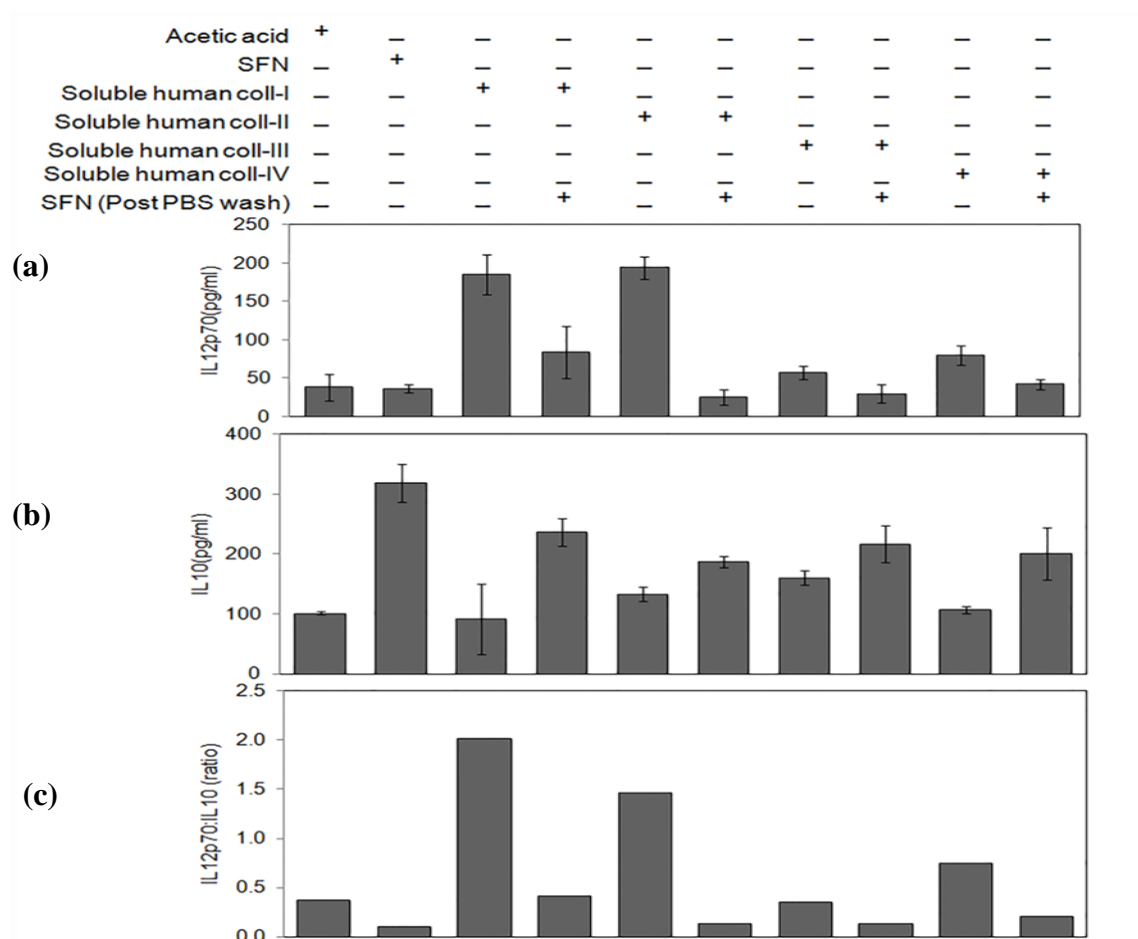
Fig.4.23. SFN modifies cytokine milieu to regulate M1 macrophage plasticity. Quantification of the production of IL12p70 and IL10 and their ratio was obtained by sandwich ELISA for each experimental set up (**described in Fig.22**). Error bars represent mean ± SEM.

Results: Cellular responses to phytochemical, SFN

4.4.   DISCUSSIONS

SFN had been shown to alleviate several effector cells of autoimmune arthritis e.g. autoreactive inflammatory fibroblasts and auto-antigen specific T cells and exerts protective effects. However, the possible cellular mechanisms that SFN adapt to suppress soluble collagen (biomarker for different arthritis) induced inflammatory, highly aggressive M1 macrophages have not been fully elucidated. Therefore, in the present study, we investigated *in vitro* the effect of SFN on monocytes/macrophages mediated inflammatory reaction during autoimmune arthritis conditions. To study the potential molecular mechanisms an *in vitro* monocytes/macrophages based cellular model of collagen induced arthritis condition has been developed.

In immune system, cellular phenotypes (surface protein expression) and activities (cytokine secretion and alteration in endogenous proteins) play important roles to receive or recognize any physiological alteration (e.g. infection or inflammation) as well as display that alteration to the others. Here we studied human monocytes/macrophages specific phenotype and function modulatory activities of SFN and its implication as therapeutic in autoimmunity associated inflammation. All the results demonstrated under the **section 4.4** suggested that SFN not only polarizes THP1 differentiation but also regulates plasticity of already polarized macrophages in favor of M2 type. Experimental results obtained using positive (conventional M1/M2 cells) and negative controls (solvent controls) had also validated SFN's ability in shifting monocytes to macrophages differentiation towards anti-inflammatory M2 type and its potential implication in overall immune suppression. SFN activity outstandingly resembled to the status of IL-4/IL-13-driven alternatively activated M2 macrophages.

SFN significantly inhibited the expression of iNOS and COX-2, attenuated the level of pro-inflammatory cytokine, IL12p70 and elevated the level of anti-inflammatory IL10 at various stages of PMA induced THP derived monocytes to macrophage differentiation. In addition, results also indicated an interesting role of MAPKs, especially MEK-1/2 and JNK1/2 in SFN activity. It was

observed that non-cytotoxic, M2 polarizing activity (suppression of COX-2 accumulation) of SFN is MEK-1/2 and JNK1/2 dependent.

Further studies with this newly developed *in vitro* monocytes/macrophages model revealed that SFN can alter cellular phenotypes especially those surface markers (surface CD14 and CD36) which had been characterized to be associated with M1/M2 polarization and plasticity (surface CD197 and CD206) and are reported to be positively/ negatively involved in soluble collagen induced autoimmune disease pathogenesis.

Cumulatively, this chapter had enlightened the possible implication of SFN in the treatment and control of autoimmune inflammation specifically arthritis (RA/OA) pathogenesis.

Results: Cellular responses to phytochemical, SFN

CHAPTER-5

Non Cytotoxic SFN Regulates Phenotypic and Functional Switching of Spontaneously Differentiating Human Monocytes

Results: Cellular responses to phytochemical, SFN

5.1. BRIEF BACKGROUND INFORMATION

Functional skewing of monocytes also takes place *in vivo* under various physiological or pathological conditions (e.g., chronic inflammation, tissue repair and cancer). As mentioned in previous chapter, *in vivo* the monocytes-macrophages system also exists in at least two distinct phenotypes: classical/pro-inflammatory (M1) and alternative/anti-inflammatory (M2). Similarly their activation states also get influenced by variety of external stimuli (cytokines and microbial products). Despite of such similarities, the human monocytic cell lines (e.g. THP1) and the monocytes isolated from human peripheral blood differ from each other in their ability to get differentiate. Apart from M1 and M2 stimulants, these human monocytic cell line need external agents to get differentiate *in vitro* e.g PMA, MCSF, GMCSF [207, 208]. In addition, i*n vitro* MCSF or GMCSF exposed human peripheral blood derived monocytes get differentiate into macrophages and had been characterized as polarized population, i.e, M2 and M1 respectively [209, 265, 266]. However, i*n vitro* in the presence of animal (e.g. FBS) or human serum, human peripheral blood monocytes can also differentiate spontaneously, more specifically in absence of specific macrophage growth factors e.g. MCSF or GMCSF or PMA [256, 267, 268]. As reports suggested, these spontaneously differentiated monocytes/macrophages also respond in similar fashion, following exposure to conventional exogenous polarizing agents and display all the features of M1 and M2 cells [261, 268].

Spontaneous differentiation found to be more relevant during testing the potential impact of pharmacological interventions targeting macrophage functions. So far, PPARγ agonists, dexamethasone and statins have been shown to promote M2 like polarization, whereas glucocorticoids induce M2c activation state [261, 268, 269]. However, no studies have been conducted so far demonstrating similar effect of SFN on spontaneously differentiating human peripheral blood derived monocytes.

Results: Cellular responses to phytochemical, SFN

Therefore, in the current chapter, spontaneously differentiating, peripheral blood derived human monocytes had been used to evaluate polarizing effects of SFN.

5.2. METHODS

5.2.1. Ethics statement

Kalinga Hospital Limited, Blood Bank Unit and hospital authority collected and provided the bloods drawn from willing (for research purpose) donors. Information of each human subject was protected throughout this study. Bloods was obtained from healthy males who were not undergoing any drug treatment and belong to different blood groups. Blood quality (e.g. hepatitis infection, AIDS) was verified by the competent authority in the hospital.

For the whole studies with human PBMCs, blood was first drawn at blood bank and PBMCs were isolated at Super Religare Laboratories (SRL) Ltd in Kalinga Hospital Limited maintaining proper ethics.

5.2.2. Peripheral blood mononuclear cells (PBMCs) isolation

PBMCs from each donor blood were isolated using HISTOPAQUE® 1077 (#0219083780 MP biomedicals). At first collected blood samples were diluted with (1:1) with PBS (usually 25 ml blood + 25 ml PBS). Histopaque 1077 (5 ml solution) were added to the 15 ml tube and mentioned diluted blood samples (9 ml) were layered carefully on the top of it. It is important not to mix the blood and Histopaque solution. Then this two layered solution was centrifuged at 400x g for 40 minutes at 24°C. Following centrifugation 4 layers were appeared, in order from the top: plasma/serum, white blood cells, histopaque 1077 (transparent) and at the bottom- dark red layer of the erythrocytes and granulocytes. Cellular white fractions comprising lymphocytes/monocytes were collected in a separate fresh 15ml tube and washed twice with ice cold PBS (100x g for 10 min at 24°C). Ice cold PBS prevents the adhesion of the monocytes to the test tube walls. Fresh serum (complete RPMI-1640) containing media was added to the cells after the final washing.

Results: Cellular responses to phytochemical, SFN

5.2.3. *Primary monocytes culture*

Fig. 5.1 has been given as the work plan during the studies performed with human PBMCs. Experiments were performed only when viability (assessed by trypan-blue staining; see **section. 3.1.5**) was found more than 95%. Isolated PBMCs were dissolve in complete RPMI1640 (contains 10% FBS and 1% Pen-strep) media and 2×10^6/ml of them were seeded in each well of a 24 well plate in and incubated for 2 h at 37°C and 5% CO2. Non-adherent cells were removed by washing (twice) with PBS. In next phase, cells were once again kept at 37 °C and 5% CO2 for the indicated time period (mentioned in **Fig. 5.1**).The medium was not replaced throughout the culture period and no further exogenous agent was added until fourth day after seeding in order to allow un-polarized spontaneous differentiation. On fourth day, supernatants were collected and stored at -80 °C freezer. As spontaneous differentiation of monocytes required atleast 7 days to transform into completely differentiated macrophages were cultured up to 5 days at 37 °C in 5% CO_2 to evaluate role of SFN in spontaneous differentiation.
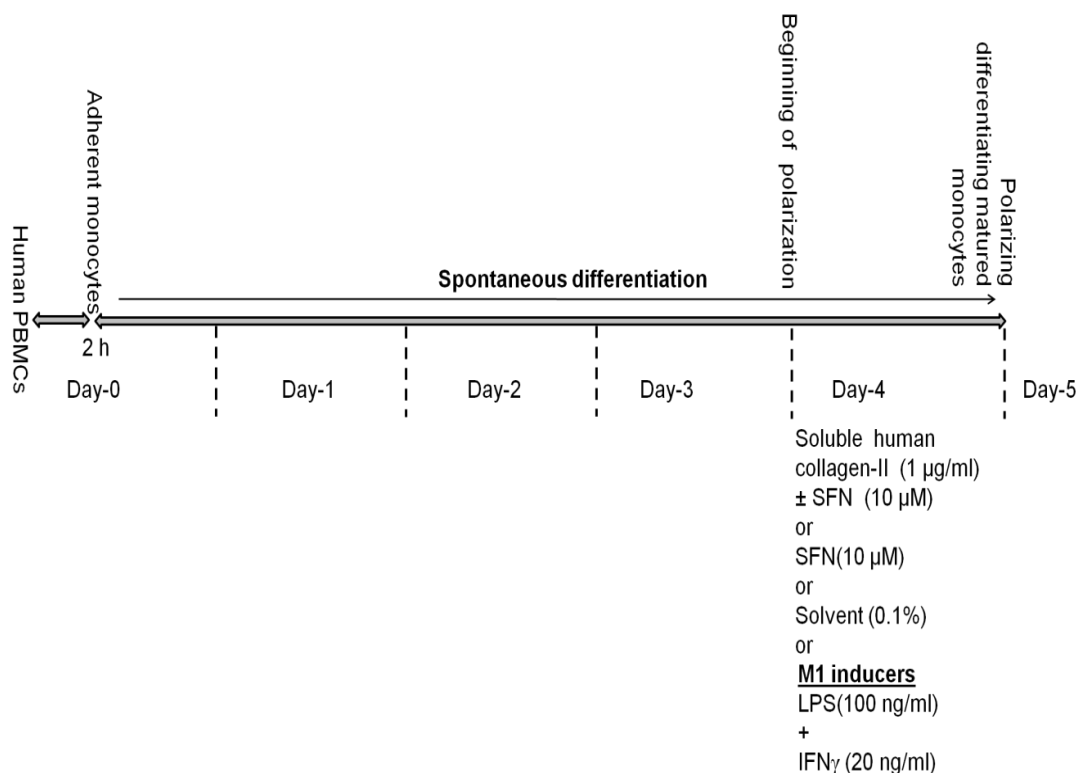
Fig.5.1. Schematic illustration of work plans, chemicals used and respective conc.

Results: Cellular responses to phytochemical, SFN

5.2.4. Protocols for polarization of primary human monocytes

On the fourth day from initial seeding, spontaneously differentiating primary Mns were exposed to M1 polarizers, LPS and IFNγ and incubated for another 24 h. Similarly, soluble human collagen-II and SFN were also added individually or together in culture media (**Fig.5.1**). After 24 h cells were harvested to study the phenotypes and supernatants were collected, followed by stored at -80°C freezer.

5.2.5. Phenotypes determination using flow cytometry

Treated (mentioned at **Fig.5.1**), solvent treated (0.1% DMSO) and floating cells (separated after 2 h from initial seeding) were harvested on day 5. Samples had been prepared (staining, followed by acquisition and analysis) following the protocol mentioned at **section 3.6.1.**

5.2.6. Quantification of cytokine production by ELISA

As mentioned in **Fig.5.1,** spent cell culture media had collected from the polarized (5 day old treated or solvent treated) and unpolarized (4 day old) samples. Quantitative ELISA had performed to determine the desired cytokines productions at each condition, following the protocol mentioned at **section 3.8.**

5.3. RESULTS

5.3.1. Determination of purity of isolated human peripheral blood derived spontaneously differentiating monocytes

Human and mouse blood contains three distinct Mn subsets with differential migratory and functional properties based on expression of CD14 and CD16 antigens. CD14 is one of the most reliable and well established markers of monocytes isolated from human PBMCs.

Purity of the lineage of isolated primary cells was assessed on fifth day from initial seeding by detecting percentages of $CD14^+$ cells in both adhered and supernatant cell population using

Results: Cellular responses to phytochemical, SFN

flowcytometry. Statistically analyzed results suggested that following staining with optimized conc. of fluorophore tagged anti human CD14 antibody on 5 th day more than 70% adherent cells were found to be CD14$^+$. However, less than 20% cells were appeared to be CD14$^+$ monocytes in supernatant fractions (separated after 2 h from initial seeding).
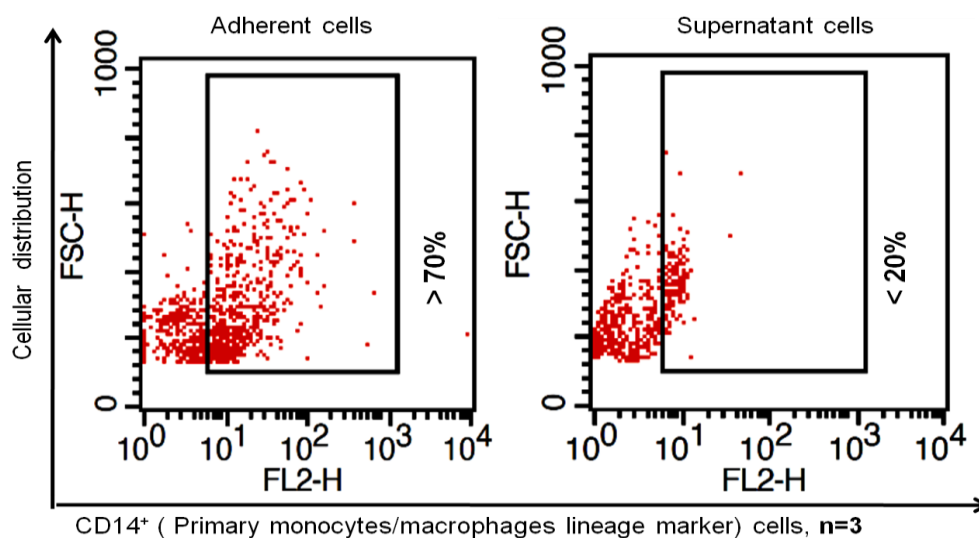
Fig.5.2. Flow cytometry based purity assessment of spontaneously differentiating primary human monocytes. Staining was performed with spontaneously (grown in absence of external M1/M2 inducers) differentiating 5 days old monocytes

5.3.2. *Effect of SFN treatment on M1 specific phenotypic marker expression on human peripheral blood derived, spontaneously differentiating monocytes*

M1 macrophage lineage specific marker, CD197 was selected to determine role of SFN in skewing polarization of spontaneously differentiated primary human monocytes. It has been observed, in terms of percentages of 10000 gated populations, CD197$^+$ M1 polarizing spontaneously differentiating primary human monocytes were generally low (3.1 ± 1 %). It also observed that conventional M1 polarizers (LPS and IFNγ at optimized conc.) had induced CD197$^+$ cells number (10 ± 1%). Another efficient *in vitro* auto-reactive M1 polarizer, soluble human collagen-II also showed to induce the accumulation of CD197$^+$ M1 polarizing cells (8 ± 0.7%). However, in presence of non cytotoxic conc. of SFN (10 μM) alone or together with soluble human

Results: Cellular responses to phytochemical, SFN

coll-II in culture media, number of those CD197$^+$ M1 polarizing cells became diminished (**see Fig.5.3.b and d**).
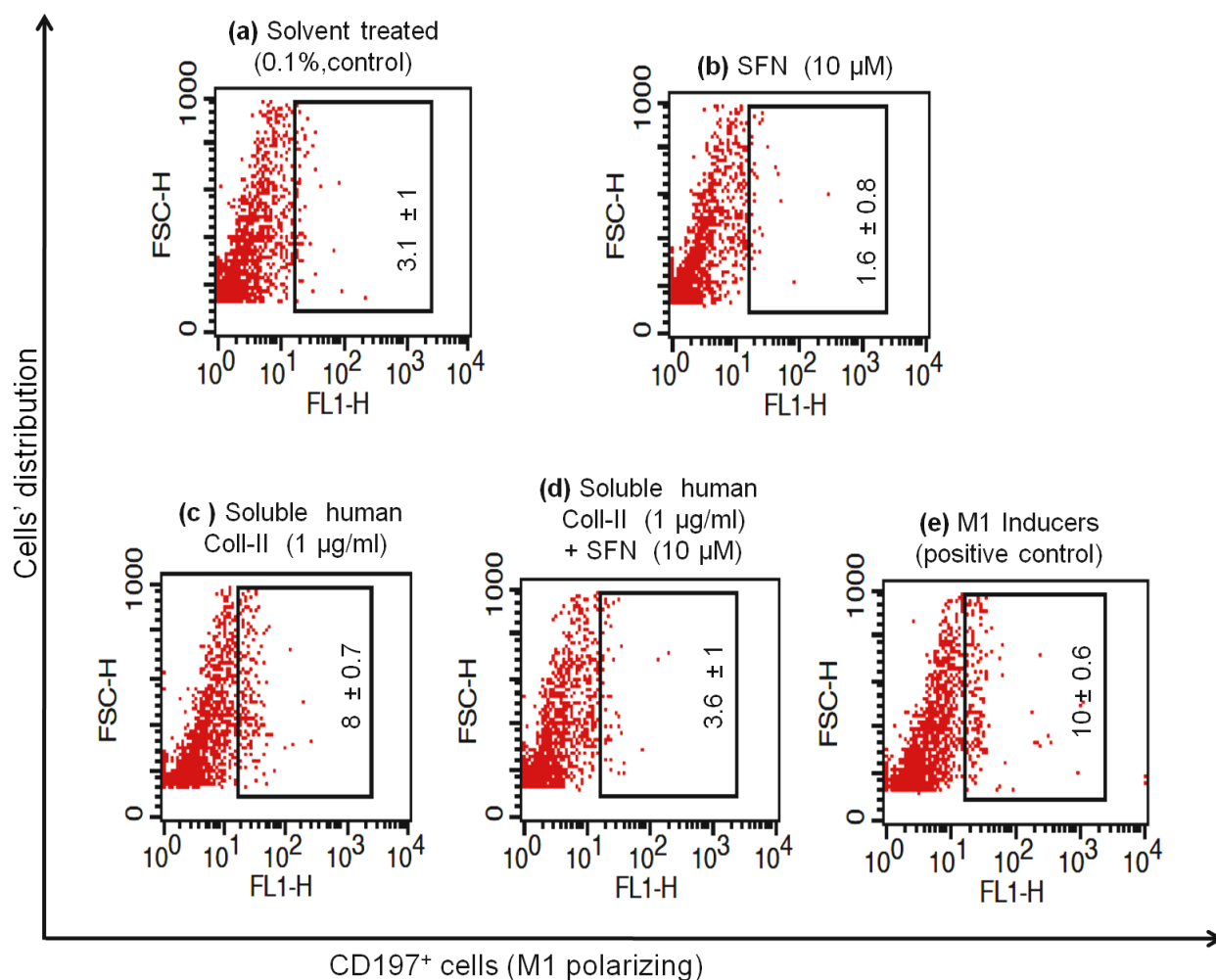
Fig.5.3. SFN prevents spontaneous differentiation of primary human monocytes to M1 type. 4 day old spontaneously differentiating primary human Mns were treated with (a) solvent (0.1% DMSO) (b) 10 µM SFN (c) Soluble human collagen-II (1 µg/ml) (d) Soluble human collagen-II (1 µg/ml) +10 µM SFN (e) LPS (100 ng/ml) + IFNγ (20 ng/ml) for another 24 h (until day 5). Cells were harvested and percentage of M1 polarized cells populations (CD197$^+$) at each treated condition was determined using flow-cytometry.

5.3.3. Effect of SFN treatment on M2 specific phenotypic marker expression on human peripheral blood derived, spontaneously differentiating monocytes

M2 lineage specific marker, CD36 was selected to determine role of SFN in skewing polarization of spontaneously differentiated primary human Mns. In terms of percentages of 10000 gated populations, CD36$^+$ M2 polarizing spontaneously differentiating primary human Mns were found to be comparatively high (48.1 ± 14 %), indicating default differentiation towards partially M2 type . In addition, conventional M1 polarizers (LPS and IFNγ at optimized conc.) had shown to reduce CD36$^+$ cells number (29.3 ± 5%). Another efficient *in vitro* auto-reactive M1 polarizer, soluble human coll-II also showed to reduce the accumulation of CD36$^+$ M2 polarizing cells (29.9 ± 6%) as compared to both SFN treated and respective solvent (DMSO) treated cells. However, in presence of non cytotoxic conc. of SFN (10 µM) alone (58.2 ± 14 %) or together with soluble human coll-II (43.8 ± 10) in culture media, number of those CD36$^+$ M2 polarizing cells showed a significant increase (**see Fig.5.3.b and d**).

Results: Cellular responses to phytochemical, SFN
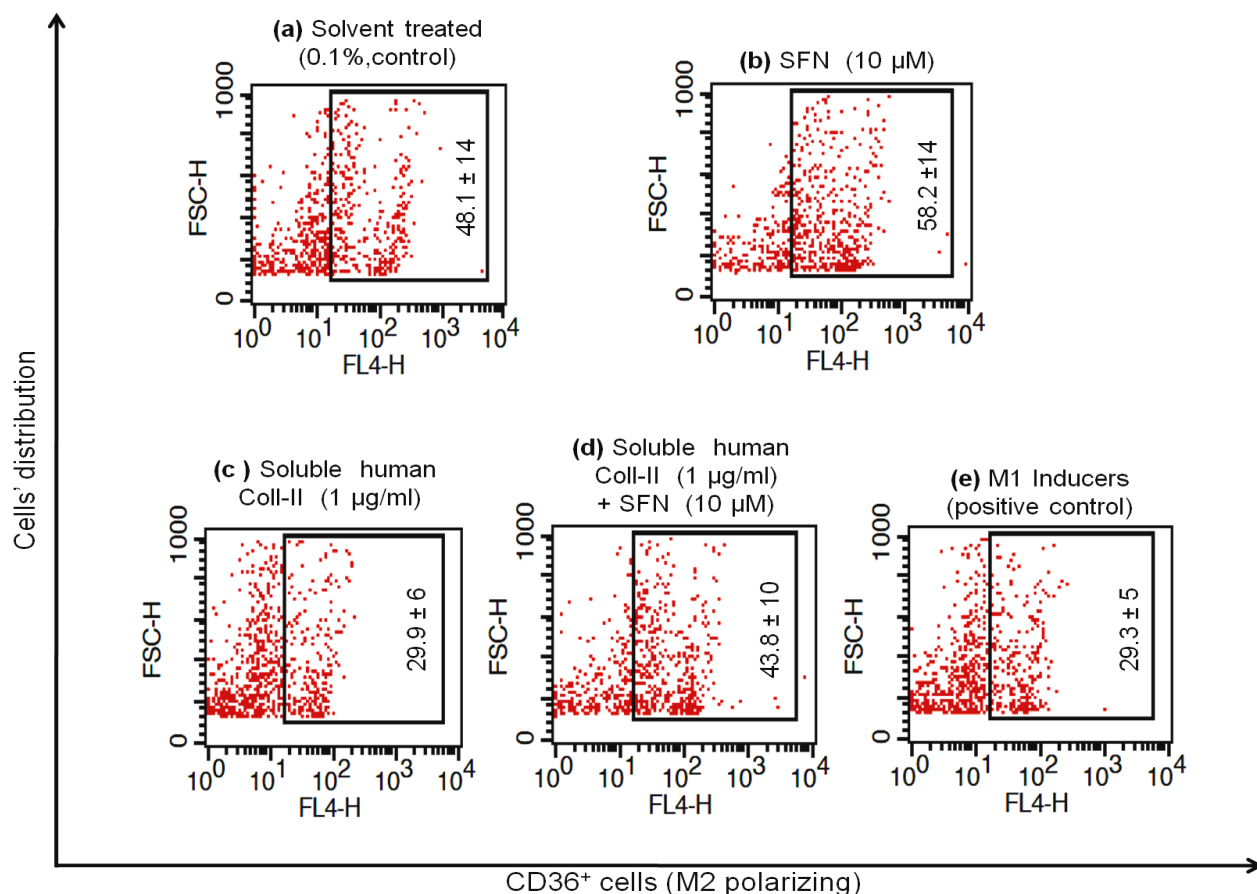
Fig.5.4. SFN skews spontaneous differentiation of primary human monocytes to M2 type. 4 day old spontaneously differentiating primary human Mns were treated with (a) solvent (0.1% DMSO) (b) 10 µM SFN (c) Soluble human collagen-II (1 µg/ml) (d) Soluble human collagen-II (1 µg/ml) +10 µM SFN (e) LPS (100 ng/ml) + IFNγ (20 ng/ml) for another 24 h (until day 5). Cells were harvested and percentage of M2 polarized cells populations (CD36$^+$) at each treated condition was determined using flow-cytometry.

5.3.4. *Effect of SFN treatment on the cytokine productions by human peripheral blood derived, spontaneously differentiating monocytes*

M1 (IL12p70) and M2 (IL10) polarization specific cytokines productions by both unpolarized (4 day old) and polarized (indicated external stimuli exposed 5 day old cells, **see Fig.5.5**) spontaneously differentiating cells were evaluated using sandwich ELISA technique. It was observed that As compared to solvent treated (**IL10:** 48 ± 12 pg/ml, **IL12p70:** 64.1 ± 9.7 pg/ml), conventional M1 polarized (**IL10:** 33.7 ± 13.6 pg/ml, **IL12p70:** 130.5 ± 18.9 pg/ml), autoreactive M1 polarized (**IL10:** 23.4 ± 15.9 pg/ml, **IL12p70:** 121.1 ± 11.5pg/ml),and 4 day old unpolarized cells (**IL10:** 24 ± 7.5 pg/ml, **IL12p70:** 37.6 ± 2.9 pg/ml), SFN treatment alone caused an induction of **IL10** (66 ± 11.5 pg/ml) and reduction of **IL12p70** (27.5 ± 9.5 pg/ml) production by spontaneously differentiating primary Mns. This observed induction of M2 specific cytokine indicated a functional polarization of spontaneously differentiating primary human Mns.

As expected, SFN treatment was proved to be efficient to suppress autoreactive M1 polarization of differentiating primary Mns by increasing the IL10 to IL12p70 ratio in the micro environment when cells were treated with both soluble coll-II and SFN at the begining of polarization (on day 4)

Results: Cellular responses to phytochemical, SFN
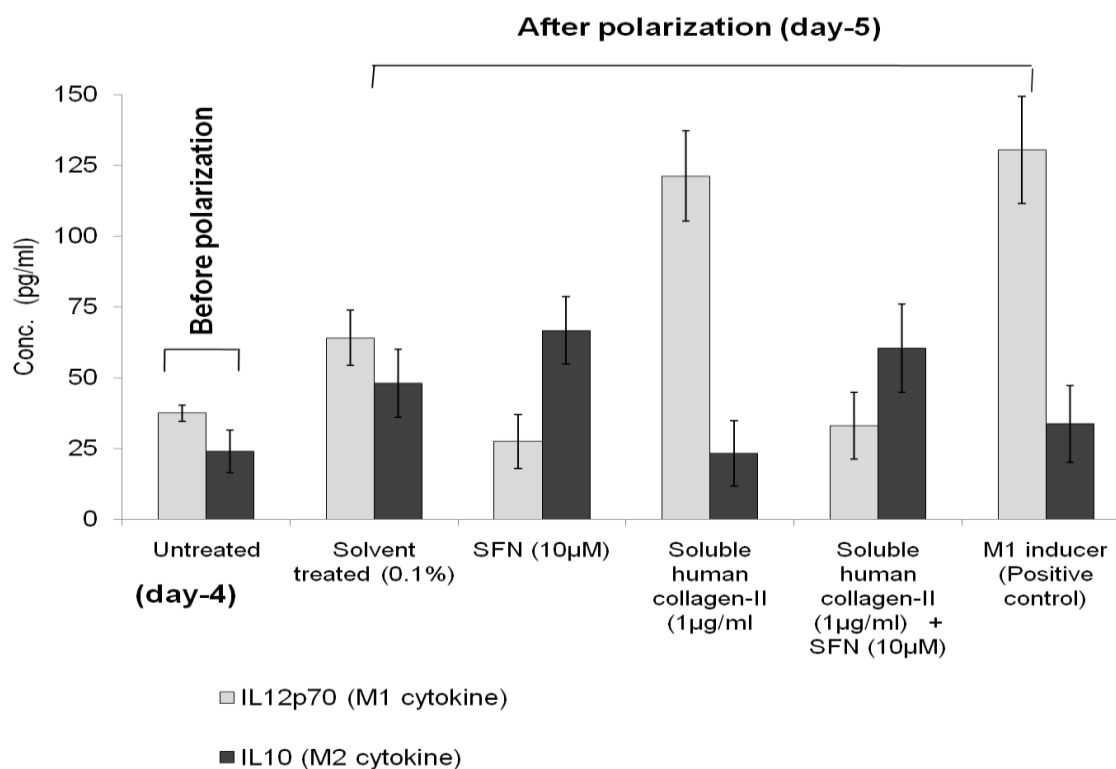
Fig.5.5. SFN alters both M1 and M2 specific cytokines production during spontaneous differentiation of primary human monocytes. Spent cell media consisting of secreted cytokines/chemokines by both 4 day old spontaneously differentiating unpolarized and 5 day old polarized [Soluble human collagen-II (1 μg/ml) or LPS (100 ng/ml) + IFNγ (20 ng/ml or 10 μM SFN or Soluble human collagen-II (1 μg/ml) +10 μM SFN treated) primary human Mns were collected and level of both IL10 (M2 type) and IL12p70 (M1 type) cytokines at each treatment condition was determined using ELISA.

5.4. DISCUSSIONS

In this chapter, polarizing effect of SFN on human peripheral blood derived spontaneously differentiating monocytes had been studied. After assuring the monocyte / macrophage lineage specific purity (CD14$^+$ cells> 70%) of isolated primary monocytes, cells had been employed to examine the previously described M1 and M2 specific surface biomarkers expressions (**Fig. 5.3 and 5.4**) and cytokines production (**Fig. 5.5**). Results suggested that SFN also capable of influencing spontaneous differentiation of primary monocytes and shifts their phenotypes and activity towards M2 type. It had also restrained the spontaneous differentiation to auto-reactive M1 type (by soluble collagen-II) and drifted them to M2 type (CD36^{high} IL10^{high} CD197$^{extremely\ low}$, IL12p70$^{extremely\ low}$).

CHAPTER-6

Regulation of Endogenous *Fas/FasL* Proteins During SFN and

Soluble Human Collagens Mediated Polarization of PMA

Induced Differentiating THP1 Monocytes/ Macrophages

Results: Cellular responses to phytochemical, SFN

6.1.   BRIEF BACKGROUND INFORMATION

Functional interactions between two members of tumor necrosis factor (TNF) receptor super-family, Fas receptor (CD95) and Fas ligand (CD178) majorly act as cell death inducers *via* apoptosis [270, 271]. However, several reports also suggested their apoptosis-independent, immune modulatory activities [272-276]. Any alteration in intracellular control or distributions of this highly regulated system (Fas/FasL) is committed to various disease associated pathogenesis [277-282]. Experimental evidences suggest that altered regulation in Fas-mediated apoptosis in T cells is associated with inflammatory autoimmune diseases and successful Fas-FasL interactions are capable of eliminating auto-reactive T and B cells through apoptosis [279]. Here, the functional implications for Fas and FasL vary depending on their maturation status; whether they are membrane bound or soluble. Both the sFas and/or sFasL act as disease-promoting mediators in autoimmune patients [283-288]. According to experimental evidence, a significant impairment in the activation of Fas/FasL system leads to COX-2 dependent inflammation by the autoimmune responsive cells [289]. Several therapeutic targeting of Fas/FasL system have been developed, only a few reports are available regarding the endogenous regulation of Fas and FasL to prevent generation of auto-reactive macrophages especially during monocytes differentiation, polarization and maturation under the influence of pro-inflammatory auto-immunogenic mediators.

Although cell death (*via* apoptosis) is reported to be a predominant outcome in multifunctional SFN exposed cells, but being a hormetic agent it remains functional (anti-inflammatory and anti-oxidant) even at non-cytotoxic concentrations. Therefore, at non-cytotoxic concentration, SFN capable of regulating the expression or function or post-translational modification of biomolecules those ultimately help to develop immune-suppression without causing any cell death. *In vitro* studies are also revealed Fas/FasL proteins as important target molecules for the induction of two paradoxical events (survival autophagy to apoptosis) by SFN [87, 290-292].

Results: Cellular responses to phytochemical, SFN

A significant increase in macrophage population positively correlates with the degree of inflammation and considered as one of the biomarkers for active inflammatory autoimmune diseases [234]. It is well established fact that autoreactive immune cells (T cell, macrophages) are highly proliferative and resistant to Fas/FasL mediated apoptosis [254, 293-296]. In recent years anti-inflammatory effects of SFN were examined using different inflammatory auto-reactive immune cells but its potential to abrogate the abnormality of Fas/FasL process in auto-reactive monocytes or macrophages remained unclear.

Recently, soluble collagen has used to develop auto-reactive Jurkat T cells (human leukemic T cells) which conferred resistance against Fas-mediated apoptosis [254]. However, any kind of modification in Fas/FasL system in soluble collagens treated *in vitro* differentiating monocytes or matured macrophages has not been evaluated. The classical autoimmune (arthritis) model are developed using chicken type II collagen mediated immunization *in vivo* in genetically susceptible models (rats or mice) [255, 297, 298]. But how far the immune reactivity of chicken can be extrapolated to human collagen is not clear to date. Therefore we used soluble forms of both chicken and human collagens as *in vitro* inflammatory mediators (auto-antigen) for monocytes/macrophages.

In this chapter, attempts had been made to find out any abnormality in endogenous FasL dependent molecular event during *in vitro* differentiation of monocytes into soluble collagens induced inflammatory autoreactive macrophages and also delineate the therapeutic potential of SFN to inhibit such autoimmune conditions.

6.2. METHODS

6.2.1. *In vitro* cell culture

In this chapter, human monocytic leukemic cell line THP1 was maintained, differentiated and polarized into M1/M2 macrophages as described in **Fig.4.1.** in RPMI 1640 medium supplemented with 10% FBS and 1% Pen-Strep at 37 °C in 5% CO_2. Polarizing THP1-Mns (6h+

24 h) or already polarized and differentiated THP1 derived macrophages (6 h+ 48 h) were harvested in ice cold PBS at indicated time points and used for western blotting.

6.2.2. Protein immunoblotting

Freshly prepared total cell extracts of THP1 cells belonging to various maturity and treatment groups were used for the measurement of total protein content, followed by western blotting as described in **section 3.5.**

6.2.3. Statistical analysis

Western blotting for each experimental setup was performed for at least twice-thrice.

6.3. RESULTS

6.3.1. Differential regulation in endogenous FasL protein within M1/M2 polarizing, differentiating monocytes

The presence of 26KDa cleaved products of FasL (one of the key maturation or endogenous control of SFN) have already noticed in whole cell lysates of differentiating matured Mns exposed to indicated concentrations of solvents used to dissolve the polarizers **Fig. 6.1.lane-1, 3**. To examine the existence of any positive or negative effects of soluble collagens (from various origins) and SFN on this particular endogenous process protein-immuno blotting were performed.

. In the following experiment, auto-immunogenic soluble collagens (chicken type-II and human type-I), immune suppressive SFN and respective solvent controls (DMSO and acetic acids) were added to the differentiating THP1 cells. **Fig. 6.1.lane-4 and 5** clearly shows that FasL maturation (formation of 26KDa protein product) process gets hindered in 30 h old THP1 moncytes (6 h PMA differentiating cells were exposed to soluble collagens for last 24 h). However, above mentioned endogenous FasL maturation process remained unaffected (as compared to any solvent control) in similarly differentiating THP1 monocytes those are destined to be immune suppressive M2 macrophages by SFN **(Fig. 6.1. lane-2).**

Results: Cellular responses to phytochemical, SFN

PMA(20ng/ml)	+	+	+	+	+
DMSO (0.1%)	+	-	-	-	-
Acetic acid (0.01%)	-	-	+	-	-
Chicken collagen (20µg/ml)	-	-	-	+	-
Human collagen (1µg/ml)	-	-	-	-	+
SFN (10µM)	-	+	-	-	-

40KDa,FasL

26KDa, cleaved FasL

45KDa,β-actin

1　2　3　4　5
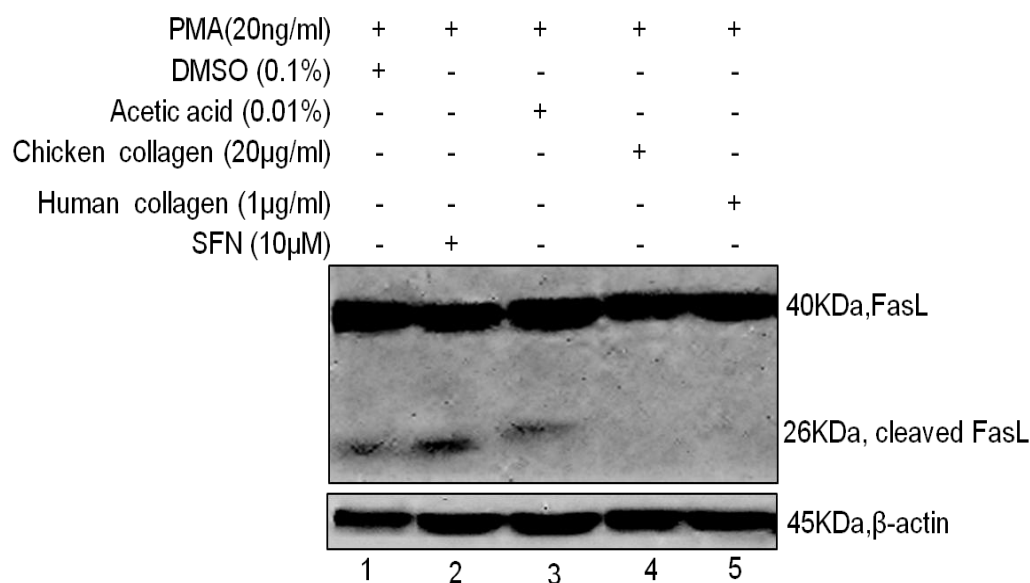
Fig. 6.1. Regulation of FasL maturation in M1/M2 polarizing THP1 monocytes. Soluble collagens inhibit FasL maturation (absence of 26KDa product) in differentiating monocytes (at 24h). However, SFN treatment causes slight increase in mature FasL (26KDa product) formation.

6.3.2. Effect of SFN and soluble collagens on endogenous Fas protein expression

Studies have also been conducted to examine endogenous control on Fas protein accumulation in SFN and soluble collagens treated cells. Whole cell proteins isolated from similar experimental set ups (THP1 monocytes differentiating in presence of either auto-antigen soluble collagen or anti-inflammatory SFN) were separated and western blotting was performed using Fas specific antibody. **Fig.6.2** clearly showcases that endogenous Fas protein expression or accumulation remained almost unaltered in presence of SFN and soluble collagen independently.

PMA(20ng/ml)	+	+	+
Acetic acid(0.01%)	+	-	-
Chicken collagen (20µg/ml)	-	+	-
SFN(10µM)	-	-	+

40KDa, Fas

45KDa, β-actin

1　2　3

Results: Cellular responses to phytochemical, SFN
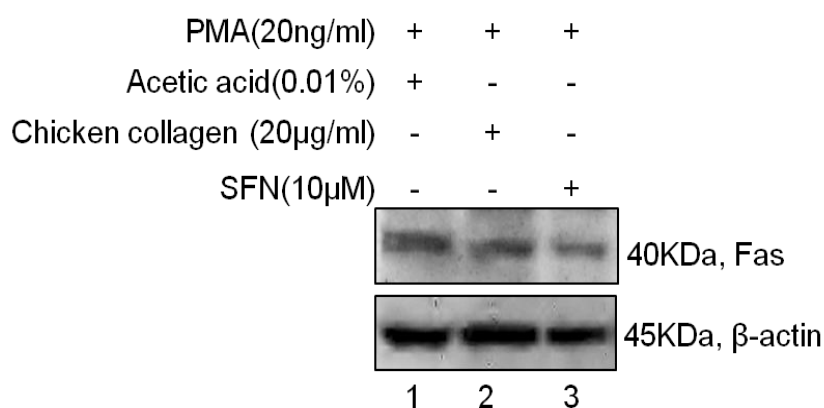
Fig. 6.2. Unaffected endogenous Fas expression during polarized differentiation. Whole cell proteins were collected from 24 h treated (soluble collagens or SFN) and untreated (solvent control) differentiating THP1 derived Mns and western blotting was performed to detect endogenous Fas protein. Data reveals there were no differences in endogenous level of Fas protein in soluble collagen treated or SFN treated differentiating monocytes.

6.3.3. *SFN resumes endogenous FasL maturation in soluble collagens induced auto-reactive M1 macrophages*

Differentiating THP1 monocytes clearly showed existence of differential FasL maturation in presence of different M1 or M2 type external polarizing stimuli. In this study, it has also analyzed whether soluble collagens can completely shut down the endogenous FasL maturation after driving cells to become completely matured, differentiated, auto-reactive M1 type macrophages. Therefore, we performed western blot analysis with the whole cell lysates obtained from completely differentiated but either immunogenic or immune suppressive macrophages.

We observed different degree of accumulation of both 26KDa and 40KDa forms of FasL protein (**Fig.6.3**) in matured, polarized macrophages belong to mentioned treatment groups. According to the observations, accumulation of 26KDa product (cleaved form of 40KDa FasL) is significantly higher in the lysates of SFN pretreated macrophages **(Fig. 6.3.a Lane-5)** than in that of the different soluble collagens pretreated auto-reactive inflammatory macrophages **(Fig. 6.3.a Lane-2, 3).**

However, FasL targeting (especially FasL maturation) anti-arthritic, therapeutic potential of SFN have been determined by co-treating differentiating monocytes with 10 μM SFN and 20μg/ml soluble collagen (chicken) *in vitro*. Due to presence of SFN, these specific pretreated macrophages can resist any inhibitory signals on FasL maturation (exerted by soluble collagen) during differentiation and displayed almost equivalent level of accumulation of 26KDa FasL peptide (**Fig.6.3.a Lane-4**) as compared to only SFN induced M2 macrophages.

Fig.6.3.b is the representative bar graph for the above mentioned differential accumulation of endogenous FasL in different experimental cell lysates.

(a)

Acetic acid (0.01%)	+	-	-	-	-
Chicken collagen (20µg/ml)	-	+	-	-	-
Human collagen (1µg/ml)	-	-	+	-	-
Chicken collagen (20µg/ml)+ SFN(10µM)	-	-	-	+	-
SFN (10µM)	-	-	-	-	+

40KDa, FasL

26KDa,cleaved FasL

45KDa, β-actin

(b)

Density(INT/mm2)

	1	2	3	4	5
☐26KDa	230	164	135	726	910
■40KDa	737	1061	1460	263	446

0 h 6 h   24 h   48 h   WB
72 h

PBS wash

PMA(20ng/ml)

Soluble collagens/
SFN/
Solvent/
Soluble collagens + SFN
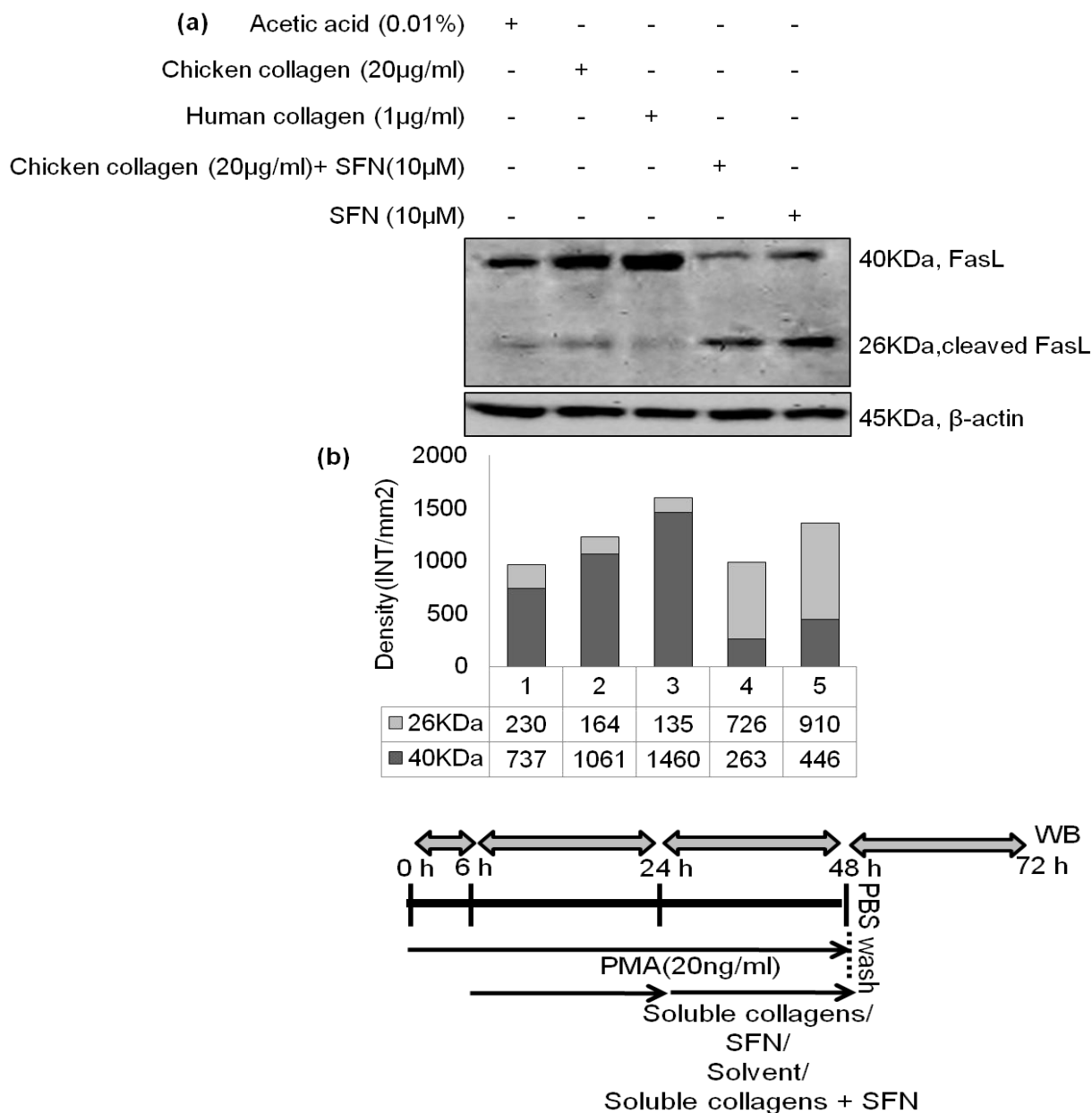
Fig. 6.3. Differential level of FasL maturation in soluble collagens induced M1 macrophages and SFN induced M2 macrophages. a) After 72h from initial polarization, minimal accumulation of 26KDa product was observed only in soluble collagens polarized auto-reactive inflammatory macrophages. However, in presence/absence of soluble collagens, SFN resumes FasL cleavage. **b)** Representative bar graph obtained from the densitometric analysis of each FasL band (both 40KDa and 26KDa) Work plan has been provided schematically.

6.4.   DISCUSSIONS

Abnormal proliferation and/or longer persistence of auto-reactive inflammatory cells at inflamed sites are the characteristic features of several autoimmune diseases. Numerous studies

have already connected altered Fas/FasL system mediated apoptosis with the development of autoimmunity. Delayed Fas mediated apoptosis in auto reactive T cells has already been reported. Not only expression but also altered Fas and FasL maturation, trafficking or secretion may also take part in expanding (by developing apoptosis resistance) any auto-reactive inflammatory immune cells at inflamed tissues. Though a particular population of monocytes/macrophages (M1 type) also participates in disease pathogenesis, yet a very little attention has been given on auto-reactive monocytes/macrophages development and their persistence in the same regards. Above all almost negligible amount of attention has given to study the Fas/FasL maturation process during polarized differentiation of monocytes. Therefore, therapeutic intervention targeting the autoimmunity associated abnormalities in Fas/FasL pathway in monocytes/macrophages may be beneficial for reversing the resistance inflammatory monocytes/macrophages against Fas/FasL mediated death.

In previous chapter, it has been shown how soluble collagens act as stimuli for classical activation (M1 type) in THP1 monocytes differentiation whereas anti-inflammatory SFN shifts the differentiation in alternative pathway and generates a specific M2 type macrophage population. To understand whether endogenous FasL can be a target in auto-antigens (soluble collagens) exposed differentiating monocytes or completely differentiated autoreactive macrophages in general, we examined endogenous status of Fas and FasL in those M1 polarized cells. Simultaneously Fas/FasL targeting therapeutic role of anti-inflammatory SFN was also evaluated.

First, our *in vitro* data revealed that soluble collagens impaired the endogenous FasL maturation process in the differentiating monocytes. For the first time it has been demonstrated that the differential maturation status of endogenous FasL (presence or absence of cleaved product of FasL) in THP1 derived monocytes, differentiating in presence of either inflammatory or anti-inflammatory agents. FasL maturation (cleavage into 26KDa peptide by proteases) process displays a delay in experimental auto-reactive inflammatory macrophages. This delay might have occurred due to induction of inhibitory signal/s on endogenous proteolytic cleavage FasL by inflammatory inducers at the time monocyte differentiation. FasL maturation process returns to its normalcy when

differentiating monocytes were co treated with SFN and soluble collagens. However no significant changes in endogenous Fas level had been found in differentiating monocytes exposed to either SFN or soluble collagens.

Therefore, profound suppression of M1 cells (at the level of polarization and plasticity) and normalization of FasL maturation *in vitro* directly link to the probable protective monocytes/macrophages dependent actions of SFN in autoimmunity. Cumulatively data in current chapter suggested that in the course of development of inflammatory macrophages, the FasL maturation process never gets completely shutdown; only gets delayed. The delay has happened due to initiation of inhibitory signal/s by inflammatory stimuli during differentiation. Though further studies required but results indicated, alteration in FasL maturation process may be one of the reasons (not only) for their characteristic resistance to Fas/FasL mediated apoptosis.

All the observations (**Chapter-4 to 6**) together indicated regulatory roles of anti-inflammatory agent, SFN on FasL maturation process in soluble collagens induced autoreactive inflammatory M1 monocytes/macrophages which schematically presented in **Fig. 6.4**
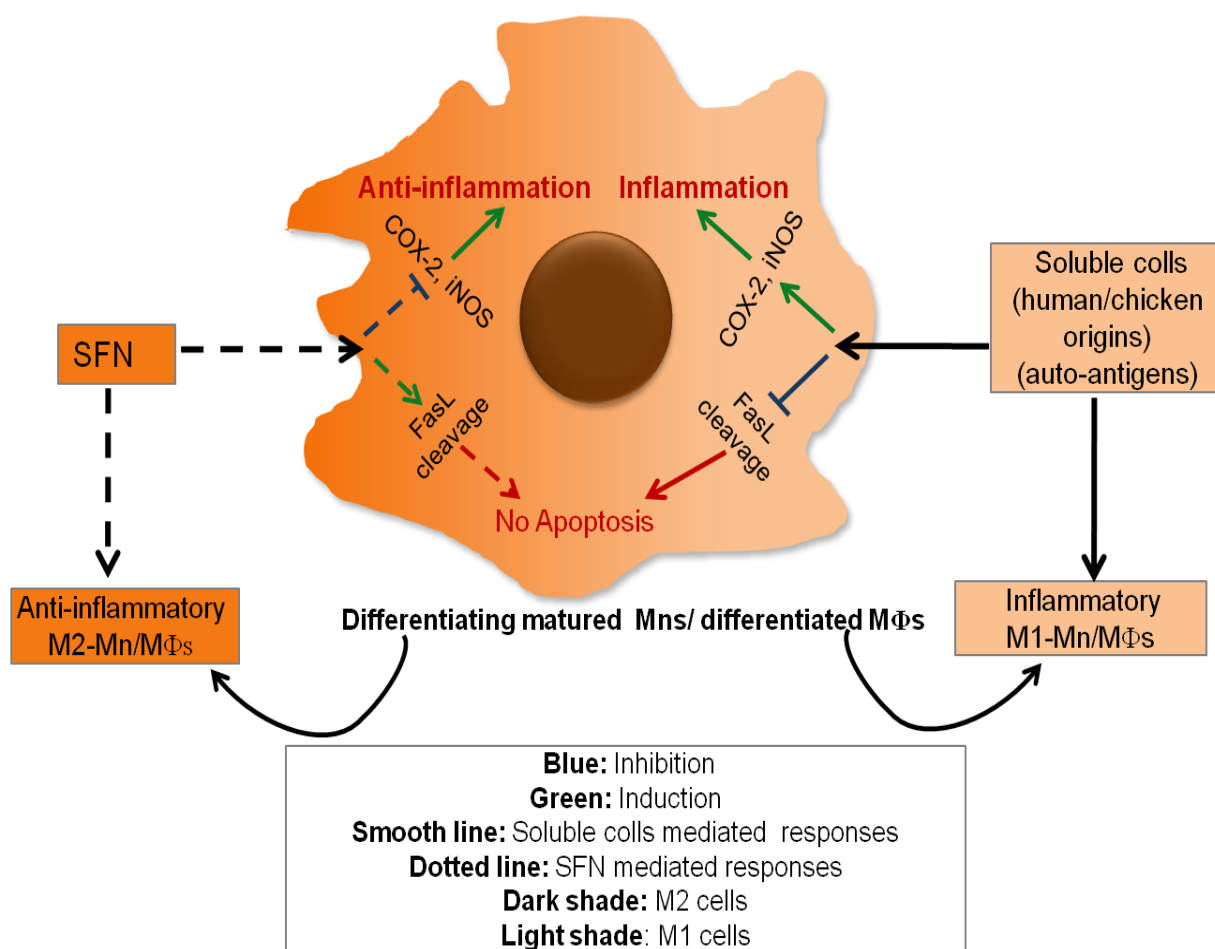
Fig. 6.4. Schematic overview of anti-inflammatory SFN and auto-antigenic, inflammatory soluble collagens mediated regulation during induced differentiation of monocytes. Mn = monocytes, MΦ = macrophage

CHAPTER-7

Screening for Bioactivity and Mechanistic Characterization of Novel, Synthetic Benzo[α]phenoxazines (BPZs) In Different *In Vitro* Experimental Models

Results: Cellular responses to synthetic derivatives of BPZs

7.1. BRIEF BACKGROUND INFORMATION

In cancer cells, chemo or apoptosis refractory mutations at one or more genes often exist and a large numbers of researchers are actively seeking bioactive synthetic/semi-synthetic agents for chemotherapeutic interventions. Most Cancers possess genetic heterogeneity [299], and often relapse following many therapies due to their intrinsic and adaptive ability to evolve as chemo- resistant and immortal [300]. However, every acquired mutation often aids in altering the overall cellular/physiological micro-environments in cancer patients e.g. alterations in the RAS-RAF-MAP2K (MEK)-MAPK signaling are one of the predominant drivers in carcinogenesis. In presence of chemotherapeutic agents, most treatment refractory cancer cells can easily adapt to the through mutations or expression changes of key genes that control drug metabolism or response to damage [300]. It is now well documented that the tumor microenvironments also have an important impact on the success of chemotherapy. Therefore, development of chemo-resistance with predominant intracellular networks maintaining immortality in malignant cells remains a major obstacle to the successful use of chemotherapeutic drugs for cancer therapy.

Cancer cells are expected to be more sensitive than non-transformed/non-malignant cells to any of the chemotherapeutic agents those can halt uncontrolled cell cycle progression and induce cell death. However, in the search for potent synthetic bioactive agents with cancer therapeutic potential, a tendency exists to overlook their adverse effects on non-malignant cells or dismiss weak ligands that could prove effective in cancer prevention following further scaffold modifications. Altogether treatment failures in cancer chemotherapy are common and mainly attributed due to wrong choice of the chemotherapeutics or acquisition of intrinsic resistance passed to the accumulation of mutations within multiple genes. As mentioned in the **section 1.2,** three newly synthesized –Cl/ -CH$_3$/ -H substituted compounds belong to BPZ family have been chosen to establish as selective anticancer agents for two different malignant tissue types over non-malignant cells.

Results: Cellular responses to synthetic derivatives of BPZs

Programmed cell deaths (PCD) referring to apoptosis, autophagy, programmed necrosis and so on are important terminal pathways for cells of multicellular organisms [129]. These death modes commence a variety of biological events including morphogenesis, maintenance of tissue homeostasis, and elimination of harmful cells. Dysfunctional PCDs are intricately associated with cancer development, progression and pathogenesis [301, 302]. Cells undergoing apoptosis, autophagy and programmed necrosis showcase distinct morphological characteristics, intracellular molecular events and physiological processes. Apoptosis (type I PCD) is the major type of cell death after any irreparable DNA damage. Generally suppression of apoptosis triggers autophagy (type II PCD) whereas in other situations apoptosis and autophagy can exert synergetic effects [303].

Induction of apoptosis comprises of two core pathways, the extrinsic– death receptor pathway and intrinsic – mitochondrial pathway [304]. The extrinsic pathway is triggered by Fas-FasL, a death complex. Upon receiving a specific stimulus, Fas/FasL composite gets activated and initiates a signaling array which leads to form death-inducing signaling complex (DISC) with death domain containing protein (FADD) and pro-caspase-8. DISC activates pro-caspase-8, which proceeds to trigger expression of pro-caspase-3, an enzyme for executing the apoptotic process. The intrinsic pathway involves mitochondrial pro-enzymes to induce apoptosis. Following either extracellular or intracellular irreparable insults, outer mitochondrial membranes become permeable to internal cytochrome c, which is then released into the cytosol. Cytochrome c recruits Apaf–1 and pro-caspase-9 to compose the apoptosome, which downstream triggers a caspase 9/3 signaling cascade. Under most circumstances, conclusive endpoint signaling in both pathways involves caspase-3 (cleaved active form is regarded as biomarker) to commence apoptosis.

Autophagy is an evolutionarily conserved, regulated, catabolic, cellular homeostatic process. During this process cells involve lysosomes, membrane bound autophagosomes (LC3II A/B; cleaved form is regarded as authenticate biomarker [305]) to degrade cytoplasmic proteins, macromolecules and organelles, tightly regulated autophagy-related genes (ATGs) and a number of pathways involving Beclin-1, Bcl-2, Class III and I PI3K, mTORC1/C2, p53 [306, 307]. Role of

autophagy in cancer promotion or suppression is always a topic of controversy [308]. According to the available reports, depending on the context, stage of carcinogenesis, cellular micro-environment, cell type or attempted therapeutic interventions autophagy displays contradicting roles e.g either induces malignant transformation or suppresses carcinogenesis [130, 131, 309]. Relationships between autophagy and cancer, a common challenge is to determine whether ongoing autophagy is pro-cell survival or pro- death [310, 311]. Depending on the cell type, especially in fully transformed cancer cells where impaired autophagy is associated with malignant transformation and carcinogenesis, it essentially plays a critical tumour suppressive role [312, 313].

Tumor cells those display resistance to anticancer agents induced-apoptosis may become sensitive upon autophagy inhibition. However, when an extensive autophagic stimulus is activated, cell death *via* autophagy is inevitable [314-316]. Therefore, few cancer cell types tend to undergo pro-survival autophagy and continue to display aggressive growth when put under nutrient stress e.g *in vitro* low serum condition. Meanwhile for an anti-cancer therapeutic intervention, few pro-death autophagy inducers work like tumour suppressors.

Most of the anti-cancer therapies follow apoptotic pathway and related cell death networks to eliminate malignant cells. However, in cancer, occurrence of dysfunctional apoptotic signaling, particularly the activation of anti-apoptotic cell death escaping networks is common and eventually lead to therapeutic resistance and recurrence of cancer. This resistance is a complicated phenomenon that involves presence, interactions of various molecules and signaling pathways. In this comprehensive study two cellular models, COLO205 and MIA PaCa-2 have been chosen to provide a roadmap for the development of successful BPZ mediated anti-cancer strategies that overcome resistance to chemotherapy and apoptosis for better therapeutic outcome in patients with cancer.

Oncogenes, RAS and RAF are parts of the RAS-RAF-MAP2K (MEK)-MAPK signaling and constitutive activation of this pathway is associated with uncontrolled cellular growth, invasion and metastasis [317, 318]. This particular pathway also responds to several growth factors and cytokines.

Results: Cellular responses to synthetic derivatives of BPZs

Mutational activation of either KRAS (Kirsten rat sarcoma viral oncogene homolog) or its downstream key effector molecules, B-RAF (V-raf murine sarcoma viral oncogene homolog B1,a serine/threonine protein kinase) generally appear at the early stage of the carcinogenesis and considered as the powerful treatment refractory prognostic and predictive markers for several cancer types. Either KRAS or BRAF mutation is associated with inferior prognosis in several cancer types. Though a large number of established chemo-therapeutic agents are capable of identifying such altered conditions to some extent but later suffered due to lack of their ability to identify non-malignant cells (causes side effects) and development of resistance after uninhibited application. For this current study, two cancer models e.g colon and pancreatic those have been reported to bear distinct chemo- and death (apoptosis) resistance, have been selected.

Among all the patients diagnosed with cancer per year, colorectal cancer counts are the third (10% of total case) while the corresponding death rate is more than 600000 per year (fourth in worldwide) [319-322]. Recent population based on time trend studies also demonstrated a sudden increasing trend in the incidence of CRC in India [323].

Mutations at either KRAS or BRAF genes are also predominantly present in cancer e.g colon and pancreatic [317, 318, 323, 324]. Most the colon cancer cells harboring such mutations are highly metastatic and non responsive to established treatment regime e.g., monoclonal antibody against EGFR, inhibitors, against mutated gene products, kinases and other established chemotherapeutic agents [325-329]. Occurrence of BRAF mutations are clearly lower than the KRAS mutations (50%) and only observed in approx 15% of colorectal adenocarcinoma [330-333]. Surprisingly, in KRAS wild type metastatic colorectal cancer patients, existence of mutation/s at BRAF often serves as an established marker for poor prognosis [334, 335]. A specific point mutation (c.1799T-A derived; BRAF V600E) within the kinase activation domain of the B-RAF protein is the most common (95% among all types of mutated BRAF) in colon cancer and significantly associated worst cancer specific patient survival [333, 335, 336]. Although targeted treatment of BRAF V600E mutation (specific inhibitors) is demonstrated as beneficial for the survival of the

melanoma patients, in colorectal cancer such procedure is not feasible due to innate resistance harboured by the cancer cells. These BRAF mutated cancer cells and cell lines display the chemo-resistance because of several reasons, e.g, amplification of BRAF genes, altered status of EGFR (elevated expression, phosphorylation, and alternative innate activation via inhibiting CDC25c) [337, 338]. Similar effect has also been demonstrated by the available *BRAF* mutated colon cancer cell lines (COLO205, HT-29) [331, 339]. In this study, COLO205 cell line which showcases above mentioned chemo-resistance served as the background for screening effectiveness of newly synthesized BPZs against BRAF mutated status.

Pancreatic adenocarcinoma is one of the major untreatable and fourth leading cause of cancer death estimated to be <7% worldwide [340, 341]. According to the established phenomenon, concurrent occurrence of highly penetrance mutations in several types of tumor suppressor (e.g. p53) and oncogenes (KRAS, BRAF, PTEN) enable the cancer cells to modulate the controlled signaling network of programmed cell deaths and those mutations are considered as the hallmarks of carcinogenesis [341, 342].

KRAS is a small GTP binding protein which belongs to KRAS superfamily including Rho, Raf, Rac and extensively involved in diverse cellular functions such as cytokinesis, cell motility, cell adhesion and proliferation. Thus constitutive activation of KRAS and its downstream signaling molecules promote as well as aggravate several hallmarks of metastatic tumour [343]. A single point mutation within KRAS gene causes an intracellular stress condition whereby chances of co-existence of several other mutated genes e.g, p53, p16 tend to increase [344, 345]. Several studies report coexistence of significant mutations of KRAS (GTP binding protein which belongs to RAS super family and found almost in >90% diagnosed patients) and p53 (more than 50-70% pancreatic cancer patients) to be one of the critical factors for developing pancreatic cancer associated invasions, resistance to apoptosis as well as chemotherapeutics [344, 346-349]. According to reports almost all targeted therapeutic clinical approaches against mutant KRAS have failed miserably and

these paved the path for the screening of novel anti cancer ligands which may indirectly be effective against pancreatic cancer [341, 346].

Hence extensive studies are going on to perceive the underpinning pathobiology of pancreatic cancer for the development of novel and effective therapies against it. Rosenfeldt *et. al.* has also shown *in vivo* that lack of p53 could aggravate the tumor pancreatic tumour development and progression in mice containing oncogenic KRAS along with functionally impaired or deleted essential autophagy genes, Atg5 or Atg7 [350]. These results indicated that induction of pro-death autophagy might be beneficial alternative approach for the treatment of pancreatic cancer patients lacking wild type p53, KRAS as well as other few wild type genes mentioned and above all extremely resistant to virtually all chemotherapy and radiation induced apoptosis [351-353]. Despite of few promising published results at the preclinical stage, introduction of novel therapeutic approaches for such condition is still required. In this study, newly synthesized BPZs have been screened in MIA PaCa-2 cell line which bears characteristics of both chemo- and apoptosis-resistance simultaneously [215, 216, 354, 355]. Apoptosis resistant pancreatic ductal adenocarcinoma cell line, MIA PaCa-2 (p53-R248W, KRAS-G12D, mutated DPC4 /SMAD family member 4 and CDKN2A / p16 / p16INK4a) also exhibits aggressive growth under metabolite stress (serum free/ low) [356] along with above mentioned chemorefractory characteristics [216, 357-359]. Published information on the genotype of pancreatic cell lines bestows a background for screening of novel compounds with prominent cytotoxic effect against such chemo and apoptosis resistance.

In **chapter-7** under section **7.3.1** and **7.3.2** we determined potential anticancer bioactivities of three novel benzo[α]phenoxazines/BPZs after evaluating their anti-proliferative effects (promotion of apoptosis or pro-death autophagy) on two malignant cells (COLO205-BRAF-V600E and MIA PaCa-2- p53-R248W, KRAS-G12D, mutated DPC4 /SMAD family member 4 and CDKN2A / p16 / p16INK4a) harboring defined apoptosis and chemorefractory mutations in tumor suppressor genes and oncogenes and a non-malignant cell line, HEK293T.

7.2. METHODS

7.2.1. Chemicals

Three fluorescent BPZ, **1B** (10-chloro-benzo[α]phenoxazine-5-one), **2B** (10-methyl-benzo[α]phenoxazine-5-one) and **3B** (benzo[α]phenoxazine-5-one) synthesized and reported in by Dr. Sunita Salunke Gawali and her lab members. 20 mM concentration of each stock of **1B, 2B** and **3B** was prepared in dimethyl sulfoxide and kept at -20 °C freezer. For every experimental assay, 0.5% DMSO was considered as solvent control.

7.2.2. *In vitro* cell culture

A human colon cancer cell line, COLO205 (BRAF:c.1799T>A or p.V600E), a human pancreatic cancer cell line, MIA PaCa-2 and a non-malignant human embryonic kidney cell line, HEK293T (SV40 large T antigen mediated inactivated wild type p53 but BRAF-wt, KRAS-wt) were maintained in complete growth media as described in **section-3.1.2, 3.1.3, 3.1.4** respectively. During each experiment final FBS concentration was maintained 5% in both types of growth medium.

7.2.3. Cell viability assay

Colorimetric XTT assay was performed to study the anti-proliferative activity of three BPZs (1B, 2B and 3B) on the above mentioned two malignant cell lines and one non-malignant cell line. The percentage viable cell (as compared to solvent treated control) was calculated and concomitantly IC_{50} concentrations for each test compound (also for each cell type) were determined as mentioned in **section 3.10**.

7.2.4. Colony formation assay

To determine bioactive BPZs indeed cause reproductive death of this metastatic cell, growing under serum (5%) stress condition colony formation assay was performed with adhered cell lines, MIA PaCa-2 and HEK293T. Detailed protocol had been discussed in **section 3.11**. As

Results: Cellular responses to synthetic derivatives of BPZs

reported in other studies, the result outcome of this assay is important and can be extrapolated to assess the *in vivo* tumour growth inhibitory abilities of these compounds.

7.2.5. Quantitative Cellular uptake assay using flow cytometry

In order to quantify the cellular uptake and retention kinetics of the testes BPZs in all three cell lines, flow-cytometry had been done. Detailed protocol for this study had been discussed in the **section 3.6.2.**

7.2.6. Qualitative cellular uptake and determination of intracellular localization using fluorescence microscopy

In order to visualize the fluorescent BPZs are getting internalized into cells, fluorescent microscopy technique had been used. Detailed protocol for this had been discussed in **section 3.9.2**.

7.2.7. Cell cycle analysis

Effects of **1B, 2B** and **3B** on cell cycle progression of both malignant and non-malignant models were studied using flow cytometry. Protocols to obtain histograms based on the DNA contents present as each phase of cell cycle before and after 24 h treatment with BPZ derivatives have been vividly discussed at the **section 3.12**.

7.2.8. Cellular granularity determination assay

Changes in the cellular granularity occur when dying cell follow few non apoptotic cell deaths, e.g. autophagy, senescence. For this study, changes in cellular granularity upon BPZs treatment in a apoptosis resistant model, MIA PaCa-2 have been measured using flow-cytometry. Protocol has been discussed briefly in the following section.

About 1×10^6 cells/ml were seeded in each well of a 24-well plate with complete growth medium (containing 5% FBS) and incubated overnight at 37°C in 5% CO_2. Adhered MIA PaCa-2 cells were treated with either a low dose (5 µM) or a high dose (50 µM) or respective IC_{50} concentrations separately. Following 15 min, 2 h, 24 h of each treatment, cells were harvested with

Results: Cellular responses to synthetic derivatives of BPZs

cold PBS and single-cell suspensions for each experimental set up were prepared. 10000 gated live cell populations were acquired for each set up using FACS-Calibur.

In flow cytometry, auto-fluorescence or side-scattered light (SSC) has been used to determine the changes in cellular granularity or internal complexity. To study the increment in intracellular granularity upon treatment with the three compounds under study along with their accumulation within those highly granular cells, dot plots [auto-fluorescence (SSC) *vs* cellular uptake in terms of percentage of cells under FL-1 channel] were prepared for each experimental sample. Bar graphs were prepared after comparing the percentage of compound accumulated highly granular cells with that of DMSO treated control samples.

7.2.9. Apoptosis determination assay

7.2.9.a. Annexin V-PE/7-AAD assay:

Annexin V/7-AAD assay was carried out using flow cytometry to examine the possibility of apoptosis induction in COLO205 and HEK293T cells in response to the treatment with these compounds. Staining was performed as per protocol mentioned in **section 3.6.3.** Cells undergoing apoptosis after treatment were determined and represented in terms of percentage by comparing test samples with DMSO treated solvent control.

7.2.9.b. DNA fragmentation assay:

For further confirmation and to establish these novel BPZs as cancer type selective pro-apoptotic agent, DNA fragmentation assay was performed.

7.2.9.c. Determination of caspase 3 activation using western blot technique:

Though various independent processes have already been reported, still caspase--3 is considered as the executioner marker for apoptosis induction [219]. In **section.3.2.1**, a detailed protocol had been given to find out whether tested BPZs were caspase-3 dependent apoptotic inducers for COLO205, MIA PaCa-2 and HEK293T cells. An established pro-apoptotic agent staurosporine (MP

Results: Cellular responses to synthetic derivatives of BPZs

biomedicals, Cat no.191400) had been used as the positive control for the experiments performed to detect caspase-3 activation.

7.2.10. Determination of autophagy induction using western blot technique

Induction of autophagy mediated cell death requires a cascade of signaling events comprising of a particular cleaved form of microtubule-associated protein 1A/1B-light chain 3 (LC3) , few enzymes e.g. autophagy-related gene products (e.g. Atg-5, 7, 12, 14), autophagosomes formation [305, 360]. Whole cell lysates of BPZs treated or 0.5% DMSO treated MIA PaCa-2 cells had been used for detecting reliable biomarkers of autophagy, LC3A/B-I/II, Atg-7 and beclin-1. Western blotting was performed (protocol mentioned in **section 3.2.1**) with these cells lysates with a minute modification at the time of transfer (required at 15 V for 1 h) of electrophoresed samples to methanol pre-activated PVDF membrane using semi dry blotter (Biorad)

7.2.11. Data analysis and statistics

`   Statistical analyses were performed using origin-pro Software and microsoft Excel. All data were normalized to control values for each assay and presented as means ± SD (bar graphs) or histograms (obtained from cell-Quest pro software) from an experiment.

7.3.   RESULTS

7.3.1. *Molecular structures of three novel, synthetic and fluorescent derivatives of BPZ*

To screen bioactive chemical entities for the treatment in above mentioned mutated conditions three newly synthesized, redox active, intrinsically fluorescent BPZs, **1B** (10-chloro-benzo[α]phenoxazine-5-one), **2B** (10-methyl-benzo[α]phenoxazine-5-one) and **3B** (benzo[α]phenoxazine-5-one) were collected from Dr. Sunita Salunke. Molecular structures of these three compounds have been displayed in **Fig.7.1.** The complete reaction mechanism of 1B, 2B and 3B synthesis have showcased in **Fig.1.10.** In that scheme, the presented reaction mechanism revealed that BPZ derivatives **1B, 2B** and **3B** were synthesized by Michael addition of the phenolic

Results: Cellular responses to synthetic derivatives of BPZs

hydroxyl groups of 4R-2-aminophenol (R = Cl; **1B**, CH₃; **2B** and H; **3B**) to 2-hydroxy-1,4-naphthoquinone [361]. **1B, 2B** and **3B** are the minor products of the reaction between 2-hydroxy-1,4-naphthoquinone and aminophenol derivatives.
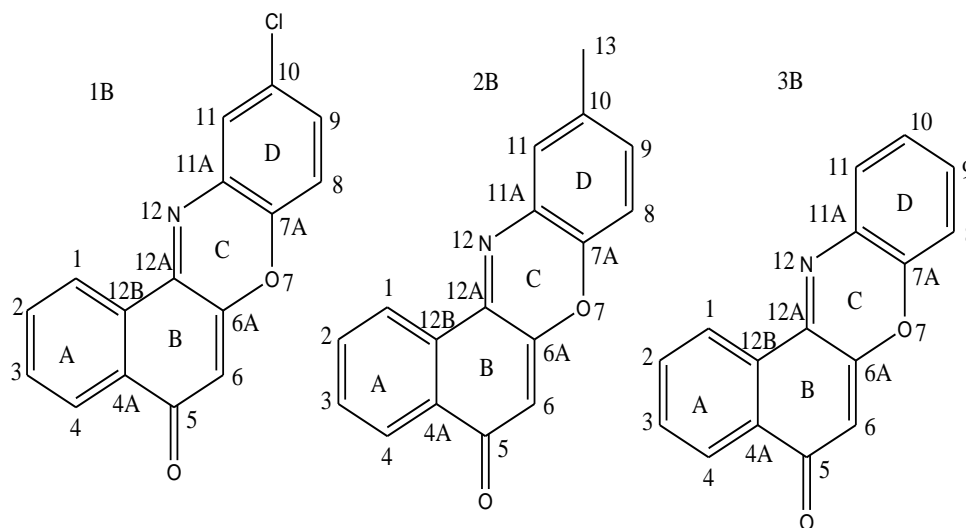
Fig.7.1. Molecular structures of 1B, 2B and 3B

7.3.2. *Evaluation of cytotoxicity, membrane permeability and intra-cellular localization of novel BPZs using in vitro malignant and non-malignant models*

7.3.2.1. Anti-proliferative effects of novel BPZs on malignant (pancreatic and colon cancer) models

Data obtained from XTT assay (Fig.7.2) demonstrated that both 2B and 3B induce dose dependent cytotoxicity only in tumor cells after 72 h from initial treatment. Though differ in IC_{50} concentrations for respective cell lines, **3B** were found to execute maximum level of anti-proliferative activity only on cells with malignant origin, e.g. COLO205 (IC_{50}: 9 μM, **Fig.7.2.a**) and MIA PaCa-2 (IC_{50}: 5 μM, **Fig.7.2.b**). Compound **2B** also exerted anti-proliferative effects on these malignant cells, COLO205 and MIA PaCa-2 with IC_{50} concentrations, 13 μM (**Fig.7.2.a**) and 20 μM (**Fig.7.2.b**) respectively. Another tested compound **1B** showed cytotoxicity on these malignant cells at very high concentration (≥100 μM) but failed to demonstrate any IC_{50} concentration within *in vitro* permissible limit. Altogether these IC_{50} values indicated the order of anti-proliferative effect

of tested BPZs on malignant cells, **3B** >**2B** >>**1B**. Potent anticancer drug, doxorubicin (DOX) had been used as positive control.

Table.6.1. showcases estimated IC$_{50}$ values for each cell and compound type and corresponding working concentrations employed in further experiments.
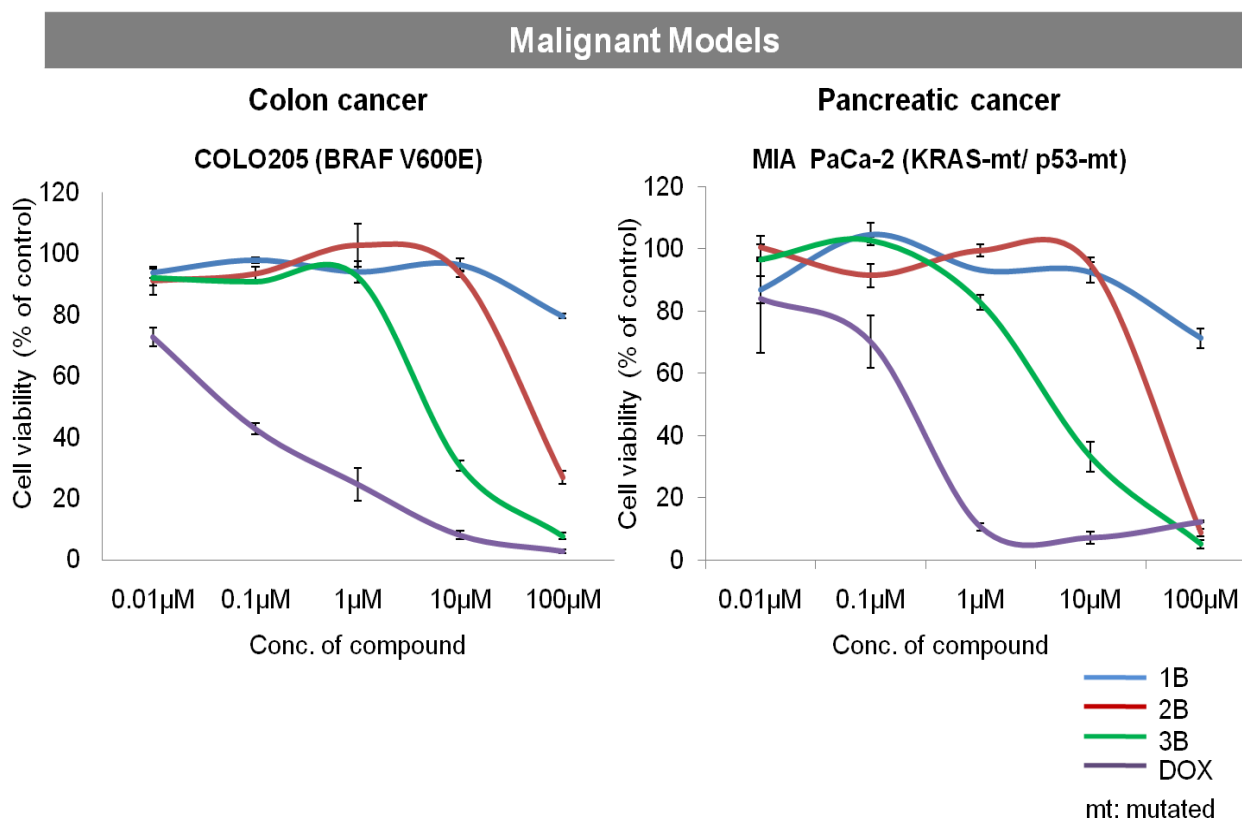
Fig.7.2. Dose-response curve upon treatment of COLO205 and MIA PaCa-2 cell line with BPZ derivatives, 1B, 2B and 3B. As compared to positive control, only 2B and 3B showed anti-proliferative effect on these malignant cell lines.

7.3.2.2. BPZs, 1B, 2B and 3B showed insignificant anti-proliferative effect on a non-malignant (HEK293T) models

Bioactivity activities of **1B**, **2B** and **3B** were also screened using a non malignant cell line HEK293T. However, all these three BPZs showed extremely insignificant inhibition in HEK293T cell proliferation (IC$_{50}$ >100μM, **Fig.6.3**). Therefore, they were considered to be non-cytotoxic for non-malignant cell growth.

Results: Cellular responses to synthetic derivatives of BPZs

Table.6.1. showcases individual compound type dependent IC$_{50}$ values and working concentrations.
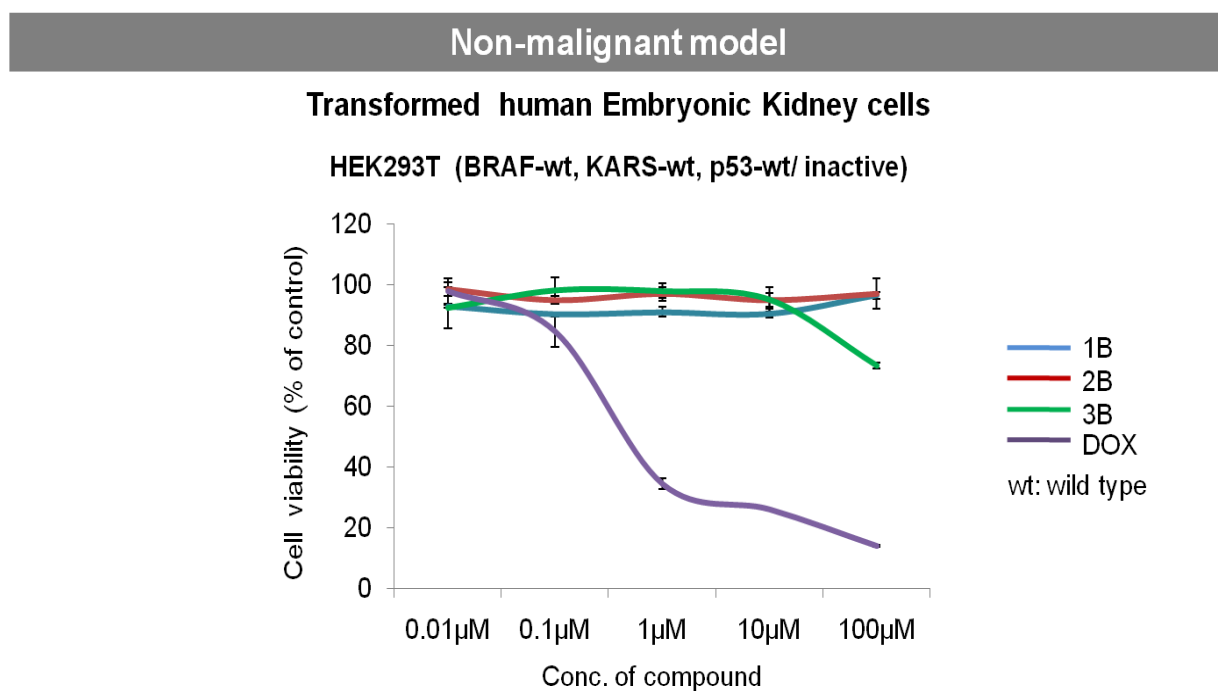
Fig.7.3. **Dose-response curve upon treatment of HEK293T cell line with BPZ derivatives, 1B, 2B and 3B**. As compared to positive control, **1B**, **2B** and **3B** failed to show anti-proliferative effect on this non-malignant cell lines.

Table.7.1. Summarized cell type dependent IC$_{50}$ values and working conc. of novel derivatives of BPZs (M = malignant, NM = Non-malignant)

Cell lines	Type	Genetic background		1B	2B	3B	DOX
				R= -Cl	R= -CH$_3$	R= -H	Doxorubicin
			Ex wl	475 nm	480 nm	470 nm	ND
			Em wl	535nm	538 nm	540 nm	ND
COLO205	M	BRAF V600E, KRAS-wt	IC$_{50}$	>100 µM	13 µM	9 µM	67.8 nM
			Working Conc.	50 µM	13 µM	9 µM	ND
			Remarks	Inactive	Active	Active	Positive control
MIA PaCa-2	M	KRAS-G12D, p53-R248W, SMAD4-mt, p16INK4a-mt	IC$_{50}$	>100 µM	20 µM	5 µM	0.37 µM
			Working Conc.	5 µM, 50 µM	5 µM, 20 µM, 50 µM	5 µM, 50 µM	ND

Results: Cellular responses to synthetic derivatives of BPZs

				Inactive	Active	Active	Positive control
			Remarks	Inactive	Active	Active	Positive control
HEK293T	NM	p53-wt (Inactivated by SV40 large T antigen), BRAF-wt, KRAS-wt	**IC$_{50}$**	>100 μM	>100 μM	>100 μM	0.77 μM
			Working Conc.	50 μM	50 μM	50 μM	ND
			Remarks	Inactive	Inactive	Inactive	Positive control

7.3.2.3. Effect of tested BPZs on colony forming ability of a malignant cellular model for pancreatic cancer and a non-malignant model

The colony formation assay was performed on highly metastatic, MIA PaCa-2 (adhered) and non-malignant/metastatic HEK293T (adhered) cells. MIA PaCa-2 cells were treated separately with three BPZs at *in vitro* concentrations corresponding to low dose (5 μM; for **1B** and **2B** but IC$_{50}$ for **3B**), IC$_{50}$ dose (20 μM for **2B** and 5 μM for **3B)** and high dose (50 μM; for **1B**, **2B** and **3B**) for 24 h. Because of the determined inactivity (**Fig.7.3**), non-malignant cellular model, HEK293T cells were treated with high dose (50 μM) of all three tested compounds.

Reduced or absence of crystal violet stained colonies following 24h treatment and 15 days of maintenance in ligand free fresh media (as shown in **Fig.7.4.a**) firmly confirms a long term irreversible effect (cell death) of bioactive **2B** and **3B** on colony forming ability of metastatic MIA PaCa-2 cells at determined IC$_{50}$ concentrations. The effects observed at the determined IC$_{50}$ concentrations of **2B** and **3B** were extremely significant as compared to the observations where cells were treated at low dose **1B** and **2B**. As expected, colony forming ability of inactive **1B** treated cells remained almost unaltered (at low dose, 5 μM) or mildly altered (at high dose, 50 μM) upon short span of exposure (24 h) and followed by removal.

Similar study was performed with non-malignant HEK293T cells (KRAS-wt, inactive p53-wt) where despite treating them with very high doses of all three compounds (50 μM), their colony forming ability remained unaltered (**Fig.7.4.b**), indicating only malignancy selective bioactivity of

2B and **3B** and their ability to inhibit reproductive growth of malignant cells (here MIA PaCa-2) upon short exposure.

Images of these colonies formed in all treated and untreated samples were captured by phase contrast microscope (Invirogen, USA) and displayed as **Fig.7.4.c.i and ii.**

Results: Cellular responses to synthetic derivatives of BPZs
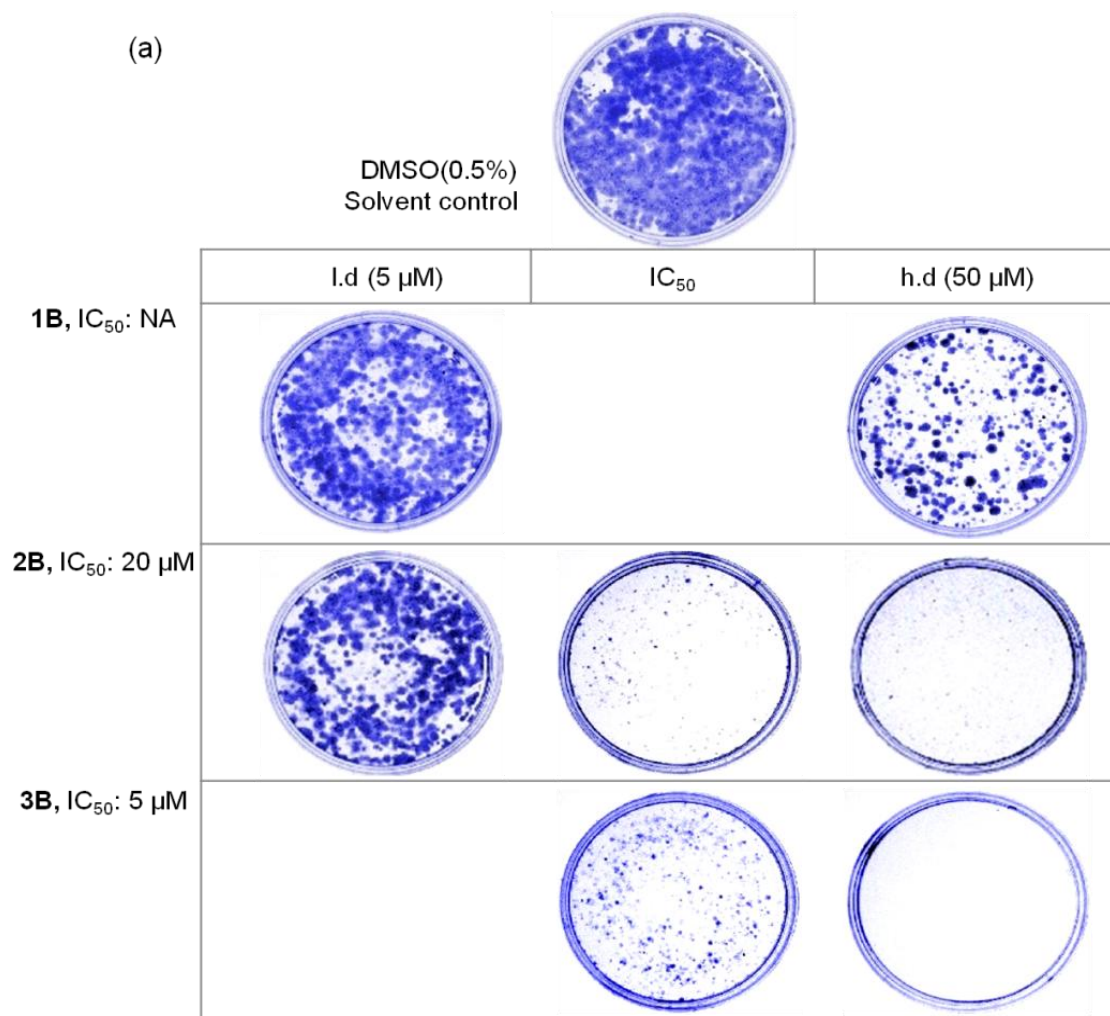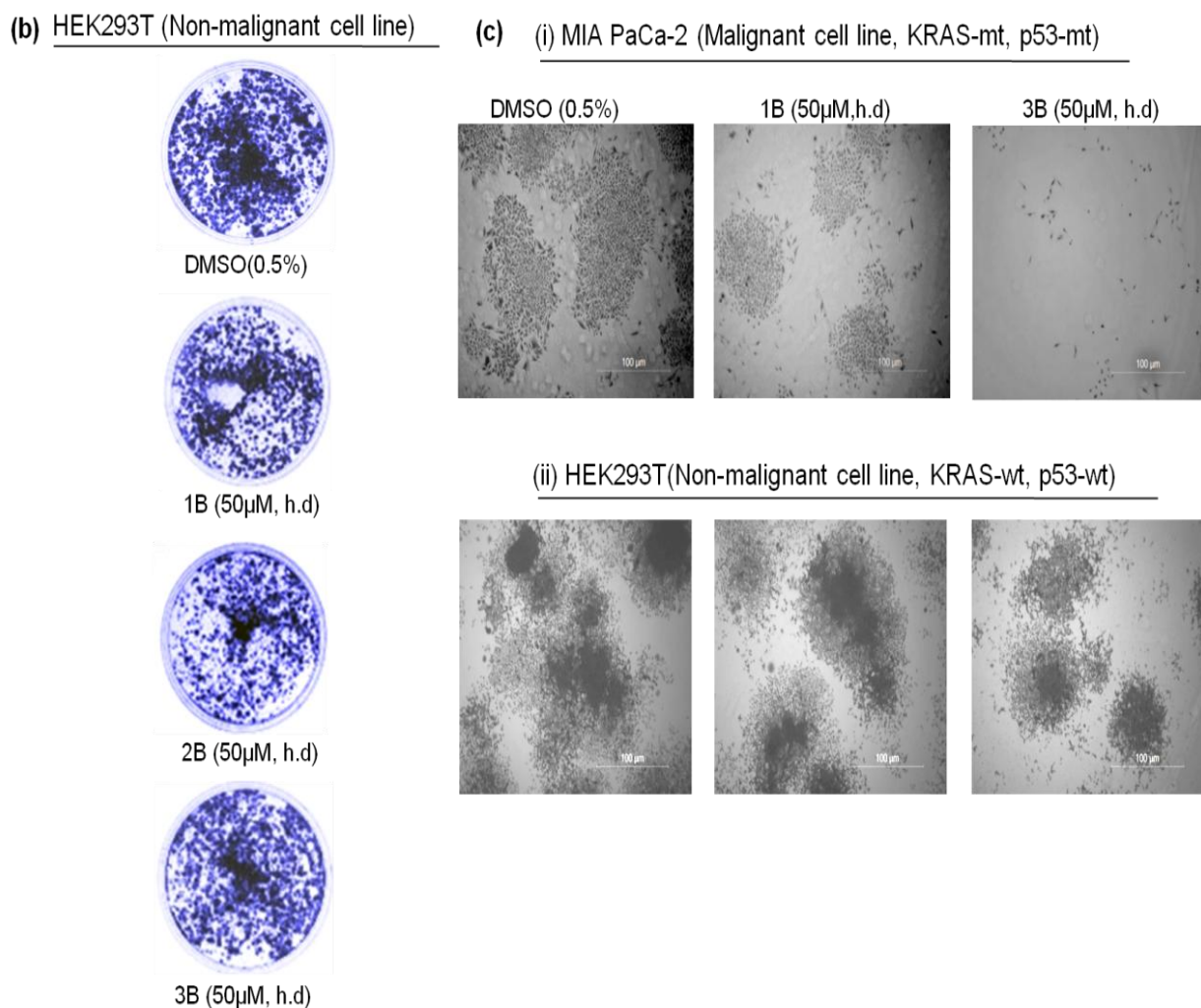
Fig. 7.4. Clonogenic assay of malignant MIA PaCa-2 and non-malignant HEK293T cells treated with BPZ derivatives 1B, 2B and 3B, Photographs of 35mm dishes in a representative experiment are shown. **(a)** Anti-colonogenic effects with different efficiency by **2B** and **3B** on MIA PaCa-2. **(b)** Unaltered colony forming ability in BPZs treated HEK293T cells (c) Images of representative colonies (treated/untreated).

7.3.2.4. Bioactivity, cellular origin, time, and dose dependent internalization of BPZs

A flow cytometry based cellular penetration/internalization and retention determination assay was developed as these compounds are intrinsically fluorescent and their emission spectra are compatible with FL-1 channel (**Table.7.1**) of FACS Calibur. Histograms were prepared based on cell count *vs* MFI obtained at equivalent and compensated voltage for each experimental sample (0.5% DMSO treated, low-5 µM / IC$_{50}$ / high-50 µM BPZ treated three different cell lines) collected

Results: Cellular responses to synthetic derivatives of BPZs

after 15 min, 2 h, 24 h. Later analysis revealed that irrespective to the cellular origin (malignant *vs* non-malignant), all these compounds (**1B**, **2B** and **3B**) penetrated as well as sustained within cells in a time dependent and dose dependent manner.

All three COLO205 (malignant), MIA PaCa-2 (malignant) and HEK293T (non-malignant) cells were treated separately with 50 µM of inactive **1B** and after comparing with the respective solvent (DMSO) treated controls, it was revealed that it had much less uptake for all cell lines at any time point tested. As expected, 5 µM of **1B** treated MIA PaCa-2 cells demonstrated lesser uptake even after 24 h of treatment.

COLO205 (malignant), MIA PaCa-2 (malignant) were treated with corresponding IC_{50} concentrations of bioactive **2B** and **3B** (mentioned in **Table.7.1**) and level of their cellular internalization and retention were estimated (in terms of MFIs) after indicated time points. At these IC_{50} concentrations, both **2B** and **3B** showed significant amount of time dependent uptake and retention (upto 24 h) within these malignant cells as compared to their respective solvent controls. In other experiments, malignant MIA PaCa-2 cells were also treated with both a low (5 µM; IC_{50} for **3B**) and high (50 µM) concentration of both **2B** and **3B.** In every experimental set up, level of both **2B** and **3B** uptake had increased with concentration (MFI were high for 50 µM treated samples than 5 µM at time points) and time of exposure (MFI were high after 24 h than 15 min).

Despite treating HEK293T (non-malignant) cells at a dose of 50µM, that is approximately two to ten times higher than the IC_{50} concentrations used for **2B** and **3B** in MIA PaCa-2 and COLO205 respectively, uptake were either always less (**2B** and **3B** treated MIA PaCa-2), almost the same (**3B** treated COLO205) and high (**2B** treated COLO205) at all time-points (**Fig.7.5**).

(a.i)

(a.ii)

Results: Cellular responses to synthetic derivatives of BPZs

(b)
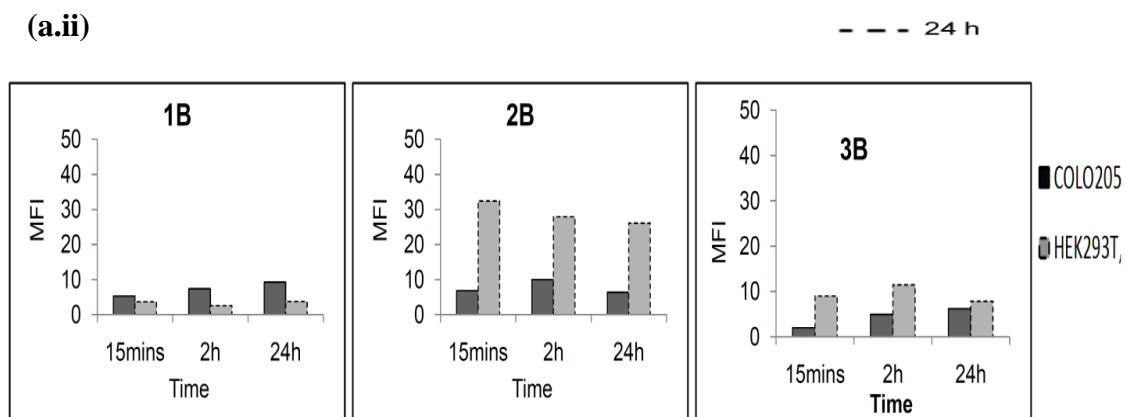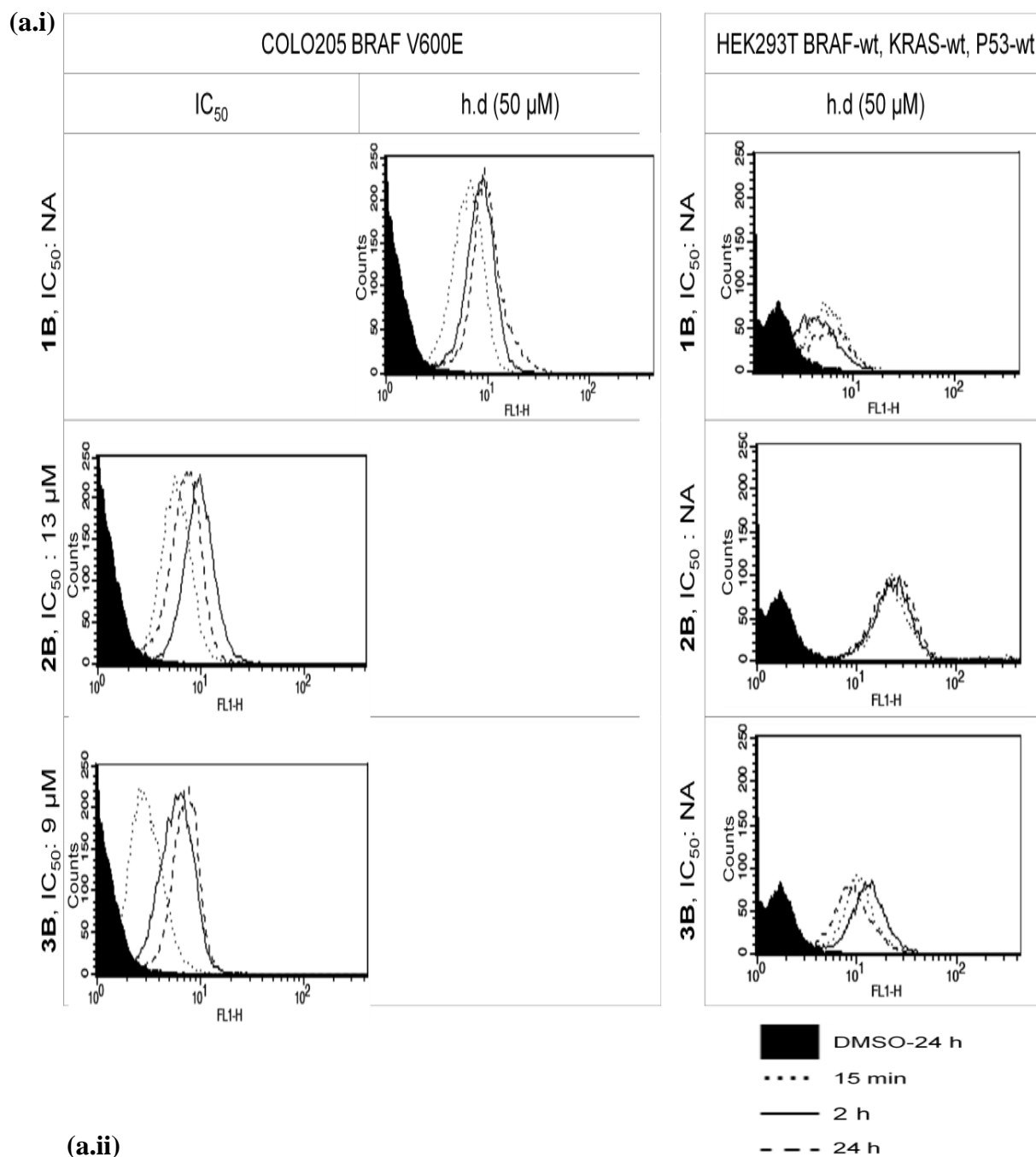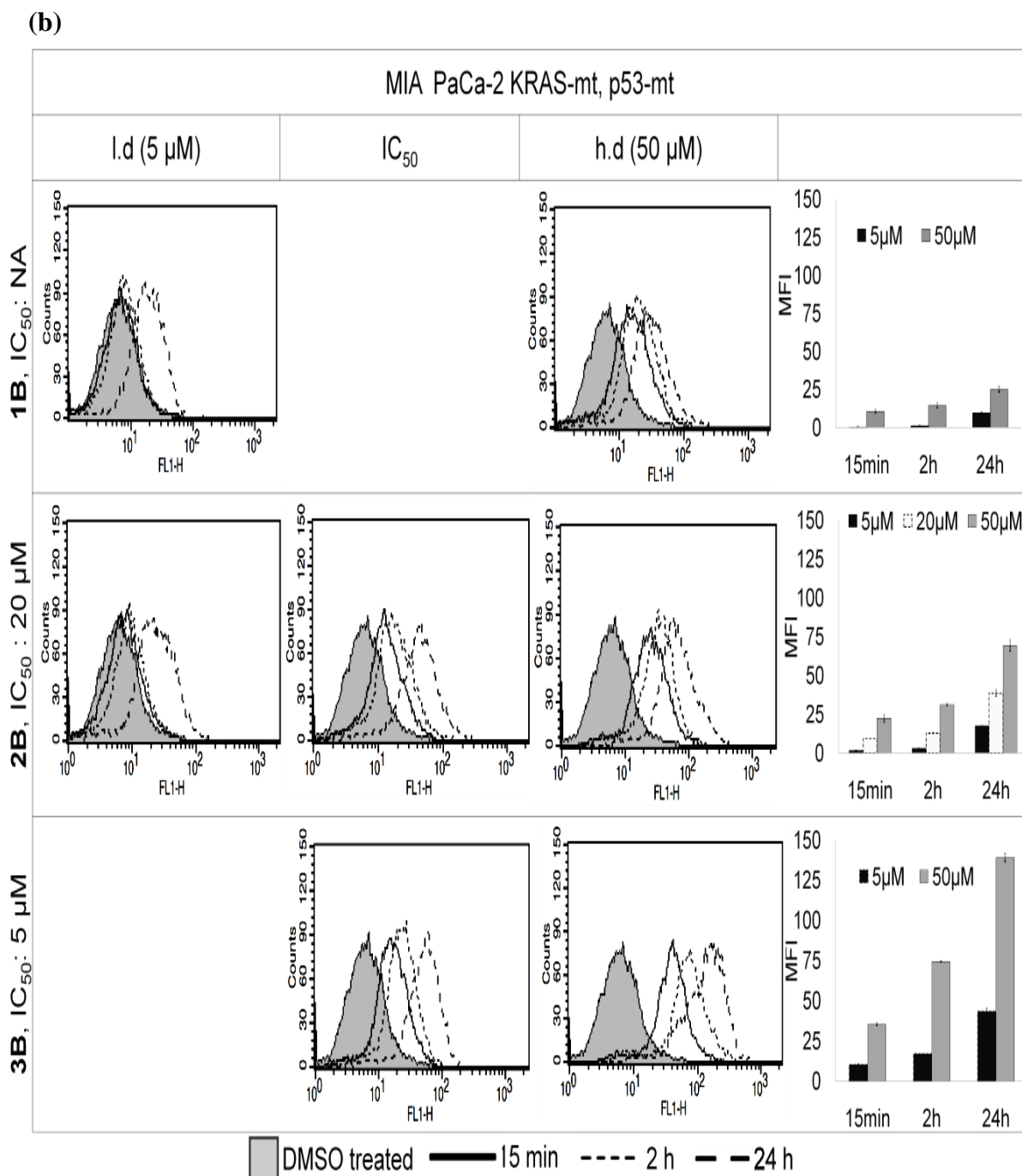
Fig.7.5. Time and dose dependent internalization of BPZs within different cellular models. Cellular internalization of each BPZ was analyzed by flow cytometry. Histograms displayed are showing relative fluorescence intensity (from 15 min post treatment to 24 h) of each BPZ (**1B, 2B**, and **3B** alone) treated and untreated cells for indicated time and concentration. From the data given, it is also confirmed that level of internalization of each compound depends upon the degree of its bioactivity. (**a.i and ii**) A comparative study on differential internalization and retention of BPZs in malignant COLO205 and non-malignant HEK293T cell lines. (**b**) Comparative bar diagrams have been given at the right panel ; showcasing dose and time dependent internalization of bioactive (**2B** and **3B**) and inactive (**1B**) BPZs. Dotted borders in the bar graphs are showcasing the level of compound accumulation within MIA PaCa-2 cells at respective IC50 doses of indicated compounds. h.d: High dose; l.d: low dose.

Results: Cellular responses to synthetic derivatives of BPZs

7.3.2.5. Intracellular localization and distribution of internalized BPZs

Fluorescent microscopic images (green fluorescence) were captured from the slides obtained following 15 min incubation and fixing both malignant and non-malignant cell types treated with the three compounds and solvent DMSO independently (at mentioned working concentrations **Table.7.1**). Results demonstrated an extremely fast cellular uptake for these compounds (especially for bioactive **2B** and **3B**) in all cases. From DAPI stained nuclei, preferential cytoplasmic accumulation of the uptaken compounds was confirmed for all three compounds in each cell lines.

For treated (Data shown for 15 min) COLO205 (**Fig.7.6.a**) and HEK293T cells (**Fig.7.6.b**), cytoplasmic accumulations of these BPZ derivatives were diffused type.   Displayed (**Fig.7.6.c**) fluorescent microscopic images of MIA PaCa-2 cells were obtained after 24 h treatment (15 min data was not shown) with indicated working concentrations of each compound. Surprisingly, cytoplamic distribution of **1B**, **2B** and **3B** within MIA PaCa-2 (malignant, apoptosis resistant) cells were not diffused and internalized compounds were majorly found within some vesicles like structures. These undefined vesicles appeared as bright green fluorescent clusters (indicating BPZ accumulation) and predominantly aggregated within the cytosol. However, accumulation of these tested BPZs within these vesicles like structures in MIA PaCa-2 was found to be dose dependent. **3B** showed extremely high accumulation as well as aggregation of those compound internalized vesicle like structures even at low concentration, 5 µM as compared to other two.

Results: Cellular responses to synthetic derivatives of BPZs

(a) COLO205 (BRAF V600E)

(b) HEK293T (BRAF-WT)

Results: Cellular responses to synthetic derivatives of BPZs
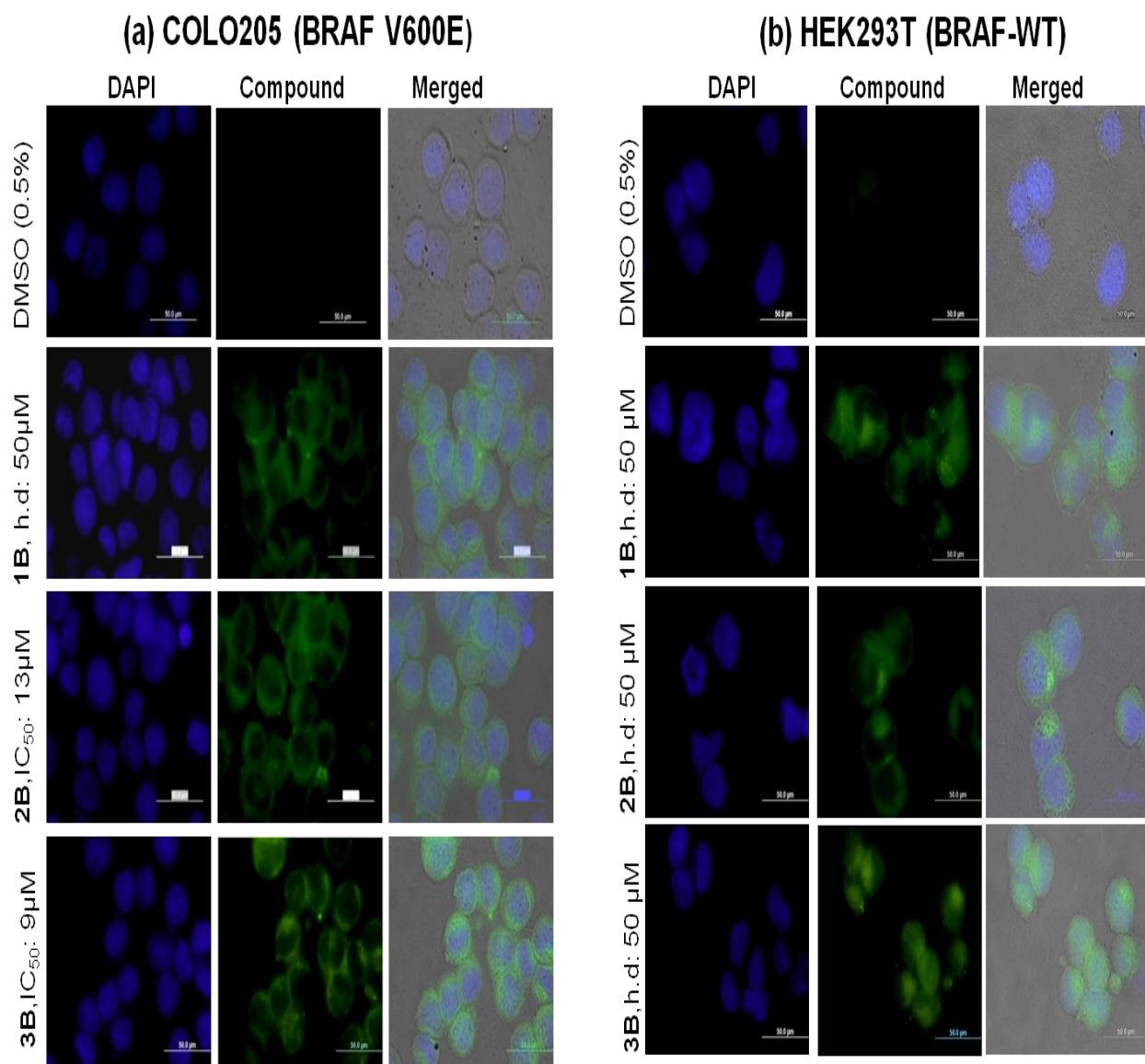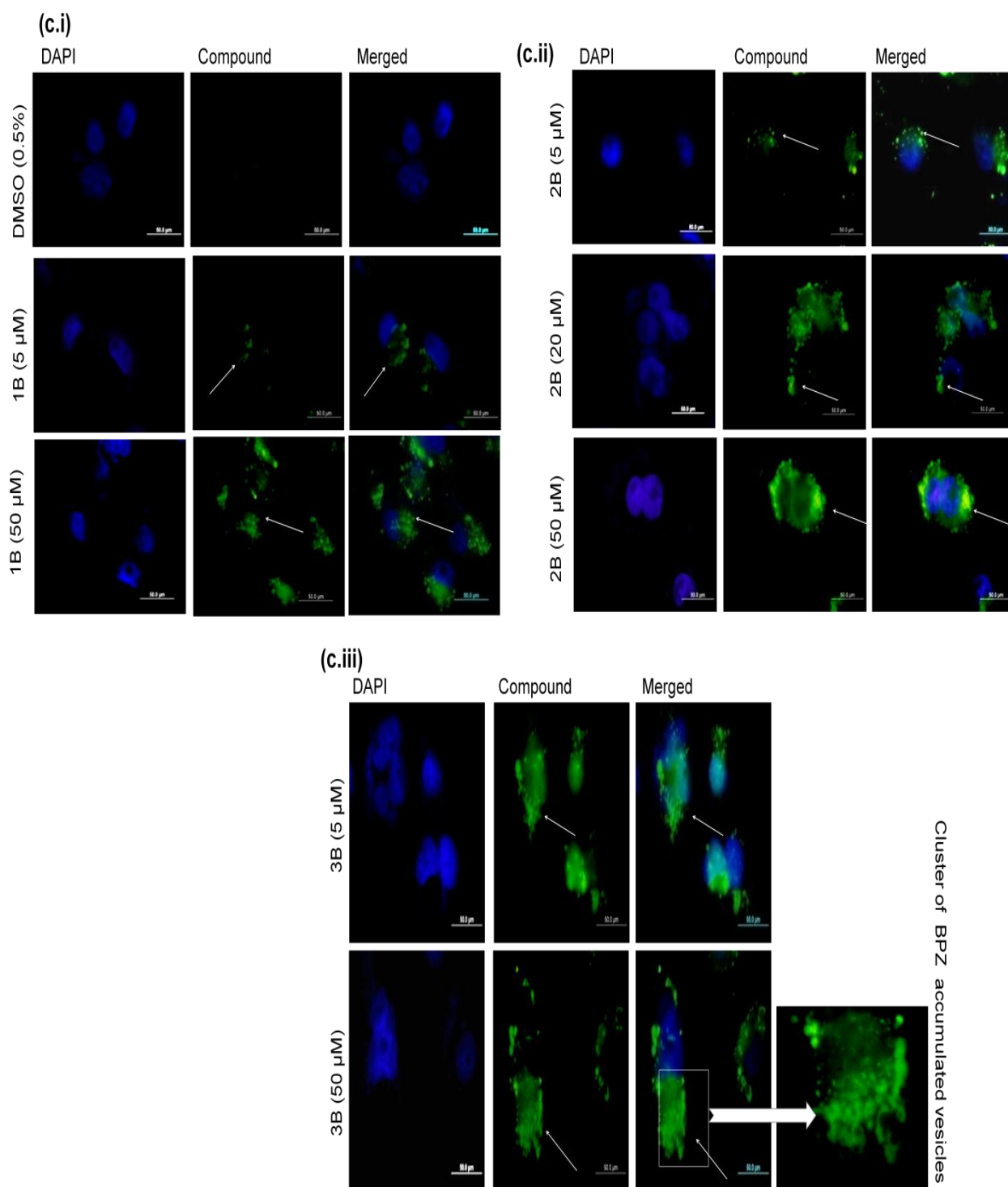
Fig.7.6. Cell type dependent differential intracellular localization and accumulation of BPZs. The fluorescence microscopic images are the representative of 15 min treated or untreated (**a**) malignant COLO205 and (**b**) non-malignant HEK293T cells in which tested BPZs accumulation were cytosolic and diffuse type. (**c**) 24 h treated or untreated malignant MIA PaCa-2 cells showed dose and bioactivity dependent centralized accumulation (within vesicle like structures) of tested BPZs within cytosol. From the images it has been confirmed that after entering inside the cells compounds got accumulated within the unidentified vesicles like structures which appeared as clusters and predominantly aggregated within the cytosol in a dose dependent manner. **White arrows:** Indicating vesicle like structures. **White bold arrow:** Indicating aggregation/clusters of unidentified vesicle like structures

Results: Cellular responses to synthetic derivatives of BPZs

7.3.2.6. Effect of bioactive BPZs on intracellular granularity

Flow cytometry was used to study whether the observed dose and bioactivity dependent clustering of BPZ internalized vesicles like structures concomitantly caused a time and dose dependent increase in intracellular granularity. Both BPZ treated (at respective working concentrations) and respective solvent control (0.5% DMSO) treated MIA PaCa-2 cells were collected after 15 min, 2 h and 24 h from the treatment. Changes in cellular distribution (dot plots as FSC *vs* SSC), increment in auto fluorescence (SSC) associated with altered intracellular granularity and increased in probability of getting highly granular, fluorescent individuals in treated cells as compared to untreated solvent control were sequentially analyzed. Within 24 h of treatment, **2B** and **3B** increases the density (in terms of percentage) of highly granular cells (SSC≥10^2; directly proportional to high intra cellular granularity) in MIA PaCa-2 population in a time (15 mins to 24 h from initial addition) and dose (5 μM, IC$_{50}$ and 50 μM) dependent manner. However, solvent 0.5% DMSO failed to show such effects on MiaPaCa-2 cells. For inactive **1B**, internalization was observed only when treated at high dose for 24 h which have mildly elevated the intra-cellular granularity in treated cells. The densities of compound accumulated granular cells (high SSC, high Fl-1) were found in an order of **3B**>**2B** treated cells and gradually increased with working concentrations as well as time of exposure **(Fig.7.7).** We predicted this increased appearance of number of compound internalized highly granular cells following effective **2B** (≥20 μM) and **3B** (≥5 M) treatment, have positive correlation with the results observed in previously mentioned assays and may also play a role to initiate any specific mode of cell death.

(a)

DMSO (0.5%) treated

l.d (5 μM)   IC$_{50}$ h.d(50 μM)

1B, IC$_{50}$:NA

2B,IC$_{50}$:20 μM

3B, IC$_{50}$: 5 μM

(b)

Post 24 h treatment in MIA PaCa-2

Results: Cellular responses to synthetic derivatives of BPZs
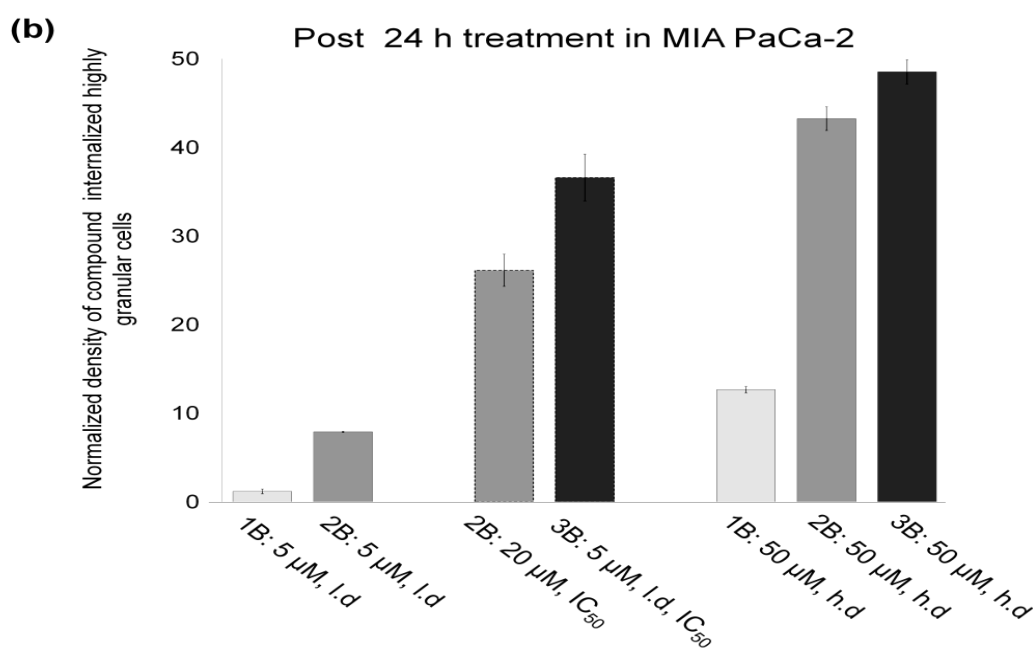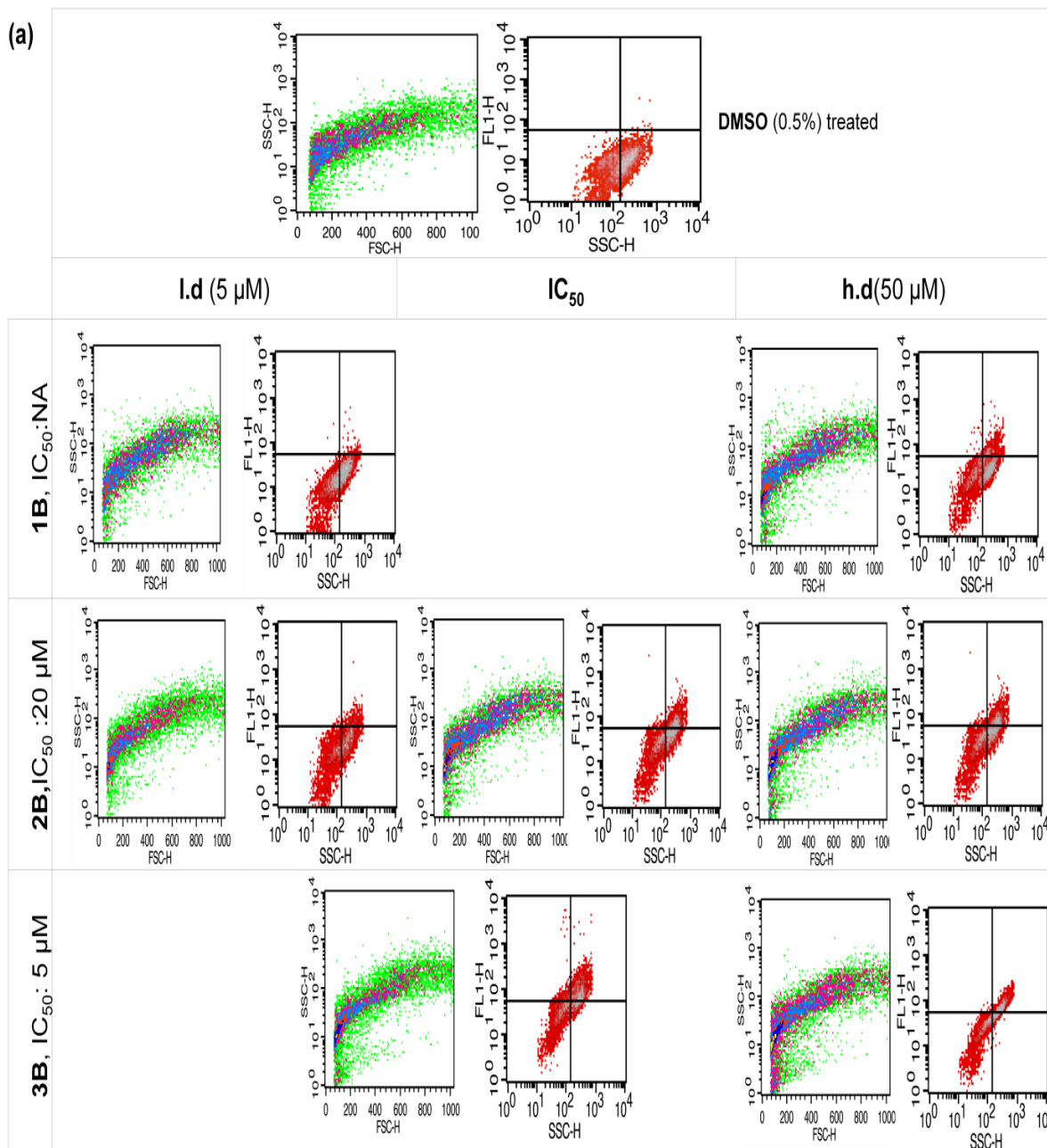
Fig.7.7. Cytosolic accumulation of active BPZs increase intracellular granularity. (a) Above mentioned phenomenon was validated using flow cytometry. We analyzed the changes in auto fluorescence (FSC vs SSC) and increased fluorescence of individual treated cells as compared to untreated solvent control. Within 24 h of treatment, **2B** and **3B** increases the density (in terms of percentage and density distribution) of highly granular cells (SSC$\geq 10^2$; directly proportional to high intra cellular granularity) in a time and dose dependent manner. However, solvent DMSO failed to show such effects on MIA PaCa-2 cells. **(b)** Further analysis have revealed that these compounds generally accumulated within these highly granular cells and such effects occurred in an order of the bioactivity of used BPZs; **3B>2B>1B**. Dotted border in bar graphs represent the IC$_{50}$ doses of **2B** (20 μM) and **3B** (5 μM). After 24 h from initial treatment, IC$_{50}$ concentration (5 μM; lower dose for other two compounds) of **3B** accumulated within a large number of highly granular cells which is significantly higher than that observed in 50μM (high dose) **1B** treated cells or 20 μM (IC$_{50}$) **2B** treated cells. h.d = high dose, l.d = low dose

7.3.3. Evaluation of differential modes of cellular responses to BPZ treatment

Results demonstrated under **section 6.3.2** have provided ample indications of the selective (anti-malignant) anti-proliferative activity of tested derivatives of BPZs. But their cell specific mechanistic mode of actions (induction of cell death) remained obscure. Following experiments have been performed to execute their either pro-apoptotic or pro-death autophagy inducing properties.

7.3.3.1. Cellular origin specific induction of cell cycle arrest by bioactive BPZs

To evaluate the effect of BPZ derivatives in cell cycle distribution of these three model cell lines, the percentage of DNA contents (PI tagged, fluorescent) were measured by flow cytometry. Analysis (**Fig.7.8.a**) had revealed that following 24 h of independent exposure to **1B** (used at a very high concentration; 50 μM) , **2B** (used at IC$_{50}$) and **3B** (used at IC$_{50}$)**,** cell cycle progression of malignant COLO205 cells were inhibited at G$_0$/G$_1$ phase along with accumulation of DNA contents at sub G$_1$ (may be due to either apoptosis or necrosis) stage.

However, data given in the **Fig.7.8.b** displayed the dose dependent cell cycle blocking activity of only **2B** and **3B** in malignant MIA PaCa-2 cells**.** In earlier experiments it was observed that at any concentrations (5 μM, IC$_{50}$, 50 μM) and any time intervals (15 min 2 h, 24 h), intracellular retention ability of **3B** was highest, while **2B** was moderate and **1B** was negligible in MIA PaCa-2 cells. In this experiment it was found that at any concentration (Low/ high dose/ IC$_{50}$) **3B** can block (comparatively weak) cell cycle progression together at G$_0$/G$_1$ and S-phase within 24

Results: Cellular responses to synthetic derivatives of BPZs

h of treatment. While at low dose (5 μM) and also at IC$_{50}$ (20 μM) concentration, **2B** induced only S-phase arrest because of its moderate capacity to get internalized into cells. In addition, high concentration (50 μM) of **2B** initiated mild cell cycle arrest both at G$_0$/G$_1$ and S phase. Though very weak, inactive **1B** enabled to block cell cycle progression only at S-phase when treated at a very high concentration (50 μM). However, active BPZs failed to induce accumulation of apoptotic DNA contents at phase A (unlike COLO205) in MIA PaCa-2 cells. These results indicated different modes of cell deaths in active BPZ exposed malignant cells with differential tissue and genetic background.

Even though HEK293T cells were treated with very high concentrations (50 μM) of these BPZ derivatives, their cell cycle progressions were seemed to be unaffected even after 24 h of treatment (**Fig.6.8.c**). We further studied the preferred mode of induction of cell death by these compounds at the indicated doses.

Results: Cellular responses to synthetic derivatives of BPZs

(a.ii)

(c.ii)
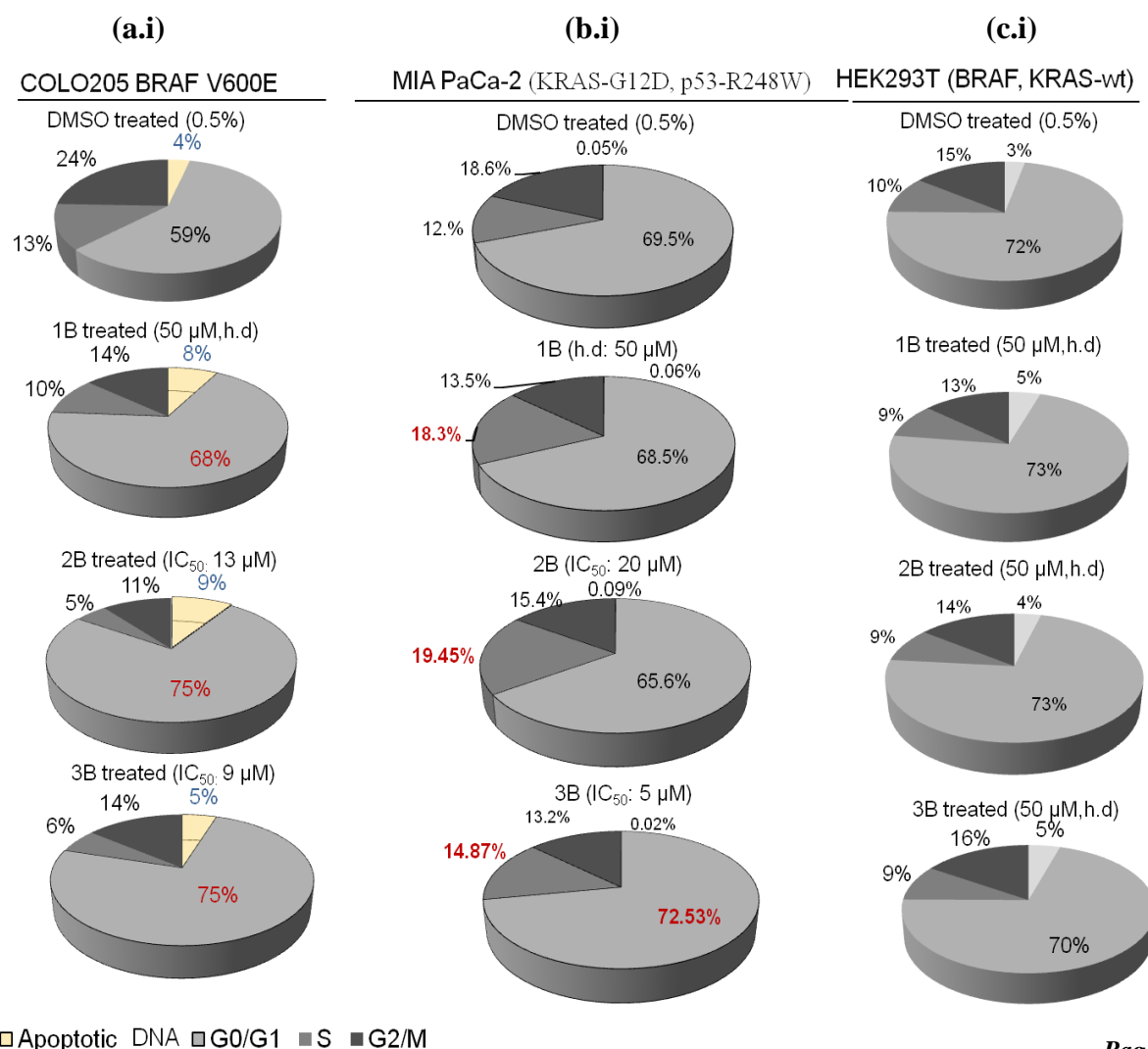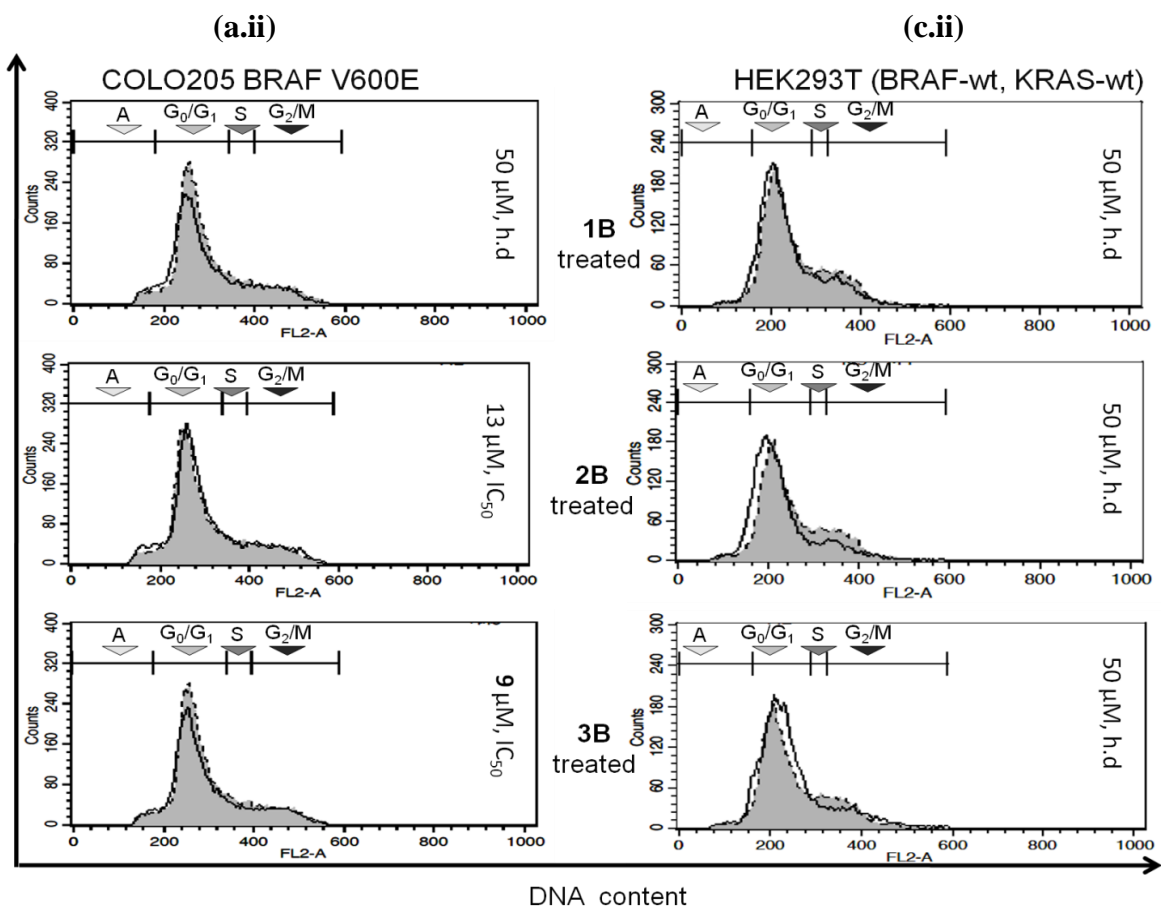
DNA content

(b.ii) MIA PaCa-2 (KRAS-mt, p53-mt)

Results: Cellular responses to synthetic derivatives of BPZs
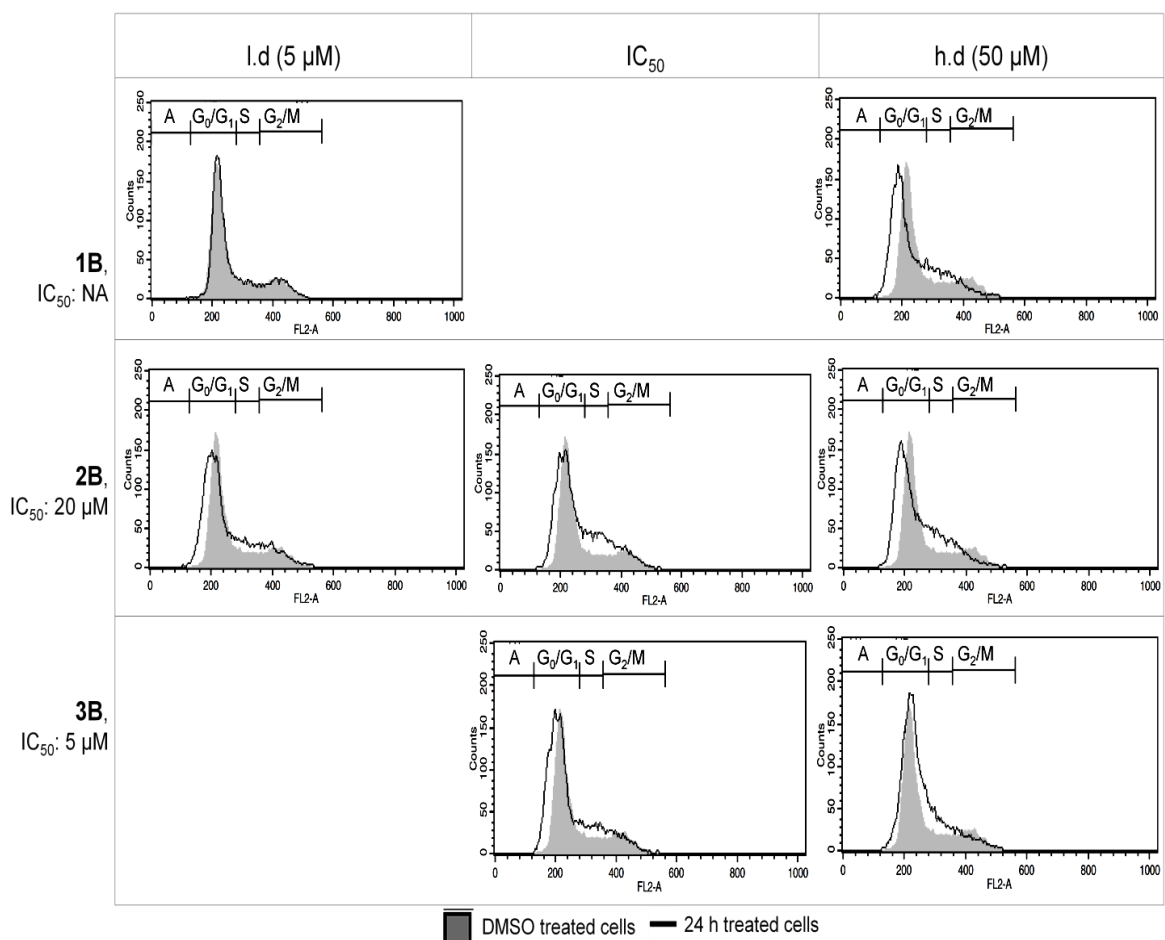
Fig.6.8. Determination of the DNA content at different phases of cell cycle in BPZ derivatives treated cells. G_0/G_1 phase arrest in the cell cycle was observed in both MIA PaCa-2 (**b.i and ii**) and COLO205 cells (**ai and ii**). Although weak but **2B** and **3B** block S-phase at low conc. Compounds **2B** and **3B** were able to show equivalent activity to block cell cycle progression and apoptotic DNA accumulation at concentrations 5 times lower than that of compound **1B**. No cell cycle arrest was observed in the HEK293T cells (**c.i and ii**) with the compounds even when treated at a high dose (h.d.) of 50 μM.

7.3.3.2. Cellular origin specific pro-apoptotic effect of bioactive BPZs

Apoptosis is reported to be altered or deregulated almost in every tumor cell and also has been proved to play a significant role in promoting malignancy. Apoptosis promoting ability of these three BPZs were assessed using three conventional techniques those can detect **(a)** early marker **(b)** end point executioner marker **(c)** late marker of apoptosis induction following treatment at various time intervals.

(a) Induction of early marker of apoptosis (membrane exposed phosphatidyl serine) by tested BPZs

Within 2 h of treatment with determined doses, all three BPZs (though doses used for 1B was extremely high, 50μM) have seen to induce alteration in membrane asymmetry. Therefore, number of annexin V positive early apoptotic cells (in terms of percentage) had increased in BPZs treated COLO205 cells (18.41% in **1B**, 22.69% in **2B** and 29.14% in **3B** treated cells) as compared to the 0.5% DMSO treated cells (9.94%) (**Fig.7.9.a**). While after 24h treatment, only COLO205 cells had shown undergoing severe cell death as evaluated by the increment in the percentage of 7AAD-annexin V double positive cells (**Fig.7.9.a**). But treated HEK293T cells remained unaffected even after 24h treatment with very high doses (50 μM) (**Fig.7.9.a**). Time dependent (at 2 h and 24 h) fold changes in number of early apoptotic cells have been displayed as bar diagrams (fig.) and only significant changes have been observed for malignant COLO205 cells.

Despite of exposing the MIA PaCa-2 cells independently with extremely high concentrations (50μM) of inactive **1B** and active **3B,** these BPZs failed to induce any plasma membrane asymmetry or significant increase in early apoptotic cell numbers at any time points (following 2 h and 24 h). **Fig.7.9.b** displays a comparative bar graph of time dependent fold changes

Results: Cellular responses to synthetic derivatives of BPZs

in the number of early apoptotic cells in both treated (**1B** and **3B** at indicated doses) and solvent treated malignant (COLO205, MIA PaCa-2) and non-malignant (HEK293T) cells. Despite of using 5 times high conc. (50 μM) of **3B** in MIA PaCa-2 and HEK293T than that of COLO205 (9 μM), there were no significant changes in the number of apoptotic cells, even after 24 h.

Results: Cellular responses to synthetic derivatives of BPZs
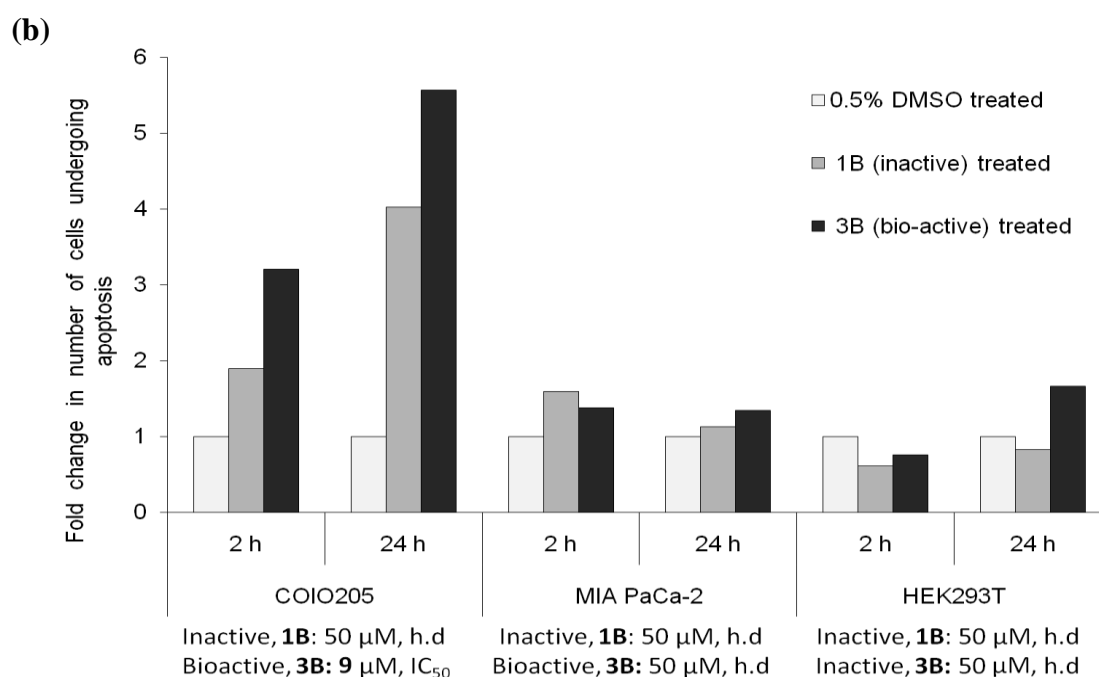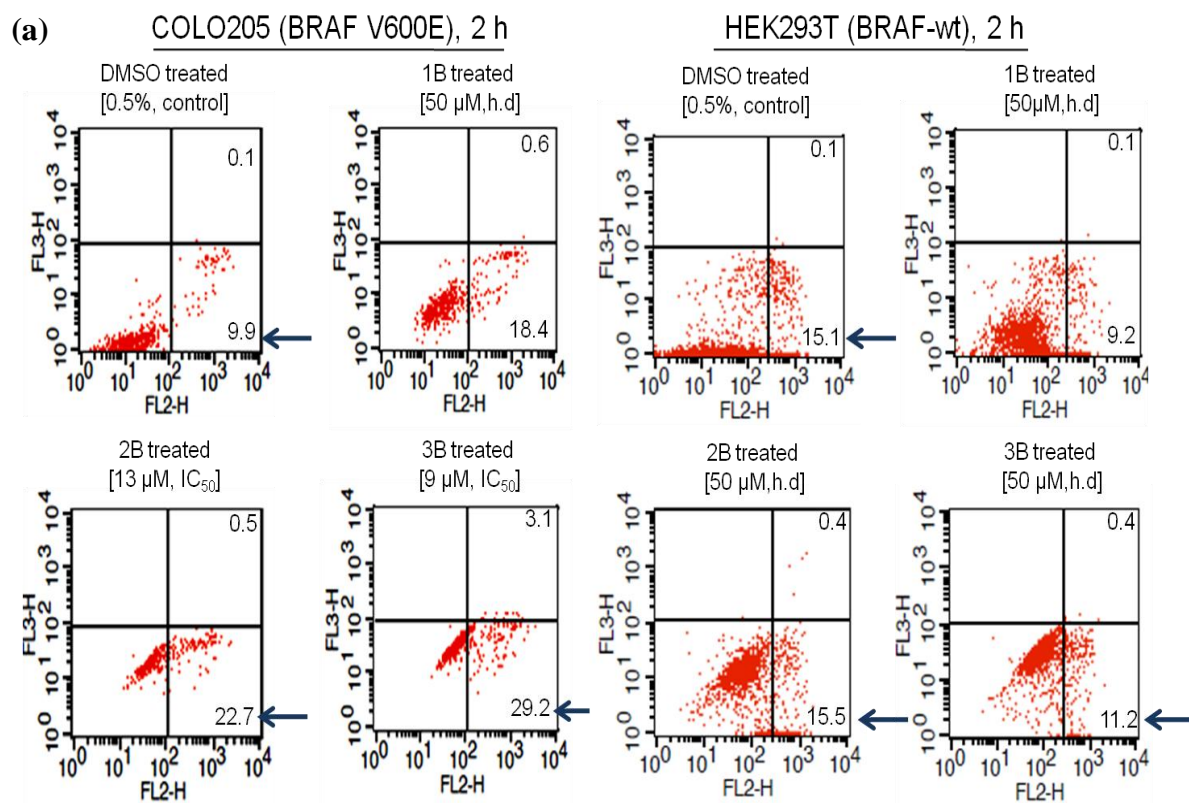
Fig. 7.9. Annexin-V assay for the assessment of pro-apoptotic activity in 1B, 2B and 3B treated cells. Apoptosis was determined after treating cell lines with compounds 1B, 2B and 3B followed by staining with annexin-V/7-AAD after 2 h (top). Flow cytometry profiles (dot plots) represent annexin-V-PE staining along the X-axis (FL2-H) and 7-AAD along the y-axis (FL3-H). (b) Comparative bar graph showing time dependent (2 h, 24 h) fold changes in the number cells undergoing apoptosis in 1B and 3B treated cell lines.. Time dependent increase in number of early apoptotic cells were observed only in COLO205 cells exposed to very high conc. (50 µM) inactive **1B** and IC$_{50}$ conc. (9 µM) of **3B.**

(b) *Induction of executioner of apoptosis (active caspase-3) by tested BPZs*

Appearance of cleaved caspase-3 is the hall mark of caspase dependent apoptosis. To investigate whether these BPZs caspase-3 dependent apoptosis in COLO205 cells, western blotting was performed with whole cell lysates. The accumulation of active caspase-3 (cleaved 17 KDa and 19 KDa bands) was found in 12 h BPZ treated COLO205 cells. While active form of this executioner pro-apoptotic protein was absent in each BPZ treated HEK293T cell lysates (**Fig. 7.10.a**).

Fig.**7.10.b.** showcased, instead of using very high doses (50 µM), all three compounds failed to induce apoptosis (absence of active form of caspase-3, 17 KDa and 19 KDa bands) in MIA PaCa-2 cells those are already intrinsically resistant to apoptosis.

1 µM Staurosporine (STU) treated colon cancer as well as pancreatic cancer cell lysates were used as positive control for every experiment.

(a)

Results: Cellular responses to synthetic derivatives of BPZs
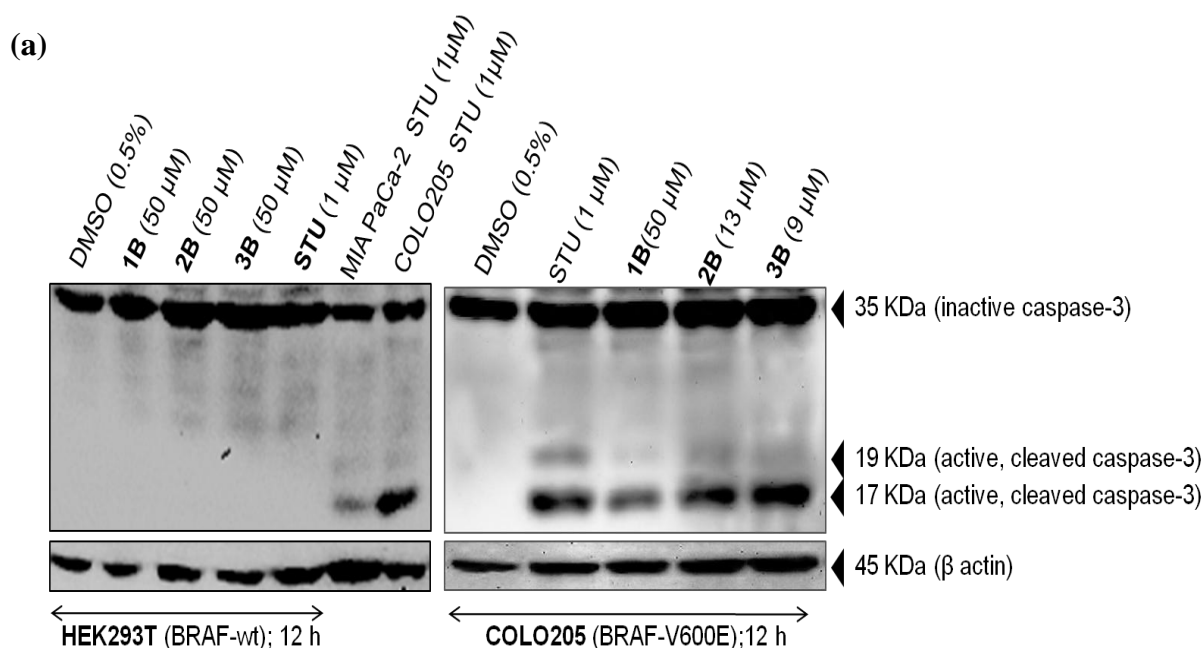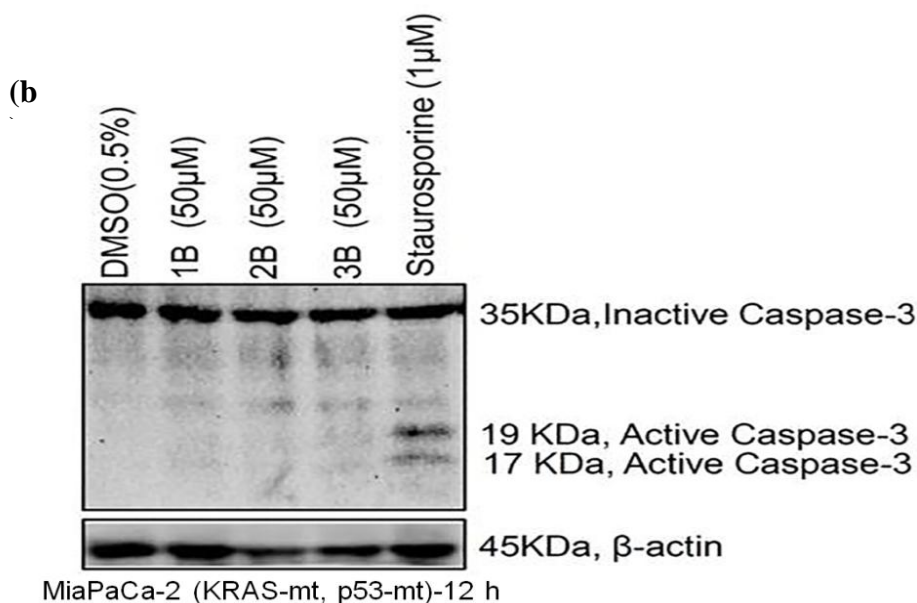
Fig. 7.10. Caspase-3 dependent and independent cell deaths in BPZ treated malignant cells. (a) Caspase-3 activation (17 KDa band) by compounds **1B, 2B** and **3B** after 12 h of treatment was detected using western blot analysis. Capase-3 dependent apoptosis in COLO205 (BRAF V600E) was observed only when cell were treated with IC_{50} conc. of **2B** and **3B** (**1B** had been used at physiologically non permissible conc. β-actin was used as a loading control. **(b)** Despite of treating with very high conc. of [50 μM] of **1B, 2B and 3B**, apoptosis hallmark, active caspase-3 (cleaved product of 35 KDa Caspase-3) was found to be absent in treated cells. This result also confirms the reason behind the absence of DNA at **phase A** (apoptotic DNA) in cell cycle analysis. Pro-apoptotic agent, 1 μM staurosporine (STU) treated cell lysates were used as a positive control.

(c) *Induction of late marker of apoptosis (sequentially fragmented DNA) by tested BPZs*

To detect the formation of specific fragmented DNAs, malignant COLO205 cells were treated with very low IC_{50} doses (except **1B; 50 μM**) of BPZs as compared to the corresponding non malignant cells, HEK293T for 48 h. Formation of DNA ladder (late marker of apoptosis) were observed only in **1B**, **2B** and **3B** treated COLO205 cells. But there were no fragmented chromosomal DNA (apoptosis) or smears (necrosis) have been observed in treated HEK293T cell lines (**Fig.7.11**). These results have confirmed that these compounds were genuinely apoptosis inducers only in malignant colon cancer. DNA extracted from 48h Doxorubicin treated COLO205 cells were used as positive control especially for this DNA fragmentation assay.

Results: Cellular responses to synthetic derivatives of BPZs

COLO205 (BRAF V600E)-48h **HEK293T (BRAF-WT)-48h**
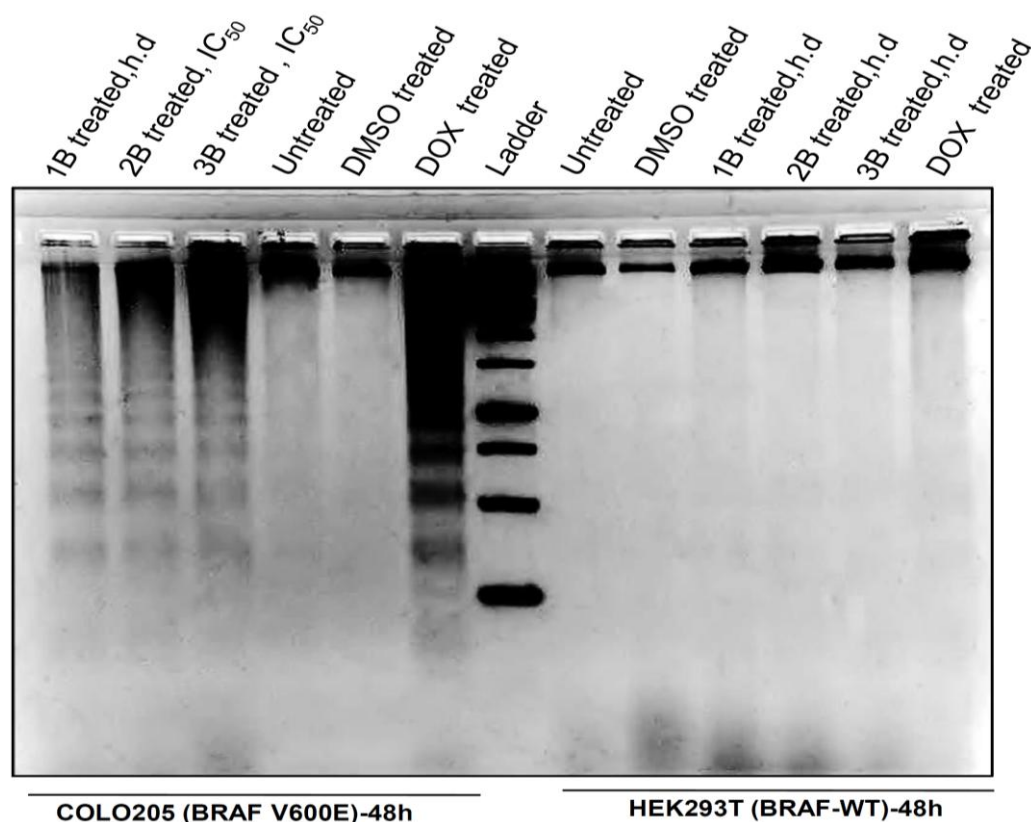
Fig. 7.11. Compounds 1B, 2B and 3B induced DNA fragmentation in colon cancer cells, COLO205 BRAF V600E. (a) After a 48 h treatment of both COLO205 and HEK293T cells with compounds **1B, 2B** and **3B** at the indicated doses (high dose of 50 μM for inactive and IC_{50} dose for active compounds), the chromosomal DNA was extracted. On a 1.8% agarose gel, a DNA laddering profile was observed for the COLO205 (BRAF V600E) cell lines when cell were treated with compounds **1B** (used very concentration), **2B** and **3B** for 48 h indicating stronger apoptotic activity. This particular cell death pathway was not activated in the HEK293T cells where the BRAF is wild-type. **(b)** No fragmented DNAs have been observed despite of treating MIA PaCa-2 cells with high conc.of bioactive BPZs (50 μM: **2B** and **3B**)

7.3.3.3. Cellular origin specific pro-death autophagy inducing role of bioactive BPZs

It is reported that specific vesicle formation (autophagosomes) along with increased intracellular granularity (increased number of autophagosomes) is associated with induction of autophagy, type II PCD. Already it has been observed that tested derivatives of BPZs failed to induce apoptosis in MIA PaCa-2 cells even after treating with very high concentration. Therefore, further experiments have been done with whole cell protein lysates to determine pro-death autophagy inducing activity of BPZs in MIA PaCa-2. Active BPZ (**2B** and **3B**) are already shown to be cytotoxic to malignant MIA PaCa-2 cells and by detecting the accumulation of biomarkers for

autophagosome formation (LC3A/B-II, Atg-7, beclin-1 [362, 363]) in BPZ treated cells may confirm their potential to be count as pro-death autophagy inducers.

For detecting the BPZ treatment induced autophagic cell deaths in BPZ treated MIA PaCa-2 cell lysates, cells were treated 24 h. Both **2B** and **3B** (though IC$_{50}$ of **3B** > IC$_{50}$ of **2B**) significantly induced LC3A/B-II accumulation within MIA PaCa-2 cells as compared to corresponding solvent control and **1B** treated cells (**Fig.7.12**). The induction of pro-death autophagy is seemed to be dependent on exposed concentration and bioactivity of the compound tested. However, within the same time point, **1B**, both at 5 µM and 50 µM concentrations failed to induce formation of significant amount of LC-3 A/B-II, clearly indicating the reason of its inefficiency to induce significant inhibition in cell proliferation, cell cycle arrest and death as compared to **2B** and **3B**.
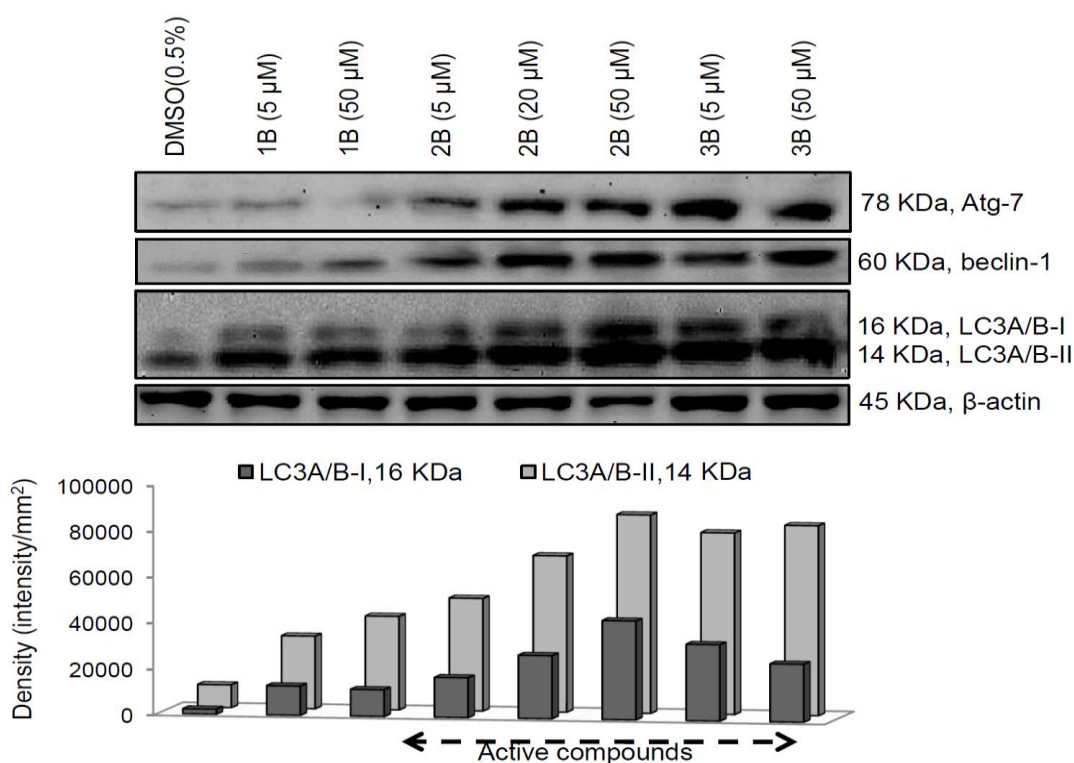
5 µM: l.d of 1B and 2B and IC$_{50}$ of 3B, 20 µM: IC$_{50}$ of 2B, 50 µM: h.d

Fig. 7.12. Active BPZs induce cytotoxic autophagy. Formation of LC3A/B-II (14 KDa) is the biomarker of autophagy. MIA PaCa-2 cells undergo cytotoxic autophagy within 24 h of treatment with by bioactive BPZs in an order of **3B** >**2B**. Any doses of **1B** and lower dose of **2B** though induced formation of LC 3B-II, Atg-7, beclin-1 within 24 h but were significantly lower than those formed in IC$_{50}$ dose of **3B** and **2B** treated cells. l.d : low dose, h.d : high dose.

Results: Cellular responses to synthetic derivatives of BPZs

7.3.3.4. DISCUSSIONS

Intrinsically fluorescent BPZ class compounds remain under investigations for the development of cell permeable, intracellular DNA, lipid and protein binding dyes for last few decades. However, studies to explore their roles as potential anticancer agents have just begun in last few decades and still at the stage of infancy. However, their roles in promoting tumor cell death via autophagy still obscure.

Genetic alterations (mutations independently at BRAF, KRAS) are associated with chemo-refractory tumorigencity of both colon and pancreatic cancers cells and render them one of the non-curable malignant entities for ages. Despite of few successful results, still researchers are thriving to find new clinically applicable pro-drugs. Till date there are very few positive reports are available only on combined treatment which included sustained suppression of EGFR and MAPK signaling pathway together. Therefore, single treatment strategies against these malignant conditions remain unavailable. In the era of personalized medicine, here efforts have been given to screen new BPZ derivatives those can evoke selective cytotoxic responses against chemorefractory and apoptosis refractory malignant backgrounds.

Obtained results eventually demonstrated that **2B** and **3B** were highly cytotoxic to malignant tumour cells (MIA PaCa-2 and COLO205) grown under the nutrient deprived condition (5% FBS) while they affect non-malignant cell (HEK293T) growth at minimal level. For **2B** and **3B** the treatment doses and cellular uptakes in chemo-refractory COLO205 were low in comparison to HEK293T (treated with 5 times higher concentration), but still these two compounds were highly cell permeable and able to effectively inhibit proliferation of COLO205 by 50%. Similar activities were also observed in another chemo- and apoptosis refractory model, MIA PaCa-2. However, **2B** and **3B** were found to be anti-colonogenic as well as efficient inducers of intracellular granularity (associated formation and accumulation of vesicle like structures) in MIA PaCa-2. In these malignant cell lines and non-malignant cell line, the cell viability, colonogenic and cellular uptake assays revealed the poor uptake of **1B** even at very high concentration. Therefore, results confirmed

Results: Cellular responses to synthetic derivatives of BPZs

their inability to reach the cell type specific intracellular cytotoxic threshold concentrations required to promote any modes of cell deaths. Despite of these, at extremely high concentration (50 µM, beyond clinically permissible limit), **1B** selectively showed pro-apoptotic effect on malignant COLO205 cells.

Not only cytotoxicity, these data had confirmed that **3B** (≥ 5 µM) and 2B (≥ **13** µM) in are highly efficient and irreversible cell cycle blocker in used cellular models for different malignancy. May be differential level of accumulation of **2B** and **3B** within this metastatic cancer cells is the reason behind such dose dependent disparity in arresting cell cycle progression.

In this dissertation, these screened BPZ derivatives treatment associated dose dependent mechanistic mode of cell death has also been elucidated. Conducted *in vitro* assays for determining induction of apoptosis or pro-death autophagy allowed us to draw a conclusion on bioactivities of newly synthesized BPZs; **2B** and **3B** initially affect cell cycle progression following internalization into malignant cells. In COLO205 cells with intact apoptotic machinery, both **2B** and **3B** induced caspase-3 dependent apoptotic cell death while in MIA PaCa-2 cells with deregulated apoptotic machineries, tested bioactive BPZ caused cellular demise *via* autophagy.

Cumulatively, I have determined the level of efficacy of all three BPZs under investigation [**3B** >**2B** >> **1B**].

Results: Cellular responses to synthetic derivatives of BPZs

CHAPTER-8

SUMMARY

AND

CONCLUSIONS

8.1. SUMMARY OF THE WORK

8.1.1. Chapter-4

SFN remained differentially non cytotoxic to differentiating (PMA induced) THP1 derived monocytes in comparison to non differentiating THP1 monocytes. It simultaneously regulates PMA induced differentiation of THP1, ameliorating the inflammatory responses (here soluble collagen induced *in vitro* autoimmune arthritic condition) at the level of monocytes/macrophages (Mns/MΦs). Under such conditions, it not only shifted human monocytes to macrophage differentiation (PMA induced) towards a specific M2 type but also converted already developed auto-immune responsive M1 polarized macrophages into M2 type. Observed *in vitro,* non cytotoxic yet immune modulatory activity of SFN suggests its potential application as a therapeutic intervention to improve inflammatory autoimmune conditions in patients.

8.1.2. Chapter-5

In connection with the studies conducted in previous chapter, similar M2 polarizing role of SFN had been evaluated using spontaneously (in absence of external stimuli e.g. PMA) differentiating, human peripheral blood derived monocytes. Data suggest, below and at a particular concentration (10μM), SFN mediates polarization of these spontaneously differentiating human monocytes towards immune-suppressive M2 type and this activity had also correlated well with decreased inflammatory responses by soluble human collagen-II induced polarization to auto-reactive M1 macrophages in presence of same concentration of SFN.

8.1.3. Chapter-6

Studies in this chapter enlighten a specific therapeutic potential of M2 macrophage inducer, SFN. Data suggest its potential to perturb soluble collagens (both human and chicken) induced pro-inflammatory autoimmune responses by targeting impaired endogenous FasL maturation pathway *in*

vitro. SFN treatment recues the delayed FasL maturation in autoimmune responsive inflammatory M1 macrophages, indicating a pivotal role to target and combat with autoimmunity associated altered Fas/FasL mediated apoptosis machinery.

8.1.4. Chapter-7

Summarizing all the experimental results it may be concluded, **3B** is the most potential anticancer agent among three BPZ derivatives. **3B** remained effective at very low dose (IC_{50} is 5 µM in MIA PaCa-2 and 9 µM in COLO205) than **2B** (IC_{50} is 20 µM in MIA PaCa-2 and 13 µM in COLO205). However, both of them may be utilized as lead compounds for the development of another set of novel fluorescent anticancer agents in future. In addition, insignificant level of bioactivity confirmed the potential usage of **1B** as non cytotoxic fluorescent dye or lead scaffold structure to develop new set of halogenated bioactive BPZs in future.

Results specifically indicate **2B** and **3B** (cytotoxicity of **1B** was observed only when very high concentration; 50 µM was used for treating COLO205) or their prototypes to be used as potential anticancer agents to trigger apoptotic cell death at particular IC_{50} doses only in malignant colon cancer cells harboring chemo-resistance inducer, BRAF-V600E protein. These data also suggest that these compounds might have great implication in individualized treatment against colon cancer.

However, data also allowed us to conclude that these examined bioactive BPZs (**3B** > **2B**) are efficient enough to trigger a p53 independent cytotoxic autophagy (non-apoptotic cell death) in chemo-and apoptosis refractory pancreatic cancer model, MIA PaCa-2 harboring mutated forms of KRAS, p53, p16 proteins and so on.

Summary and Conclusions

8.2. CONCLUSIONS

Current study has emphasized a few obscure cellular responses to SFN and three derivatives (R= -Cl, -CH$_3$, -H) of BPZs. Depending on the aim and respective objectives (non cytotoxic to cytotoxic and anti-autoimmune or anti-cancer activities) of the studies, few interesting human beneficiary bioactivities of these compounds of different origins have been deduced in this dissertation.

Both SFN (economical, well-accepted, naturally occurring non-nutrient dietary compound) and two chemically synthesized derivatives of BPZs (well established lipid, DNA and protein staining class of dyes) can be used as effective, selective chemopreventive agents. From this study it is obeserved that well established anticancer agent; SFN may also be employed as anti-autoimmune-regulator both *in vitro* or *ex-vivo* at non-cytotoxic (for macrophage lineage) concentration. Moreover, these novel derivatives of a most frequently used family of fluorescent probes or dyes, BPZs may be used as lead or selective drug candidates for the treatment of chemo-refractory and apoptosis resistant cancer types (pancreatic and colon cancer).

Though a great deal of work needs to be done before the respective anti autoimmune and cancer chemopreventive role of these chemical entities may find its way into mainstream medicine, this study can be considered as one of the preliminary but pivotal report in those regards. Enhanced interdisciplinary and collaborative efforts by researchers need to drive the field of biomedicine forward and help to secure a disease-free or atleast diminished effects in future.

8.3.   FUTURE PERSPECTIVE AND SHORTCOMINGS OF THE STUDY

- Current dissertation demonstrates differential bioactivities of a phytochemical, SFN and three newly synthesized BPZs (at C-10, R= -Cl, -CH$_3$ and –H) using only *in vitro/ex vivo* cell based studies.

- Here, non-cytotoxic, effective, beneficial and monocytes/macrophages dependent possible anti-arthritic role of SFN was studied and reported. But further studies with patients' samples are necessary to determine proper treatment regimes for SFN.

- Similarly, immune-suppressive M2 macrophage generating role of SFN needs to be verified in other chronic inflammatory autoimmune disease conditions.

- Both active and inactive derivatives of BPZ may be modified at molecular level to redeem their respective IC$_{50}$ values up to nano-molar range.

- To establish all our conclusions on bioactivities of BPZs. in broader aspects, further *in vitro* studies with other intrinsically apoptosis resistant cancer cell lines of same or different tissue origins as well as *in vivo* studies with similar cancer or other cancer models or patients' samples are required.

- These BPZ derivatives were unable to induce apoptosis in MIA PaCa-2 cells (KRAS-mt, BRAF-wt, P53-mt) and HEK293T (KRAS-wt, BRAF-wt, p53-wt/inactive) but were pro-apoptotic to COLO205 (BRAF-V600E, KRAS-wt, p53-wt/active). It would be interesting to find out existence of any relationships among the cytotoxicity of BPZs, p53 and EGFR signaling events.

BIBLIOGRAPHY

[1]   Biesalski, H.K.; Dragsted, L.O.; Elmadfa, I.; Grossklaus, R.; Muller, M.; Schrenk, D.*, et al.* Bioactive compounds: safety and efficacy. *Nutrition,* **2009**, *25* (11-12), 1206-1211.

[2]   Siem, H.; Bjertness, E.; Meltzer, M.H.*e.a.* Bioactive compounds in plants –benefits and risks for man and animals. *Proceedings from a symposium held at The Norwegian Academy of Science and Letters,Oslo, 13 – 14 November 2008,* **2008**.

[3]   Mangal, M.; Sagar, P.; Singh, H.; Raghava, G.P.; Agarwal, S.M. NPACT: Naturally Occurring Plant-based Anti-cancer Compound-Activity-Target database. *Nucleic Acids Res,* **2013**, *41* (Database issue), D1124-1129.

[4]   Scarpa, E.S.; Ninfali, P. Phytochemicals as Innovative Therapeutic Tools against Cancer Stem Cells. *Int J Mol Sci,* **2015**, *16* (7), 15727-15742.

[5]   Lee, S. Artemisinin, promising lead natural product for various drug developments. *Mini Rev Med Chem,* **2007**, *7* (4), 411-422.

[6]   Kumar, G.; Tuli, H.S.; Mittal, S.; Shandilya, J.K.; Tiwari, A.; Sandhu, S.S. Isothiocyanates: a class of bioactive metabolites with chemopreventive potential. *Tumour Biol,* **2015**, *36* (6), 4005-4016.

[7]   Ahn, Y.H.; Hwang, Y.; Liu, H.; Wang, X.J.; Zhang, Y.; Stephenson, K.K.*, et al.* Electrophilic tuning of the chemoprotective natural product sulforaphane. *Proc Natl Acad Sci U S A,* **2010**, *107* (21), 9590-9595.

[8]   Zhang, Y.; Talalay, P.; Cho, C.G.; Posner, G.H. A major inducer of anticarcinogenic protective enzymes from broccoli: isolation and elucidation of structure. *Proc Natl Acad Sci U S A,* **1992**, *89* (6), 2399-2403.

[9]   Vasanthi, H.R.; Mukherjee, S.; Das, D.K. Potential health benefits of broccoli- a chemico-biological overview. *Mini Rev Med Chem,* **2009**, *9* (6), 749-759.

[10]   Steinkellner, H.; Rabot, S.; Freywald, C.; Nobis, E.; Scharf, G.; Chabicovsky, M.*, et al.* Effects of cruciferous vegetables and their constituents on drug metabolizing enzymes involved in the bioactivation of DNA-reactive dietary carcinogens. *Mutat Res,* **2001**, *480-481*, 285-297.

[11]   Zanichelli, F.; Capasso, S.; Cipollaro, M.; Pagnotta, E.; Carteni, M.; Casale, F.*, et al.* Dose-dependent effects of R-sulforaphane isothiocyanate on the biology of human mesenchymal stem cells, at dietary amounts, it promotes cell proliferation and reduces senescence and apoptosis, while at anti-cancer drug doses, it has a cytotoxic effect. *Age (Dordr),* **2012**, *34* (2), 281-293.

[12]   Pal, S.; Konkimalla, V.B. Hormetic potential of Sulforaphane (SFN) in switching cells' fate towards survival or death. *Mini Rev Med Chem,* **2015**.

[13]   Abdull Razis, A.F.; Iori, R.; Ioannides, C. The natural chemopreventive phytochemical R-sulforaphane is a far more potent inducer of the carcinogen-detoxifying enzyme systems in rat liver and lung than the S-isomer. *Int J Cancer,* **2011**, *128* (12), 2775-2782.

[14] Posner, G.H.; Cho, C.G.; Green, J.V.; Zhang, Y.; Talalay, P. Design and synthesis of bifunctional isothiocyanate analogs of sulforaphane: correlation between structure and potency as inducers of anticarcinogenic detoxication enzymes. *J Med Chem,* **1994**, *37* (1), 170-176.

[15] Kim, M.J.; Kim, S.H.; Lim, S.J. Comparison of the apoptosis-inducing capability of sulforaphane analogues in human colon cancer cells. *Anticancer Res,* **2010**, *30* (9), 3611-3619.

[16] Gerhauser, C.; You, M.; Liu, J.; Moriarty, R.M.; Hawthorne, M.; Mehta, R.G.*, et al.* Cancer chemopreventive potential of sulforamate, a novel analogue of sulforaphane that induces phase 2 drug-metabolizing enzymes. *Cancer Res,* **1997**, *57* (2), 272-278.

[17] Dinkova-Kostova, A.T.; Kostov, R.V. Glucosinolates and isothiocyanates in health and disease. *Trends Mol Med,* **2012**, *18* (6), 337-347.

[18] Zhang, Y.; Kensler, T.W.; Cho, C.G.; Posner, G.H.; Talalay, P. Anticarcinogenic activities of sulforaphane and structurally related synthetic norbornyl isothiocyanates. *Proc Natl Acad Sci U S A,* **1994**, *91* (8), 3147-3150.

[19] Wang, G.C.; Farnham, M.; Jeffery, E.H. Impact of Thermal Processing on Sulforaphane Yield from Broccoli (Brassica oleracea L. ssp. italica). *J Agric Food Chem,* **2012**, *60* (27), 6743-6748.

[20] Conaway, C.C.; Getahun, S.M.; Liebes, L.L.; Pusateri, D.J.; Topham, D.K.; Botero-Omary, M.*, et al.* Disposition of glucosinolates and sulforaphane in humans after ingestion of steamed and fresh broccoli. *Nutr Cancer,* **2000**, *38* (2), 168-178.

[21] Wu, X.; Zhou, Q.H.; Xu, K. Are isothiocyanates potential anti-cancer drugs? *Acta Pharmacol Sin,* **2009**, *30* (5), 501-512.

[22] Zhang, Y.; Talalay, P. Mechanism of differential potencies of isothiocyanates as inducers of anticarcinogenic Phase 2 enzymes. *Cancer Res,* **1998**, *58* (20), 4632-4639.

[23] Koo, J.E.; Park, Z.Y.; Kim, N.D.; Lee, J.Y. Sulforaphane inhibits the engagement of LPS with TLR4/MD2 complex by preferential binding to Cys133 in MD2. *Biochem Biophys Res Commun,* **2013**, *434* (3), 600-605.

[24] Shibata, T.; Kimura, Y.; Mukai, A.; Mori, H.; Ito, S.; Asaka, Y.*, et al.* Transthiocarbamoylation of proteins by thiolated isothiocyanates. *J Biol Chem,* **2011**, *286* (49), 42150-42161.

[25] Youn, H.S.; Kim, Y.S.; Park, Z.Y.; Kim, S.Y.; Choi, N.Y.; Joung, S.M.*, et al.* Sulforaphane suppresses oligomerization of TLR4 in a thiol-dependent manner. *J Immunol,* **2010**, *184* (1), 411-419.

[26] Hong, F.; Freeman, M.L.; Liebler, D.C. Identification of sensor cysteines in human Keap1 modified by the cancer chemopreventive agent sulforaphane. *Chem Res Toxicol,* **2005**, *18* (12), 1917-1926.

[27] Mi, L.; Hood, B.L.; Stewart, N.A.; Xiao, Z.; Govind, S.; Wang, X.*, et al.* Identification of potential protein targets of isothiocyanates by proteomics. *Chem Res Toxicol,* **2011**, *24* (10), 1735-1743.

[28]   Zhang, Y. Molecular mechanism of rapid cellular accumulation of anticarcinogenic isothiocyanates. *Carcinogenesis,* **2001**, *22* (3), 425-431.

[29]   Zhang, Y. Role of glutathione in the accumulation of anticarcinogenic isothiocyanates and their glutathione conjugates by murine hepatoma cells. *Carcinogenesis,* **2000**, *21* (6), 1175-1182.

[30]   Mi, L.; Wang, X.; Govind, S.; Hood, B.L.; Veenstra, T.D.; Conrads, T.P.*, et al.* The role of protein binding in induction of apoptosis by phenethyl isothiocyanate and sulforaphane in human non-small lung cancer cells. *Cancer Res,* **2007**, *67* (13), 6409-6416.

[31]   Mi, L.; Xiao, Z.; Hood, B.L.; Dakshanamurthy, S.; Wang, X.; Govind, S.*, et al.* Covalent binding to tubulin by isothiocyanates. A mechanism of cell growth arrest and apoptosis. *J Biol Chem,* **2008**, *283* (32), 22136-22146.

[32]   Mi, L.; Xiao, Z.; Veenstra, T.D.; Chung, F.L. Proteomic identification of binding targets of isothiocyanates: A perspective on techniques. *J Proteomics,* **2011**, *74* (7), 1036-1044.

[33]   de Figueiredo, S.M.; Binda, N.S.; Nogueira-Machado, J.A.; Vieira-Filho, S.A.; Caligiorne, R.B. The antioxidant properties of organosulfur compounds (sulforaphane). *Recent Pat Endocr Metab Immune Drug Discov,* **2015**, *9* (1), 24-39.

[34]   Harada, N.; Kanayama, M.; Maruyama, A.; Yoshida, A.; Tazumi, K.; Hosoya, T.*, et al.* Nrf2 regulates ferroportin 1-mediated iron efflux and counteracts lipopolysaccharide-induced ferroportin 1 mRNA suppression in macrophages. *Arch Biochem Biophys,* **2011**, *508* (1), 101-109.

[35]   Hernandez-Rabaza, V.; Cabrera-Pastor, A.; Taoro-Gonzalez, L.; Gonzalez-Usano, A.; Agusti, A.; Balzano, T.*, et al.* Neuroinflammation increases GABAergic tone and impairs cognitive and motor function in hyperammonemia by increasing GAT-3 membrane expression. Reversal by sulforaphane by promoting M2 polarization of microglia. *J Neuroinflammation,* **2016**, *13* (1), 83.

[36]   Cook, A.L.; Vitale, A.M.; Ravishankar, S.; Matigian, N.; Sutherland, G.T.; Shan, J.*, et al.* NRF2 activation restores disease related metabolic deficiencies in olfactory neurosphere-derived cells from patients with sporadic Parkinson's disease. *PLoS One,* **2011**, *6* (7), e21907.

[37]   Higgins, L.G.; Hayes, J.D. Mechanisms of induction of cytosolic and microsomal glutathione transferase (GST) genes by xenobiotics and pro-inflammatory agents. *Drug Metab Rev,* **2011**, *43* (2), 92-137.

[38]   Lin, L.C.; Yeh, C.T.; Kuo, C.C.; Lee, C.M.; Yen, G.C.; Wang, L.S.*, et al.* Sulforaphane Potentiates the Efficacy of Imatinib against Chronic Leukemia Cancer Stem Cells through Enhanced Abrogation of Wnt/beta-Catenin Function. *J Agric Food Chem,* **2012**, *60* (28), 7031-7039.

[39]   Sakao, K.; Singh, S.V. D,L-sulforaphane-induced apoptosis in human breast cancer cells is regulated by the adapter protein p66Shc. *J Cell Biochem,* **2012**, *113* (2), 599-610.

[40] Rodriguez-Cantu, L.N.; Gutierrez-Uribe, J.A.; Arriola-Vucovich, J.; Diaz-De La Garza, R.I.; Fahey, J.W.; Serna-Saldivar, S.O. Broccoli (Brassica oleracea var. italica) sprouts and extracts rich in glucosinolates and isothiocyanates affect cholesterol metabolism and genes involved in lipid homeostasis in hamsters. *J Agric Food Chem,* **2011**, *59* (4), 1095-1103.

[41] Gan, N.; Wu, Y.C.; Brunet, M.; Garrido, C.; Chung, F.L.; Dai, C*., et al.* Sulforaphane activates heat shock response and enhances proteasome activity through up-regulation of Hsp27. *J Biol Chem,* **2010**, *285* (46), 35528-35536.

[42] Balasubramanian, S.; Chew, Y.C.; Eckert, R.L. Sulforaphane suppresses polycomb group protein level via a proteasome-dependent mechanism in skin cancer cells. *Mol Pharmacol,* **2011**, *80* (5), 870-878.

[43] Pei, Y.; Wu, B.; Cao, Q.; Wu, L.; Yang, G. Hydrogen sulfide mediates the anti-survival effect of sulforaphane on human prostate cancer cells. *Toxicol Appl Pharmacol,* **2011**, *257* (3), 420-428.

[44] Jeong, J.K.; Moon, M.H.; Seo, J.S.; Seol, J.W.; Lee, Y.J.; Park, S.Y. Sulforaphane blocks hypoxia-mediated resistance to TRAIL-induced tumor cell death. *Mol Med Report,* **2011**, *4* (2), 325-330.

[45] Bryant, C.S.; Kumar, S.; Chamala, S.; Shah, J.; Pal, J.; Haider, M*., et al.* Sulforaphane induces cell cycle arrest by protecting RB-E2F-1 complex in epithelial ovarian cancer cells. *Mol Cancer,* **2010**, *9*, 47.

[46] Choi, S.; Singh, S.V. Bax and Bak are required for apoptosis induction by sulforaphane, a cruciferous vegetable-derived cancer chemopreventive agent. *Cancer Res,* **2005**, *65* (5), 2035-2043.

[47] Tanito, M.; Masutani, H.; Kim, Y.C.; Nishikawa, M.; Ohira, A.; Yodoi, J. Sulforaphane induces thioredoxin through the antioxidant-responsive element and attenuates retinal light damage in mice. *Invest Ophthalmol Vis Sci,* **2005**, *46* (3), 979-987.

[48] Rajendran, P.; Dashwood, W.M.; Li, L.; Kang, Y.; Kim, E.; Johnson, G*., et al.* Nrf2 status affects tumor growth, HDAC3 gene promoter associations, and the response to sulforaphane in the colon. *Clin Epigenetics,* **2015**, *7* (1), 102.

[49] Watson, G.W.; Wickramasekara, S.; Palomera-Sanchez, Z.; Black, C.; Maier, C.S.; Williams, D.E*., et al.* SUV39H1/H3K9me3 attenuates sulforaphane-induced apoptotic signaling in PC3 prostate cancer cells. *Oncogenesis,* **2014**, *3*, e131.

[50] Meeran, S.M.; Patel, S.N.; Li, Y.; Shukla, S.; Tollefsbol, T.O. Bioactive dietary supplements reactivate ER expression in ER-negative breast cancer cells by active chromatin modifications. *PLoS One,* **2012**, *7* (5), e37748.

[51] Kaufman-Szymczyk, A.; Majewski, G.; Lubecka-Pietruszewska, K.; Fabianowska-Majewska, K. The Role of Sulforaphane in Epigenetic Mechanisms, Including Interdependence between Histone Modification and DNA Methylation. *Int J Mol Sci,* **2015**, *16* (12), 29732-29743.

[52] Tomczyk, J.; Olejnik, A. [Sulforaphane--a possible agent in prevention and therapy of cancer]. *Postepy Hig Med Dosw (Online),* **2010**, *64*, 590-603.

[53] Sestili, P.; Fimognari, C. Cytotoxic and Antitumor Activity of Sulforaphane: The Role of Reactive Oxygen Species. *Biomed Res Int,* **2015**, *2015*, 402386.

[54] Cross, J.V.; Rady, J.M.; Foss, F.W.; Lyons, C.E.; Macdonald, T.L.; Templeton, D.J. Nutrient isothiocyanates covalently modify and inhibit the inflammatory cytokine macrophage migration inhibitory factor (MIF). *Biochem J,* **2009**, *423* (3), 315-321.

[55] Wang, W.; He, Y.; Yu, G.; Li, B.; Sexton, D.W.; Wileman, T.*, et al.* Sulforaphane Protects the Liver against CdSe Quantum Dot-Induced Cytotoxicity. *PLoS One,* **2015**, *10* (9), e0138771.

[56] Jo, C.; Kim, S.; Cho, S.J.; Choi, K.J.; Yun, S.M.; Koh, Y.H.*, et al.* Sulforaphane induces autophagy through ERK activation in neuronal cells. *FEBS Lett,* **2014**, *588* (17), 3081-3088.

[57] Southam, C.; Ehrlic, J. Effects of extracts of western red-cedar heartwood on certain wood-decaying fungi in culture. *Phytopathology,* **1943**, *33*, 517-524.

[58] Calabrese, E.J. Paradigm lost, paradigm found: The re-emergence of hormesis as a fundamental dose response model in the toxicological sciences. *Environmental Pollution,* **2005**, *138*, 378–411.

[59] Mattson, M.P. Hormesis defined. *Ageing Res Rev,* **2008**, *7* (1), 1-7.

[60] Mattson, M.P. Dietary factors, hormesis and health. *Ageing Res Rev,* **2008**, *7* (1), 43-48.

[61] Bao, Y.; Wang, W.; Zhou, Z.; Sun, C. Benefits and risks of the hormetic effects of dietary isothiocyanates on cancer prevention. *PLoS One,* **2014**, *9* (12), e114764.

[62] Zhang, Y.; Li, J.; Tang, L. Cancer-preventive isothiocyanates: dichotomous modulators of oxidative stress. *Free Radic Biol Med,* **2005**, *38* (1), 70-77.

[63] Blum, N.M.; Mueller, K.; Hirche, F.; Lippmann, D.; Most, E.; Pallauf, J.*, et al.* Glucoraphanin does not reduce plasma homocysteine in rats with sufficient Se supply via the induction of liver ARE-regulated glutathione biosynthesis enzymes. *Food Funct,* **2011**, *2* (11), 654-664.

[64] Guerrero-Beltran, C.E.; Calderon-Oliver, M.; Pedraza-Chaverri, J.; Chirino, Y.I. Protective effect of sulforaphane against oxidative stress: recent advances. *Exp Toxicol Pathol,* **2012**, *64* (5), 503-508.

[65] Guerrero-Beltran, C.E.; Mukhopadhyay, P.; Horvath, B.; Rajesh, M.; Tapia, E.; Garcia-Torres, I.*, et al.* Sulforaphane, a natural constituent of broccoli, prevents cell death and inflammation in nephropathy. *J Nutr Biochem,* **2012**, *23* (5), 494-500.

[66] Cheung, K.L.; Kong, A.N. Molecular targets of dietary phenethyl isothiocyanate and sulforaphane for cancer chemoprevention. *AAPS J,* **2010**, *12* (1), 87-97.

[67] Tortorella, S.M.; Royce, S.G.; Licciardi, P.V.; Karagiannis, T.C. Dietary Sulforaphane in Cancer Chemoprevention: The Role of Epigenetic Regulation and HDAC Inhibition. *Antioxid Redox Signal,* **2014**.

[68]   Amjad, A.I.; Parikh, R.A.; Appleman, L.J.; Hahm, E.R.; Singh, K.; Singh, S.V. Broccoli-Derived Sulforaphane and Chemoprevention of Prostate Cancer: From Bench to Bedside. *Curr Pharmacol Rep,* **2015**, *1* (6), 382-390.

[69]   Steward, W.P.; Brown, K. Cancer chemoprevention: a rapidly evolving field. *Br J Cancer,* **2013**, *109* (1), 1-7.

[70]   Yang, L.; Palliyaguru, D.L.; Kensler, T.W. Frugal chemoprevention: targeting Nrf2 with foods rich in sulforaphane. *Semin Oncol,* **2016**, *43* (1), 146-153.

[71]   Tan, H.; Bi, J.; Wang, Y.; Zhang, J.; Zuo, Z. Transfusion of Old RBCs Induces Neuroinflammation and Cognitive Impairment. *Crit Care Med,* **2015**.

[72]   Suppipat, K.; Lacorazza, H.D. From the Table to the Bedside: Can Food-Derived Sulforaphane be used as a Novel Agent to Treat Leukemia? *Curr Cancer Drug Targets,* **2014**.

[73]   Sun, C.; Yang, C.; Xue, R.; Li, S.; Zhang, T.; Pan, L.*, et al.* Sulforaphane alleviates muscular dystrophy in mdx mice by activation of Nrf2. *J Appl Physiol (1985),* **2015**, *118* (2), 224-237.

[74]   Ryoo, I.G.; Shin, D.H.; Kang, K.S.; Kwak, M.K. Involvement of Nrf2-GSH signaling in TGFbeta1-stimulated epithelial-to-mesenchymal transition changes in rat renal tubular cells. *Arch Pharm Res,* **2015**, *38* (2), 272-281.

[75]   Royston, K.J.; Tollefsbol, T.O. The Epigenetic Impact of Cruciferous Vegetables on Cancer Prevention. *Curr Pharmacol Rep,* **2015**, *1* (1), 46-51.

[76]   Gupta, S.C.; Kim, J.H.; Prasad, S.; Aggarwal, B.B. Regulation of survival, proliferation, invasion, angiogenesis, and metastasis of tumor cells through modulation of inflammatory pathways by nutraceuticals. *Cancer Metastasis Rev,* **2010**, *29* (3), 405-434.

[77]   Gabriel, D.; Roedl, D.; Gordon, L.B.; Djabali, K. Sulforaphane enhances progerin clearance in Hutchinson-Gilford progeria fibroblasts. *Aging Cell,* **2015**, *14* (1), 78-91.

[78]   Amin, P.J.; Shankar, B.S. Sulforaphane induces ROS mediated induction of NKG2D ligands in human cancer cell lines and enhances susceptibility to NK cell mediated lysis. *Life Sci,* **2015**, *126*, 19-27.

[79]   Chu, W.F.; Wu, D.M.; Liu, W.; Wu, L.J.; Li, D.Z.; Xu, D.Y.*, et al.* Sulforaphane induces G2-M arrest and apoptosis in high metastasis cell line of salivary gland adenoid cystic carcinoma. *Oral Oncol,* **2009**, *45* (11), 998-1004.

[80]   Clarke, J.D.; Hsu, A.; Yu, Z.; Dashwood, R.H.; Ho, E. Differential effects of sulforaphane on histone deacetylases, cell cycle arrest and apoptosis in normal prostate cells versus hyperplastic and cancerous prostate cells. *Mol Nutr Food Res,* **2011**, *55* (7), 999-1009.

[81]   Fahey, J.W.; Zhang, Y.; Talalay, P. Broccoli sprouts: an exceptionally rich source of inducers of enzymes that protect against chemical carcinogens. *Proc Natl Acad Sci U S A,* **1997**, *94* (19), 10367-10372.

[82] Feitelson, M.A.; Arzumanyan, A.; Kulathinal, R.J.; Blain, S.W.; Holcombe, R.F.; Mahajna, J.*, et al.* Sustained proliferation in cancer: Mechanisms and novel therapeutic targets. *Semin Cancer Biol,* **2015**.

[83] Gamet-Payrastre, L.; Li, P.; Lumeau, S.; Cassar, G.; Dupont, M.A.; Chevolleau, S.*, et al.* Sulforaphane, a naturally occurring isothiocyanate, induces cell cycle arrest and apoptosis in HT29 human colon cancer cells. *Cancer Res,* **2000**, *60* (5), 1426-1433.

[84] Jakubikova, J.; Bao, Y.; Sedlak, J. Isothiocyanates induce cell cycle arrest, apoptosis and mitochondrial potential depolarization in HL-60 and multidrug-resistant cell lines. *Anticancer Res,* **2005**, *25* (5), 3375-3386.

[85] Liu, M.; Yao, X.D.; Li, W.; Geng, J.; Yan, Y.; Che, J.P.*, et al.* Nrf2 sensitizes prostate cancer cells to radiation via decreasing basal ROS levels. *Biofactors,* **2015**, *41* (1), 52-57.

[86] Pastorek, M.; Simko, V.; Takacova, M.; Barathova, M.; Bartosova, M.; Hunakova, L.*, et al.* Sulforaphane reduces molecular response to hypoxia in ovarian tumor cells independently of their resistance to chemotherapy. *Int J Oncol,* **2015**.

[87] Singh, S.V.; Srivastava, S.K.; Choi, S.; Lew, K.L.; Antosiewicz, J.; Xiao, D.*, et al.* Sulforaphane-induced cell death in human prostate cancer cells is initiated by reactive oxygen species. *J Biol Chem,* **2005**, *280* (20), 19911-19924.

[88] Wang, L.; Tian, Z.; Yang, Q.; Li, H.; Guan, H.; Shi, B.*, et al.* Sulforaphane inhibits thyroid cancer cell growth and invasiveness through the reactive oxygen species-dependent pathway. *Oncotarget,* **2015**, *6* (28), 25917-25931.

[89] Burnett, J.P.; Korkaya, H.; Ouzounova, M.D.; Jiang, H.; Conley, S.J.; Newman, B.W.*, et al.* Trastuzumab resistance induces EMT to transform HER2(+) PTEN(-) to a triple negative breast cancer that requires unique treatment options. *Sci Rep,* **2015**, *5*, 15821.

[90] Islam, S.S.; Mokhtari, R.B.; Akbari, P.; Hatina, J.; Yeger, H.; Farhat, W.A. Simultaneous Targeting of Bladder Tumor Growth, Survival, and Epithelial-to-Mesenchymal Transition with a Novel Therapeutic Combination of Acetazolamide (AZ) and Sulforaphane (SFN). *Target Oncol,* **2016**, *11* (2), 209-227.

[91] Clarke, J.D.; Hsu, A.; Riedl, K.; Bella, D.; Schwartz, S.J.; Stevens, J.F.*, et al.* Bioavailability and inter-conversion of sulforaphane and erucin in human subjects consuming broccoli sprouts or broccoli supplement in a cross-over study design. *Pharmacol Res,* **2011**, *64* (5), 456-463.

[92] Zuryn, A.; Litwiniec, A.; Safiejko-Mroczka, B.; Klimaszewska-Wisniewska, A.; Gagat, M.; Krajewski, A.*, et al.* The effect of sulforaphane on the cell cycle, apoptosis and expression of cyclin D1 and p21 in the A549 non-small cell lung cancer cell line. *Int J Oncol,* **2016**.

[93] Byun, S.; Shin, S.H.; Park, J.; Lim, S.; Lee, E.; Lee, C.*, et al.* Sulforaphene suppresses growth of colon cancer-derived tumors via induction of glutathione depletion and microtubule depolymerization. *Mol Nutr Food Res,* **2016**.

[94] Wu, J.; Han, J.; Hou, B.; Deng, C.; Wu, H.; Shen, L. Sulforaphane inhibits TGF-beta-induced epithelial-mesenchymal transition of hepatocellular carcinoma cells via the reactive oxygen species-dependent pathway. *Oncol Rep,* **2016**, *35* (5), 2977-2983.

[95] Shang, H.S.; Shih, Y.L.; Lee, C.H.; Hsueh, S.C.; Liu, J.Y.; Liao, N.C.*, et al.* Sulforaphane-induced apoptosis in human leukemia HL-60 cells through extrinsic and intrinsic signal pathways and altering associated genes expression assayed by cDNA microarray. *Environ Toxicol,* **2016**.

[96] Jackson, S.J.; Singletary, K.W.; Murphy, L.L.; Venema, R.C.; Young, A.J. Phytonutrients Differentially Stimulate NAD(P)H:Quinone Oxidoreductase, Inhibit Proliferation, and Trigger Mitotic Catastrophe in Hepa1c1c7 Cells. *J Med Food,* **2016**, *19* (1), 47-53.

[97] Shen, G.; Xu, C.; Chen, C.; Hebbar, V.; Kong, A.N. p53-independent G1 cell cycle arrest of human colon carcinoma cells HT-29 by sulforaphane is associated with induction of p21CIP1 and inhibition of expression of cyclin D1. *Cancer Chemother Pharmacol,* **2006**, *57* (3), 317-327.

[98] Wang, L.; Liu, D.; Ahmed, T.; Chung, F.L.; Conaway, C.; Chiao, J.W. Targeting cell cycle machinery as a molecular mechanism of sulforaphane in prostate cancer prevention. *Int J Oncol,* **2004**, *24* (1), 187-192.

[99] Chiao, J.W.; Wu, H.; Ramaswamy, G.; Conaway, C.C.; Chung, F.L.; Wang, L.*, et al.* Ingestion of an isothiocyanate metabolite from cruciferous vegetables inhibits growth of human prostate cancer cell xenografts by apoptosis and cell cycle arrest. *Carcinogenesis,* **2004**, *25* (8), 1403-1408.

[100] Jiang, L.L.; Zhou, S.J.; Zhang, X.M.; Chen, H.Q.; Liu, W. Sulforaphane suppresses in vitro and in vivo lung tumorigenesis through downregulation of HDAC activity. *Biomed Pharmacother,* **2016**, *78*, 74-80.

[101] Chang, L.C.; Yu, Y.L. Dietary components as epigenetic-regulating agents against cancer. *Biomedicine (Taipei),* **2016**, *6* (1), 2.

[102] Thaler, R.; Maurizi, A.; Roschger, P.; Sturmlechner, I.; Khani, F.; Spitzer, S.*, et al.* Anabolic and Antiresorptive Modulation of Bone Homeostasis by the Epigenetic Modulator Sulforaphane, a Naturally Occurring Isothiocyanate. *J Biol Chem,* **2016**, *291* (13), 6754-6771.

[103] Abbas, A.; Hall, J.A.; Patterson, W.L., 3rd; Ho, E.; Hsu, A.; Al-Mulla, F.*, et al.* Sulforaphane modulates telomerase activity via epigenetic regulation in prostate cancer cell lines. *Biochem Cell Biol,* **2016**, *94* (1), 71-81.

[104] Fuentes, F.; Paredes-Gonzalez, X.; Kong, A.T. Dietary Glucosinolates Sulforaphane, Phenethyl Isothiocyanate, Indole-3-Carbinol/3,3'-Diindolylmethane: Anti-Oxidative Stress/Inflammation, Nrf2, Epigenetics/Epigenomics and Cancer Chemopreventive Efficacy. *Curr Pharmacol Rep,* **2015**, *1* (3), 179-196.

[105] Kheiri Manjili, H.; Ma'mani, L.; Tavaddod, S.; Mashhadikhan, M.; Shafiee, A.; Naderi-Manesh, H. D, L-Sulforaphane Loaded Fe3O4@ Gold Core Shell Nanoparticles: A Potential Sulforaphane Delivery System. *PLoS One,* **2016**, *11* (3), e0151344.

[106] Li, Y.P.; Wang, S.L.; Liu, B.; Tang, L.; Kuang, R.R.; Wang, X.B*., et al.* Sulforaphane prevents rat cardiomyocytes from hypoxia/reoxygenation injury in vitro via activating SIRT1 and subsequently inhibiting ER stress. *Acta Pharmacol Sin,* **2016**, *37* (3), 344-353.

[107] Rizzo, V.L.; Levine, C.B.; Wakshlag, J.J. The effects of sulforaphane on canine osteosarcoma proliferation and invasion. *Vet Comp Oncol,* **2016**.

[108] Shih, Y.L.; Wu, L.Y.; Lee, C.H.; Chen, Y.L.; Hsueh, S.C.; Lu, H.F*., et al.* Sulforaphane promotes immune responses in a WEHI3induced leukemia mouse model through enhanced phagocytosis of macrophages and natural killer cell activities in vivo. *Mol Med Rep,* **2016**, *13* (5), 4023-4029.

[109] Watson, G.W.; Wickramasekara, S.; Maier, C.S.; Williams, D.E.; Dashwood, R.H.; Ho, E. Assessment of global proteome in LNCaP cells by 2D-RP/RP LC-MS/MS following sulforaphane exposure. *EuPA Open Proteom,* **2015**, *9*, 34-40.

[110] Zhang, Z.; Li, C.; Shang, L.; Zhang, Y.; Zou, R.; Zhan, Y*., et al.* Sulforaphane induces apoptosis and inhibits invasion in U251MG glioblastoma cells. *Springerplus,* **2016**, *5*, 235.

[111] Fisher, M.L.; Adhikary, G.; Grun, D.; Kaetzel, D.M.; Eckert, R.L. The Ezh2 polycomb group protein drives an aggressive phenotype in melanoma cancer stem cells and is a target of diet derived sulforaphane. *Mol Carcinog,* **2015**.

[112] Rudolf, K.; Cervinka, M.; Rudolf, E. Sulforaphane-induced apoptosis involves p53 and p38 in melanoma cells. *Apoptosis,* **2014**, *19* (4), 734-747.

[113] Kallifatidis, G.; Labsch, S.; Rausch, V.; Mattern, J.; Gladkich, J.; Moldenhauer, G*., et al.* Sulforaphane increases drug-mediated cytotoxicity toward cancer stem-like cells of pancreas and prostate. *Mol Ther,* **2011**, *19* (1), 188-195.

[114] Labsch, S.; Liu, L.; Bauer, N.; Zhang, Y.; Aleksandrowicz, E.; Gladkich, J*., et al.* Sulforaphane and TRAIL induce a synergistic elimination of advanced prostate cancer stem-like cells. *Int J Oncol,* **2014**, *44* (5), 1470-1480.

[115] Wang, Y.; Dacosta, C.; Wang, W.; Zhou, Z.; Liu, M.; Bao, Y. Synergy between sulforaphane and selenium in protection against oxidative damage in colonic CCD841 cells. *Nutr Res,* **2015**, *35* (7), 610-617.

[116] Wang, X.; Govind, S.; Sajankila, S.P.; Mi, L.; Roy, R.; Chung, F.L. Phenethyl isothiocyanate sensitizes human cervical cancer cells to apoptosis induced by cisplatin. *Mol Nutr Food Res,* **2011**, *55* (10), 1572-1581.

[117] Thakkar, A.; Chenreddy, S.; Wang, J.; Prabhu, S. Evaluation of ibuprofen loaded solid lipid nanoparticles and its combination regimens for pancreatic cancer chemoprevention. *Int J Oncol,* **2015**, *46* (4), 1827-1834.

[118] Sutaria, D.; Grandhi, B.K.; Thakkar, A.; Wang, J.; Prabhu, S. Chemoprevention of pancreatic cancer using solid-lipid nanoparticulate delivery of a novel aspirin, curcumin and sulforaphane drug combination regimen. *Int J Oncol,* **2012**, *41* (6), 2260-2268.

[119] Shen, G.; Khor, T.O.; Hu, R.; Yu, S.; Nair, S.; Ho, C.T.*, et al.* Chemoprevention of familial adenomatous polyposis by natural dietary compounds sulforaphane and dibenzoylmethane alone and in combination in ApcMin/+ mouse. *Cancer Res,* **2007**, *67* (20), 9937-9944.

[120] Saw, C.L.; Cintron, M.; Wu, T.Y.; Guo, Y.; Huang, Y.; Jeong, W.S.*, et al.* Pharmacodynamics of dietary phytochemical indoles I3C and DIM: Induction of Nrf2-mediated phase II drug metabolizing and antioxidant genes and synergism with isothiocyanates. *Biopharm Drug Dispos,* **2011**, *32* (5), 289-300.

[121] Pawlik, A.; Slominska-Wojewodzka, M.; Herman-Antosiewicz, A. Sensitization of estrogen receptor-positive breast cancer cell lines to 4-hydroxytamoxifen by isothiocyanates present in cruciferous plants. *Eur J Nutr,* **2016**, *55* (3), 1165-1180.

[122] Li, D.; Wang, W.; Shan, Y.; Barrera, L.N.; Howie, A.F.; Beckett, G.J.*, et al.* Synergy between sulforaphane and selenium in the up-regulation of thioredoxin reductase and protection against hydrogen peroxide-induced cell death in human hepatocytes. *Food Chem,* **2012**, *133* (2), 300-307.

[123] Kalra, S.; Zhang, Y.; Knatko, E.V.; Finlayson, S.; Yamamoto, M.; Dinkova-Kostova, A.T. Oral azathioprine leads to higher incorporation of 6-thioguanine in DNA of skin than liver: the protective role of the Keap1/Nrf2/ARE pathway. *Cancer Prev Res (Phila),* **2011**, *4* (10), 1665-1674.

[124] Hussain, A.; Priyani, A.; Sadrieh, L.; Brahmbhatt, K.; Ahmed, M.; Sharma, C. Concurrent sulforaphane and eugenol induces differential effects on human cervical cancer cells. *Integr Cancer Ther,* **2012**, *11* (2), 154-165.

[125] Hussain, A.; Mohsin, J.; Prabhu, S.A.; Begum, S.; Nusri Qel, A.; Harish, G.*, et al.* Sulforaphane inhibits growth of human breast cancer cells and augments the therapeutic index of the chemotherapeutic drug, gemcitabine. *Asian Pac J Cancer Prev,* **2013**, *14* (10), 5855-5860.

[126] Guo, S.; Qiu, P.; Xu, G.; Wu, X.; Dong, P.; Yang, G.*, et al.* Synergistic anti-inflammatory effects of nobiletin and sulforaphane in lipopolysaccharide-stimulated RAW 264.7 cells. *J Agric Food Chem,* **2012**, *60* (9), 2157-2164.

[127] Doudican, N.A.; Wen, S.Y.; Mazumder, A.; Orlow, S.J. Sulforaphane synergistically enhances the cytotoxicity of arsenic trioxide in multiple myeloma cells via stress-mediated pathways. *Oncol Rep,* **2012**, *28* (5), 1851-1858.

[128] Doudican, N.A.; Bowling, B.; Orlow, S.J. Enhancement of arsenic trioxide cytotoxicity by dietary isothiocyanates in human leukemic cells via a reactive oxygen species-dependent mechanism. *Leuk Res,* **2010**, *34* (2), 229-234.

[129] Ouyang, L.; Shi, Z.; Zhao, S.; Wang, F.T.; Zhou, T.T.; Liu, B*., et al.* Programmed cell death pathways in cancer: a review of apoptosis, autophagy and programmed necrosis. *Cell Prolif,* **2012**, *45* (6), 487-498.

[130] Morselli, E.; Galluzzi, L.; Kepp, O.; Vicencio, J.M.; Criollo, A.; Maiuri, M.C*., et al.* Anti- and pro-tumor functions of autophagy. *Biochim Biophys Acta,* **2009**, *1793* (9), 1524-1532.

[131] Levine, B.; Yuan, J. Autophagy in cell death: an innocent convict? *J Clin Invest,* **2005**, *115* (10), 2679-2688.

[132] Darvekar, S.R.; Elvenes, J.; Brenne, H.B.; Johansen, T.; Sjottem, E. SPBP is a sulforaphane induced transcriptional coactivator of NRF2 regulating expression of the autophagy receptor p62/SQSTM1. *PLoS One,* **2014**, *9* (1), e85262.

[133] Lee, J.H.; Jeong, J.K.; Park, S.Y. Sulforaphane-induced autophagy flux prevents prion protein-mediated neurotoxicity through AMPK pathway. *Neuroscience,* **2014**, *278*, 31-39.

[134] Naumann, P.; Fortunato, F.; Zentgraf, H.; Buchler, M.W.; Herr, I.; Werner, J. Autophagy and cell death signaling following dietary sulforaphane act independently of each other and require oxidative stress in pancreatic cancer. *Int J Oncol,* **2011**, *39* (1), 101-109.

[135] Litwak, S.A.; Wali, J.A.; Pappas, E.G.; Saadi, H.; Stanley, W.J.; Varanasi, L.C*., et al.* Lipotoxic Stress Induces Pancreatic beta-Cell Apoptosis through Modulation of Bcl-2 Proteins by the Ubiquitin-Proteasome System. *J Diabetes Res,* **2015**, *2015*, 280615.

[136] Jeong, H.S.; Choi, H.Y.; Lee, E.R.; Kim, J.H.; Jeon, K.; Lee, H.J*., et al.* Involvement of caspase-9 in autophagy-mediated cell survival pathway. *Biochim Biophys Acta,* **2011**, *1813* (1), 80-90.

[137] Wang, M.; Chen, S.; Qing, Y.; Wu, D.; Lin, Y.M.; Chen, J*., et al.* Effects of autophagy modulator on autophagy and uridine 5'-diphospho-glucuronosyltransferase 1A1 induced by sulforaphane. *Zhonghua Yi Xue Za Zhi,* **2013**, *93* (8), 614-618.

[138] Kanematsu, S.; Uehara, N.; Miki, H.; Yoshizawa, K.; Kawanaka, A.; Yuri, T*., et al.* Autophagy inhibition enhances sulforaphane-induced apoptosis in human breast cancer cells. *Anticancer Res,* **2010**, *30* (9), 3381-3390.

[139] Liu, H.; Talalay, P. Relevance of anti-inflammatory and antioxidant activities of exemestane and synergism with sulforaphane for disease prevention. *Proc Natl Acad Sci U S A,* **2013**, *110* (47), 19065-19070.

[140] Harvey, C.J.; Thimmulappa, R.K.; Sethi, S.; Kong, X.; Yarmus, L.; Brown, R.H*., et al.* Targeting Nrf2 signaling improves bacterial clearance by alveolar macrophages in patients with COPD and in a mouse model. *Sci Transl Med,* **2011**, *3* (78), 78ra32.

[141]   Starrett, W.; Blake, D.J. Sulforaphane inhibits de novo synthesis of IL-8 and MCP-1 in human epithelial cells generated by cigarette smoke extract. *J Immunotoxicol,* **2011**, *8* (2), 150-158.

[142]   Zeng, X.; Liu, X.; Bao, H.; Zhang, Y.; Wang, X.; Shi, K.*, et al.* [Effects of sulforaphane on Toll-like receptor 4/myeloid differentiation factor 88 pathway of monocyte-derived macrophages from patients with chronic obstructive pulmonary disease]. *Zhonghua Jie He He Hu Xi Za Zhi,* **2014**, *37* (4), 250-254.

[143]   Choi, K.; Chen, J.; Mitra, S.; Sarna, S.K. Impaired integrity of DNA after recovery from inflammation causes persistent dysfunction of colonic smooth muscle. *Gastroenterology,* **2011**, *141* (4), 1293-1301, 1301 e1291-1293.

[144]   Kerns, M.L.; DePianto, D.; Dinkova-Kostova, A.T.; Talalay, P.; Coulombe, P.A. Reprogramming of keratin biosynthesis by sulforaphane restores skin integrity in epidermolysis bullosa simplex. *Proc Natl Acad Sci U S A,* **2007**, *104* (36), 14460-14465.

[145]   Cho, H.Y.; Imani, F.; Miller-DeGraff, L.; Walters, D.; Melendi, G.A.; Yamamoto, M.*, et al.* Antiviral activity of Nrf2 in a murine model of respiratory syncytial virus disease. *Am J Respir Crit Care Med,* **2009**, *179* (2), 138-150.

[146]   Kesic, M.J.; Simmons, S.O.; Bauer, R.; Jaspers, I. Nrf2 expression modifies influenza A entry and replication in nasal epithelial cells. *Free Radic Biol Med,* **2011**, *51* (2), 444-453.

[147]   Nioi, P.; McMahon, M.; Itoh, K.; Yamamoto, M.; Hayes, J.D. Identification of a novel Nrf2-regulated antioxidant response element (ARE) in the mouse NAD(P)H:quinone oxidoreductase 1 gene: reassessment of the ARE consensus sequence. *Biochem J,* **2003**, *374* (Pt 2), 337-348.

[148]   Chang, Y.W.; Jang, J.Y.; Kim, Y.H.; Kim, J.W.; Shim, J.J. The Effects of Broccoli Sprout Extract Containing Sulforaphane on Lipid Peroxidation and Helicobacter pylori Infection in the Gastric Mucosa. *Gut Liver,* **2015**, *9* (4), 486-493.

[149]   Fahey, J.W.; Haristoy, X.; Dolan, P.M.; Kensler, T.W.; Scholtus, I.; Stephenson, K.K.*, et al.* Sulforaphane inhibits extracellular, intracellular, and antibiotic-resistant strains of Helicobacter pylori and prevents benzo[a]pyrene-induced stomach tumors. *Proc Natl Acad Sci U S A,* **2002**, *99* (11), 7610-7615.

[150]   Fahey, J.W.; Stephenson, K.K.; Wade, K.L.; Talalay, P. Urease from Helicobacter pylori is inactivated by sulforaphane and other isothiocyanates. *Biochem Biophys Res Commun,* **2013**, *435* (1), 1-7.

[151]   Haristoy, X.; Fahey, J.W.; Scholtus, I.; Lozniewski, A. Evaluation of the antimicrobial effects of several isothiocyanates on Helicobacter pylori. *Planta Med,* **2005**, *71* (4), 326-330.

[152]   Johansson, N.L.; Pavia, C.S.; Chiao, J.W. Growth inhibition of a spectrum of bacterial and fungal pathogens by sulforaphane, an isothiocyanate product found in broccoli and other cruciferous vegetables. *Planta Med,* **2008**, *74* (7), 747-750.

[153]   Moon, J.K.; Kim, J.R.; Ahn, Y.J.; Shibamoto, T. Analysis and anti-Helicobacter activity of sulforaphane and related compounds present in broccoli (Brassica oleracea L.) sprouts. *J Agric Food Chem,* **2010**, *58* (11), 6672-6677.

[154]   Yanaka, A. Sulforaphane enhances protection and repair of gastric mucosa against oxidative stress in vitro, and demonstrates anti-inflammatory effects on Helicobacter pylori-infected gastric mucosae in mice and human subjects. *Curr Pharm Des,* **2011**, *17* (16), 1532-1540.

[155]   Yanaka, A.; Fahey, J.W.; Fukumoto, A.; Nakayama, M.; Inoue, S.; Zhang, S*., et al.* Dietary sulforaphane-rich broccoli sprouts reduce colonization and attenuate gastritis in Helicobacter pylori-infected mice and humans. *Cancer Prev Res (Phila),* **2009**, *2* (4), 353-360.

[156]   Yanaka, A.; Zhang, S.; Tauchi, M.; Suzuki, H.; Shibahara, T.; Matsui, H*., et al.* Role of the nrf-2 gene in protection and repair of gastric mucosa against oxidative stress. *Inflammopharmacology,* **2005**, *13* (1-3), 83-90.

[157]   Zhao, L.; Lee, J.Y.; Hwang, D.H. Inhibition of pattern recognition receptor-mediated inflammation by bioactive phytochemicals. *Nutr Rev,* **2011**, *69* (6), 310-320.

[158]   Reddy, S.A.; Shelar, S.B.; Dang, T.M.; Lee, B.N.; Yang, H.; Ong, S.M*., et al.* Sulforaphane and its methylcarbonyl analogs inhibit the LPS-stimulated inflammatory response in human monocytes through modulating cytokine production, suppressing chemotactic migration and phagocytosis in a NF-kappaB- and MAPK-dependent manner. *Int Immunopharmacol,* **2015**, *24* (2), 440-450.

[159]   Choi, Y.J.; Lee, W.S.; Lee, E.G.; Sung, M.S.; Yoo, W.H. Sulforaphane inhibits IL-1beta-induced proliferation of rheumatoid arthritis synovial fibroblasts and the production of MMPs, COX-2, and PGE2. *Inflammation,* **2014**, *37* (5), 1496-1503.

[160]   Amin, A.R.; Dave, M.; Attur, M.; Abramson, S.B. COX-2, NO, and cartilage damage and repair. *Curr Rheumatol Rep,* **2000**, *2* (6), 447-453.

[161]   Davidson, R.K.; Jupp, O.; de Ferrars, R.; Kay, C.D.; Culley, K.L.; Norton, R*., et al.* Sulforaphane represses matrix-degrading proteases and protects cartilage from destruction in vitro and in vivo. *Arthritis Rheum,* **2013**, *65* (12), 3130-3140.

[162]   Healy, Z.R.; Liu, H.; Holtzclaw, W.D.; Talalay, P. Inactivation of tautomerase activity of macrophage migration inhibitory factor by sulforaphane: a potential biomarker for anti-inflammatory intervention. *Cancer Epidemiol Biomarkers Prev,* **2011**, *20* (7), 1516-1523.

[163]   Heiss, E.; Herhaus, C.; Klimo, K.; Bartsch, H.; Gerhauser, C. Nuclear factor kappa B is a molecular target for sulforaphane-mediated anti-inflammatory mechanisms. *J Biol Chem,* **2001**, *276* (34), 32008-32015.

[164]   Lin, W.; Wu, R.T.; Wu, T.; Khor, T.O.; Wang, H.; Kong, A.N. Sulforaphane suppressed LPS-induced inflammation in mouse peritoneal macrophages through Nrf2 dependent pathway. *Biochem Pharmacol,* **2008**, *76* (8), 967-973.

[165] Olagnier, D.; Lavergne, R.A.; Meunier, E.; Lefevre, L.; Dardenne, C.; Aubouy, A.*, et al.* Nrf2, a PPARgamma alternative pathway to promote CD36 expression on inflammatory macrophages: implication for malaria. *PLoS Pathog,* **2011**, *7* (9), e1002254.

[166] Ho, J.N.; Kang, E.R.; Yoon, H.G.; Jeon, H.; Jun, W.; Watson, R.R.*, et al.* Inhibition of premature death by isothiocyanates through immune restoration in LP-BM5 leukemia retrovirus-infected C57BL/6 mice. *Biosci Biotechnol Biochem,* **2011**, *75* (7), 1234-1239.

[167] Hushmendy, S.; Jayakumar, L.; Hahn, A.B.; Bhoiwala, D.; Bhoiwala, D.L.; Crawford, D.R. Select phytochemicals suppress human T-lymphocytes and mouse splenocytes suggesting their use in autoimmunity and transplantation. *Nutr Res,* **2009**, *29* (8), 568-578.

[168] Kong, J.S.; Yoo, S.A.; Kim, H.S.; Kim, H.A.; Yea, K.; Ryu, S.H.*, et al.* Inhibition of synovial hyperplasia, rheumatoid T cell activation, and experimental arthritis in mice by sulforaphane, a naturally occurring isothiocyanate. *Arthritis Rheum,* **2010**, *62* (1), 159-170.

[169] Geisel, J.; Bruck, J.; Glocova, I.; Dengler, K.; Sinnberg, T.; Rothfuss, O.*, et al.* Sulforaphane protects from T cell-mediated autoimmune disease by inhibition of IL-23 and IL-12 in dendritic cells. *J Immunol,* **2014**, *192* (8), 3530-3539.

[170] Fragoulis, A.; Laufs, J.; Muller, S.; Soppa, U.; Siegl, S.; Reiss, L.K.*, et al.* Sulforaphane has opposing effects on TNF-alpha stimulated and unstimulated synoviocytes. *Arthritis Res Ther,* **2012**, *14* (5), R220.

[171] Shankar, S.; Ganapathy, S.; Srivastava, R.K. Sulforaphane enhances the therapeutic potential of TRAIL in prostate cancer orthotopic model through regulation of apoptosis, metastasis, and angiogenesis. *Clin Cancer Res,* **2008**, *14* (21), 6855-6866.

[172] Jeong, S.I.; Choi, B.M.; Jang, S.I. Sulforaphane suppresses TARC/CCL17 and MDC/CCL22 expression through heme oxygenase-1 and NF-kappaB in human keratinocytes. *Arch Pharm Res,* **2010**, *33* (11), 1867-1876.

[173] Jiang, X.; Bai, Y.; Zhang, Z.; Xin, Y.; Cai, L. Protection by sulforaphane from type 1 diabetes-induced testicular apoptosis is associated with the up-regulation of Nrf2 expression and function. *Toxicol Appl Pharmacol,* **2014**, *279* (2), 198-210.

[174] Song, M.Y.; Kim, E.K.; Moon, W.S.; Park, J.W.; Kim, H.J.; So, H.S.*, et al.* Sulforaphane protects against cytokine- and streptozotocin-induced beta-cell damage by suppressing the NF-kappaB pathway. *Toxicol Appl Pharmacol,* **2009**, *235* (1), 57-67.

[175] Berenbaum, F. Does broccoli protect from osteoarthritis? *Joint Bone Spine,* **2014**, *81* (4), 284-286.

[176] Jose, J.; Burgess, K. Benzophenoxazine-based fluorescent dyes for labeling biomolecules. *Tetrahedron,* **2006**, *62*, 11021–11037.

[177] Stužka, V.; Šimánek, V.; Stránský, Z. Infra-red spectroscopy of benzo(α)phenoxazines. *Spectroscopy,* **1967**, *23* (7), 2175-2183.

[178] Greenspan, P.; Mayer, E.P.; Fowler, S.D. Nile red: a selective fluorescent stain for intracellular lipid droplets. *J Cell Biol,* **1985**, *100* (3), 965-973.

[179] Soto, C.Y.; Andreu, N.; Gibert, I.; Luquin, M. Simple and rapid differentiation of Mycobacterium tuberculosis H37Ra from M. tuberculosis clinical isolates through two cytochemical tests using neutral red and nile blue stains. *J Clin Microbiol,* **2002**, *40* (8), 3021-3024.

[180] Firmino, A.D.G.; Gonçalves, M.S.T. Bifunctionalised long-wavelength fluorescent probes for biological applications. *Tetrahedron Letters,* **2012**, *53* (37), 4946–4950.

[181] Raju, B.R.; Firmino, A.D.G.; Costa, A.L.S.; Coutinho, P.J.G.; Gonçalves, M.S.T. Synthesis and photophysical properties of side-chain chlorinated benzo[a]phenoxazinium chlorides. *Tetrahedron,* **2013**, *69* (11), 2451-2461.

[182] Pal, S.; Konkimalla, V.B.; Kathwate, L.; Rao, S.S.; S. P. Gejji; Puranik, V.*, et al.* Targeting chemorefractory COLO205 (BRAF V600E) cell lines using substituted benzo[α]phenoxazines†. *RSC Advances,* **2015**, *5*, 82549.

[183] Cincotta, L.; Foley, J.W.; Cincotta, A.H. Phototoxicity, redox behavior, and pharmacokinetics of benzophenoxazine analogues in EMT-6 murine sarcoma cells. *Cancer Res,* **1993**, *53* (11), 2571-2580.

[184] Liu, W.; Sun, R.; Ge, J.F.; Xu, Y.J.; Xu, Y.; Lu, J.M.*, et al.* Reversible near-infrared pH probes based on benzo[a]phenoxazine. *Anal Chem,* **2013**, *85* (15), 7419-7425.

[185] Karolin, J.; Panek, D.; MacMillan, A.; Rolinski, O.; Birch, D. Fluorescence biosensing in nanopores. *Conf Proc IEEE Eng Med Biol Soc,* **2009**, *2009*, 4154-4157.

[186] Ramoino, P.; Margallo, E.; Nicolo, G. Age-related changes in neutral lipid content of Paramecium primaurelia as revealed by nile red. *J Lipid Res,* **1996**, *37* (6), 1207-1212.

[187] Jose, J.; Loudet, A.; Ueno, Y.; Barhoumi, R.; Burghardt, R.C.; Burgess, K. Intracellular imaging of organelles with new water-soluble benzophenoxazine dyes. *Org Biomol Chem,* **2010**, *8* (9), 2052-2059.

[188] Greenspan, P.; Fowler, S.D. Spectrofluorometric studies of the lipid probe, nile red. *J Lipid Res,* **1985**, *26* (7), 781-789.

[189] Diaz, G.; Melis, M.; Batetta, B.; Angius, F.; Falchi, A.M. Hydrophobic characterization of intracellular lipids in situ by Nile Red red/yellow emission ratio. *Micron,* **2008**, *39* (7), 819-824.

[190] Alba, F.J.; Bartolome, S.; Bermudez, A.; Daban, J.R. Fluorescent labeling of proteins and its application to SDS-PAGE and western blotting. *Methods Mol Biol,* **2009**, *536*, 407-416.

[191] Alba, F.J.; Bartolome, S.; Bermudez, A.; Daban, J.R. Fluorescent Labeling of Proteins and Its Application to SDS-PAGE and Western Blotting. *Methods Mol Biol,* **2015**, *1314*, 41-50.

[192] Fowler, S.D.; Brown, W.J.; Warfel, J.; Greenspan, P. Use of nile red for the rapid in situ quantitation of lipids on thin-layer chromatograms. *J Lipid Res,* **1987**, *28* (10), 1225-1232.

[193]   Daban, J.R.; Bartolome, S.; Samso, M. Use of the hydrophobic probe Nile red for the fluorescent staining of protein bands in sodium dodecyl sulfate-polyacrylamide gels. *Anal Biochem,* **1991**, *199* (2), 169-174.

[194]   Lahti, R.; Salminen, T.; Latonen, S.; Heikinheimo, P.; Pohjanoksa, K.; Heinonen, J. Genetic engineering of Escherichia coli inorganic pyrophosphatase. Tyr55 and Tyr141 are important for the structural integrity. *Eur J Biochem,* **1991**, *198* (2), 293-297.

[195]   Ogita, S.; Lee, J.B.; Kurosaki, F.; Kato, Y. The biosynthetic activities of primary and secondary metabolites in suspension cultures of Aquilaria microcarpa. *Nat Prod Commun,* **2015**, *10* (5), 779-782.

[196]   Hernando, V.; Rieutord, A.; Brion, F.; Prognon, P. Evidence for lipids-calcium ions interactions using fluorescent probing in paediatric nutrition admixtures. *Talanta,* **2003**, *60* (2-3), 543-554.

[197]   Hernando, V.; Rieutord, A.; Pansu, R.; Brion, F.; Prognon, P. Immobilised artificial membrane chromatography coupled with molecular probing. Mimetic system for studying lipid-calcium interactions in nutritional mixtures. *J Chromatogr A,* **2005**, *1064* (1), 75-84.

[198]   Chen, J.; Zeng, F.; Wu, S.; Su, J.; Zhao, J.; Tong, Z. A facile approach for cupric ion detection in aqueous media using polyethyleneimine/PMMA core-shell fluorescent nanoparticles. *Nanotechnology,* **2009**, *20* (36), 365502.

[199]   Chadar Dattatray; Rao S. Soniya; Khan Ayesha; Gejji P. Shridhar; Kiesar, B.S.; Thomas, W.*, et al.* Benzo[a]phenoxazines and benzo[a]phenothiazine from vitamin K3: synthesis, molecular structures, DFT studies and cytotoxic activity. *RSC Advances,* **2015**, *5*, 57917–57929.

[200]   Wesolowska, O.; Molnar, J.; Westman, G.; Samuelsson, K.; Kawase, M.; Ocsovszki, I.*, et al.* Benzo[a]phenoxazines: a new group of potent P-glycoprotein inhibitors. *In Vivo,* **2006**, *20* (1), 109-113.

[201]   McLuckie, K.I.; Waller, Z.A.; Sanders, D.A.; Alves, D.; Rodriguez, R.; Dash, J.*, et al.* G-quadruplex-binding benzo[a]phenoxazines down-regulate c-KIT expression in human gastric carcinoma cells. *J Am Chem Soc,* **2011**, *133* (8), 2658-2663.

[202]   Thorne, S.H.; Barak, Y.; Liang, W.; Bachmann, M.H.; Rao, J.; Contag, C.H.*, et al.* CNOB/ChrR6, a new prodrug enzyme cancer chemotherapy. *Mol Cancer Ther,* **2009**, *8* (2), 333-341.

[203]   Motohashi, N. [Interaction between 9-substituted benzo[alpha]phenoxazine derivatives and DNA and relationships to their antibacterial activities]. *Yakugaku Zasshi,* **1982**, *102* (7), 646-650.

[204]   Motohashi, N. [Test for antitumor, antibacterial and antifungal activities of 9-substituted benzo[a]phenoxazine derivatives]. *Yakugaku Zasshi,* **1982**, *102* (10), 992-994.

[205] Hara, K.; Okamoto, M.; Aki, T.; Yagita, H.; Tanaka, H.; Mizukami, Y*., et al.* Synergistic enhancement of TRAIL- and tumor necrosis factor alpha-induced cell death by a phenoxazine derivative. *Mol Cancer Ther,* **2005**, *4* (7), 1121-1127.

[206] Shi, X.L.; Ge, J.F.; Liu, B.Q.; Kaiser, M.; Wittlin, S.; Brun, R*., et al.* Synthesis and in vitro antiprotozoal activities of 5-phenyliminobenzo[a]phenoxazine derivatives. *Bioorg Med Chem Lett,* **2011**, *21* (19), 5804-5807.

[207] Chanput, W.; Mes, J.J.; Savelkoul, H.F.; Wichers, H.J. Characterization of polarized THP-1 macrophages and polarizing ability of LPS and food compounds. *Food Funct,* **2013**, *4* (2), 266-276.

[208] Chanput, W.; Mes, J.J.; Wichers, H.J. THP-1 cell line: an in vitro cell model for immune modulation approach. *Int Immunopharmacol,* **2014**, *23* (1), 37-45.

[209] Daigneault, M.; Preston, J.A.; Marriott, H.M.; Whyte, M.K.; Dockrell, D.H. The identification of markers of macrophage differentiation in PMA-stimulated THP-1 cells and monocyte-derived macrophages. *PLoS One,* **2010**, *5* (1), e8668.

[210] Fleit, H.B.; Kobasiuk, C.D. The human monocyte-like cell line THP-1 expresses Fc gamma RI and Fc gamma RII. *J Leukoc Biol,* **1991**, *49* (6), 556-565.

[211] Genin, M.; Clement, F.; Fattaccioli, A.; Raes, M.; Michiels, C. M1 and M2 macrophages derived from THP-1 cells differentially modulate the response of cancer cells to etoposide. *BMC Cancer,* **2015**, *15*, 577.

[212] Park, E.; Jung, H.; Yang, H.; Yoo, M.; Kim, C.; Kim, K. Optimized THP-1 differentiation is required for the detection of responses to weak stimuli. *Inflamm Res. ,* **2007**, *56* (1), 45-50.

[213] Little, A.S.; Balmanno, K.; Sale, M.J.; Newman, S.; Dry, J.R.; Hampson, M*., et al.* Amplification of the driving oncogene, KRAS or BRAF, underpins acquired resistance to MEK1/2 inhibitors in colorectal cancer cells. *Sci Signal,* **2011**, *4* (166), ra17.

[214] Peng, W.; Hu, J.; Zhu, X.D.; Liu, X.; Wang, C.C.; Li, W.H*., et al.* Overexpression of miR-145 increases the sensitivity of vemurafenib in drug-resistant colo205 cell line. *Tumour Biol,* **2014**, *35* (4), 2983-2988.

[215] Deer, E.L.; Gonzalez-Hernandez, J.; Coursen, J.D.; Shea, J.E.; Ngatia, J.; Scaife, C.L*., et al.* Phenotype and genotype of pancreatic cancer cell lines. *Pancreas,* **2010**, *39* (4), 425-435.

[216] Sipos, B.; Moser, S.; Kalthoff, H.; Torok, V.; Lohr, M.; Kloppel, G. A comprehensive characterization of pancreatic ductal carcinoma cell lines: towards the establishment of an in vitro research platform. *Virchows Arch,* **2003**, *442* (5), 444-452.

[217] Jiang, Q.; Zhang, Z.; Hu, Y.; Ma, Y. Function of Hsf1 in SV40 Tantigentransformed HEK293T cells. *Mol Med Rep,* **2014**, *10* (6), 3139-3144.

[218] Vermes, I.; Haanen, C.; Steffens-Nakken, H.; Reutelingsperger, C. A novel assay for apoptosis. Flow cytometric detection of phosphatidylserine expression on early apoptotic cells using fluorescein labelled Annexin V. *J Immunol Methods,* **1995**, *184* (1), 39-51.

[219] Nagata, S. Apoptotic DNA fragmentation. *Exp Cell Res,* **2000**, *256* (1), 12-18.

[220] Scudiero, D.A.; Shoemaker, R.H.; Paull, K.D.; Monks, A.; Tierney, S.; Nofziger, T.H.*, et al.* Evaluation of a soluble tetrazolium/formazan assay for cell growth and drug sensitivity in culture using human and other tumor cell lines. *Cancer Res,* **1988**, *48* (17), 4827-4833.

[221] Zips, D.; Thames, H.D.; Baumann, M. New anticancer agents: in vitro and in vivo evaluation. *In Vivo,* **2005**, *19* (1), 1-7.

[222] Gupta, V.; Krishan, A.; Zubrod, C.G. Correlation of in vitro clonogenic assay data with in vivo growth delays and cell cycle changes of a human melanoma xenograft. *Cancer Res,* **1983**, *43* (6), 2560-2564.

[223] Franken, N.A.; Rodermond, H.M.; Stap, J.; Haveman, J.; van Bree, C. Clonogenic assay of cells in vitro. *Nat Protoc,* **2006**, *1* (5), 2315-2319.

[224] Gordon, S.; Taylor, P.R. Monocyte and macrophage heterogeneity. *Nat Rev Immunol,* **2005**, *5* (12), 953-964.

[225] Martinez, F.O.; Gordon, S. The evolution of our understanding of macrophages and translation of findings toward the clinic. *Expert Rev Clin Immunol,* **2015**, *11* (1), 5-13.

[226] Mills, C.D.; Kincaid, K.; Alt, J.M.; Heilman, M.J.; Hill, A.M. M-1/M-2 macrophages and the Th1/Th2 paradigm. *J Immunol,* **2000**, *164* (12), 6166-6173.

[227] Mills, C.D.; Ley, K. M1 and M2 macrophages: the chicken and the egg of immunity. *J Innate Immun,* **2014**, *6* (6), 716-726.

[228] Murray, P.J.; Allen, J.E.; Biswas, S.K.; Fisher, E.A.; Gilroy, D.W.; Goerdt, S.*, et al.* Macrophage activation and polarization: nomenclature and experimental guidelines. *Immunity,* **2014**, *41* (1), 14-20.

[229] Natoli, G.; Monticelli, S. Macrophage activation: glancing into diversity. *Immunity,* **2014**, *40* (2), 175-177.

[230] Koch, A.E.; Burrows, J.C.; Skoutelis, A.; Marder, R.; Domer, P.H.; Anderson, B.*, et al.* Monoclonal antibodies detect monocyte/macrophage activation and differentiation antigens and identify functionally distinct subpopulations of human rheumatoid synovial tissue macrophages. *Am J Pathol,* **1991**, *138* (1), 165-173.

[231] Maruotti, N.; Cantatore, F.P.; Crivellato, E.; Vacca, A.; Ribatti, D. Macrophages in rheumatoid arthritis. *Histol Histopathol,* **2007**, *22* (5), 581-586.

[232] Peters, K.M.; Koberg, K.; Rosendahl, T.; Klosterhalfen, B.; Straub, A.; Zwadlo-Klarwasser, G. Macrophage reactions in septic arthritis. *Arch Orthop Trauma Surg,* **1996**, *115* (6), 347-350.

[233] Elsaid, K.A.; Chichester, C.O. Review: Collagen markers in early arthritic diseases. *Clin Chim Acta,* **2006**, *365* (1-2), 68-77.

[234] Hamilton, J.A.; Tak, P.P. The dynamics of macrophage lineage populations in inflammatory and autoimmune diseases. *Arthritis Rheum,* **2009**, *60* (5), 1210-1221.

[235] Han, Z.; Boyle, D.L.; Chang, L.; Bennett, B.; Karin, M.; Yang, L*., et al.* c-Jun N-terminal kinase is required for metalloproteinase expression and joint destruction in inflammatory arthritis. *J Clin Invest,* **2001**, *108* (1), 73-81.

[236] Haringman, J.J.; Gerlag, D.M.; Zwinderman, A.H.; Smeets, T.J.; Kraan, M.C.; Baeten, D*., et al.* Synovial tissue macrophages: a sensitive biomarker for response to treatment in patients with rheumatoid arthritis. *Ann Rheum Dis,* **2005**, *64* (6), 834-838.

[237] Li, J.; Hsu, H.C.; Mountz, J.D. The Dynamic Duo-Inflammatory M1 macrophages and Th17 cells in Rheumatic Diseases. *J Orthop Rheumatol,* **2013**, *1* (1), 4.

[238] Risteli, J.; Elomaa, I.; Niemi, S.; Novamo, A.; Risteli, L. Radioimmunoassay for the pyridinoline cross-linked carboxy-terminal telopeptide of type I collagen: a new serum marker of bone collagen degradation. *Clin Chem,* **1993**, *39* (4), 635-640.

[239] Aman, S.; Risteli, J.; Luukkainen, R.; Risteli, L.; Kauppi, M.; Nieminen, P*., et al.* The value of synovial fluid analysis in the assessment of knee joint destruction in arthritis in a three year follow up study. *Ann Rheum Dis,* **1999**, *58* (9), 559-562.

[240] Hakala, M.; Aho, K.; Aman, S.; Luukkainen, R.; Kauppi, M.; Risteli, J. Type I collagen degradation does not diminish with RA disease duration. *Ann Rheum Dis,* **2001**, *60* (4), 420-422.

[241] Koike, T. [Destruction of articular cartilage]. *Clin Calcium,* **2006**, *16* (9), 1543-1547.

[242] Meng, F.W.; Slivka, P.F.; Dearth, C.L.; Badylak, S.F. Solubilized extracellular matrix from brain and urinary bladder elicits distinct functional and phenotypic responses in macrophages. *Biomaterials,* **2015**, *46*, 131-140.

[243] Asquith, D.L.; Miller, A.M.; McInnes, I.B.; Liew, F.Y. Animal models of rheumatoid arthritis. *Eur J Immunol,* **2009**, *39* (8), 2040-2044.

[244] Bevaart, L.; Vervoordeldonk, M.J.; Tak, P.P. Evaluation of therapeutic targets in animal models of arthritis: how does it relate to rheumatoid arthritis? *Arthritis Rheum,* **2010**, *62* (8), 2192-2205.

[245] Hu, Y.; Cheng, W.; Cai, W.; Yue, Y.; Li, J.; Zhang, P. Advances in research on animal models of rheumatoid arthritis. *Clin Rheumatol,* **2013**, *32* (2), 161-165.

[246] Backlund, J.; Nandakumar, K.S.; Bockermann, R.; Mori, L.; Holmdahl, R. Genetic control of tolerance to type II collagen and development of arthritis in an autologous collagen-induced arthritis model. *J Immunol,* **2003**, *171* (7), 3493-3499.

[247] Odom, D.T.; Dowell, R.D.; Jacobsen, E.S.; Gordon, W.; Danford, T.W.; MacIsaac, K.D*., et al.* Tissue-specific transcriptional regulation has diverged significantly between human and mouse. *Nat Genet,* **2007**, *39* (6), 730-732.

[248] Perel, P.; Roberts, I.; Sena, E.; Wheble, P.; Briscoe, C.; Sandercock, P.*, et al.* Comparison of treatment effects between animal experiments and clinical trials: systematic review. *BMJ,* **2007**, *334* (7586), 197.

[249] Ambarus, C.A.; Krausz, S.; van Eijk, M.; Hamann, J.; Radstake, T.R.; Reedquist, K.A.*, et al.* Systematic validation of specific phenotypic markers for in vitro polarized human macrophages. *J Immunol Methods,* **2012**, *375* (1-2), 196-206.

[250] Tjiu, J.W.; Chen, J.S.; Shun, C.T.; Lin, S.J.; Liao, Y.H.; Chu, C.Y.*, et al.* Tumor-associated macrophage-induced invasion and angiogenesis of human basal cell carcinoma cells by cyclooxygenase-2 induction. *J Invest Dermatol,* **2009**, *129* (4), 1016-1025.

[251] Mantovani, A.; Sozzani, S.; Locati, M.; Allavena, P.; Sica, A. Macrophage polarization: tumor-associated macrophages as a paradigm for polarized M2 mononuclear phagocytes. *Trends Immunol,* **2002**, *23* (11), 549-555.

[252] Chesney, J.; Metz, C.; Stavitsky, A.B.; Bacher, M.; Bucala, R. Regulated production of type I collagen and inflammatory cytokines by peripheral blood fibrocytes. *J Immunol,* **1998**, *160* (1), 419-425.

[253] Gabriel, S.E.; Michaud, K. Epidemiological studies in incidence, prevalence, mortality, and comorbidity of the rheumatic diseases. *Arthritis Res Ther,* **2009**, *11* (3), 229.

[254] Lin, Y.P.; Su, C.C.; Huang, J.Y.; Lin, H.C.; Cheng, Y.J.; Liu, M.F.*, et al.* Aberrant integrin activation induces p38 MAPK phosphorylation resulting in suppressed Fas-mediated apoptosis in T cells: implications for rheumatoid arthritis. *Mol Immunol,* **2009**, *46* (16), 3328-3335.

[255] Ye, L.; Wen, Z.; Li, Y.; Chen, B.; Yu, T.; Liu, L.*, et al.* Interleukin-10 attenuation of collagen-induced arthritis is associated with suppression of interleukin-17 and retinoid-related orphan receptor gammat production in macrophages and repression of classically activated macrophages. *Arthritis Res Ther,* **2014**, *16* (2), R96.

[256] Tedesco, S.; Bolego, C.; Toniolo, A.; Nassi, A.; Fadini, G.P.; Locati, M.*, et al.* Phenotypic activation and pharmacological outcomes of spontaneously differentiated human monocyte-derived macrophages. *Immunobiology,* **2015**, *220* (5), 545-554.

[257] Li, B.; Cui, W.; Liu, J.; Li, R.; Liu, Q.; Xie, X.H.*, et al.* Sulforaphane ameliorates the development of experimental autoimmune encephalomyelitis by antagonizing oxidative stress and Th17-related inflammation in mice. *Exp Neurol,* **2013**, *250*, 239-249.

[258] Gomez-Banuelos, E.; Martin-Marquez, B.T.; Martinez-Garcia, E.A.; Figueroa-Sanchez, M.; Nunez-Atahualpa, L.; Rocha-Munoz, A.D.*, et al.* Low levels of CD36 in peripheral blood monocytes in subclinical atherosclerosis in rheumatoid arthritis: a cross-sectional study in a Mexican population. *Biomed Res Int,* **2014**, *2014*, 736786.

[259] Rossol, M.; Kraus, S.; Pierer, M.; Baerwald, C.; Wagner, U. The CD14(bright) CD16+ monocyte subset is expanded in rheumatoid arthritis and promotes expansion of the Th17 cell population. *Arthritis Rheum,* **2012**, *64* (3), 671-677.

[260] Soler Palacios, B.; Estrada-Capetillo, L.; Izquierdo, E.; Criado, G.; Nieto, C.; Municio, C.*, et al.* Macrophages from the synovium of active rheumatoid arthritis exhibit an activin A-dependent pro-inflammatory profile. *J Pathol,* **2015**, *235* (3), 515-526.

[261] Tontonoz, P.; Nagy, L.; Alvarez, J.G.; Thomazy, V.A.; Evans, R.M. PPARgamma promotes monocyte/macrophage differentiation and uptake of oxidized LDL. *Cell,* **1998**, *93* (2), 241-252.

[262] Wintergerst, E.S.; Jelk, J.; Asmis, R. Differential expression of CD14, CD36 and the LDL receptor on human monocyte-derived macrophages. A novel cell culture system to study macrophage differentiation and heterogeneity. *Histochem Cell Biol,* **1998**, *110* (3), 231-241.

[263] Martinez, F.O.; Gordon, S. The M1 and M2 paradigm of macrophage activation: time for reassessment. *F1000Prime Rep,* **2014**, *6*, 13.

[264] Arthur, J.S.; Ley, S.C. Mitogen-activated protein kinases in innate immunity. *Nat Rev Immunol,* **2013**, *13* (9), 679-692.

[265] Xu, W.; Schlagwein, N.; Roos, A.; van den Berg, T.K.; Daha, M.R.; van Kooten, C. Human peritoneal macrophages show functional characteristics of M-CSF-driven anti-inflammatory type 2 macrophages. *Eur J Immunol,* **2007**, *37* (6), 1594-1599.

[266] Li, M.; Piao, L.; Chen, C.P.; Wu, X.; Yeh, C.C.; Masch, R.*, et al.* Modulation of Decidual Macrophage Polarization by Macrophage Colony-Stimulating Factor Derived from First-Trimester Decidual Cells: Implication in Preeclampsia. *Am J Pathol,* **2016**, *186* (5), 1258-1266.

[267] Cullen, P.; Cignarella, A.; Brennhausen, B.; Mohr, S.; Assmann, G.; von Eckardstein, A. Phenotype-dependent differences in apolipoprotein E metabolism and in cholesterol homeostasis in human monocyte-derived macrophages. *J Clin Invest,* **1998**, *101* (8), 1670-1677.

[268] Eligini, S.; Crisci, M.; Bono, E.; Songia, P.; Tremoli, E.; Colombo, G.I.*, et al.* Human monocyte-derived macrophages spontaneously differentiated in vitro show distinct phenotypes. *J Cell Physiol,* **2013**, *228* (7), 1464-1472.

[269] Zizzo, G.; Cohen, P.L. IL-17 stimulates differentiation of human anti-inflammatory macrophages and phagocytosis of apoptotic neutrophils in response to IL-10 and glucocorticoids. *J Immunol,* **2013**, *190* (10), 5237-5246.

[270] Nagata, S.; Golstein, P. The Fas death factor. *Science,* **1995**, *267* (5203), 1449-1456.

[271] Nagata, S. Apoptosis by death factor. *Cell,* **1997**, *88* (3), 355-365.

[272] Bien, K.; Sokolowska, J.; Baska, P.; Nowak, Z.; Stankiewicz, W.; Krzyzowska, M. Fas/FasL pathway participates in regulation of antiviral and inflammatory response during mousepox infection of lungs. *Mediators Inflamm,* **2015**, *2015*, 281613.

[273] Krzyzowska, M.; Baska, P.; Grochowska, A.; Orlowski, P.; Nowak, Z.; Winnicka, A. Fas/FasL pathway participates in resolution of mucosal inflammatory response early during HSV-2 infection. *Immunobiology,* **2014**, *219* (1), 64-77.

[274] Krzyzowska, M.; Baska, P.; Orlowski, P.; Zdanowski, R.; Winnicka, A.; Eriksson, K.*, et al.* HSV-2 regulates monocyte inflammatory response via the Fas/FasL pathway. *PLoS One,* **2013**, *8* (7), e70308.

[275] Krzyzowska, M.; Shestakov, A.; Eriksson, K.; Chiodi, F. Role of Fas/FasL in regulation of inflammation in vaginal tissue during HSV-2 infection. *Cell Death Dis,* **2011**, *2*, e132.

[276] Ramaswamy, M.; Cleland, S.Y.; Cruz, A.C.; Siegel, R.M. Many checkpoints on the road to cell death: regulation of Fas-FasL interactions and Fas signaling in peripheral immune responses. *Results Probl Cell Differ,* **2009**, *49*, 17-47.

[277] Wahlsten, J.L.; Gitchell, H.L.; Chan, C.C.; Wiggert, B.; Caspi, R.R. Fas and Fas ligand expressed on cells of the immune system, not on the target tissue, control induction of experimental autoimmune uveitis. *J Immunol,* **2000**, *165* (10), 5480-5486.

[278] Telegina, E.; Reshetnyak, T.; Moshnikova, A.; Proussakova, O.; Zhukova, A.; Kuznetsova, A.*, et al.* A possible role of Fas-ligand-mediated "reverse signaling" in pathogenesis of rheumatoid arthritis and systemic lupus erythematosus. *Immunol Lett,* **2009**, *122* (1), 12-17.

[279] Sumida, T.; Hoa, T.T.; Asahara, H.; Hasunuma, T.; Nishioka, K. T cell receptor of Fas-sensitive T cells in rheumatoid synovium. *J Immunol,* **1997**, *158* (4), 1965-1970.

[280] Pittoni, V.; Sorice, M.; Circella, A.; Cangemi, R.; Conti, L.; Ramenghi, U.*, et al.* Specificity of antinuclear and antiphospholipid antibodies in sera of patients with autoimmune lymphoproliferative disease (ALD). *Clin Exp Rheumatol,* **2003**, *21* (3), 377-385.

[281] Hong, S.; Kim, E.J.; Lee, E.J.; San Koo, B.; Min Ahn, S.; Bae, S.H.*, et al.* TNF-alpha confers resistance to Fas-mediated apoptosis in rheumatoid arthritis through the induction of soluble Fas. *Life Sci,* **2015**, *122*, 37-41.

[282] Grosjean, M.B.; Lenzlinger, P.M.; Stahel, P.F.; Yatsiv, I.; Shohami, E.; Trentz, O.*, et al.* Immunohistochemical characterization of Fas (CD95) and Fas Ligand (FasL/CD95L) expression in the injured brain: relationship with neuronal cell death and inflammatory mediators. *Histol Histopathol,* **2007**, *22* (3), 235-250.

[283] Audo, R.; Calmon-Hamaty, F.; Papon, L.; Combe, B.; Morel, J.; Hahne, M. Distinct effects of soluble and membrane-bound fas ligand on fibroblast-like synoviocytes from rheumatoid arthritis patients. *Arthritis Rheumatol,* **2014**, *66* (12), 3289-3299.

[284] Cheng, J.; Zhou, T.; Liu, C.; Shapiro, J.P.; Brauer, M.J.; Kiefer, M.C.*, et al.* Protection from Fas-mediated apoptosis by a soluble form of the Fas molecule. *Science,* **1994**, *263* (5154), 1759-1762.

[285] Desbarats, J.; Duke, R.C.; Newell, M.K. Newly discovered role for Fas ligand in the cell-cycle arrest of CD4+ T cells. *Nat Med,* **1998**, *4* (12), 1377-1382.

[286] Proussakova, O.V.; Rabaya, N.A.; Moshnikova, A.B.; Telegina, E.S.; Turanov, A.; Nanazashvili, M.G., *et al.* Oligomerization of soluble Fas antigen induces its cytotoxicity. *J Biol Chem,* **2003**, *278* (38), 36236-36241.

[287] Silvestris, F.; Grinello, D.; Tucci, M.; Cafforio, P.; Dammacco, F. Enhancement of T cell apoptosis correlates with increased serum levels of soluble Fas (CD95/Apo-1) in active lupus. *Lupus,* **2003**, *12* (1), 8-14.

[288] Calmon-Hamaty, F.; Audo, R.; Combe, B.; Morel, J.; Hahne, M. Targeting the Fas/FasL system in Rheumatoid Arthritis therapy: Promising or risky? *Cytokine,* **2014**.

[289] Xu, L.; Zhang, L.; Yi, Y.; Kang, H.K.; Datta, S.K. Human lupus T cells resist inactivation and escape death by upregulating COX-2. *Nat Med,* **2004**, *10* (4), 411-415.

[290] Kim, H.; Kim, E.H.; Eom, Y.W.; Kim, W.H.; Kwon, T.K.; Lee, S.J., *et al.* Sulforaphane sensitizes tumor necrosis factor-related apoptosis-inducing ligand (TRAIL)-resistant hepatoma cells to TRAIL-induced apoptosis through reactive oxygen species-mediated up-regulation of DR5. *Cancer Res,* **2006**, *66* (3), 1740-1750.

[291] Pledgie-Tracy, A.; Sobolewski, M.D.; Davidson, N.E. Sulforaphane induces cell type-specific apoptosis in human breast cancer cell lines. *Mol Cancer Ther,* **2007**, *6* (3), 1013-1021.

[292] Sayed, R.H.; Khalil, W.K.; Salem, H.A.; Kenawy, S.A.; El-Sayeh, B.M. Sulforaphane increases the survival rate in rats with fulminant hepatic failure induced by D-galactosamine and lipopolysaccharide. *Nutr Res,* **2014**, *34* (11), 982-989.

[293] Bohm, B.B.; Freund, I.; Krause, K.; Kinne, R.W.; Burkhardt, H. ADAM15 adds to apoptosis resistance of synovial fibroblasts by modulating focal adhesion kinase signaling. *Arthritis Rheum,* **2013**, *65* (11), 2826-2834.

[294] Lowin, T.; Straub, R.H. Synovial fibroblasts integrate inflammatory and neuroendocrine stimuli to drive rheumatoid arthritis. *Expert Rev Clin Immunol,* **2015**, *11* (10), 1069-1071.

[295] Perlman, H.; Pagliari, L.J.; Georganas, C.; Mano, T.; Walsh, K.; Pope, R.M. FLICE-inhibitory protein expression during macrophage differentiation confers resistance to fas-mediated apoptosis. *J Exp Med,* **1999**, *190* (11), 1679-1688.

[296] Rapetti, L.; Chavele, K.M.; Evans, C.M.; Ehrenstein, M.R. B cell resistance to Fas-mediated apoptosis contributes to their ineffective control by regulatory T cells in rheumatoid arthritis. *Ann Rheum Dis,* **2015**, *74* (1), 294-302.

[297] Schoen, R.T.; Mehlman, H.; Trentham, D.E.; Perry, L.; Greene, M.I.; David, J.R. Autoimmunity induced by type II collagen-coupled spleen cells. *J Immunol,* **1981**, *127* (6), 2275-2279.

[298] Brand, D.D.; Kang, A.H.; Rosloniec, E.F. Immunopathogenesis of collagen arthritis. *Springer Semin Immunopathol,* **2003**, *25* (1), 3-18.

[299] Vogelstein, B.; Papadopoulos, N.; Velculescu, V.E.; Zhou, S.; Diaz, L.A., Jr.; Kinzler, K.W. Cancer genome landscapes. *Science,* **2013**, *339* (6127), 1546-1558.

[300] Morin, P.J. Drug resistance and the microenvironment: nature and nurture. *Drug Resist Updat,* **2003**, *6* (4), 169-172.

[301] Tan, M.L.; Ooi, J.P.; Ismail, N.; Moad, A.I.; Muhammad, T.S. Programmed cell death pathways and current antitumor targets. *Pharm Res,* **2009**, *26* (7), 1547-1560.

[302] Sun, Y.; Peng, Z.L. Programmed cell death and cancer. *Postgrad Med J,* **2009**, *85* (1001), 134-140.

[303] Mohammad, R.M.; Muqbil, I.; Lowe, L.; Yedjou, C.; Hsu, H.Y.; Lin, L.T.*, et al.* Broad targeting of resistance to apoptosis in cancer. *Semin Cancer Biol,* **2015**, *35 Suppl*, S78-103.

[304] Elmore, S. Apoptosis: a review of programmed cell death. *Toxicol Pathol,* **2007**, *35* (4), 495-516.

[305] Tanida, I.; Ueno, T.; Kominami, E. LC3 and Autophagy. *Methods Mol Biol,* **2008**, *445*, 77-88.

[306] Gozuacik, D.; Kimchi, A. Autophagy as a cell death and tumor suppressor mechanism. *Oncogene,* **2004**, *23* (16), 2891-2906.

[307] Lindqvist, L.M.; Simon, A.K.; Baehrecke, E.H. Current questions and possible controversies in autophagy. *Cell Death Discov,* **2015**, *1*.

[308] Ogier-Denis, E.; Codogno, P. Autophagy: a barrier or an adaptive response to cancer. *Biochim Biophys Acta,* **2003**, *1603* (2), 113-128.

[309] White, E. Deconvoluting the context-dependent role for autophagy in cancer. *Nat Rev Cancer,* **2012**, *12* (6), 401-410.

[310] Mizushima, N. Autophagy: process and function. *Genes Dev,* **2007**, *21* (22), 2861-2873.

[311] Moretti, L.; Yang, E.S.; Kim, K.W.; Lu, B. Autophagy signaling in cancer and its potential as novel target to improve anticancer therapy. *Drug Resist Updat,* **2007**, *10* (4-5), 135-143.

[312] Hoyer-Hansen, M.; Jaattela, M. Autophagy: an emerging target for cancer therapy. *Autophagy,* **2008**, *4* (5), 574-580.

[313] Chen, H.Y.; White, E. Role of autophagy in cancer prevention. *Cancer Prev Res (Phila),* **2011**, *4* (7), 973-983.

[314] Dalby, K.N.; Tekedereli, I.; Lopez-Berestein, G.; Ozpolat, B. Targeting the prodeath and prosurvival functions of autophagy as novel therapeutic strategies in cancer. *Autophagy,* **2010**, *6* (3), 322-329.

[315] Li, L.; Leung, P.S. Use of herbal medicines and natural products: An alternative approach to overcoming the apoptotic resistance of pancreatic cancer. *Int J Biochem Cell Biol,* **2014**, *53*, 224-236.

[316] Macintosh, R.L.; Ryan, K.M. Autophagy in tumour cell death. *Semin Cancer Biol,* **2013**, *23* (5), 344-351.

[317] McCubrey, J.A.; Steelman, L.S.; Chappell, W.H.; Abrams, S.L.; Franklin, R.A.; Montalto, G.*, et al.* Ras/Raf/MEK/ERK and PI3K/PTEN/Akt/mTOR cascade inhibitors: how mutations can result in therapy resistance and how to overcome resistance. *Oncotarget,* **2012**, *3* (10), 1068-1111.

[318] McCubrey, J.A.; Steelman, L.S.; Chappell, W.H.; Abrams, S.L.; Montalto, G.; Cervello, M.*, et al.* Mutations and deregulation of Ras/Raf/MEK/ERK and PI3K/PTEN/Akt/mTOR cascades which alter therapy response. *Oncotarget,* **2012**, *3* (9), 954-987.

[319] Brenner, H.; Kloor, M.; Pox, C.P. Colorectal cancer. *Lancet,* **2014**, *383* (9927), 1490-1502.

[320] Center, M.M.; Jemal, A.; Smith, R.A.; Ward, E. Worldwide variations in colorectal cancer. *CA Cancer J Clin,* **2009**, *59* (6), 366-378.

[321] Center, M.M.; Jemal, A.; Ward, E. International trends in colorectal cancer incidence rates. *Cancer Epidemiol Biomarkers Prev,* **2009**, *18* (6), 1688-1694.

[322] Ferlay, J.; Shin, H.R.; Bray, F.; Forman, D.; Mathers, C.; Parkin, D.M. Estimates of worldwide burden of cancer in 2008: GLOBOCAN 2008. *Int J Cancer,* **2010**, *127* (12), 2893-2917.

[323] Mohandas, K.M. Colorectal cancer in India: controversies, enigmas and primary prevention. *Indian J Gastroenterol,* **2011**, *30* (1), 3-6.

[324] Sameer, A.S. Colorectal cancer: molecular mutations and polymorphisms. *Front Oncol,* **2013**, *3*, 114.

[325] Solit, D.B.; Garraway, L.A.; Pratilas, C.A.; Sawai, A.; Getz, G.; Basso, A.*, et al.* BRAF mutation predicts sensitivity to MEK inhibition. *Nature,* **2006**, *439* (7074), 358-362.

[326] Sideris, M.; Papagrigoriadis, S. Molecular biomarkers and classification models in the evaluation of the prognosis of colorectal cancer. *Anticancer Res,* **2014**, *34* (5), 2061-2068.

[327] Rizzo, S.; Bronte, G.; Fanale, D.; Corsini, L.; Silvestris, N.; Santini, D.*, et al.* Prognostic vs predictive molecular biomarkers in colorectal cancer: is KRAS and BRAF wild type status required for anti-EGFR therapy? *Cancer Treat Rev,* **2010**, *36 Suppl 3*, S56-61.

[328] De Roock, W.; Claes, B.; Bernasconi, D.; De Schutter, J.; Biesmans, B.; Fountzilas, G.*, et al.* Effects of KRAS, BRAF, NRAS, and PIK3CA mutations on the efficacy of cetuximab plus chemotherapy in chemotherapy-refractory metastatic colorectal cancer: a retrospective consortium analysis. *Lancet Oncol,* **2010**, *11* (8), 753-762.

[329] De Roock, W.; De Vriendt, V.; Normanno, N.; Ciardiello, F.; Tejpar, S. KRAS, BRAF, PIK3CA, and PTEN mutations: implications for targeted therapies in metastatic colorectal cancer. *Lancet Oncol,* **2011**, *12* (6), 594-603.

[330] Bamford, S.; Dawson, E.; Forbes, S.; Clements, J.; Pettett, R.; Dogan, A.*, et al.* The COSMIC (Catalogue of Somatic Mutations in Cancer) database and website. *Br J Cancer,* **2004**, *91* (2), 355-358.

[331] Corcoran, R.B.; Ebi, H.; Turke, A.B.; Coffee, E.M.; Nishino, M.; Cogdill, A.P*., et al.* EGFR-mediated re-activation of MAPK signaling contributes to insensitivity of BRAF mutant colorectal cancers to RAF inhibition with vemurafenib. *Cancer Discov,* **2012**, *2* (3), 227-235.

[332] Ogino, S.; Shima, K.; Meyerhardt, J.A.; McCleary, N.J.; Ng, K.; Hollis, D*., et al.* Predictive and prognostic roles of BRAF mutation in stage III colon cancer: results from intergroup trial CALGB 89803. *Clin Cancer Res,* **2012**, *18* (3), 890-900.

[333] Thiel, A.; Ristimaki, A. Toward a Molecular Classification of Colorectal Cancer: The Role of BRAF. *Front Oncol,* **2013**, *3*, 281.

[334] Reimers, M.S.; Zeestraten, E.C.; Kuppen, P.J.; Liefers, G.J.; van de Velde, C.J. Biomarkers in precision therapy in colorectal cancer. *Gastroenterol Rep (Oxf),* **2013**, *1* (3), 166-183.

[335] Sharma, S.G.; Gulley, M.L. BRAF mutation testing in colorectal cancer. *Arch Pathol Lab Med,* **2010**, *134* (8), 1225-1228.

[336] Pratilas, C.A.; Solit, D.B. Therapeutic strategies for targeting BRAF in human cancer. *Rev Recent Clin Trials,* **2007**, *2* (2), 121-134.

[337] Prahallad, A.; Sun, C.; Huang, S.; Di Nicolantonio, F.; Salazar, R.; Zecchin, D*., et al.* Unresponsiveness of colon cancer to BRAF(V600E) inhibition through feedback activation of EGFR. *Nature,* **2012**, *483* (7387), 100-103.

[338] Cichowski, K.; Janne, P.A. Drug discovery: inhibitors that activate. *Nature,* **2010**, *464* (7287), 358-359.

[339] Straussman, R.; Morikawa, T.; Shee, K.; Barzily-Rokni, M.; Qian, Z.R.; Du, J*., et al.* Tumour micro-environment elicits innate resistance to RAF inhibitors through HGF secretion. *Nature,* **2012**, *487* (7408), 500-504.

[340] Sousa, C.M.; Kimmelman, A.C. The complex landscape of pancreatic cancer metabolism. *Carcinogenesis,* **2014**, *35* (7), 1441-1450.

[341] Singh, D.; Upadhyay, G.; Srivastava, R.K.; Shankar, S. Recent advances in pancreatic cancer: biology, treatment, and prevention. *Biochim Biophys Acta,* **2015**, *1856* (1), 13-27.

[342] Viale, A.; Pettazzoni, P.; Lyssiotis, C.A.; Ying, H.; Sanchez, N.; Marchesini, M*., et al.* Oncogene ablation-resistant pancreatic cancer cells depend on mitochondrial function. *Nature,* **2014**, *514* (7524), 628-632.

[343] Liu, J.; Ji, S.; Liang, C.; Qin, Y.; Jin, K.; Liang, D*., et al.* Critical role of oncogenic KRAS in pancreatic cancer (Review). *Mol Med Rep,* **2016**.

[344] Fryzek, J.P.; Garabrant, D.H.; Schenk, M.; Kinnard, M.; Greenson, J.K.; Sarkar, F.H. The association between selected risk factors for pancreatic cancer and the expression of p53 and K-ras codon 12 mutations. *Int J Gastrointest Cancer,* **2006**, *37* (4), 139-145.

[345] Padavano, J.; Henkhaus, R.S.; Chen, H.; Skovan, B.A.; Cui, H.; Ignatenko, N.A. Mutant K-RAS Promotes Invasion and Metastasis in Pancreatic Cancer Through GTPase Signaling Pathways. *Cancer Growth Metastasis,* **2015**, *8* (Suppl 1), 95-113.

[346] Kolodecik, T.; Shugrue, C.; Ashat, M.; Thrower, E.C. Risk factors for pancreatic cancer: underlying mechanisms and potential targets. *Front Physiol,* **2014**, *4*, 415.

[347] Eser, S.; Schnieke, A.; Schneider, G.; Saur, D. Oncogenic KRAS signalling in pancreatic cancer. *Br J Cancer,* **2014**, *111* (5), 817-822.

[348] Collins, M.A.; Pasca di Magliano, M. Kras as a key oncogene and therapeutic target in pancreatic cancer. *Front Physiol,* **2014**, *4*, 407.

[349] Bryant, K.L.; Mancias, J.D.; Kimmelman, A.C.; Der, C.J. KRAS: feeding pancreatic cancer proliferation. *Trends Biochem Sci,* **2014**, *39* (2), 91-100.

[350] Rosenfeldt, M.T.; O'Prey, J.; Morton, J.P.; Nixon, C.; MacKay, G.; Mrowinska, A*., et al.* p53 status determines the role of autophagy in pancreatic tumour development. *Nature,* **2013**, *504* (7479), 296-300.

[351] Fiorini, C.; Cordani, M.; Padroni, C.; Blandino, G.; Di Agostino, S.; Donadelli, M. Mutant p53 stimulates chemoresistance of pancreatic adenocarcinoma cells to gemcitabine. *Biochim Biophys Acta,* **2015**, *1853* (1), 89-100.

[352] Yang, A.; Rajeshkumar, N.V.; Wang, X.; Yabuuchi, S.; Alexander, B.M.; Chu, G.C*., et al.* Autophagy is critical for pancreatic tumor growth and progression in tumors with p53 alterations. *Cancer Discov,* **2014**, *4* (8), 905-913.

[353] Udelnow, A.; Kreyes, A.; Ellinger, S.; Landfester, K.; Walther, P.; Klapperstueck, T*., et al.* Omeprazole inhibits proliferation and modulates autophagy in pancreatic cancer cells. *PLoS One,* **2011**, *6* (5), e20143.

[354] Ozawa, F.; Friess, H.; Kleeff, J.; Xu, Z.W.; Zimmermann, A.; Sheikh, M.S*., et al.* Effects and expression of TRAIL and its apoptosis-promoting receptors in human pancreatic cancer. *Cancer Lett,* **2001**, *163* (1), 71-81.

[355] Yoshikawa, H.; Nagashima, M.; Khan, M.A.; McMenamin, M.G.; Hagiwara, K.; Harris, C.C. Mutational analysis of p73 and p53 in human cancer cell lines. *Oncogene,* **1999**, *18* (22), 3415-3421.

[356] Wu, C.Y.; Guo, X.Z.; Li, H.Y. Hypoxia and Serum deprivation protected MiaPaCa-2 cells from KAI1-induced proliferation inhibition through autophagy pathway activation in solid tumors. *Clin Transl Oncol,* **2015**, *17* (3), 201-208.

[357] Madden, M.E.; Heaton, K.M.; Huff, J.K.; Sarras, M.P., Jr. Comparative analysis of a human pancreatic undifferentiated cell line (MIA PaCa-2) to acinar and ductal cells. *Pancreas,* **1989**, *4* (5), 529-537.

[358]   Mujumdar, N.; Saluja, A.K. Autophagy in pancreatic cancer: an emerging mechanism of cell death. *Autophagy,* **2010**, *6* (7), 997-998.

[359]   Xue, Z.X.; Zheng, J.H.; Zheng, Z.Q.; Cai, J.L.; Ye, X.H.; Wang, C*., et al.* Latexin inhibits the proliferation of CD133+ miapaca-2 pancreatic cancer stem-like cells. *World J Surg Oncol,* **2014**, *12*, 404.

[360]   Schneider, J.L.; Cuervo, A.M. Autophagy and human disease: emerging themes. *Curr Opin Genet Dev,* **2014**, *26*, 16-23.

[361]   Pal, S.; Konkimalla, V.B.; Kathwate, L.; Rao, S.S.; S. P. Gejji; Puranik, V*., et al.* Targeting chemorefractory COLO205 (BRAF V600E) cell lines using substituted benzo[α]phenoxazines†. *RSC Adv.,* **2015**, *5*, 82549.

[362]   Klionsky, D.J.; Abdalla, F.C.; Abeliovich, H.; Abraham, R.T.; Acevedo-Arozena, A.; Adeli, K*., et al.* Guidelines for the use and interpretation of assays for monitoring autophagy. *Autophagy,* **2012**, *8* (4), 445-544.

[363]   Fu, L.L.; Cheng, Y.; Liu, B. Beclin-1: autophagic regulator and therapeutic target in cancer. *Int J Biochem Cell Biol,* **2013**, *45* (5), 921-924.